REPUBLIC OF CAMEROON

PEACE-WORK-FATHERLAND

****

THE UNIVERSITY OF YAOUNDE I

****

POSTGRADUATE SCHOOL OF SCIENCE, TECHNOLOGY AND GEOSCIENCES

REPUBLIQUE DU CAMEROUN

PAIX-TRAVAIL-PATRIE

****

UNIVERSITE DE YAOUNDE I

****

CENTRE DE RECHERCHE ET DE FORMATION DOCTORALE EN SCIENCES, TECHNOLOGIES ET GÉOSCIENCES

DOCTORAL RESEARCH UNIT FOR CHEMISTRY AND APPLICATIONS

UNITE DE RECHERCHE ET DE FORMATION DOCTORALE EN CHIMIE ET APPLICATIONS

Speciality: Natural Products

Spécialité: Substances Naturelles

****

Bioguided chemical studies of *Boswellia dalzielii* (Burseraceae) for antimicrobial agents

Thesis

Presented and defended publicly for the fulfilment of the award of the degree of

Doctorat/PhD.

By

TEGASNE Catherine

Registration number: 06T511

Master in Organic Chemistry

Under the supervision of

KAPCHE WABO FOTSO Gilbert Deccaux, Professor

Year 2023

ACADEMIC YEAR 2022/2023
(Per Department and Grade)
Update 31 MAI 2023

ADMINISTRATION

DEAN : TCHOUANKEU Jean- Claude, *Associate professor*
VICE-DEAN / DPSAA : ATCHADE Alex de Théodore, *Associate professor*
VICE-DEAN / DSSE : NYEGUE Maximilienne Ascension**,** *Professor*
VICE-DEAN / DRC : ABOSSOLO ANGUE Monique, *Associate professor*
Head of Division of Administrative and Financial Affairs: NDOYE FOE Marie C. F., *Associate professor*
Head of Division of Academics Affairs, admission and research DAASR: AJEAGAH Gideon AGHAINDUM, *professor*

1- DÉPARTEMENT DE BIOCHIMIE (BC) (43)

N°	NOMS ET PRÉNOMS	GRADE	OBSERVATIONS
1.	BIGOGA DAIGA Jude	Professor	On duty
2.	FEKAM BOYOM Fabrice	Professor	On duty
3.	KANSCI Germain	Professor	On duty
4.	MBACHAM FON Wilfred	Professor	On duty
5.	MOUNDIPA FEWOU Paul	Professor	Head of Department
6.	NGUEFACK Julienne	Professor	On duty
7.	NJAYOU Frédéric Nico	Professor	On duty
8.	OBEN Julius ENYONG	Professor	On duty

N°	NOMS ET PRÉNOMS	GRADE	OBSERVATIONS
9.	ACHU Merci BIH	Associate Professor	On duty
10.	ATOGHO Barbara MMA	Associate Professor	On duty
11.	AZANTSA KINGUE GABIN BORIS	Associate Professor	On duty
12.	BELINGA née NDOYE FOE F. M. C.	Associate Professor	*Chef DAF / FS*
13.	DJUIDJE NGOUNOUE Marceline	Associate Professor	On duty
14.	DJUIKWO NKONGA Ruth Viviane	Associate Professor	On duty
15.	EFFA ONOMO Pierre	Associate Professor	Head DAF / FS
16.	EWANE Cécile Annie	Associate Professor	On duty
17.	KOTUE TAPTUE Charles	Associate Professor	On duty
18.	LUNGA Paul KEILAH	Associate Professor	On duty
19.	MBONG ANGIE M. Mary Anne	Associate Professor	On duty

20.	MOFOR née TEUGWA Clotilde	Associate Professor	*Dean FS UDs*
21.	NANA Louise épouse WAKAM	Associate Professor	On duty
22.	NGONDI Judith Laure	Associate Professor	On duty
23.	TCHANA KOUATCHOUA Angèle	Associate Professor	On duty

24.	AKINDEH MBUH NJI	Lecturer	On duty
25.	BEBEE Fadimatou	Lecturer	On duty
26.	BEBOY EDJENGUELE Sara Nathalie	Lecturer	On duty
27.	DAKOLE DABOY Charles	Lecturer	On duty
28.	DONGMO LEKAGNE Joseph Blaise	Lecturer	On duty
29.	FONKOUA Martin	Lecturer	On duty
30.	FOUPOUAPOUOGNIGNI Yacouba	Lecturer	On duty
31.	KOUOH ELOMBO Ferdinand	Lecturer	On duty
32.	MANANGA Marlyse Joséphine	Lecturer	On duty
33.	OWONA AYISSI Vincent Brice	Lecturer	On duty
34.	Palmer MASUMBE NETONGO	Lecturer	On duty
35.	PECHANGOU NSANGOU Sylvain	Lecturer	On duty
36.	WILFRED ANGIE ABIA	Lecturer	On duty

37.	BAKWO BASSOGOG Christian Bernard	Assistant Lecturer	On duty
38.	ELLA Fils Armand	Assistant Lecturer	On duty
39.	EYENGA Eliane Flore	Assistant Lecturer	On duty
40.	MADIESSE KEMGNE Eugenie Aimée	Assistant Lecturer	On duty
41.	MANJIA NJIKAM Jacqueline	Assistant Lecturer	On duty
42.	MBOUCHE FANMOE Marceline Joëlle	Assistant Lecturer	On duty
43.	WOGUIA Alice Louise	Assistant Lecturer	On duty

2- DÉPARTEMENT DE BIOLOGIE ET PHYSIOLOGIE ANIMALES (BPA) (52)

1.	AJEAGAH Gideon AGHAINDUM	Professor	*DAARS/FS*
2.	BILONG BILONG Charles-Félix	Professor	Head of Department
3.	DIMO Théophile	Professor	On duty
4.	DJIETO LORDON Champlain	Professor	On duty
5.	DZEUFIET DJOMENI Paul Désiré	Professor	On duty
6.	ESSOMBA née NTSAMA MBALA	Professor	*HD and Dean /FMSB/UYI*
7.	FOMENA Abraham	Professor	On duty
8.	KEKEUNOU Sévilor	Professor	On duty
9.	NJAMEN Dieudonné	Professor	On duty
10.	NJIOKOU Flobert	Professor	On duty

11.	NOLA Moïse	Professor	On duty
12.	TAN Paul VERNYUY	Professor	On duty
13.	TCHUEM TCHUENTE Louis Albert	Professor	*Inspector of Service Coord.Progr./MINSANTE*
14.	ZEBAZE TOGOUET Serge Hubert	Professor	On duty

15.	ALENE Désirée Chantal	Associate Professor	*Vice Dean/ Uty Ebwa*
16.	BILANDA Danielle Claude	Associate Professor	On duty
17.	DJIOGUE Séfirin	Associate Professor	On duty
18.	GOUNOUE KAMKUMO Raceline épse FOTSING	Associate Professor	On duty
19.	JATSA BOUKENG Hermine épse MEGAPTCHE	Associate Professor	On duty
20.	LEKEUFACK FOLEFACK Guy B.	Associate Professor	On duty
21.	MAHOB Raymond Joseph	Associate Professor	On duty
22.	MBENOUN MASSE Paul Serge	Associate Professor	On duty
23.	MEGNEKOU Rosette	Associate Professor	On duty
24.	MOUNGANG Luciane Marlyse	Associate Professor	On duty
25.	NOAH EWOTI Olive Vivien	Associate Professor	On duty
26.	MONY Ruth épse NTONE	Associate Professor	On duty
27.	NGUEGUIM TSOFACK Florence	Associate Professor	On duty
28.	NGUEMBOCK	Associate Professor	On duty
29.	TAMSA ARFAO Antoine	Associate Professor	On duty
30.	TOMBI Jeannette	Associate Professor	On duty

31.	ATSAMO Albert Donatien	Lecturer	On duty
32.	BASSOCK BAYIHA Etienne Didier	Lecturer	On duty
33.	ETEME ENAMA Serge	Lecturer	On duty
34.	FEUGANG YOUMSSI François	Lecturer	On duty
35.	FOKAM Alvine Christelle Epse KENGNE	Lecturer	On duty
36.	GONWOUO NONO Legrand	Lecturer	On duty
37.	KANDEDA KAVAYE Antoine	Lecturer	On duty
38.	KOGA MANG DOBARA	Lecturer	On duty
39.	LEME BANOCK Lucie	Lecturer	On duty
40.	MAPON NSANGOU Indou	Lecturer	On duty
41.	METCHI DONFACK MIREILLE FLAURE EPSE GHOUMO	Lecturer	On duty
42.	MVEYO NDANKEU Yves Patrick	Lecturer	On duty
43.	NGOUATEU KENFACK Omer Bébé	Lecturer	On duty
44.	NJUA Clarisse YAFI	Lecturer	*Head of Division. Uty Bamenda*
45.	NWANE Philippe Bienvenu	Lecturer	On duty
46.	TADU Zephyrin	Lecturer	On duty
47.	YEDE	Lecturer	On duty
48.	YOUNOUSSA LAME	Lecturer	On duty

49.	AMBADA NDZENGUE GEORGIA ELNA	Assistant Lecturer	On duty
50.	KODJOM WANCHE Jacguy Joyce	Assistant Lecturer	On duty
51.	NDENGUE Jean De Matha	Assistant Lecturer	On duty
52.	ZEMO GAMO Franklin	Assistant Lecturer	On duty

3- DÉPARTEMENT DE BIOLOGIE ET PHYSIOLOGIE VÉGÉTALES (BPV) (34)

1.	AMBANG Zachée	Professor	*Head of Department*
2.	DJOCGOUE Pierre François	Professor	On duty
3.	MBOLO Marie	Professor	On duty
4.	MOSSEBO Dominique Claude	Professor	On duty
5.	YOUMBI Emmanuel	Professor	On duty
6.	ZAPFACK Louis	Professor	On duty

7.	ANGONI Hyacinthe	Associate Professor	On duty
8.	BIYE Elvire Hortense	Associate Professor	On duty
9.	MAHBOU SOMO TOUKAM. Gabriel	Associate Professor	On duty
10	MALA Armand William	Associate Professor	On duty
11	MBARGA BINDZI Marie Alain	Associate Professor	*DAAC /UDla*
12	NDONGO BEKOLO	Associate Professor	On duty
13	NGALLE Hermine BILLE	Associate Professor	On duty
14	NGODO MELINGUI Jean Baptiste	Associate Professor	On duty
15	NGONKEU MAGAPTCHE Eddy L.	Associate Professor	*CT / MINRESI*
16	TONFACK Libert Brice	Associate Professor	On duty
17	TSOATA Esaïe	Associate Professor	On duty
18	ONANA JEAN MICHEL	Associate Professor	On duty

19.	DJEUANI Astride Carole	Lecturer	On duty
20.	GONMADGE CHRISTELLE	Lecturer	On duty
21.	MAFFO MAFFO Nicole Liliane	Lecturer	On duty
22.	NNANGA MEBENGA Ruth Laure	Lecturer	On duty
23.	NOUKEU KOUAKAM Armelle	Lecturer	On duty
24.	NSOM ZAMBO EPSE PIAL ANNIE CLAUDE	Lecturer	*UNESCO MALI*
25.	GODSWILL NTSOMBOH NTSEFONG	Lecturer	On duty
26.	KABELONG BANAHO Louis-Paul-Roger	Lecturer	On duty
27.	KONO Léon Dieudonné	Lecturer	On duty
28.	LIBALAH Moses BAKONCK	Lecturer	On duty
29.	LIKENG-LI-NGUE Benoit C	Lecturer	On duty
30.	TAEDOUNG Evariste Hermann	Lecturer	On duty
31.	TEMEGNE NONO Carine	Lecturer	On duty

32.	MANGA NDJAGA JUDE	Assistant Lecturer	On duty
33.	DIDA LONTSI Sylvere Landry	Assistant Lecturer	On duty
34.	METSEBING Blondo-Pascal	Assistant Lecturer	On duty

4- DÉPARTEMENT DE CHIMIE INORGANIQUE (CI) (28)

1.	GHOGOMU Paul MINGO	Professor	*Minister in Charge of Miss.PR*
2.	NANSEU NJIKI Charles Péguy	Professor	On duty
3.	NDIFON Peter TEKE	Professor	*CT MINRESI*
4.	NENWA Justin	Professor	On duty
5.	NGAMENI Emmanuel	Professor	*Dean FS Univ.Ngaoundere*
6.	NGOMO Horace MANGA	Professor	*Vice Chancelor/UB*
7.	NJOYA Dayirou	Professor	On duty

8.	ACAYANKA Elie	Associate Professor	On duty
9.	EMADAK Alphonse	Associate Professor	On duty
10	KAMGANG YOUBI Georges	Associate Professor	On duty
11	KEMMEGNE MBOUGUEM Jean C.	Associate Professor	On duty
12	KENNE DEDZO GUSTAVE	Associate Professor	On duty
13	MBEY Jean Aime	Associate Professor	On duty
14	NDI NSAMI Julius	Associate Professor	Head of department
15	NEBAH Née NDOSIRI Bridget NDOYE	Associate Professor	*Senator/SENAT*
16	NJIOMOU C. épse DJANGANG	Associate Professor	On duty
17	NYAMEN Linda Dyorisse	Associate Professor	On duty
18	PABOUDAM GBAMBIE AWAWOU	Associate Professor	On duty
19	TCHAKOUTE KOUAMO Hervé	Associate Professor	On duty
20	BELIBI BELIBI Placide Désiré	Associate Professor	*Chief Service/ ENS Bertoua*
21	CHEUMANI YONA Arnaud M.	Associate Professor	On duty
22	KOUOTOU DAOUDA	Associate Professor	On duty

23.	MAKON Thomas Beauregard	Lecturer	On duty
24.	NCHIMI NONO KATIA	Lecturer	On duty
25.	NJANKWA NJABONG N. Eric	Lecturer	On duty
26.	PATOUOSSA ISSOFA	Lecturer	On duty
27.	SIEWE Jean Mermoz	Lecturer	On duty
28.	BOYOM TATCHEMO Franck W.	Assistant Lecturer	On duty

5- DÉPARTEMENT DE CHIMIE ORGANIQUE (CO) (37)

1.	Alex de Théodore ATCHADE	Professor	*Vice-Dean / DPSAA*
2.	DONGO Etienne	Professor	*Vice-Dean/FSE/UYI*
3.	NGOUELA Silvère Augustin	Professor	Head of department *UDS*
4.	PEGNYEMB Dieudonné Emmanuel	Professor	*Director/ MINESUP/* Head of department
5.	WANDJI Jean	Professor	On duty
6.	MBAZOA née DJAMA Céline	Professor	On duty

7.	AMBASSA Pantaléon	Associate Professor	On duty
8.	EYONG Kenneth OBEN	Associate Professor	On duty
9.	FOTSO WABO Ghislain	Associate Professor	On duty
10.	KAMTO Eutrophe Le Doux	Associate Professor	On duty
11.	KENMOGNE Marguerite	Associate Professor	On duty
12.	KEUMEDJIO Félix	Associate Professor	On duty
13.	KOUAM Jacques	Associate Professor	On duty
14.	MKOUNGA Pierre	Associate Professor	On duty
15.	MVOT AKAK CARINE	Associate Professor	On duty
16.	NGO MBING Joséphine	Associate Professor	*Chief of Cel MINRESI*
17.	NGONO BIKOBO Dominique Serge	Associate Professor	*C.E.A/ MINESUP*
18.	NOTE LOUGBOT Olivier Placide	Associate Professor	*DAAC/Uty Bertoua*
19.	NOUNGOUE TCHAMO Diderot	Associate Professor	On duty
20.	TABOPDA KUATE Turibio	Associate Professor	On duty
21.	TAGATSING FOTSING Maurice	Associate Professor	On duty
22.	TCHOUANKEU Jean-Claude	Associate Professor	*Dean /FS/ UYI*
23.	YANKEP Emmanuel	Associate Professor	On duty
24.	ZONDEGOUMBA Ernestine	Associate Professor	On duty

25.	MESSI Angélique Nicolas	Lecturer	On duty
26.	NGNINTEDO Dominique	Lecturer	On duty
27.	NGOMO Orléans	Lecturer	On duty
28.	NONO NONO Éric Carly	Lecturer	On duty
29.	OUAHOUO WACHE Blandine M.	Lecturer	On duty
30.	OUETE NANTCHOUANG Judith Laure	Lecturer	On duty
31.	SIELINOU TEDJON Valérie	Lecturer	On duty
32.	TCHAMGOUE Joseph	Lecturer	On duty
33.	TSAFFACK Maurice	Lecturer	On duty
34.	TSAMO TONTSA Armelle	Lecturer	On duty
35.	TSEMEUGNE Joseph	Lecturer	On duty

36	MUNVERA MFIFEN Aristide	Assistant Lecturer	On duty
37	NDOGO ETEME Olivier	Assistant Lecturer	On duty

6- DÉPARTEMENT D'INFORMATIQUE (IN) (22)

1.	ATSA ETOUNDI Roger	Professor	*Chief Div.MINESUP*
2.	FOUDA NDJODO Marcel Laurent	Professor	*Inspector Général/ MINESUP*

3.	NDOUNDAM Réné	Associate Professor	On duty
4.	TSOPZE Norbert	Associate Professor	On duty

5	ABESSOLO ALO'O Gislain	Lecturer	*Chief Cell MINFOPRA*
6	AMINOU HALIDOU	Lecturer	Head of department
7	DJAM Xaviera YOUH - KIMBI	Lecturer	On duty
8	DOMGA KOMGUEM Rodrigue	Lecturer	On duty
9	EBELE Serge Alain	Lecturer	On duty
10	HAMZA Adamou	Lecturer	On duty
11	JIOMEKONG AZANZI Fidel	Lecturer	On duty
12	KOUOKAM KOUOKAM E. A.	Lecturer	On duty
13	MELATAGIA YONTA Paulin	Lecturer	On duty
14	MESSI NGUELE Thomas	Lecturer	On duty
15	MONTHE DJIADEU Valery M.	Lecturer	On duty
16	NZEKON NZEKO'O ARMEL JACQUES	Lecturer	On duty
17	OLLE OLLE Daniel Claude Georges Delort	Lecturer	*Vice Director ENSET. Ebolowa*
18	TAPAMO Hyppolite	Lecturer	On duty

19	BAYEM Jacques Narcisse	Assistant Lecturer	On duty
20	EKODECK Stéphane Gaël Raymond	Assistant Lecturer	On duty
21	MAKEMBE. S . Oswald	Assistant Lecturer	*Director CUTI*
22	NKONDOCK. MI. BAHANACK.N.	Assistant Lecturer	On duty

7- DÉPARTEMENT DE MATHÉMATIQUES (MA) (33)

1.	AYISSI Raoult Domingo	Professor	Head of Department

2.	KIANPI Maurice	Associate Professor	On duty
3.	MBANG Joseph	Associate Professor	On duty
4.	MBEHOU Mohamed	Associate Professor	On duty
5.	MBELE BIDIMA Martin Ledoux	Associate Professor	On duty
6.	NOUNDJEU Pierre	Associate Professor	*Chief Service of Programs & Diplomas/FS/UYI*
7.	TAKAM SOH Patrice	Associate Professor	On duty
8.	TCHAPNDA NJABO Sophonie B.	Associate Professor	*Director/AIMS Rwanda*
9.	TCHOUNDJA Edgar Landry	Associate Professor	On duty

10	AGHOUKENG JIOFACK Jean Gérard	Lecturer	*Chief Cell MINEPAT*
11	BOGSO ANTOINE Marie	Lecturer	On duty
12	CHENDJOU Gilbert	Lecturer	On duty
13	DJIADEU NGAHA Michel	Lecturer	On duty
14	DOUANLA YONTA Herman	Lecturer	On duty
15	KIKI Maxime Armand	Lecturer	On duty
16	LOUMNGAM KAMGA Victor	Lecturer	On duty
17	MBAKOP Guy Merlin	Lecturer	On duty
18	MBATAKOU Salomon Joseph	Lecturer	On duty
19	MENGUE MENGUE David Joël	Lecturer	*Head of Department /HS Uty d'Ebolowa*
20	MBIAKOP Hilaire George	Lecturer	On duty
21	NGUEFACK Bernard	Lecturer	On duty
22	NIMPA PEFOUKEU Romain	Lecturer	On duty
23	OGADOA AMASSAYOGA	Lecturer	On duty
24	POLA DOUNDOU Emmanuel	Lecturer	*En stage*
25	TCHEUTIA Daniel Duviol	Lecturer	On duty
26	TETSADJIO TCHILEPECK M. Eric.	Lecturer	On duty

27	BITYE MVONDO Esther Claudine	Assistant Lecturer	On duty
28	FOKAM Jean Marcel	Assistant Lecturer	On duty
29	GUIDZAVAI KOUCHERE Albert	Assistant Lecturer	On duty
30	MANN MANYOMBE Martin Luther	Assistant Lecturer	On duty
31	MEFENZA NOUNTU Thiery	Assistant Lecturer	On duty
32	NYOUMBI DLEUNA Christelle	Assistant Lecturer	On duty
33	TENKEU JEUFACK Yannick Léa	Assistant Lecturer	On duty

8- DÉPARTEMENT DE MICROBIOLOGIE (MIB) (24)

1.	ESSIA NGANG Jean Justin	Professor	*Head of Department*
2.	NYEGUE Maximilienne Ascension	Professor	*VICE-Dean / DSSE*

3.	ASSAM ASSAM Jean Paul	Associate Professor	On duty
4.	BOUGNOM Blaise Pascal	Associate Professor	On duty
5.	BOYOMO ONANA	Associate Professor	On duty
6.	KOUITCHEU MABEKU Epse KOUAM Laure Brigitte	Associate Professor	On duty
7.	RIWOM Sara Honorine	Associate Professor	On duty
8.	NJIKI BIKOÏ Jacky	Associate Professor	On duty
9.	SADO KAMDEM Sylvain Leroy	Associate Professor	On duty

10	ESSONO Damien Marie	Lecturer	On duty
11	LAMYE Glory MOH	Lecturer	On duty
12	MEYIN A EBONG Solange	Lecturer	On duty
13	MONI NDEDI Esther Del Florence	Lecturer	On duty
14	NKOUDOU ZE Nardis	Lecturer	On duty
15	TAMATCHO KWEYANG Blandine Pulchérie	Lecturer	On duty
16	TCHIKOUA Roger	Lecturer	*Chief of education service*
17	TOBOLBAÏ Richard	Lecturer	On duty

18	NKOUE TONG Abraham	Assistant Lecturer	On duty
19	SAKE NGANE Carole Stéphanie	Assistant Lecturer	On duty
20	EZO'O MENGO Fabrice Télésfor	Assistant Lecturer	On duty
21	EHETH Jean Samuel	Assistant Lecturer	On duty
22	MAYI Marie Paule Audrey	Assistant Lecturer	On duty
23	NGOUENAM Romial Joël	Assistant Lecturer	On duty
24	NJAPNDOUNKE Bilkissou	Assistant Lecturer	On duty

9. DEPARTEMENT DE PYSIQUE(PHY) (43)

1.	BEN- BOLIE Germain Hubert	Professor	On duty

2.	DJUIDJE KENMOE épouse ALOYEM	Professor	On duty
3.	EKOBENA FOUDA Henri Paul	Professor	*Vice rector. Uty Ngaoundéré*
4.	ESSIMBI ZOBO Bernard	Professor	On duty
5.	HONA Jacques	Professor	On duty
6.	NANA ENGO Serge Guy	Professor	On duty
7.	NANA NBENDJO Blaise	Professor	On duty
8.	NDJAKA Jean Marie Bienvenu	Professor	*Head of Department*
9.	NJANDJOCK NOUCK Philippe	Professor	On duty
10.	NOUAYOU Robert	Professor	On duty
11.	SAIDOU	Professor	*Chief of center/IRGM/MINRESI*
12.	TABOD Charles TABOD	Professor	*Dean FSUniv/Bda*
13.	TCHAWOUA Clément	Professor	On duty
14.	WOAFO Paul	Professor	On duty
15.	ZEKENG Serge Sylvain	Professor	On duty
16.	BIYA MOTTO Frédéric	Associate Professor	*DG/HYDRO Mekin*
17.	BODO Bertrand	Associate Professor	On duty
18.	ENYEGUE A NYAM épse BELINGA	Associate Professor	On duty
19.	EYEBE FOUDA Jean sire	Associate Professor	On duty
20.	FEWO Serge Ibraïd	Associate Professor	On duty
21.	MBINACK Clément	Associate Professor	On duty
22.	MBONO SAMBA Yves Christian U.	Associate Professor	On duty
23.	MELI'I Joelle Larissa	Associate Professor	On duty
24.	MVOGO ALAIN	Associate Professor	On duty
25.	NDOP Joseph	Associate Professor	On duty
26.	SIEWE SIEWE Martin	Associate Professor	On duty
27.	SIMO Elie	Associate Professor	On duty
28.	VONDOU Derbetini Appolinaire	Associate Professor	On duty
29.	WAKATA née BEYA Annie Sylvie	Associate Professor	*Director/ENS/UYI*
30.	WOULACHE Rosalie Laure	Maître de Conférence	*Intership since february 2023*
31.	ABDOURAHIMI	Lecturer	On duty
32.	AYISSI EYEBE Guy François Valérie	Lecturer	On duty
33.	CHAMANI Roméo	Lecturer	On duty
34.	DJIOTANG TCHOTCHOU Lucie Angennes	Lecturer	On duty
35.	EDONGUE HERVAIS	Lecturer	On duty

x

36.	FOUEJIO David	Lecturer	*Chief Cell. MINADER*
37.	KAMENI NEMATCHOUA Modeste	Lecturer	On duty
38.	LAMARA Maurice	Lecturer	On duty
39.	OTTOU ABE Martin Thierry	Lecturer	Director of reagent production unit /IMPM
40.	TEYOU NGOUPO Ariel	Lecturer	On duty
41.	WANDJI NYAMSI William	Lecturer	On duty
42.	NGA ONGODO Dieudonné	Assistant Lecturer	On duty
43.	SOUFFO TAGUEU Merimé	Assistant Lecturer	On duty

10- DÉPARTEMENT DE SCIENCES DE LA TERRE (ST) (42)

1.	BITOM Dieudonné-Lucien	Professor	*Dean / FASA /UDs*
2.	NDAM NGOUPAYOU Jules-Remy	Professor	On duty
3.	NDJIGUI Paul-Désiré	Professor	*Head of Department*
4.	NGOS III Simon	Professor	On duty
5.	NKOUMBOU Charles	Professor	On duty
6.	NZENTI Jean-Paul	Professor	On duty
7.	ONANA Vincent Laurent	Professor	*Head of Department /Uty. Eb.*
8.	YENE ATANGANA Joseph Q.	Professor	*Chief Div. /MINTP*

9.	ABOSSOLO née ANGUE Monique	Associate Professor	*Vice-Dean / DRC*
10.	BISSO Dieudonné	Associate Professor	On duty
11.	EKOMANE Emile	Associate Professor	*Chief Div./Uty Ebolowa*
12.	Elisé SABABA	Maitre de Conférences	On duty
13.	FUH Calistus Gentry	Associate Professor	*Sec. of State /MINMIDT*
14.	GANNO Sylvestre	Associate Professor	On duty
15.	GHOGOMU Richard TANWI	Associate Professor	*Chief of Div. /Uty Bertoua*
16.	MBIDA YEM	Maitre de Conférences	On duty
17.	MOUNDI Amidou	Associate Professor	*CT/MINIMDT*
18.	NGO BIDJECK Louise Marie	Associate Professor	On duty
19.	NGUEUTCHOUA Gabriel	Associate Professor	*CEA/MINRESI*
20.	NJILAH Isaac KONFOR	Associate Professor	On duty
21.	NYECK Bruno	Associate Professor	On duty
22.	TCHAKOUNTE Jacqueline épse NUMBEM	Associate Professor	*Chief. Cell /MINRESI*
23.	TCHOUANKOUE Jean-Pierre	Associate Professor	On duty
24.	TEMGA Jean Pierre	Associate Professor	On duty
25.	ZO'O ZAME Philémon	Associate Professor	*DG/ART*

26.	ANABA ONANA Achille Basile	Lecturer	On duty
27.	BEKOA Etienne	Lecturer	On duty
28.	ESSONO Jean	Lecturer	On duty
29.	EYONG John TAKEM	Lecturer	On duty
30.	MAMDEM TAMTO Lionelle Estelle, épouse BITOM	Lecturer	On duty
31.	MBESSE Cécile Olive	Lecturer	On duty
32.	METANG Victor	Lecturer	On duty
33.	MINYEM Dieudonné	Lecturer	*Chief Serv./Uty Maroua*
34.	NGO BELNOUN Rose Noël	Lecturer	On duty
35.	NOMO NEGUE Emmanuel	Lecturer	On duty
36.	NTSAMA ATANGANA Jacqueline	Chargée de Cours	On duty
37.	TCHAPTCHET TCHATO De P.	Lecturer	On duty
38.	TEHNA Nathanaël	Lecturer	On duty
39.	FEUMBA Roger	Lecturer	On duty
40.	MBANGA NYOBE Jules	Lecturer	On duty

41.	KOAH NA LEBOGO Serge Parfait	Assistant Lecturer	On duty
42.	NGO'O ZE ARNAUD	Assistant Lecturer	On duty
43.	TENE DJOUKAM Joëlle Flore, épouse KOUANKAP NONO	Assistant Lecturer	On duty

Distribution of permanent lecturers in the faculty of science of University of Yaoundé I

NUMBER OF LECTURERS

DEPARTMENT	Professors	Associate Professors	Lecturers	Assistant Lecturers	Total
BCH	8 (01)	15 (11)	13 (03)	7 (05)	**43 (20)**
BPA	14 (01)	16 (09)	18 (04)	4 (02)	**52 (16)**
BPV	6 (01)	12 (02)	13 (07)	3 (00)	**34 (10)**
CI	7 (01)	15 (04)	5 (01)	1 (00)	**28 (06)**
CO	6 (01)	18 (04)	11 (04)	2 (00)	**37 (09)**
IN	2 (00)	2 (00)	14 (01)	4 (00)	**22 (01)**
MAT	1 (00)	8 (00)	17 (01)	7 (02)	**33 (03)**
MIB	2 (01)	7 (03)	8 (04)	7 (02)	**24 (10)**
PHY	15 (01)	15 (04)	11 (01)	2 (00)	**43 (06)**
ST	8 (00)	17 (03)	15 (04)	3 (01)	**43 (08)**
Total	**69 (07)**	**125 (40)**	**125 (30)**	**40 (12)**	**359 (89)**

	Total of	**359 (89)** then :
-	Professors	**69 (07)**
-	Associate Professors	**125 (40)**
-	Lecturers	**125 (30)**
-	Assistant Lecturers	**40 (12)**

( ) = Number of Ladies **89**

DEDICATION

TO MY MOTHER AND FATHER

ACKNOWLEDGEMENTS

LIST OF CONTENTS

LIST OF FIGURES

LIST OF TABLES

LIST OF SCHEME

INITIALISMS AND ACRONYMS

^{13}C NMR: Carbon-13 Nuclear Magnetic Resonance

1D-NMR: One-dimensional Nuclear Magnetic Resonance

^{1}H NMR: Proton Nuclear Magnetic Resonance

2D-NMR: Two-dimensional Nuclear Magnetic Resonance

4CL: 4-coumaroylcoenzyme A ligase

B. dalzielii: Boswellia dalzielii

C4H: cinnamate 4-hydroxylase

CC: Column Chromatography

CHI: chalcone isomerase

CHR: chalcone reductase

CHS: chalcone synthase

CI: Chemical Ionisation

CoA: Coenzyme A

COSY: Correlation Spectroscopy

d: doublet

DCM: Dichloromethane

dd: doublet of doublet

ddd: doublet of doublet of doublet

DEPT: Distortionless Enhancement by Polarization Transfer

DI: Desorption Ionisation

DMAPP: Dimethylallyl diphosphate

DMSO: Dimethylsulfoxide

dq: doublet of quartet

DRF: dihydroxyflavonol-4-reductase

dt: doublet of triplet

EA: Ethyl Acetate

EI-MS: Electronic Impact Mass Spectrometry

ESI-MS: Electro Spray Ionization Mass Spectrometry

F3H: flavone-3-hydroxylase

FAB: Fast Atom Bombardment

FLS: flavonol synthase

FPP: Farnesyl diphosphate

FS: flavone synthase

GGPP: Geranyl Geranyl diphosphate

GPP: Geranyl diphosphate

Hex: Hexane

HMBC: Heteronuclear Multiple Bond Correlation

HMQC: Heteronuclear Multiple Quantum Coherence

HPLC: High Performance Liquid Chromatography

HR-EIMS: High Resolution Electron Impact Mass Spectrometry

HR-ESIMS: High Resolution ElectroSpray Ionization Mass Spectrometry

HSQC: Heteronuclear Single Quanctum Coherence

Hz: Hertz

IC$_{50}$: Concentration causing 50% inhibition

IFS: isoflavone synthase

IPP: Isopentenyl diphosphate

IR: Infra Red

IRF: isoflavone reductase

J (Hz): Coupling constant (NMR) in Hertz

m: Multiplet

MHz: Megahertz

MIC: Minimal inhibitory concentration

MS: Mass spectroscopy

NMR: Nuclear Magnetic Resonance

NOESY: Nuclear Overhauser Enhanced Spectroscopy

OSCs: oxidosqualene cyclases

PAL: phenylalanine ammonialyse

PCR: polymerase chain reaction

PG: peptidoglycan

ppm: Part per million

PTLC: Preparative thin layer chromatography

q: Quadruplet

RDA: Retro Diels-Alder

ROESY: Rotating frame Overhausser enhancement spectroscopy

s: Singlet

t: Triplet
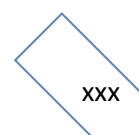
TLC: Thin layer chromatography

TOCSY: Total Correlated Spectroscopy

UV: Ultraviolet

VLC: Vacuum Liquid Chromatograpghy

WHO: World Health Organization

*δ***(ppm**): Chemical shift in parts per million

ABSTRACT

The stem bark and branches of *Boswellia dalzielii* (Burceraceae) are used in traditional medicine in the Northern part of Cameroon for the treatment of gonorrhea, syphilis and diarrhea. This plant was selected to search for bioactive constituents. The bioguided fractionation of the MeOH-CH$_2$Cl$_2$ (1:1, v/v) extract from the stem bark and branches of *Boswellia dalzielii* followed by subsequent isolation of compounds were performed using normal phase open column chromatographies. The broth microdilution method was used to evaluate the antibacterial activity of the crude extract, fractions and compounds against several bacterial strains. The crude extract of the stem bark of *Boswellia dalzielii* exhibited moderate antibacterial activity against *Staphylococcus aureus*, *Enterobacter cloacae*, *Streptococcus pneumoniae* ATCC491619 with MIC of 250 µL/mL whereas, hexane-ethyl acetate (7:3, v/v) and hexane-ethyl acetate (1:1, v/v) fractions showed significant activities against *Staphylococcus aureus, Salmonella typhi, Enterobacter cloacae, Streptococcus pneumonia* ATCC491619, *Pseudomonia aeruginosa* HM801 with MIC of 7.8 µg/mL. Actives fractions Hex-EtOAc (7:3, v/v) (39.6 g) and Hex-EtOAc (1:1, v/v) (11 g), were then subjected to separations and purifications by column chromatography, this led to isolation of six compounds (α-boswellic acid (**59**), β-boswellic acid (**17**), Acetyl-11-keto-β-boswellic acid (**20**), 3-*O*-acetyl-28-hydroxylupeolic acid (**63**), angolensin (**72**), and betulinic acid (**62**) whose chemical structures were identified based on mass and NMR spectral data. The isolated compounds were also evaluated for antimicrobial activity using the same method as extract and fractions. Four of these compounds were the most active against *S. typhi, E. cloacae, S. pneumoniae* ATCC491619, *E. coli* ATCC25322, *P. aeruginosa* HM801 with an MIC value of 3.125 *µg*/mL, these compounds are α-boswellic acid (**59**), β-boswellic acid (**17**), Acetyl-11-keto-β-boswellic acid (**20**), 3-*O*-acetyl-28-hydroxylupeolic acid (**63**). Non-active fractions of stem bark and branches were also subjected to chromatographic separations to give twenty-two compounds including **three steroids**: β-Sitosterol and stigmasterol (**66**) and (**65**), β-sitosterol-3-*O*-β-D-glucopyranoside (**67**), **nine triterpenes**: friedelin (**56**), 3α-acetyl-β-boswellic acid (**19**), lupeol (**25**), α-amyrin (**26**), β-amyrin (**58**), β-amyrin acetate (**60**), lupenone (**22**), 3α-acetyl-α-boswellic acid (**61**), Urs-12-ene-3α,24β-diol (**57**), **one tirucalan**: lanosta-7,24-dien-3-one (**64**), **four flavonoids:** 4',5-dihydroxy-7-methoxyflavanone (**68**), 5,4′-Dihydroxy-7-(γ,γ dimethylallyloxy)dihydroflavonol (**70**), Soforaflavanone B (**69**), 3-Acetoxy-4',5-dihydroxy-7-methoxyflavanone (**71**), **five phenolic compounds:** 4-methoxy-2-*O*-α-D-glucopyranosylphenyl methanol (**75**), desoxyrhapontigenin-3-*O*-rutinoside (**76**), aurantiamide

acetate **(77)** 7-(3,4-Dihydroxyphenyl)-1-(4-hydroxyphenyl)-3-heptanol (**73**) with **one new derivative** namely dalzienoside (**74**); these compounds were also tested on the same strains, only three of these compounds like 4',5-dihydroxy-7-methoxyflavanone (**68**), soforaflavanone B (**69**) 5,4′ dihydroxy-7-(γ,γ-dimethylallyloxy)dihydroflavonol (**70**) exhibited moderate antibacterial activities against *S. aureus, S. typhi, P. aeruginosa* HM801, *k. pneumoniae* NR41388, *k. pneumoniae*, with MICs ranging from 7.8 to 62.5 μg/mL. Totally twenty-eight compounds were isolated from the extract of stem bark and branches, one of these compounds namely dalzienoside (**74**) was characterized for the first time and eight compounds such as 4',5-Dihydroxy-7-methoxyflavanone (**68**), Soforaflavanone B (**69**) , 3-acetoxy-4',5-dihydroxy-7-methoxyflavanone (**71**), 5,4′ Dihydroxy-7-(γ,γ-dimethylallyloxy)dihydroflavonol (**70**), Angolensin (**72**), Aurantiamide acetate (**77**), 7-(3,4 Dihydroxyphenyl)-1-(4-hydroxyphenyl)-3(R)-heptanol (**73**), 4-methoxy-2-O-α-D glucopyranosylphenyl methanol (**75**) are herein reported for the first time from the genus *Boswellia* which may be of chemotaxonomic significance. The structures of these compounds were established by comprehensive 1D and 2D NMR spectroscopy, MS, and by comparison with literature data. In order to formulate the phytodrugs, the acute toxicity was also done. This study was performed according to the protocol of the OECD (2001) of the guideline 423 using 9 adult female rats and not pregnant. No clinical signs of toxicity were observed either on the behavior, or on the body weight of the animals, or on the weight of the organs after administration of the test substance and during the 14 days of experimentation. Thus, according to the globally harmonized classification system (SCGH), the aqueous extract of *B. dalzielii* can be classified in category 5 of non-toxic substances because of its harmlessness. Finaly pre-formulation of syrup for children was done.

Keywords: *Boswellia dalzielii*, dalzienoside, boswellic acid, chemotaxonomy, antibacterial.

RESUME

Les écorces du tronc et les branches de *Boswellia dalzielii* (Burceraceae) sont utilisées en médecine traditionnelle dans la partie septemtrionale du Cameroun pour le traitement de la gonorrhée, la syphilis et de la diarrhée. C'est ainsi que cette plante a été sélectionnée pour rechercher ses constituants bioactifs. Un fractionnement bioguidé de l'extrait CH_2Cl_2-MeOH (1 :1, v/v) de l'écorce du tronc et des branches de *Boswellia dalzielii* suivi de l'isolement des composés a été réalisé en utilisant une chromatographie sur colonne de gel de silice ouverte en phase normale. La méthode de microdilution a été utilisée pour évaluer l'activité antibactérienne de l'extrait brut, des fractions et des composés contre plusieurs souches bactériennes. L'extrait brut de l'écorce du tronc de *Boswellia dalzielii* a présenté une activité antibactérienne modérée contre *Staphylococcus aureus, Enterobacter cloacae, Streptococcus pneumoniae* ATCC491619 avec une CMI de 250 μL/mL alors que les fractions à l'hexane-acétate d'éthyle (7 :3, v/v) et l'hexane-acétate d'éthyle (1 :1, v/v) ont montré des activités significatives contre *Staphylococcus aureus, Salmonella typhi, Enterobacter cloacae, Streptococcus pneumoniae* ATCC491619*, Pseudomonia aeruginosa* HM801 avec une CMI de 7,8 μg/mL. Les fractions actives tels que la fraction à l'Hexane-acétate d'éthyle (7 :3, v/v) (39.6 g) et la fraction à l'Hexane-acétate d'éthyle (1 :1, v/v) (11 g) ont subit une separation et purification sur colonne chromatographique de gel de silice et de sephadex LH-20 pour donner six composés donc les structures ont été élucidés par la méthode spectroscopique RMN 1D et 2D, SM et par comparaison avec les données de la littérature. Ces composés ont été testés sur les mêmes souches et ont montré une activité significative contre *Salmonella typhi, Enterobacter cloacae, Streptococcus pneumoniae* ATCC491619*, Escherichia coli* ATCC25322*, Pseudomonas aeruginosa* HM801 avec une CMI allant 3,125 à 7,8 μg/mL il s'agit de : acide α-boswellique (**59**), acide β-boswellique (**17**), acide acetyl-11-keto-β-boswellique (**20**), acide 3-*O*-acetyl-28-hydroxylupeolique (**63**). Les fractions non actives des écorces du tronc et des branches de *Boswellia dalzielii* ont aussi subit une séparation sur colonne de gel de silice et de séphadex LH-20 pour conduire à 22 composés à savoir : **trois steroids**: β-Sitosterol et stigmasterol (**66**) et (**65**), β-sitosterol-3-*O*-β-*D*-glucopyranoside (**67**), **neuf triterpenes**: friedelin (**56**), 3α-acetyl-β-boswellic acid (**19**), lupeol (**25**), α-amyrin (**26**), β-amyrin (**58**), β-amyrin acetate (**60**), lupenone (**22**), 3α-acetyl-α-boswellic acid (**61**), Urs-12-ene-3α,24β-diol (**57**), **un tirucalan**: lanosta-7,24-dien-3-one (**64**), **quatre flavonoids:** 4',5-dihydroxy-7-methoxyflavanone (**68**), 5,4′-Dihydroxy-7-(γ,γ dimethylallyloxy)dihydroflavonol (**70**), Soforaflavanone B (**69**), 3-Acetoxy-4',5-dihydroxy-7-methoxyflavanone (**71**), **cinq composés phenoliques:** 4-methoxy-

2-*O*-*α*-*D*-glucopyranosylphenyl methanol **(75)**, desoxyrhapontigenin-3-*O*-rutinoside **(76)**, aurantiamide acetate **(77),** 7-(3,4-Dihydroxyphenyl)-1-(4-hydroxyphenyl)-3-heptanol **(73**), parmi lesquels **un dérivé nouveau** appelé dalzienoside **(74**). Ces composés ont également subi des tests antibacteriens sur les mêmes souches précédentes, seulement trois de ces composés à savoir la 4',5-dihydroxy-7-methoxyflavanone **(68)**, soforaflavanone B **(69)**, 5,4′ dihydroxy-7-(γ,γ dimethylallyloxy) dihydroflavonol **(70)** ont présenté une activité antibactérienne modérée avec une CMI comprise entre 7,8 et 62,5 μg/mL. En somme 28 composés ont été isolés des écorces du tronc et des branches de *Boswellia dalzielii* parmi lesquels un dérivé nouveau le dalzienoside **(74)** isolé et charactérisé pour la première fois et 8 composés à l'instar de 4',5-dihydroxy-7-methoxyflavanone **(68)**, soforaflavanone B **(69)**, 3-acetoxy-4',5-dihydroxy-7-methoxyflavanone **(71)**, 5,4′ dihydroxy-7-(γ,γ-dimethylallyloxy)dihydroflavonol **(70)**, 7-(3,4 dihydroxyphenyl)-1-(4-hydroxyphenyl)-3-heptanol **(73)**, 4-methoxy-2-*O*-*α*-*D* glucopyranosylphenyl methanol **(75)**, angolensin **(72)**, acetate d'aurantiamide **(77)**, isolés pour la première fois du genre *Boswellia* ce qui contribue à la chimiotaxonomie de ce genre. Les structures de ces composés ont été élucidées par la méthode spectroscopique RMN 1D, 2D, SM et par comparaison avec les données de la littérature. Afin de formuler un phytomédicament, la toxicité aiguë a été également faite. Cette étude a été réalisée selon le protocole de l'OCDE (2001), de la directive 423 sur 9 rats femelles adultes et non gravides. Ainsi aucun signe clinique de toxicité n'a été observé ni sur le comportement, ni sur le poids corporel des animaux, ni sur le poids des organes après administration de la substance d'essai et pendant les 14 jours d'expérimentation. De ce resultat, selon le système de classification globalement harmonisé (SCGH), l'extrait aqueux de *B. dalzielii* peut être classé dans la catégorie 5 des substances non toxiques en raison de son innocuité. Enfin, une pré-formulation de sirops pour enfants a été réalisée.

Mots-clés : *Boswellia dalzielii*, dalzienoside, boswellic acid, chimiotaxonomie, antibactérien

INTRODUCTION

For several years, people around the world have used element of their environment especially plants to treat several diseases. Microbial diseases are a serious public health problem in Africa. Although a significant number of synthesised drugs exist around the world for the treatment of microbial diseases in modern medicine, in most African countries, poverty has encouraged many communities to focus on herbal medicine (Timo et al. 2013; Gera et al. 2015). While in developed countries, populations are especially concerned about over-prescribing drugs such as anti-inflammatory drugs and antibiotics. This results in the emergence of multi-resistant strains, so many are increasingly practicing herbal self-medication (Eisenberg et al., 1993). Plants are little exploited when we consider the high percentage of plant species not yet studied either for their chemical composition or for their pharmacological properties. The pharmacological and phytochemical studies of plants used in traditional medicine could lead not only to the discovery of new antimicrobial compounds, but also to the valorisation of local plant species through the investigation on their efficacy and safety.

In fact, in the current health context, there is a continuing need for new molecules to treat many pathologies, including bacterial and fungal infections. Plants are known to possess several antimicrobial compounds and are used in all traditional medicine. Many crude preparations of "herbal drugs'' are in clinical use in medical and veterinary practice. Laboratories of the world have found literally thousands of phytodrugs which have inhibitory effects on all types of microorganisms. Many of these compounds are being subjected to animal and human studies to determine their potential to restrict growth / multiplication of pathogenic organisms as well as examination of their effects on beneficial normal micro biotech.

Plants are rich in a wide variety of secondary metabolites such as tannins, terpenoids, alkaloids, and flavonoids which have been found to have antimicrobial properties. Antimicrobials such as lichochalcones (Demizu et al., 1988; Fukui et al., 1988) benzoin and emetine (Cox, 1994) have been isolated from plants and 2 to 3 new antibiotics are introduced to the market every year (Ebimieowei and Ibemologi, 2016). However, microorganisms develop resistance against antibiotics, the cause for antibiotic resistance is overuse, misuse and indiscriminate use of antimicrobials by population.

In establishing new herbal medicines, the use of ethnopharmacological data is important. The bioguided fractionation of plant extracts according to their traditional uses can often be the basis for the discovery of new active ingredients.

In this study, a bioassay-guided approach was undertaken to further identify constituents which may contribute to the antimicrobial activity of *Boswellia dalzielii*. This plant was chosen on the basis of its use in traditional medicine. In fact, ethnobotanical studies have revealed that this plant is used in traditional medicine to treat several diseases such as dysentery, venereal disease, hemorrhoids.

The aim of this work was to search for active and non toxic extracts fractions and compounds and subsequently to preformulate a phytodrug against bacterial diseases

The specific objectives were to:

- evaluate the antibacterial activity of extracts, fractions and compounds

- characterise isolated compounds

- Evaluate the toxicity of the active extracts or fractions

- preformulate a phytodrug

This thesis includes chapters focused on literature review, the results with structure elucidation of isolated compounds, hemi-synthesized compounds and biological tests.

CHAPTER 1 : LITERATURE REVIEW

1.1. Botanical aspects

1.1.1. General information on the family Burseraceae

Burseraceae is a pantropical family of some 700 species in 19 genera (**Doyle and Hotton, 1991; Ii, 2003**). This family includes many shrubs and trees that are distributed throughout Africa, the Middle East, the Indian subcontinent and the Americas. This family has three subtribes, Bursereae (Burserinae and Boswelliinae), Canarieae and Protieae (**Group, 2009**). This family has been considered as a sister group of the Anacardiaceae (**Gadek *et al*., 1996; Weeks *et al*. 2005**). In Protieae, *Protium* consists of approximately 147 species; *Commiphora* has approximately 200 species in the Bursereae tribe and *Canarium* comprises 75 species in the tribe Canarieae (**Group, 2009**). The Canarieae plus Boswelliinae clade may have evolved from a Southeast Asian ancestor (**Gadek *et al*. 1996**). However, the basal species of this clade (*Boswellia*, *Garuga*, *and Triomma*) are African, Indian or Southeast Asian in distribution (**Gadek *et al*., 1996**). The Bursereae comprises *Bursera*, *Commiphora*, *Aucoumea*, *Beiselia*, *Boswellia*, *Triomma*, *Garuga*, *Ambilobea*, *Canarium*, *Dacryodes*, *Haplolobus*, *Pseudodacryodes*, *Rossellia*, *Santiria*, *Scutinanthe*, *Trattinnickia*, *Crepidospermum*, *Protium* and *Tetragastris* (**De-Nova *et al*., 2012; Lawrence, 1951**).

In Cameroon, the most widespread genera are *Commiphora, Canarium, Dacryodes and Boswellia* (**Onana, 2018**) which is the subject of our study.

1.1.2. General information on the genus *Boswellia*

Boswellia plants also called frankincense trees are deciduous plants known to grow on rocky terrains, solid rocks and gravel soils. The tree reaches 2–8 m in height. Normally, it branches are close to the ground, giving the appearance of multi trunks, each up to 25 cm in diameter. Its bark is easily peeled off and can be stripped in long sheets that were once used for writing. (**Coder, 2011; Hepper, 1969; Vaishnav and Janghel 2019**). The leaves are imparipinnate, mostly congested at the end of the branches, but some of the smaller leaves are glabrous in nature. All species are without thorns; they are shrubby, small-to-medium trees, and the external bark is exfoliated and the flowers are five-lobed and have five petals, with internal stamens that are disk-shaped in the centre (**Eslamieh, 2010**). The fruits and seeds are similar to capsules, and the outer layer of three-to-five-winged pyrenes falls at maturity. These plant species can selfpollinate and are bisexual. (**Thulin and Warfa, 1987**)

The genus *Boswellia* has around 25 species distributed worldwide (**Emmanuel *et al.*, 2015**) among which *Boswellia serrata, Boswellia carterii* and *Boswellia dalzielii* on which our study was focused.

1.1.3. Geographic distribution of the genus *Boswellia*

Boswellia is a genus from the Burserae tribe, it has several species distributed in the Middle East, South Asia and more specifically in African countries such as Cameroon, Somalia, Kenya, Ethiopia and Nigeria. In Cameroon, the genus *Boswellia* is found in the shrub and wooded savannas of Adamawa, the North and the Far North (**Onana, 2018**).

1.1.4. General information on *Boswellia dalzielii* Hutch

Boswellia dalzielii Hutch is a common deciduous tree in the wooded savanna growing up to 12m high, it is mostly called the "Frankincense tree*"* (**Younoussa *et al*., 2014**) (**Fig**. 1A). Its stem bark is pale brown and smooth, peeling off in thin ragged papery patches, the slash is reddish brown, exuding a whitish fragrant resin. (**Fig**. 1D). The trunk is yellow or grey with exfoliation. The leaves are arranged in alternate and imparipinnate ways. The leaves are glabrous green and approximately 20–45 cm long (**Fig**. 1B). Small white flowers may appear, while the tree is leafless, and they are fragrant (**Fig**. 1C). (**Burkill, 1985**). This species ranges from the Northern Ivory Coast to Nigeria and into Cameroun and Ubangi-Shari (**Eslamieh, 2010**).

A   **B**

| C | D |

Figure 1:tree (A), leaves (B), flowers (C) and stem bark (D) of *Boswellia dalzielii*

Pictures source A and B: **personnal source**; C and D **(Decarlo *et al*, 2019)**

1.1.5. Systematic position of *Boswellia dalzielii*

The systematic position of the *Boswellia dalzielii* species is given in Table 1.

Table 1: Systematic position of *Boswellia dalzielii*

Kingdom	Plantae
Sub-kingdom	Tracheobionta
Division	Magnoliophyta
Class	Magnoliopsida
Subclass	Rosidae
Order	Sapindales
Family	Burseraceae
Genus	*Boswellia*
Specie	*Boswellia dalzielii*

1.2. Geographical distribution of *Boswellia dalzielii*

The *Boswellia dalzielii* species is abundantly found in wooded savannas in East Africa in countries such as Ghana, Côte d'Ivoire, Central African Republic, Cameroon, Burkina Faso and northern Nigeria **(Uzama *et al.*, 2015)**. In Cameroon, this species is found in Adamawa, North and the Far North **(Kémeuzé *et al.*, 2012)**. **Figure 3** provides an overview of its distribution in West and Central Africa **(Decarlo *et al.*, 2019)**

● **areas where *Boswellia dalzielii* plants are found in the world**

Figure 2: Distribution in West and Central Africa of the *Boswellia dalzielii* (red circles) (Decarlo *et al.*, 2019)

In Cameroon, the harvest locations of *Boswellia dalzielii* are shown in Table 2.

Table 2: Harvest locations of *Boswellia dalzielii* in Northern Cameroon (Available at the National Herbarium of Cameroon).

Collection location	Collection station
Maroua	Maroua
Tinguelin	Tingueling
Gashiga	Gashiga
Mokolo	Mogodé-Mokolo road.
Dourbey	Dourbey.
Garoua	20 km au SSE de Garoua.
Dembo	Dembo
Sanguere	Sanguéré paul, 10 km S. Garoua.
Sanguere	Sangueré paul, 10 km S. garoua.
Sanguere	Sanguéré Paul, 10 km S Garoua.
Guidder	Mayo Sangonaré 17 km N. Guider.
Guidder	Marma près de Mousgay. 24 km N. Guider.
Guidder	Mayo Sangonaré 17 km N. Guider.
Guidder	Marma près de Mousgay. 24 km N. Guider.
Gashiga	Gashiga
Tinguelin	Tinguelin.
Hosere Vaimba	Route vaimba Béré, 50 km N. de Vaimbé
Bibeme	Route bere Bibeme

Plants of the genus *Boswellia* is widely used around the world and particularly in traditional medicine.

1.3. Some uses of plants of the genus *boswellia*

The plants of the genus *Boswellia* are exploited by populations for many purposes and on different planes: food, industrial, medical.

1.3.1. Plants of the genus *Boswellia* as food

One of the oldest species in the genus *Boswellia* and most valued in Ayurveda is *Boswellia serrata*. The term "Gajabhakshya" was sometimes used to refer to this plant, literally ("favorite

food of elephants"), because it was part of the diet of these mammals **(Perotto, 2013)**. The leaves of *Boswellia dalzielii* serve as flavour for some traditional drinks **(Kémeuzé *et al.*, 2012)**.

1.3.2. Domestic and industrial uses of plants of the genus *Boswellia*

In domestic use, the bark of *Boswellia dalzielii* contains a whitish exudate (secreting a scent) which is burned to fumigate clothing and is also used as an insect repellent to drive away house flies and mosquitoes **(Uzama *et al.*, 2015)**. *Boswellia serrata* gum resin was used for a long time, as was *Boswellia dalzielii* for domestic purposes, notably for disinfecting linen, hair and homes. When mixed with acacia gum, the resin from the Indian frankincense helped correct foul breath and mixed with an oily solution and applied regularly to the scalp, it helped stimulate hair growth **(Delfaut, 2018)**. Species of the genus *Boswellia* produce an aromatic resin known as real frankincense, which is incorporated into various health, care, aromatherapy, cosmetic and hygiene products, as well as food supplements.

In Kenya, *Boswellia neglecta* smoke is considered a repellent for snakes and flies **(Hay *et al.*, 2019)**.

In northern Cameroon, the leaves of *Boswellia dalzielii* are used to protect maize, millet and sorghum against Weevil attacks **(Younoussa *et al.*, 2016)**. The powder of the dried bark is used in granaries to protect the foodstuffs stored by maffa women in the far North of Cameroon **(Kémeuzé *et al.*, 2012)**.

In India, wood pulp of these species is used for paper and wood is considered a good fuel and valued coal in the smelting of iron. In India and Ethiopia, *Boswellia* wood is also used for fencing, farm implements, inexpensive furniture, packing cases, matches, plywood and veneers.

In some parts of Africa, gum and resin can be used as adhesives, dyes and lithographic inks **(Hay *et al.*, 2019)**.

In Cameroon in particular and precisely in the far North, the yellowish white, soft and medium-hard wood of *Boswellia dalzielii*, is used as matchbox wood, veneer, plywood, parquet, tool handles, framing and as firewood. The trunk is used in the same region by the Tupuri and Mundang peoples to make mortars and pestles **(Kémeuzé *et al.*, 2012)**

1.3.3. Therapeutic uses of plants of *Boswellia*

There is also a long history of using species of the genus *Boswellia* in Ayurvedic medicine (traditional Indian medicine), Urania and Chinese. The resin which is characteristic of these

species, has long been used as incense during religious ceremonies around the world (**Hay *et al*., 2019**).

In West Africa, the bark of the trunk of *Boswellia dalzielii* is the most used in pharmacopoeia. It represents 80% of the harvest and is commercially exploited (**Ouedraogo *et al.*, 2006**). Its decoction is drunk against dysentery, hemorrhoids and angina. Dried and then crushed, the bark is used in combination with other plants to treat malaria, yellow fever, stomach aches and many childhood illnesses (**Kémeuzé *et al*., 2012**). The gum resin obtained from *Boswellia dalzielii* is used with other products as a gastric medicine to increase appetite, aid digestion and is also used as a treatment for venereal diseases. Combined with *Steganotaenia aralicia*, this resin has anti-inflammatory activity. The roots and bark of the same plant are used as an antidote for arrow poisons; the fresh bark is eaten to induce vomiting and so relieve symptoms of dizziness and palpitations. The leaf extract is used for the treatment of diarrhea in poultry and humans (**Emmanuel et al., 2015**). The decoction of bark heals boils (**Gormo *et al*., 2013**). A decoction of the roots with *Hibiscus sabdariffa* is used for the treatment of syphilis and a decoction of the roots with *Daniella oliveri* is used for the healing of wounds (**Aliyu *et al.*, 2007**).

In Nigeria, the young leaves of *Boswellia dalzielii* are picked, crushed in water and the pressed liquid is collected and given orally to poultry against diarrhea (**Nwude and Ibrahim, 1980**). In the northern part of the same country, a bark decoction is used as a wash against fever and rheumatism when used in large quantities (**Nazifi *et al*, 2017**). In Côte d'Ivoire the same decoction is used as an antiseptic wash for wounds (**Uzama et al., 2015**).

In Cameroon a mixture of the roots and the bark has been used to treat snakebites and poisoning (**Nacoulma-Ouédraogo, 1996).**

Clinically and therapeutically, *Boswellia serrata* resin is described as having diaphoretic and astringent properties. Traditional Indian medicine also attributed stimulating properties (internally and externally), expectorant, diuretic, stomachic and mild depurative of the liver. It is written that this substance was used to treat respiratory ailments (asthma, bronchorrhea, chronic laryngitis) internally or in fumigation, abdominal (digestive, gynecological and urinary) disorders such as ulcers, diarrhea, dyspepsia, spasms, hemorrhoids, urinary tract infections, dysmenorrhea or jaundice (not dependent on mechanical obstruction); nervous disorders; rheumatic conditions, inflammatory disorders and bone and joint pain. The gum oleoresin was also used in the preparation of ointments (in mixture with coconut oil in particular) to treat wounds, abscesses or ringworm. It was prescribed mixed with clarified butter to treat syphilis.

It was used over long periods and in high doses (one drachma per day) to reduce obesity as well as to treat scorpion bites and snake bites **(Delfaut, 2018)**. The bark of *Boswellia odorata* treats diarrhea and dysentery by maceration **(Baggnian *et al*., 2018)**.

1.4. previous chemical and biological work on plants of the genus *boswellia*

1.4.1. Previous chemical work on the genus *Boswellia*
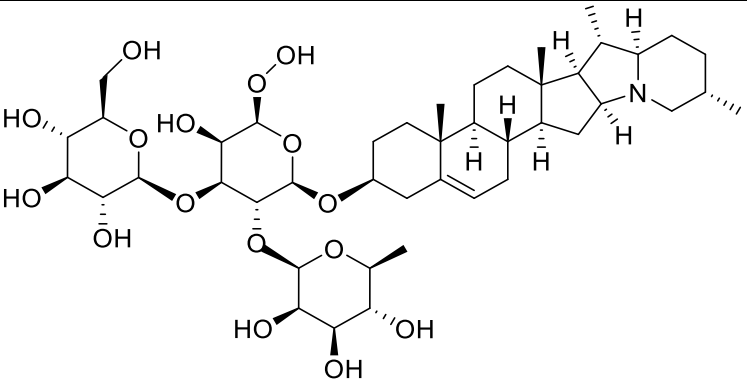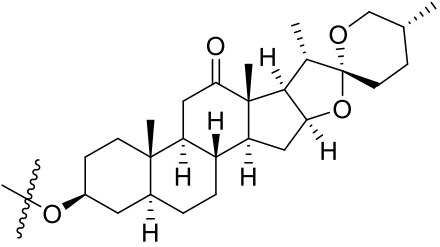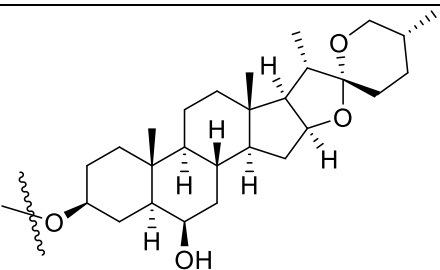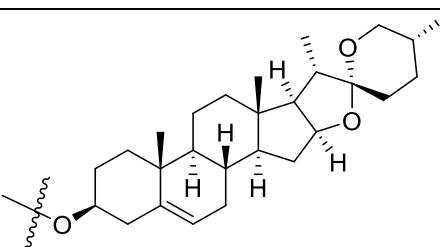
Work carried out on the species of the genus *Boswellia* showed that they contain secondary metabolites belonging to the following class: terpenoids such as: triterpenes **(Qurishi *et al*., 2010)**, diterpenes **(Alemika *et al*., 2004)**, monoterpenes, sesquiterpenes **(Sarada *et al*., 2016)**; but also tannins, saponins, steroids, flavonoids, alkaloids **(Mbiantcha *et al*., 2017)** and coumarins **(Subhashini *et al*., 2014)**. Furthermore, other studies carried out on the genus *Boswellia* have led to the isolation and characterization of secondary metabolites belonging mainly to the class of triterpenes **(Verhoff *et al*., 2014)**, steroids and their glycosides.

1.4.1.1. The identified saponins of the genus *Boswellia*

The name saponin derives from the Latin word "sapo", which means soap, because these compounds foam when stirred with water. They are made up of non-polar aglycones linked to one or more sugars. This combination of polar and non-polar structural elements in their molecules explains their foaming behaviour in aqueous solution. As a definition, it looks like a saponin is a steroid or triterpene glycoside. Thus, a fundamental distinction is made, the steroidal saponins and the triterpene saponins both derived biosynthetically from oxydosqualene **(Kone, 2009)**. Saponins are compounds used to defend the plant. Many reviews report that they exist in plants in biologically active form and are involved in antimicrobial phytoprotection. Saponins attract attention as well for their industrial exploitation in connection with their pharmacological properties. Several plants with saponins are used by the pharmaceutical industry to obtain galenical forms, others have applications in phototherapy. Saponins also find many applications in the food and cosmetic industries due to their foaming and emulsifying properties. The applications of saponins extend to agriculture, with use for soil remediation and natural pesticides **(Manase, 2013)**.

The identified saponins of the genus *Boswellia* are listed in Table 3:

Table 3: Some identified saponins of the genus *Boswellia*

Sources	Names	Structures	References
Leaves of *B. dalzielii*	α-solanine (**1**)		Onobrudu, 2017
	hecogenine (**2**)		
	neochlorogenine (**3**)		
	diosgenine (**4**)		

1.4.1.2. Isolated steroids of the genus *Boswellia*

Steroids are compounds that contain the perhydrocyclopentenophenanthrene nucleus. They include a wide variety of natural compounds, including bile acids, sex hormones, adrenocortical hormones, cardiotonic glucosides, some alkaloids, and other minor groups.
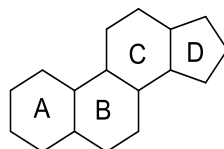
(5)

Perhydrocyclopentenophenanthrene

Steroids are distributed in the plant and animal kingdom, and formed by biosynthesis of terpene origin. The first of these compounds was isolated around 1770, from gallstones, by Poulletier de la Salle, then also found, in 1815, in animal fats, by M.E. Chevreul. It was named ≪ cholestérine ≫ (from the Greek kholé = bile and stereos = solid) in memory of the source where it was originally discovered. In 1859, M. berthelot, taking into consideration the alcohol function, changed the name to cholesterol (**Ayad, 2008**). Plant sterols are botanical analogues of cholesterol that differ from it only in their side chain. However, they are not without therapeutic potential; phytosterols like phytostanols inhibit the absorption of cholesterol by complex mechanisms, phytostanols more than phytosterols, indeed β-sitosterol has been known as cholesterol-lowering agent since 1951. We can also cite that plant sterols are raw materials in the production of therapeutic steroids, this latter role has been performed in the processes involved in the field of biotransformation alone, or biotransformations coupled with conventional chemical transformations (**Bruneton 1993**). In addition to β-sitosterol, other steroids have been isolated from the genus *Boswellia*. (Table 4)

Table 4: Some steroids isolated from the genus *Boswellia*

Sources	Names	Structures	References
Stem bark *B. serrata*	cholesterol **(6)**		**Hanaa et al, 2015**
	stigmasterol **(7)**		
	β-sitosterol **(8)**		
Stem bark *B. carterii*	sitost-4-en-3-one **(9)**		**Sarata et al, 2016**

1.4.1.3. The isolated terpenoids of the genus *Boswellia*
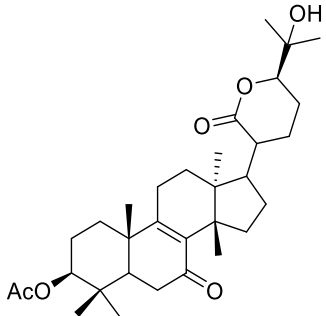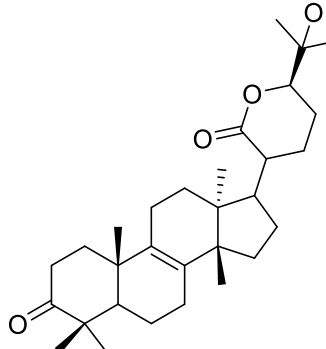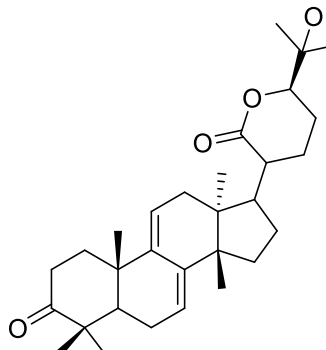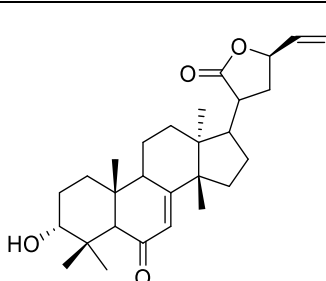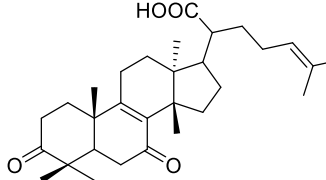
Terpenoids, also known as isoprenoids, are the most numerous and structurally diverse natural products. The generic name "terpene" was originally applied to the hydrocarbons found in turpentine, the suffix "ene" indicating the presence of olefinic bonds. Terpenoids are classified based on the number and structural organization of carbons formed by the linear arrangement of isoprene units followed by cyclization and rearrangements of the carbon
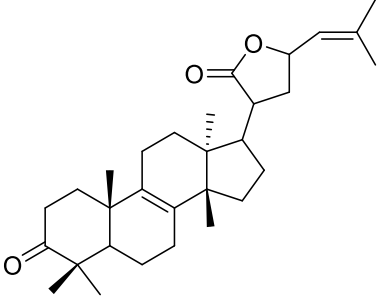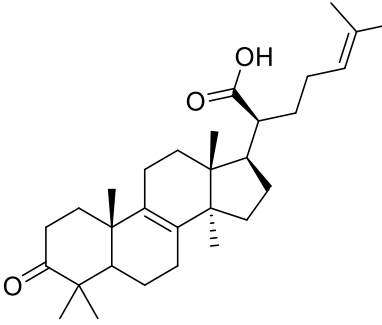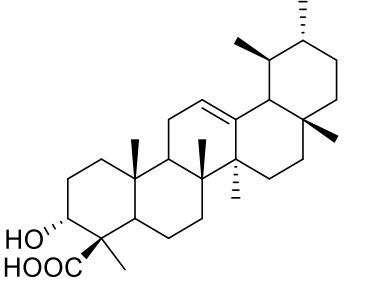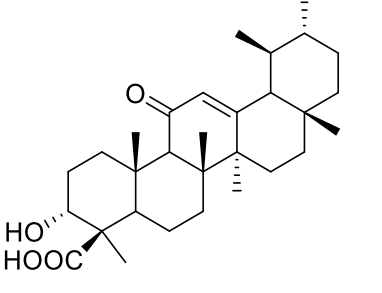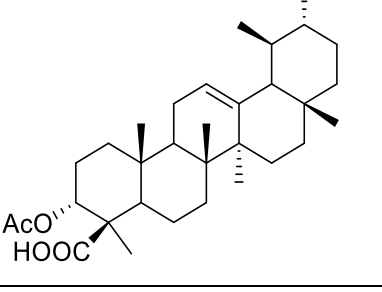
skeleton with an empirical feature known as the isoprene rule. Isoprene, the "building block" of terpenoids, is 2-methylbuta-1,3-diene (C_5H_8). The single isoprene unit, therefore, represents the most basic class of terpenoids and hemiterpenoids. The so-called isoprene rule states that all terpenoids are derived from the ordered, head-to-tail joining of isoprene units. A head-to-tail fusion is the most common; however, non-head-to-tail condensation of isoprene units also occurs. Head-to-head fusions are common among triterpenoids and carotenoids, while some compounds are formed by head-to- middle fusions e.g., irregular monoterpenoids (**Connolly et al., 1991**).
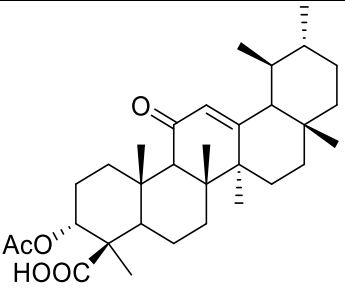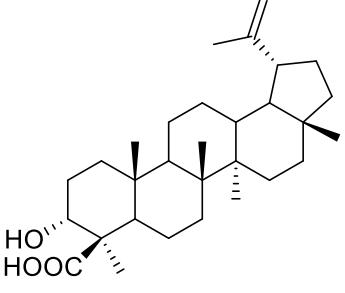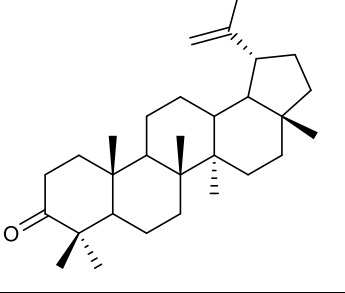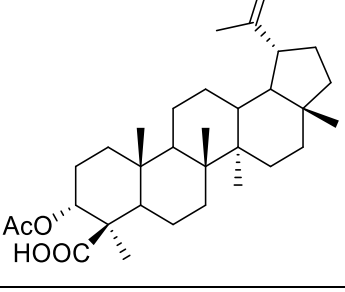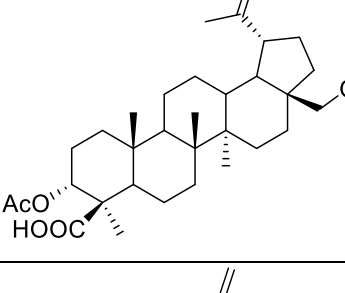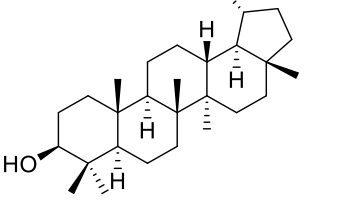
1.4.1.3.1. Some terpenoids isolated from genus *Boswellia*
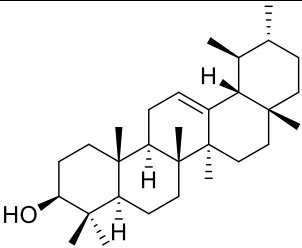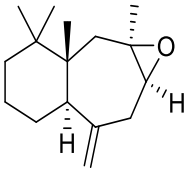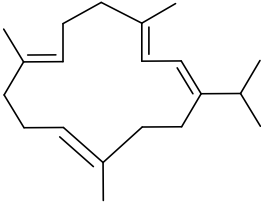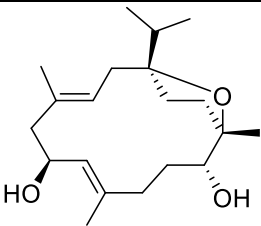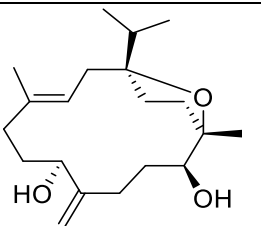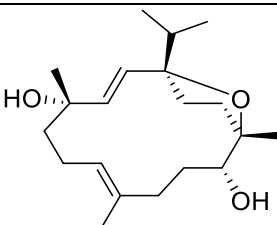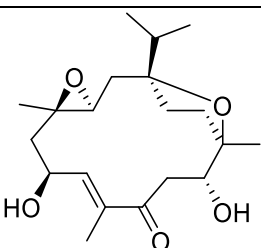
The isolation of terpenoides from plants is based on extraction with organic solvents such as methanol, chloroform, ethyl acetate and ethyl ether. The terpenoids previously isolated from genus *Boswellia* are mostly pentacyclic triterpenes. Pentacyclic triterpenes constitute about twenty structurals groups. **Table 5** contain some terpenoids previously isolated from the genus *Boswellia*.
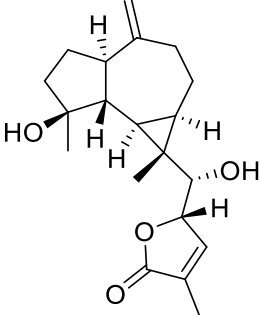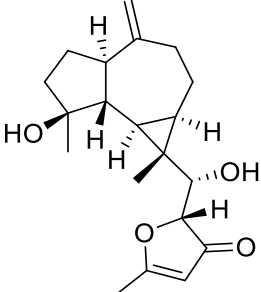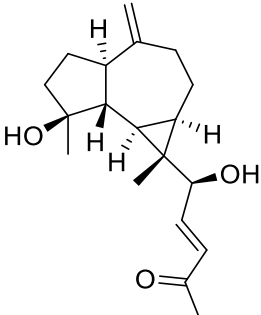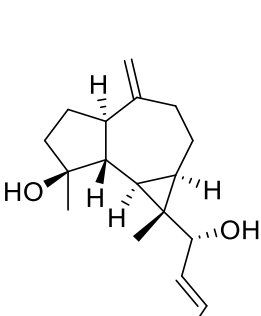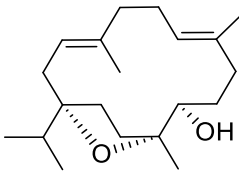
Table 5: Some isolated terpenoids of the genus *Boswellia*
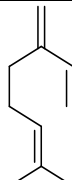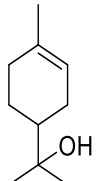
Sources	Names	Structures	Classes	References
gum resin of *B carterii*	Boscartene A (**10**)			**Wang *et al.*, 2016**
	Boscartene B (**11**)			
	Boscartene C (**12**)		Triterpenes	
	Boscartene G (**13**)			
	Boscartene D (**14**)			

	Isoflindissone **(15)** lactone			
	acide 3-oxo-tirucallique **(16)**			
gum resin of *B. serrata*	*β*-Boswellic acid **(17)**			**Belsner** *et al.*, **2003**
	11-keto-*β*-boswellic acid **(18)**			
	3-*O*-acetyl-*β*-boswellic acid **(19)**			

	3-*O*-acteyl-11-keto-β-boswellic acid **(20)**			
gum resin of *B. carterii*	Lupeolic acid **(21)**			**Verhoff** *et al.*, **2012**
	Lupenone **(22)**			
	Acetyl-lupeolic acid **(23)**			
	Acetyl-hydroxy-lupeolic acid **(24)**			
Root of *B. dalzielii*	lupeol **(25)**			**Talom** *et al.*, **2019**

Stem bark *B. rivae*	α-amyrine **(26)**			**Manguro et Wagai, 2016**
Stem bark *B. ovalifoliolata*	1a,2a,3,3-tetramethyl-7-methylenedecahydro-2H-benzo[4,5]cyclohepta[1,2-b]oxirene **(27)**		Sesquiterpenes	**Sarata *et al.*, 2016**
Resin of *B. carterii*	cembrene A **(28)**			**Aksamija, 2012**
gum resin of *B. carterii*	Boscartin I **(29)**		Diterpenes	**Jinqian, 2018**
	Boscartin K **(30)**			
	1,4-epoxy-8,13 cembrandien-5,12-diol **(31)**			
	boscartin E **(32)**			

	Boscartol K (33)			
	Boscartol L (34)			
	Boscartol M (35)			
	Boscartol N (36)			
Stem bark of *B. dalzielii*	Incensole (37)			**Alemika et *al*, 2004**

Stem bark *B. elongata*	β-myrcene (**38**)		Monoterpenes	**Ahmed, 2013**
	α-terpineol (**39**)			

1.5. Biosynthesis of terpenoids

Starting with Acetyl-CoA, the biosynthesis of terpene compounds begins with a common structural unit: the isoprene unit (C_5H_8). Terpenes are generally all formed from these units linked one after the other by a "head-tail" coupling. Generally, the carbon chain thus formed from the common unit (isoprene) can close to form one or more cycles (**Caron, 2013**).

1.5.1. Triterpenes

1.5.1.1. Generalities on triterpenes

Triterpenoids in their free and esterified forms are compounds with low polarity, and are therefore found in abundance in plant parts such as surface cuticle waxes and stem bark. Triterpenoids are widely distributed in edible and medicinal plants and are an integral part of the human diet. They are being evaluated for use in new functional foods, drugs, cosmetics and healthcare products. Screening plant material has identified fruit peel and especially fruit cuticular waxes as promising and highly available sources (**Szakiel *et al*., 2012**). Triterpenes are derived from C_{30} precursors which are themselves built up of isoprene units. Nearly 200 different triterpene skeletons are known from natural sources and represent structural cyclisation products of squalene which is the immediate biological precursor of all triterpenes.
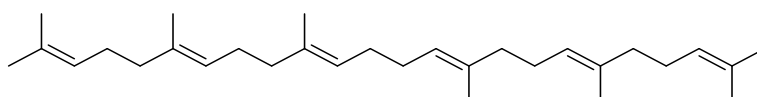
Squalene (**40)**

Most triterpenes have hydroxyl on C_3 which serve as points of attachments to aglycones (**Mahato *et al.*, 1992**).

1.5.1.2. Biosynthesis of triterpenoids

Plants biosynthesize diverse groups of triterpenoids. Although isoprene is the fundamental unit of all terpenoids, it is not the direct precursor for most members of this class. The terpenes biosynthesis can be divided into four distinct stages. The first stage involves the activation of isoprene by converting it to isopentenyl diphosphate (IPP) that is the basic building block for isoprenoids (**Thimmappa *et al*., 2014)**, which is converted then to geranyl diphosphate (GPP), and subsequently to farnesyl diphosphate (FPP) by head-to-tail condensation of two GPP units. Secondly, head-to-head condensation of two FPP units yields squalene, which is the main biological precursor of different groups of acyclic terpenoids. Thirdly, Squalene can undergo cyclisation directly and leads to terpenoids with no function, but this is rare. There is generation of different carbon skeletons as a result of the cyclization of these units. Finally, various chemical reactions such as hydroxylations and oxidations lead to the formation of individual terpenes. Most of the triterpenes are derived from squalene, which is synthesized from the reductive coupling of two molecules of farnesyl pyrophosphate by the enzyme squalene synthase. The enzyme squalene epoxidase then oxidizes squalene to generate 2, 3-oxidosqualene. Furthermore, this oxidized squalene moiety is cyclised by oxidosqualene cyclases (OSCs) to form intermediate cations. These cations then undergo structural changes by various enzymes to produce triterpene alcohols or aldehydes including α- and β-amyrin and lupeol (**Haralampidis *et al*., 2002**; **Thimmappa *et al*., 2014)**

It is well-established that different plants possess genomic machineries for multiple OSC enzymes that facilitate triterpenoid biosynthesis. These OSCs confers the structural diversity to the triterpenoids by their unique role on cyclization of 2, 3-oxidosqualene. Cyclization of 2, 3-oxidosqualene through a protosteryl cation intermediate, loss of small molecules, ring expansions or contractions generates lanosterol and cycloartenol which are structural precursors for all the steroids. Lanosterol is then converted to cholesterol, which is the precursor for most steroids. Whereas cyclization through a baccharenyl, dammarenyl and lupenyl cation intermediates produces lupeol and α/β-amyrin (**Augustin *et al*., 2011**).

The cyclisation of 2, 3-oxidosqualene by α/β-amyrin synthase enzymes results into the formation of dammarenyl cation which undergoes further ring expansion and a few rearrangements before deprotonation to α-amyrin and β-amyrin, respectively. Following cyclization, further diversity in structure is conferred by modification of the products by oxidation, hydroxylation, glycosylation and a series of concerted Wargner Meerwein 1,2 migration of protons and methyls mediated by cytochrome P450-dependent monooxygenases,

glycosyl transferases and other enzymes called cyclases. The enzymes employed for these chemical elaborations of triterpenes and triterpenoids have not been well documented (**Thimmappa** *et al***., 2014)**

The configuration will then depend on the conformation adopted by the 3S-epoxy-2,3-squalene or squalene during cyclisation. This leads to 40 or so tetra- and pentacyclic skeletons that characterise this class **(Thimmappa** *et al***., 2014).**
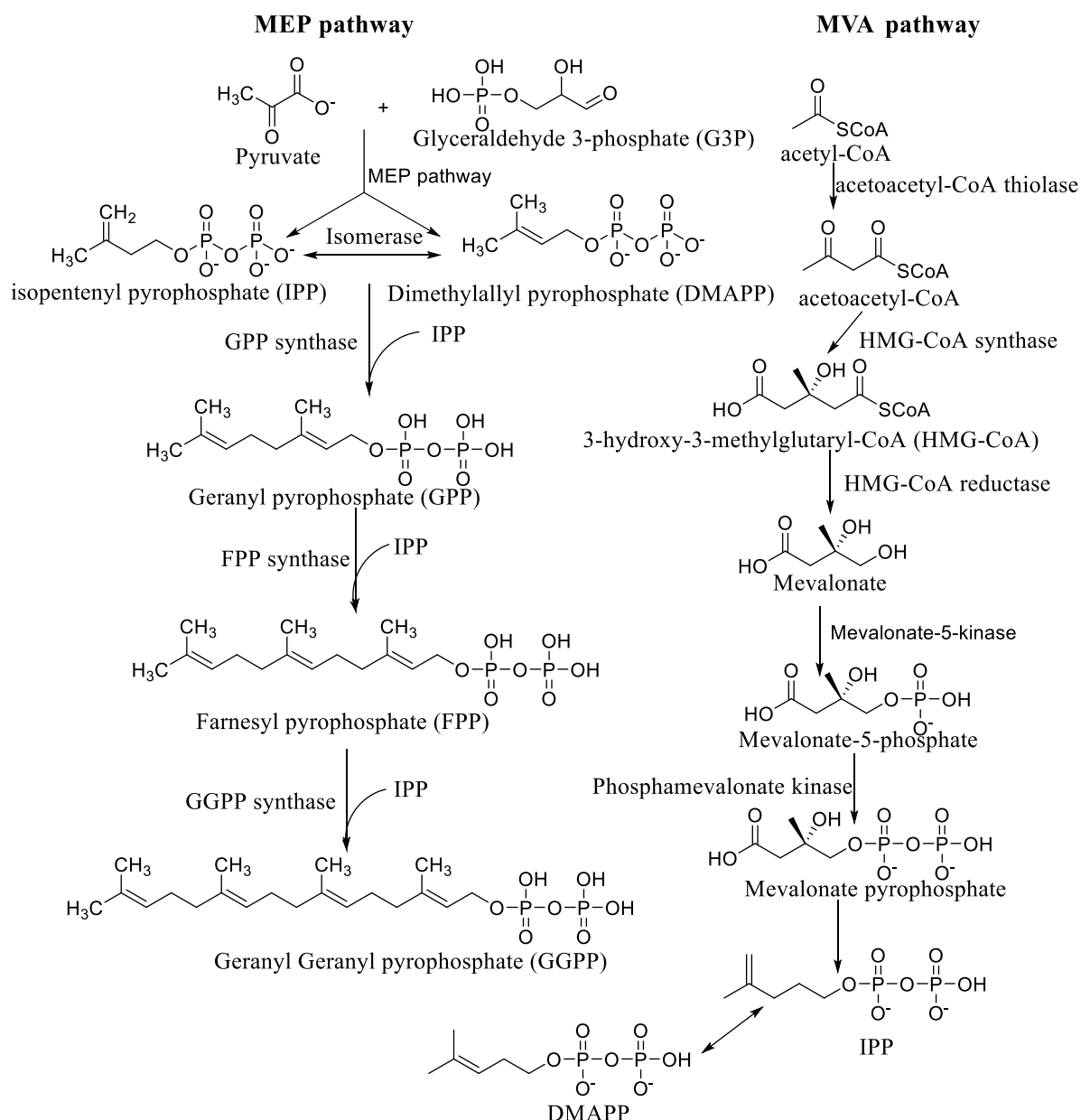
Scheme 1: Formation of epoxydosqualene (Noushah et al; 2022)

Subsequently, the epoxydosqualene will undergo a certain number of successive reactions to lead to the formation of triterpenes as shown in scheme 2
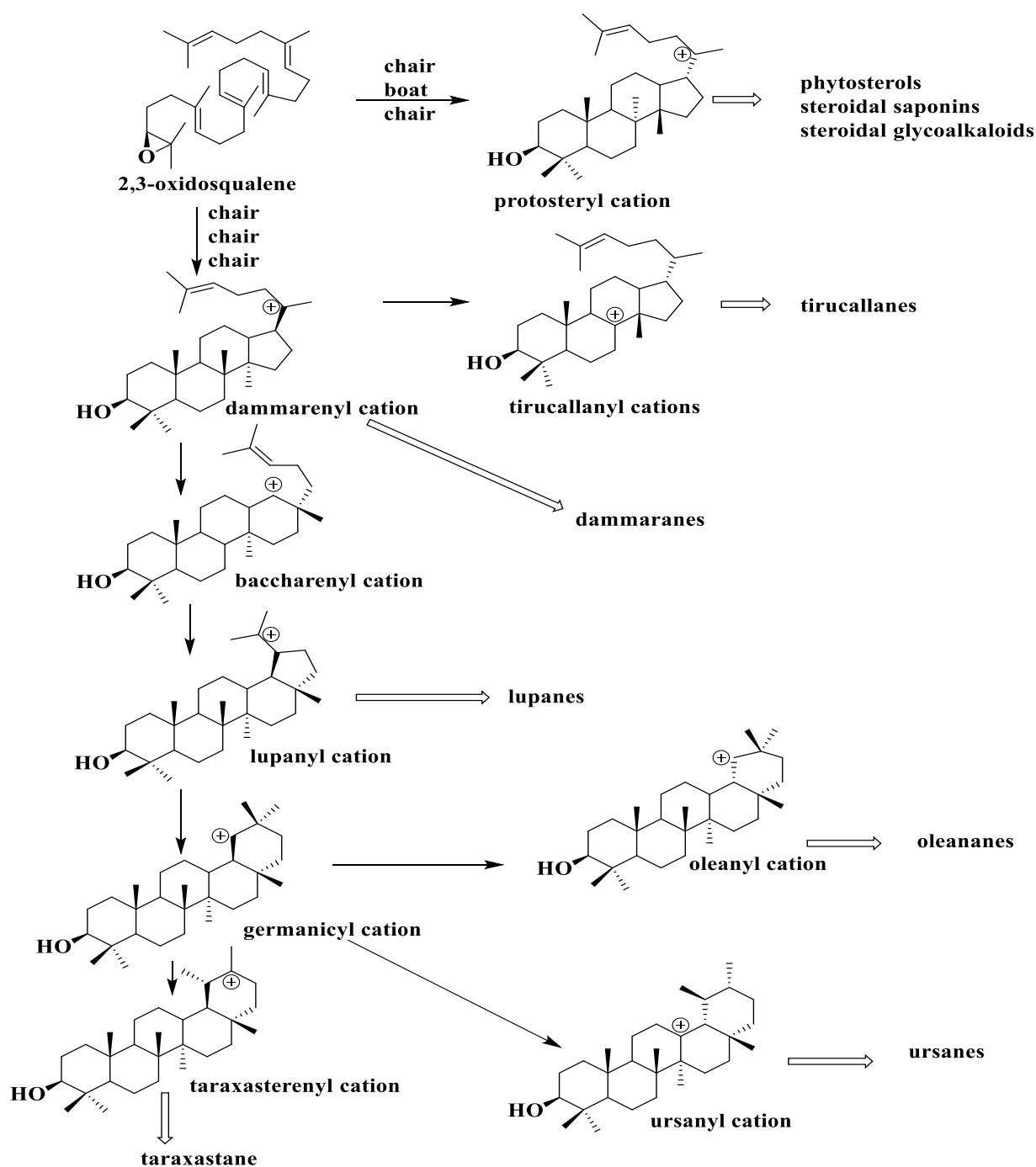
Scheme 2: Biosynthesis of triterpenoids (Augustin et *al*., 2011; Mahato and sen, 1997)

1.5.1.3. Elucidation of structures of triterpenoids and steroids

Given the considerable biological importance of triterpenes, their separation, identification and quantification in various environments represent a real challenge. The identification of organic molecular structures is generally done by the combined use of several spectroscopic techniques, mass spectrometry (MS), ultraviolet (UV) and infrared (IR) spectroscopies, 1D nuclear

magnetic resonance (^{1}H NMR, ^{13}C NMR; DEPT; APT). Indeed, these techniques are more readily used because they do not modify the structure of the compound (NMR) or require very little amount of product (UV, SM) **(Philippe, 2000)**. They also allow in a short time to have important data leading to structural clarification **(Benguerba, 2008)**. In following line, we will present the IR, ^{1}H NMR and ^{13}C NMR spectroscopies of triterpene compounds.

1.5.1.3.1. Infrared spectroscopy

Infra-red (IR) spectroscopy is mainly used to determine the types of functional groups, the modes of substitution of aromatic nuclei, etc. All functional groups such as carbonyls, phenolic hydroxyls, phenyls have corresponding IR absorptions. With regard to triterpenes, the absorption band for hydroxyl groups is in the region 3200-3300 cm^{-1}. The carbonyl groups are in the region 1700-1750 cm^{-1} **(Pine et al, 1991)**.

1.5.1.3.2. Proton Nuclear Magnetic Resonance (^{1}H NMR)

Triterpenoids are easily identified on the ^{1}H NMR by the appearance of between four and eight very intense peaks in the δ_H 0.50 to 2.00 region, each integrating for three protons **(Ageta and Arai, 1983)**. These readily discernable peaks are the angular methyls on the triterpenoid structure. Protons attached to unsaturated carbons appear further downfield after δ_H 5.00. Most triterpenoids are hydroxylated at position 3 of the triterpenoids structure, hence the oxymethine proton appears between δ_H 3.00 and 4.00. But if the proton attached to the oxygen is substituted by an ester or ether bond, then the oxymethine proton will appear further downfield after δ_H 4.00 due to the deshielding of its environment. Protons attached to any other oxygenated carbon appear downfield after δ_H 3.00. In lup-(20) (29)-enes characteristic exocyclic olefenic protons appear between δ_H 4.30 and 4.80. In the ^{1}H NMR spectrum of ursane-type triterpenoids, H-18 appears as a doublet around δ_H 2.55 while in oleanane series, it appears around δ_H 2.20 as a doublet of doublet. When the methyl C-17 is oxidized to carboxylic acid, the proton H-18 undergoes an attractor effect of the acid which then moves it downfield to about δ_H 2.84 for oleanane-type molecules and around δ_H 2.40 for ursane-type **(Connolly *et al*, 1991).** In friedelane triterpenes, there is absence of the double bond and consequently the vinylic proton signal after δ_H 5.00. The proton NMR spectrum in most cases is not sufficient even for known compounds to be identified and must be associated to other NMR and spectroscopic techniques.

1.5.1.3.3. Carbon Nuclear Magnetic Resonance (^{13}C NMR)

The ^{13}C NMR experiment is very important for structure elucidation. Generally, this technique makes it possible to highlight all the carbons in the molecule. The analysis is based on the

chemical shifts observed as a function of the environment of each of the carbon atoms (**Benguerba, 2008**). Indeed, it makes it possible to distinguish the different types of triterpene skeletons. Triterpenoids show 30 signals on their broad band decoupled ^{13}C NMR spectrum, except in cases where more than one carbon atoms possess the same magnetic environment and hence the same chemical shift value, reducing the number of signals or when other molecules like sugar moieties, esters, phenyl groups etc, add up to the triterpenoids, increasing the number of signals. The different classes of pentacyclic titerpenes are easily distinguished on their ^{13}C NMR spectrum by the appearance of some diagnostic signals pertaining to the olefinic carbons at C-12 and C-13. Olean-12-enes have signals approximately at δ_C 122.0 and 145.0 respectively; Urs-12-enes have signals at δ_C 124.0 and 139.0 and lup-(20)(29)-enes have signals at δ_C 109.0 and 150.0 for C-20 and C-29 respectively. For friedelanes, C-23 appears around δ_C 11.0 when C-3 is hydroxylated and around δ_C 7.0 when C-3 is completely oxidised to a keto function. However, these resonances are affected by the introduction of substituents (**Mahato and Kundu, 1994**).

1.5.1.3.4. Two-Dimensional Nuclear Magnetic Resonance Spectroscopy

Two-dimensional NMR spectra provide more information about a molecule than one-dimensional NMR spectra and are especially useful in determining the structure of a molecule. Each experiment consists of a sequence of radio frequency (RF) pulses with delay periods in between them. It is the timing, frequencies, and intensities of these pulses that distinguish different NMR experiments from one another. Types of 2D NMR include (DEPT, COSY, NOESY, HSQC, HMBC, and TOCSY) The ^{13}C DEPT experiments, especially DEPT 135 helps in classifying the carbons as primary (CH_3), secondary (CH_2), tertiary (CH). The HMQC or HSQC experiment permits attribution of protons to particular carbon atoms. The HMBC spectrum allows us to establish links between protons and the carbon atoms adjacent to the one bearing the proton usually up to 2, 3 and in rare cases 4 bonds. The HMBC experiment is very important in locating the positions of substituent groups in a molecule. COSY on its part useful in locating adjacent protons through bonds while NOESY helps in the attribution of the relative stereochemistry around stereogenic centres and locating protons that have spatial proximities. Finally, HOHAHA or TOCSY is very useful in the elucidation of the structure of saponins because it helps in dividing the proton signals into groups or coupling networks. (**Tommy *et al*; 2014**). The table **6** below shows Chemical shifts of some specific carbons of certain triterpene derivatives

Table 6: Chemical shifts (in ppm) of some specific carbons of certain triterpene derivatives (Kapche, 2000).

Dérivés triterpéniques	β-amyrine	Acide oléanolique	Urs-12-ène	α-amyrine	lup-20(29)-ène	Acide bétulinique
C_2	27,4	27,3	52,5	27,2	27,4	27,6
C_3	78,7	79,0	46,2	78,8	47,7	78,9
C_4	38,7	38,7	43,6	38,7	44,8	39,0
C_{12}	122,7	121,7	124,3	124,3	25,1	25,6
C_{13}	143,4	145,0	139,3	139,3	38,6	38,2
C_{16}	23,4	27,0	26,6	26,6	35,6	32,6
C_{17}	46,6	32,5	33,7	33,7	42,9	56,3
C_{18}	41,3	47,2	58,9	58,9	48,2	47,1
C_{20}	30,6	31,1	39,6	39,6	47,9	49,2
C_{27}	26,0	26,0	23,3	23,3	14,5	14,7
C_{28}	181,0	28,4	28,1	28,1	18,0	178,9
C_{29}	33,2	33,2	23,3	17,4	109,2	109,4
C_{30}	23,6	23,6	21,3	21,3	19,3	19,4

1.5.1.3.5. Mass spectroscopy (MS)

Mass spectroscopy is used to establish the molecular weight of the compound under analysis. The soft ionisation techniques such as ESI, FAB, DI, MALDI, and CI are commonly used to establish the mass of steroids, triterpenoids and their saponins from pseudomolecular ion peaks on the spectrum (**Li et *al*., 2006; Bonfill et *al*., 2005; Shipinp et *al*., 1999**). The most prominent fragmentation pattern shown by pentacyclic triterpenoids is that due to a RDA reaction common in tritepenoids with a double bond. This usually leads to a base peak at m/z 218 and a prominent peak at m/z 203 on simple unsubstituted triterpenoids like *α* and *β*-amyrin. It is thus possible to get more information about the structure of a substituted triterpenoid by making deductions from the distinctive peaks. Oleanolic and ursolic acid show base peak at m/z 203 and other prominent peaks at m/z 248 and 263 (**Ogunkoya, 1981**)
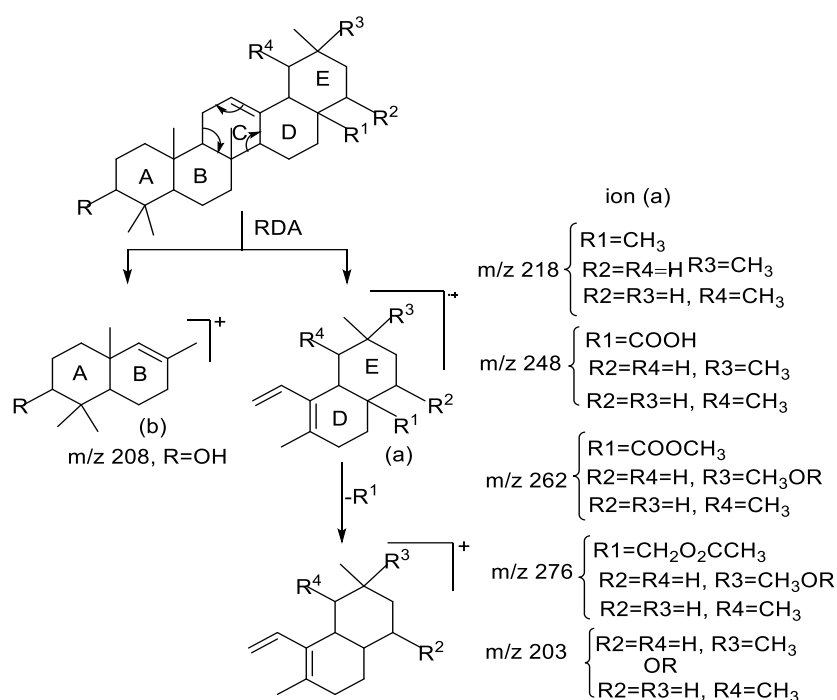
Scheme 3: Retro-Diels-Alder fragmentation pattern for Oleanane and Ursane type triterpenoids (Ogunkoya, 1981).

1.5.1.3.6. Biological activities of terpenoids

The usefulness of terpenoids has been demonstrated for the chemoprevention and chemotherapy of several diseases (taxol and artemisinin) and also for antimicrobial, antifungal, antiparasitic, anti-viral, anti-oxidant, anti-allergenic, anti-pasmodic, anti -hyperglycemic, anti-neoplastic and immunomodulatory. They also play several roles in traditional medicine and are the subject of numerous studies to understand their therapeutic effects **(Tarek, 2012)**. Terpenoids are also used therapeutically for their anti-inflammatory, antibacterial (monoterpene), and anticancer (diterpene) effects **(Nacoulma, 2012)**

1.6. Generalities on flavonoids

Considering that this work led to the isolation of one new phenolic compound and some flavonoids with good activity against bacterials strains, it will be important to give a brief overview of this class of compounds

1.6.1. Definition and general classification of flavonoids

The term ―flavonoid‖ is generally used to describe a broad collection of natural products that include a C6-C3-C6 carbon framework, or more specifically phenylbenzopyran functionality. Flavonoids contain fifteen carbons in their parent nucleus and share the common structural

feature derivatives. Depending on the position of the linkage of the aromatic ring to the benzopyrano (chromano) moiety; this group of natural products may be divided into three classes: the flavonoids (2-phenylbenzopyrans) (**42**), isoflavonoids (3-phenylbenzopyrans) (**43**), and the neoflavonoids (4-phenylbenzopyrans) (**44**) (**Bruneton, 1999).**
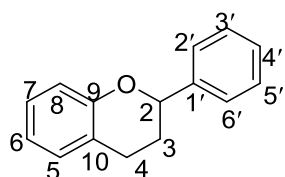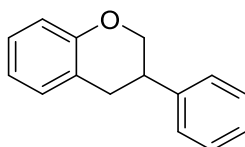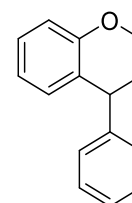
(**41**)   (**42**)   (**43**)

Based on the degree of oxidation and saturation present in the heterocyclic ring C, the flavonoids may be divided into the following groups:

Table 7: Different groups of flavonoids (Bruneton, 1999)

 Chalcone (**44**)	 Aurone (**45**)	 Flavone (**46**)
 Flavonol (**47**)	 Flavanone (**48**)	 Dihydroflavonol (**49**)
 Isoflavone (**50**)	 Isoflavanone (**51**)	 Flavane (**52**)
 Flavan-3,4-diol (**53**)	 Anthocyanidine (**54**)	 Flavan-3-ol (**55**)

1.6.2. Biosynthesis of flavonoids

Flavonoids have long sparked the interest of scientists and nonscientists alike, largely because these metabolites account for much of the red, blue, and purple pigmentation found in plants and increasingly for their association with the health benefits of wine, chocolate, and generally with diets rich in fruits and vegetables. The flavonoid pathway, illustrated in Figure 2, therefore has become one of the most well-studied of the many unique secondary metabolic systems that characterize the plant kingdom. There is good evidence that these systems are derived from primary metabolism, with a variety of enzymes, including members of the cytochrome P450 hydroxylase, 2-oxoglutarate-dependent dioxygenase (2-ODDs), short-chain dehydrogenase/reductase (SDR), O-methyltransferase (OMT), and glycosyltransferase (GT) families, having been recruited into new functions during the rapid evolution that accompanied the movement of plants onto land. **(Herbert, 1981; Belkacem, 2009)**.
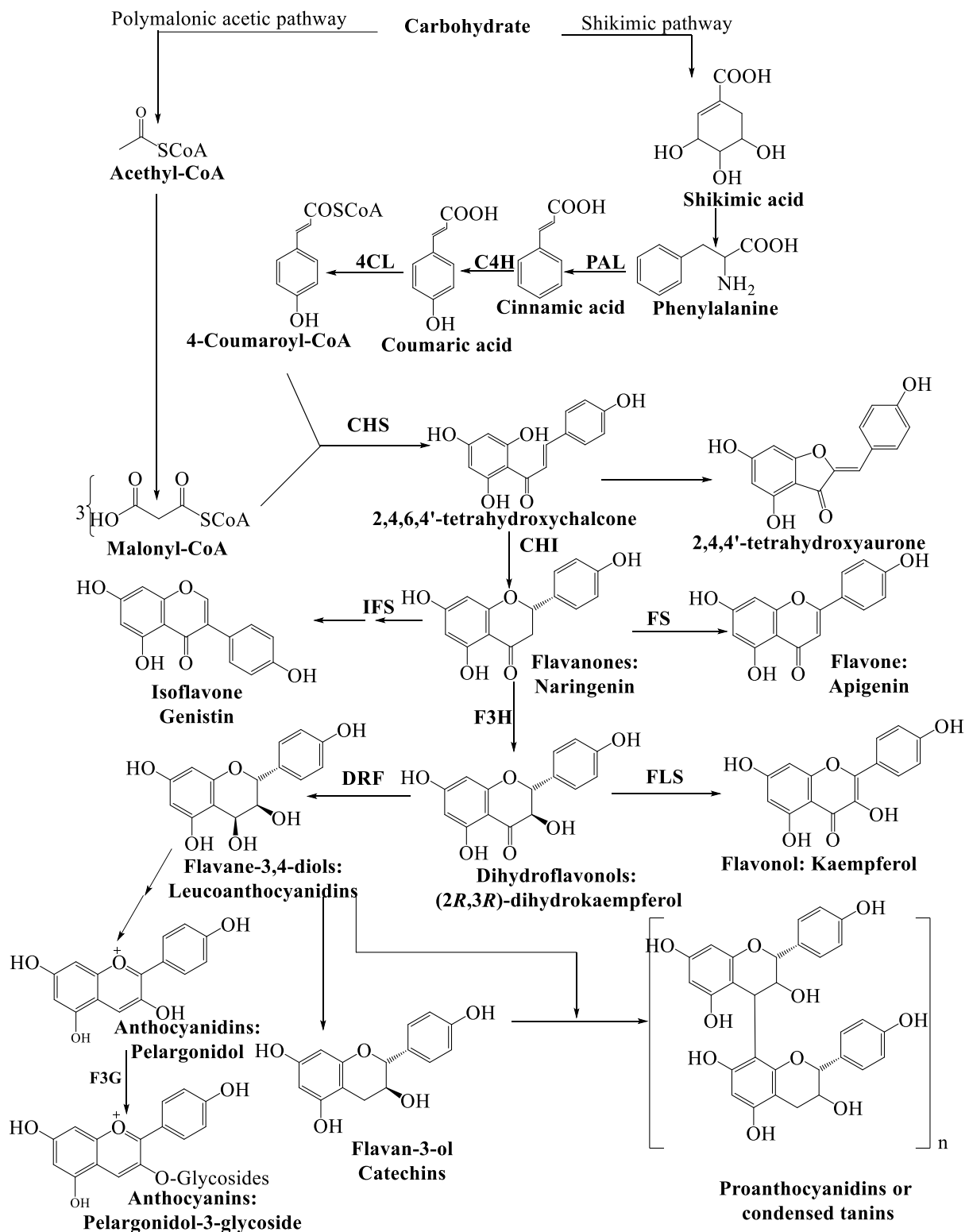
Scheme 4: Biosynthesis of flavonoids (Herbert, 1981; Belkacem, 2009)

1.6.3. Distribution of flavonoids in the nature

Flavonoids are one of the most diverse and widespread groups of natural products occupying a prominent position among the natural phenols. They are usally found in different parts (leaves, fruits, bark, stem, roots etc.) of terestial plants.

1.6.4. Extraction and purification of flavonoids

1.6.4.1. Extraction

Flowers, fruits, leaves, roots, root barks, stems and stem bark can be extracted by a single solvent or a mixture of two or more solvents in increasing polarity. These solvents could be benzene, hexane, dichloromethane, chloroform, acetone, ethyl acetate, methanol, ethanol and/or water.

1.6.4.2. Purification

Classical techniques are the column chromatography (using normal phase silica, reverse phase silica, polyamide or sephadex) and thin layer chromatography. All those techniques can use many systems of solvent mixtures depending on the nature of the stationary phase including chloroform-methanol, acetone-methanol-water, acetone-water, methanol-water, methanol-water-formic acid etc (Agrawal, 1989). Others new techniques have become available for the purification of flavonoids, they not only reduce the separation time, but simplify the isolation of previously unknown or unstable constituents from crude plant extracts or other complex biological sources (Agrawal, 1989). High-performance liquid chromatography (HPLC) and droplet counter-current chromatography (DCCC) are major innovations and are complementary to each other. While HPLC has been extensively used for analytical purposes, DCCC is an ideal method for the isolation of flavonoids on preparative scale

1.6.5. General method for flavonoid structure elucidation

Structures of flavonoids are determined by more convenient spectroscopic techniques such as IR (infra-red), UV (ultra-violet), MS (mass) and NMR (nuclear magnetic resonance) spectroscopy (Agrawal, 1989). Spectroscopic measurements in the infra-red, ultra-violet and visible regions were the first to be developed and still constitute the primary probes for the detection of used to establish the environment and the nature of carbon and hydrogen atoms **(Agrawal, 1989).**

1.6.5.1. Infra-red spectroscopy

The IR spectra of all flavonoids and isoflavonoids show absorption bands in the region of 1500─1600 cm-1 due to the aromatic rings, along with a carbonyl band at 1620─1670 cm-1.

The carbonyl absorption does not appear in flavonoids, isoflavonoids, pterocarpanoids and chalcanoids. The presence of hydroxyl groups in hydroxylflavonoids is evident by absorption in the region of 3300─3450 cm-1. An absorption band at 925 cm-1 is indicative of a methylenedioxy group and the presence of a gem-dimethyl group is indicated by the appearance of a band at 1400 cm-1. The glycosidic nature of a flavonoid is reflected by broad bands at 3250 and 1060 cm-1. However, although these absorption bands in most flavonoid glucosides, they may also occur in the spectra of polyhydroxyflavonoids (**Agrawal, 1989**).

1.6.5.2. Ultraviolet-visible absorption spectroscopy

The UV spectrum of a flavonoid is usually determined in ethanol or methanol and typically consists of two absorption maxima at the ranges of 240─285 nm (band II, primarily due to the ring A absorption), and 300─550 (band I, due to the B-ring). These precise position and relative intensities of these maxima give valuable information regarding the nature of the flavonoid and of its oxygenation pattern (Agrawal, 1989). A guide to the expected ranges of the principal maxima for each flavonoid type is given in Table 8

Table 8: Ultraviolet-visible absorption ranges for various flavonoids types (Agrawal, 1989)

Band II (nm)	Band I (nm)	Flavonoid type
250─280	304─350	Flavones
250─280	328─360	Flavonols (3-OH substituted)
250─280	350─385	Flavonols (3-OH free)
245─275	310─330 shoulder	Isoflavones
245─275	320 peak	Isoflavones (5-deoxy-6,7dioxygenated)
275─295	300─330 shoulder	Flavanones and flavanonols
230─270 (low intensity)	340─390	Chalcones
230─270 (low intensity)	380─430	Aurones
230─280	465─560	Anthocyanidins and anthocyanins

1.6.5.3. Proton nuclear magnetic resonance spectroscopy

Proton magnetic resonance (^{1}H NMR) spectroscopy has been widely employed as a method for flavonoid structure analysis. Until about 1964, ^{1}H NMR studies were limited to relatively non-polar flavonoids and to acetylated or methylated flavonoids which are soluble in

deuterochloroform (CDCl₃) or carbon tetrachloride (CCl₄). In 1964, Batterham and Highet introduced hexadeuterodimethylsulfoxide (DMSO-d6) as a solvent for more polar flavonoids and, later, trimethylsilylation was promoted as a method of derivatization for solubilizing polar flavonoids in CCl_4 or $CDCl_3$. Trimethylsilylation was preferred over other derivatization methods as signals due to trimethysilyl groups, occurring as they do in the region of 0 to 0.5 ppm, do not obscure the flavonoid signals **(Agrawal, 1989)**. The ^{1}H NMR spectrum appears predominantly in the range of 0─10 ppm downfield from the reference signal of tetramethysilane. The integral of the signal is proportional to the number of protons it represents and chemically identical protons are represented by the same signal. The chemical shift establishes the nature of the hydrogen, and coupling constants determine the presence of the ortho, meta and vicinal protons. The ortho and meta couplings have ranges of 6.5─9.0 Hz and 1.5─2.5 Hz, respectively, and are of value in establishing the aromatic substitution pattern (Agrawal, 1989).

1.6.5.4. Carbon nuclear magnetic resonance spectroscopy

The decoupled ^{13}C NMR spectrum of an unknown flavonoid permits ready differentiation between 4-keto flavonoids, flavonoids lacking a keto group, 2,3-unsaturated flavonoids and 2,3saturated flavonoids. The 4-keto flavonoids possess a carbonyl carbon resonance in the range of 170─205 ppm, which is not present in flavonoids lacking the 4-keto function. All fifteen signals due to the flavonoid nucleus resonate in the region of 90─200 ppm in case of 2,3-unsaturated flavonoids and isoflavonoids whereas 2,3-saturated flavonoids and isoflavonoids possess only thirteen signals in this region, the two additional signals resonate at higher field. Flavonoids, pterocarpanoids and chalcanes possess three aliphatic resonances and twelve aromatic resonances in above mentioned chemical shift range. The presence of many signals in the range of 60─80 ppm region is generally indicative of glycosidic carbons **(Agrawal, 1989)**. Proton-coupled ^{13}C NMR spectra, although often extraordinarily complex, can be invaluable for the reliable assignment of signals. Protonated aromatic carbons are immediately identified by their 150─170 Hz ipso-coupling and carbons ortho-, meta- or para- to ring A proton appear as signal with 1.5─4 Hz, 4.5─9 Hz, and 1─3 Hz coupling, respectively. The isoflavone C-2 signal is particularly striking because of its 200 Hz coupling with H-2. Signals of various ring C carbons show the following (approximate) coupling constants: flavones H-3/C-3, 155─170 Hz; flavones **(Agrawal, 1989)**.

Table 9: Carbon-13 resonances for ring C in flavonoids

Type of flavonoids	C-2	C-3	C-4
Chalcones	136.9―145.4	116.6―128.1	188.6―194.6
Flavanones	75.0―80.3	42.8―44.6	189.5―195.5
Flavones	160.5―165	103―111.8	176.3―184
Flavonols	145―150	136―139	172―177
Isoflavones	149.8―155.4	122.3―125.9	174.5―181
Aurones	146.1―147.7	111.6―111.9 (=CH―)	182.5―182.7
Pterocarpans	66.4―66.5 (C-6)	39.5―40.2 (C-6a)	78.4―78.5 (C-11a)

1.6.5.5. Mass spectrometry

Fragmentation of flavonoids on electron impact occurs in a limited number of predictable ways. These are detailed in a number of reviews. The first objective in interpreting a flavonoid MS is to identify the unfragmented molecular ion $[M]^+$ and then to relate other major fragments to it by rationalizing the loss in molecular weight using recognized fragmentation pathways (Agrawal, 1989). The molecular ion normally appears as a major peak in the MS of aglycones and must be an even mass number due to the presence of only oxygen, carbon and hydrogen atoms. Further, it must represent a reasonable molecular weight bearing in mind the molecular weight of basic flavonoid nucleus i.e. chalcane, 196; flavan, 208; chalcanol, 212; flavone, isoflavone and aurone, 222; flavanone, flavanol, pterocarpan and chalcone, 224; chalcanone, 226; flavonol, 238; flavanonol and chalconol, 240. Sixteen mass units (m.u.) must be added for each additional –OH, 30 m.u. for each –OCH_3, 33 m.u. for each –OCD_3 and 46 m.u. for each –OCH_2O (Agrawal, 1989). Characteristic fragments in the MS originate by fission of the molecular ion into ring A and B derived fragments. These fragmentations usually involve one of the two competing pathways, I (retro-Diels Alder) and II (Scheme 5). The dominant pathway is determined by the aglycone type, although on occasions neither pathway produces significant fragments (Agrawal, 1989).

Pathway I
with H transfer

RDA

Pathway I

C=OH⁺

+·

C=O

+

+·

C≡CH

Pathway II

+   O=C=C̄H   +   O≡⁺C
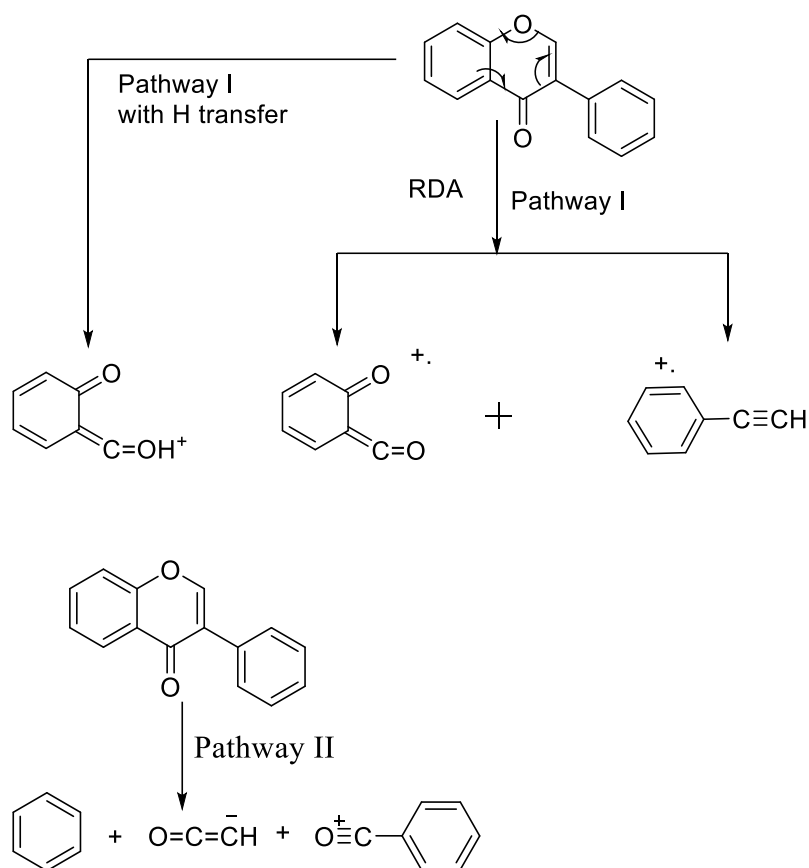
Scheme 5: Diagnostic mass spectral fragmentation pathways for flavones (Agrawal, 1989)

1.6.5.6. Biological activities of flavonoids

Due to a wide range of biological activities of flavonoids, their consumption by humans and animals, there is a high interest in the metabolism of these compounds. The most important groups of this class of natural products are the phytoestrogens (isoflavones: genistein derivatives) and antioxidants (anthocyanins: Flavonols and flavones); their interactions with proteins and their metabolites are monitored in physiological fluids (urine, blood, milk) and tissues **(Prasain et al., 2004)**. These kinds of studies will help to elucidate the influence of the flavonoids on human and animal health and permit the evaluation of their role in different kinds of epidemiological studies

1.6.5.6.1. Antimicrobial activity

The in vitro antibacterial activity against antibiotic-resistant Propionibacterium acnes of kaempferol isolated from the Impatiens balsamina alone and in combination with erythromycin or clindamycin antibiotics was investigated. The antibiotic combination effect against antibioticresistant P. acnes was studied by checkerboard test. Kaempferol and quercetin demonstrated antibacterial activities against P. acnes. Minimum inhibitory concentrations (MICs) for both compounds were ≤32 μg/ml and ≤64 μg/ml for clindamycin-sensitive and -

resistant P. acnes, respectively. The four combination formulations (kaempferol and either erythromycin or clindamycin; quercetin and either erythromycin or clindamycin) exhibited a synergistic inhibition of P. acnes growth. The combination of kaempferol with quercetin showed an indifferent effect. The combination of clindamycin with kaempferol or quercetin showed a greater synergistic effect than that of erythromycin with kaempferol or quercetin. Thus, these combinations demonstrated the potential to treat acne (**Lim et al., 2007**).

1.7. Biological activities of extracts and fractions of plants of the genus *Boswellia*

The genus *Boswellia* through its many uses has several properties in the pharmacological field, namely anti-inflammatory, antibacterial, anti-cancer properties etc. Therefore, several studies have been done on the genus *Boswellia* to highlight all these properties. Indeed, a study done on the methanol extract of the gummy resin of *Boswellia papyrifera* showed that this extract had the greatest antibacterial effect with a minimum inhibitory concentration between 62.5 and 500 μg / mL (**Al-Harrasi *et al*., 2019**). Another study by Fan et al demonstrated that the gum resin of *Boswellia carterii* given orally for ten consecutive days at a dose of 0.9 g / kg significantly reduced arthritis (inflammatory disease affecting the joints) in rats (**Al- Harrasi *et al.*, 2019**). Methanolic and aqueous extracts of *Boswellia dalzielii* have shown broad spectrum antibacterial and antifungal activities (**Alemika *et al*., 2004**). In addition, the α-amyrin compound isolated from the ethyl acetate fraction of the same species has shown a very high immunomodulatory activity (acts on the immune system) towards polymorphonyclear neutrophils (first class immune defense cells against infections) (**Talom *et al*., 2019**). The acetoxy derivatives of tirucallic acid isolated from *Boswellia serrata* have been found to inhibit proliferation induced by apoptosis in tumors and also decrease the growth of pre-established prostate tumors in nude mice (**Shenvi et al, 2014**). A mixture of α- and β-boswellic acids isolated from *Boswellia rivae* exhibited the greatest activity against *Bacillus subtilis* (a bacterium) with a minimum inhibitory concentration of 7.8 μg / mL and also showed impressive activities (minimum inhibitory concentration of 15.7 μg / mL) against *Staphylococcus albus* and *Staphylococcus aureus* (bacteria) (**Manguro and Wagai, 2016**). The anti-tripanosomal activities of extracts from different parts of *Boswellia dalzielii* have been tested in vitro and in vivo against *Trypanosoma brucei* and it has been observed that methanolic extracts from the leaves, bark of the trunk and bark from the roots of this species at a concentration of 20 mg / mL resulted in loss of mobility after 35, 25 and 20 minutes respectively. The in vivo effect of the methanolic extract of the same species on mice infected with *Trypanosoma brucei* showed a constant suppression of the parasitaemia at a dose of 300 mg / kg (**Al-Harrasi *et al*., 2019**).

1.8. Microbial diseases

Broadly, microbial pathogens are class of microbes which cause disease in humans. These microbes may be food borne, water borne, and sometimes air borne too. These organisms may be Gram-positive or Gram-negative. Few examples of pathogens include Mycobacterium sp., *Vibrios*, *Escherichia coli*, *Staphylococcus aureus*, *Shigella sp.*, *Yersinia sp.*, etc. Human body is a complex milieu of billions of cells and community of microbes which live as commensal in the gut. In the beginning of the history of human medicine, bacteria were considered as one of the large threats as in a century ago there was no potent drug for some bacterial pathogens and they were causing death of large people. After the discovery of Penicillin in 1929 by Alexander Fleming, the first antibiotic humans started doing extensive research in the area for development of novel drugs to inhibit the bacterial growth and ultimately related infections. With the development of molecular biology techniques like polymerase chain reaction (PCR) and sequencing, the identification of the microbes became more robust than the biochemical and microscopic assays used earlier **(Dethlefsen et al., 2007)**.

1.9. Antibiotic

1.9.1. Definition and generality

The term antibiotic was coined from the word antibiosis which literally means against life. In the past, antibiotics were considered to be organic compounds produced by one microorganism which are toxic to other microorganisms **(Russell, 2004)**. As a result of this notion, an antibiotic was originally, broadly defined as a substance, produced by one microorganism **(Denyer et al., 2004)**, or of biological origin **(Schlegel, 2003)** which at low concentrations can inhibit the growth of, or are lethal to other microorganisms **(Russell, 2004)**. However, this definition has been modified in modern times, to include antimicrobials that are also produced partly or wholly through synthetic means. Whilst some antibiotics are able to completely kill other bacteria, some are only able to inhibit their growth. Those that kill bacteria are termed bactericidal while those that inhibit bacterial growth are termed bacteriostatic **(Walsh, 2003)**. Although antibiotic generally refers to antibacterial, antimicrobial compounds are differentiated as antibacterials, antifungals and antivirals to reflect the group of microorganisms they antagonize **(Brooks et al., 2004; Russell, 2004)**. Penicillin was the first antibiotic discovered in September 1928 by an English Bacteriologist, late Sir Alexander Fleming who accidentally obtained the antibiotic from a soil inhabiting fungus *Penicillium notatum* but its discovery was first reported in 1929 **(Aminov, 2010)**, and clinical trials first conducted on humans in 1940 **(Russell, 2004; Schlegel, 2003)**.

Antibiotics are not totally selective in their antibacterial activity, they also antagonize the normal and useful microbiota that we all have and need in our systems as those in the gastrointestinal tract **(Walsh, 2003)**. Prescription and administration of any given antibiotics is therefore predicated on the overall intended benefit, taking into consideration the attendant side effects. For this reason, it is pertinent to understand the mechanism of action of every identified antibiotic before introduction into our health care delivery system, and recent molecular biological approaches have played very significant roles to elucidate our understanding in this regard. If used properly, antibiotics can save lives. But the use of these wonder drugs has been hampered by the rapid appearance of resistance. Antibiotic resistance occurs when a drug loses its ability to inhibit growth effectively (Levy *et al*., 2007). Bacteria become resistant and replicate in the presence of antibiotics by developing new genes. Such bacteria are called resistant bacteria and this type of resistance is called acquired resistance.

1.9.2. Causes of antibiotic resistance

An extensive range of physiological and biochemical mechanisms are responsible for antimicrobial resistance. Resistance genes can arise by spontaneous mutations in microbial DNA or by natural selection process in the presence of antimicrobials. It can also be transferred from drug resistant microbes to drug sensitive ones (Levy and Engl, 1993). Resistance occurs in a natural way, but misuse of antibiotics in humans and animals is accelerating the process **(Chopra *et al*., 2002)**. The cause for antibiotic resistance is overuse, misuse and indiscriminate use of antimicrobials by doctors, nurses and pharmacists and its use in animal husbandry and agriculture. Almost 70-80% of prescriptions are advised unnecessarily by health professionals. Antibiotics do not fight infections caused by viruses, such as common cold, flu, etc. It can cause you more harm than good and further adds to antibiotic resistance

1.9.3. Mechanisms of resistance

1.9.3.1. Intrinsic and acquired resistance

Intrinsic resistance is defined as a functional or structural characteristic conferring a certain tolerance, or even total insensitivity, to all the members of a group of bacteria (a species, a genus or sometimes a larger group tall), against a particular molecule or against a class of antimicrobials. The absence or reduced sensitivity to an antibiotic may be due to:

- A lack of affinity of the compound for the bacterial target (for example, the low affinity of nalidixic acid for the gyrase of enterococci),

- Inaccessibility of the molecule to the bacterial cell (impermeability of the outer membrane of gram-negative bacteria to glycopeptides such as vancomycin),
- Expulsion of the antibiotic by chromosomal efflux pumps (resistance to tetracyclines, chloramphenicol and quinolones in Pseudomonas aeruginosa, or even
- An innate enzymatic inactivation of the antibiotic (the production of a beta-lactamase AmpC in certain members of the Enterobacteriaceae family).

Unlike intrinsic resistance, acquired resistance is defined as a characteristic specific to a few bacterial strains of a particular genus or species, causing the emergence and spread of resistance within populations of normally sensitive germs. Two major phenomena underlying the acquisition of resistance by modification of the bacterial genome are described, namely, the mutations responsible for endogenous resistance, and the horizontal acquisition of foreign genetic material responsible for exogenous resistance. In addition, certain resistances result from the association of a mutation and a horizontal gene transfer, such as, for example, the events leading to the broadening of the spectrum of beta-lactamases or which confer resistance to beta-lactamase inhibitors. lactamases (**guardabassi and Courvalin, 2006**)

1.9.4. Consequences of antibiotic resistance

Approximately 700,000 people a year are dying from antibiotic resistance and thus it has become a major health problem and responsible for life threatening infections. It can affect anyone, in any country and at any age (**Nitu, 2018**). Antibiotic resistance is most obvious in bacterial infections contributing most to human mortality and morbidity e.g. respiratory infections, diarrhoeal diseases, meningitis, sexually transmitted diseases and hospital acquired infections. Certain resistant species include multi-resistant *Mycobacterium tuberculosis*, multi-resista nt-*Salmonella Typhi*, penicillin-resistant *Streptococcus pneumonia*. These microorganisms with resistance genes are known as superbugs (**Lipp *et al*., 2002**). Some new antibiotics are in development but are not effective against the most resistant bacteria. Thus more expensive medicines must be used for treatment that increases health care costs as well as medicines increase economic burden on families and societies. Antibiotic resistance works as a major threat to global health, food security and development today. Pharmaceutical industries have limited interest in production of new antibiotics as within no time it becomes ineffective and make them nonprofitable as compared to drugs for lifestyle related ailments. The pipeline for new drugs is drying out and putting achievements of modern medicine at risk (**Nitu, 2018**).

1.9.5. Antibiotics mode of actions

The antimicrobial potency of most classes of antibiotic are directed at some unique feature of the bacterial structure or their metabolic processes. The mechanism of antibiotic actions are as follows: inhibition of cell wall synthesis, breakdown of cell membrane structure or function, Inhibition of the structure and function of nucleic acids, inhibition of protein synthesis, Blockage of key metabolic pathways. (**Talaro and Chess, 2008; Madigan and Martinko, 2006; Wright, 2010**)

1.9.5.1. Inhibition of cell wall synthesis

Most bacterial cells are encased by a rigid layer of peptidoglycan (PG), also called murein in older sources) which both protect the cells in the face of prevailing osmotic pressure consistent with the often-harsh environment and conditions under which they exist. (Bugg and Walsh, 1992; Holtje, 1998). To stay alive, bacteria must of necessity synthesize peptidoglycan; they do this by the activity of PBPs which are transglycosylases and transpeptidases. These two enzymes play very pivotal roles by adding disaccharide pentapeptides to extend the glycan strands of existing peptidoglycan molecule and also cross-link strands of immature peptidoglycan units (Park and Uehara, 2008). Drugs like penicillins, carbapenems and cephalosporins are able to block the cross-linking of peptidoglycan units by inhibiting the peptide bond formation catalyzed by PBPs (Josephine et al., 2004).

1.9.5.2. Breakdown of the cell membrane structure or function

The classes of antibiotics that damage cell membranes of bacteria are specific in each microbial group based on the differences in the types of lipids in their cell membranes. For example, Daptomycin depolarizes calcium-dependent membrane, and that leads to the cessation of macromolecular synthesis and disruption of the cellular membrane in bacteria (Alborn et al., 1991). The polymyxins cause disintegration of bacterial cell membrane by effectively binding to the lipid moiety of the lipopolysaccharide in the bacterial cell (**Falagas et al., 2010**).

1.9.5.3. Inhibition of nuclei acid synthesis

Metabolic pathways that result in synthesis of nucleicacids are very essential; disruption of nucleic acid synthesis is inimical to both the survival and posterity of bacterial cells. Antibiotics interfere with nuclei acid synthesis by blocking replication or stopping transcription. DNA replication involves the unwinding of the traditional double helix structure, a process facilitated by the helicase enzymes (**Gale et al., 1981**). The quinolones group of antibiotics, for example, do interfere with the functionality of the helicase enzyme thereby disrupts the enzyme from playing its function of unwinding DNA. This antibiotic action of the quinolones ultimately

truncates the process of DNA replication and repair amongst susceptible bacteria (**Chen et al., 1996**).

1.9.5.4. Inhibition of protein synthesis

The 30S ribosome-inhibitors principally work by blocking the access of aminoacyl-tRNAs to the ribosome. Examples of antibiotics that function in this manner include the tetracycline, streptomycin, spectinomycin, etc. (Hong Living things including bacteria are defined by the amount and type of proteins they are composed of, and continually produce. Proteins are responsible for the structural composition, metabolic and physiological processes, and response to adverse conditions, amongst other roles. However, the type and amount of proteins produced by a bacterium at any given time is dependent on information contained in yet another very important biomolecule – Deoxyribonucleic acid (DNA). DNA determines the type of protein a bacterial cell produces through certain information it harbours within itself. The information is a set of genetic codes called codons, handed down to an identical biomolecule – Ribonucleic acid (RNA), specifically messenger RNA (mRNA). Transfer RNA (tRNA), a similar biomolecule is also formed under the directive of DNA. This biomolecule together with mRNA travels to the ribosomes – the factory for protein synthesis in a living cell. The tRNA then deciphers the codons contained in the mRNA and facilitates the translation of the sequence of codons to a sequence of amino acids which are the building blocks of proteins (**Etebu, 2013**).

The translation of mRNA into proteins occurs over three sequential phases (initiation, elongation and termination) involving the ribosome and a host of cytoplasmic accessory factors (**Gualerzi et al., 2000**). Ribosomes are made up of RNA and proteins, and are generally called RIBONUCLEOPROTEINS. The RNA component is what is referred to as Ribosomal RNA (rRNA), and comprises two subunits, one small subunit (SSU) and the other large subunit (LSU). These two subunits are usually described in terms of their sedimentation coefficients (that is, their rate of sedimentation is an ultracentrifuge), and are measured in Svedberg units (symbols) termed the 30S and 50S, respectively (**Nissen et al., 2000**).

Given the importance of proteins in the metabolic and life processes of all living organisms, antibiotics such as erythromycin, clindamycin, lincomycin, chloramphenicol, linezolid etc. have been shown to be among the 50S ribosome inhibitors (**Douthwaite, 1992; Katz and Ashley, 2005**). In general terms, antibiotics that inhibit 50S ribosome do so by physically blocking either the initiation phase of protein translation or the elongation phase of protein synthesis where the incoming amino acid is linked up with the growing nascent peptide chain (**Patel et al., 2001; Vannuffel and Cocito, et al., 2014; Chopra and Roberts, 2001**). It is

worthy to note that some earlier works have shown that tetracycline also inhibits some proteins at the 50S ribosomes (**Epe and Woolley, 1984**).

1.9.5.5. Blockage of key metabolic pathways

Some antibiotics like sulphonamides and trimethoprim have been shown to mimic a substrate needed for cellular metabolism of bacteria. This deception causes bacterial enzymes to attach themselves to the antibiotic rather than the normal substrate. In particular, sulphonamides act like tetrahydrofolate which is required for the synthesis of folic acid in bacterial cells (**Talaro and Chess, 2008**). Folic acid is vital in the metabolism of nucleic acid and amino acids; for this reason, sulphonamides ultimately disrupt the production of nucleic acids (DNA and RNA) and amino acids, as they mimic substrates required for folic acid metabolism (**Talaro and chess, 2008**).

With a view to making our contribution in the fight against these microbial diseases and the problems of resistance to several antibiotics, we undertook a bioguided study of the plant *Boswellia dalzielii* used in traditional medicine in Cameroon to treat microbial diseases.

CHAPTER 2: RESULTS AND DISCUSSION

2.1. Plant material, bioassays and isolation of compounds

2.1.1. Collection of plant material

The stem barks and arial part of *Boswellia dalzielii* were collected in 2018 at Moutourma in the far North Region of Cameroon. The plant was identified by Doctor Souare Konssala, a Botanist at the University of Maroua and then deposited in the Cameroon National Herbarium in Yaounde where a voucher specimen N° 64939/HNC is kept.

2.1.2. Preparation of crude extracts

Each part of the plant *Boswellia dalzielii* was shade-dried, milled into fine powder and extracted with dichloromethane/ methanol (1:1 v/v) during 72 hours. After filtration and evaporation, the stem bark yielded 401.6g of extract from 5 kg of powder and 184.8 g of extract from 3.4 kg of powder of branches. The Methanolic extract of stem barks and branches of *B. dalzielii* were evaluated for antimicrobial activity using the broth microdilution method as described by Eloff (1998) with slight modifications. Only the Methanolic extract of the stem barks of *Boswellia dalzielii* exhibits moderate antibacterial activity against *Staphylococcus aureus, Enterobacter cloacae, Streptococcus pneumonia* ATCC491619 with MIC of 250 μg/mL. These two extract were fractionated by VLC using solvent and mixture of solvent such as hexane, hexane-ethyl acetate with increasing polarity to yield seven fractions from the extract of stem bark labelled: Hex-EtOAc (9:1 v/v), Hex-EtOAc (8:2 v/v), Hex-EtOAc (7:3 v/v), Hex-EtOAc (1:1 v/v), EtOAc, EtOAc-MeOH (8:2 v/v) and six fractions from branches indexed: Hexane, Hex-EtOAc (7:3 v/v), Hex-EtOAc (1:1 v/v), EtOAc, EtOAc-MeOH (8:2 v/v). All fractions were evaluated for antimicrobial activity using the same strains like extracts, then Hexane-Ethyl acetate (7/3, v/v) fraction and Hexane-Ethyl acetate (1/1, v/v) fraction of stem bark exibited significant to moderate activities against *Staphylococcus aureus, Enterobacter cloacae, Streptococcus pneumoniae ATCC491619, Pseudomonas aeruginosa HM801* with MIC ranging between 7.8 and 31.2 μg/mL.

2.1.2.1. Isolation of compounds from the active fractions

Actives fractions: Hex-EtOAc (7:3, v/v) (39.6 g) and Hex-EtOAc (1:1, v/v) (11 g), were adsorbed on coarse silica gel (70-230 mesh) and subjected to repeated column chromatography, eluting with varying solvent gradients starting with n-hexane and gradually increasing the polarity with ethyl acetate and finally methanol. Through this process, six compounds were obtained and labelled BDF3, BDF3A, BDF3B, BDF3C, BDF3d and BDF4A as shown on the **scheme 6** below. These compounds were also evaluated for antimicrobial activity using the same method as extract and fractions. Compounds BDF3B, BDF3C, BDF3d and BDF4A were

the most active against *Salmonella typhi, Enterobacter cloacae, Streptococcus pneumoniae* ATCC491619, *Escherichia coli* ATCC25322, *Pseudomonas aeruginosa HM801* with the MIC value of 3.125 and 7.8 μg/mL.
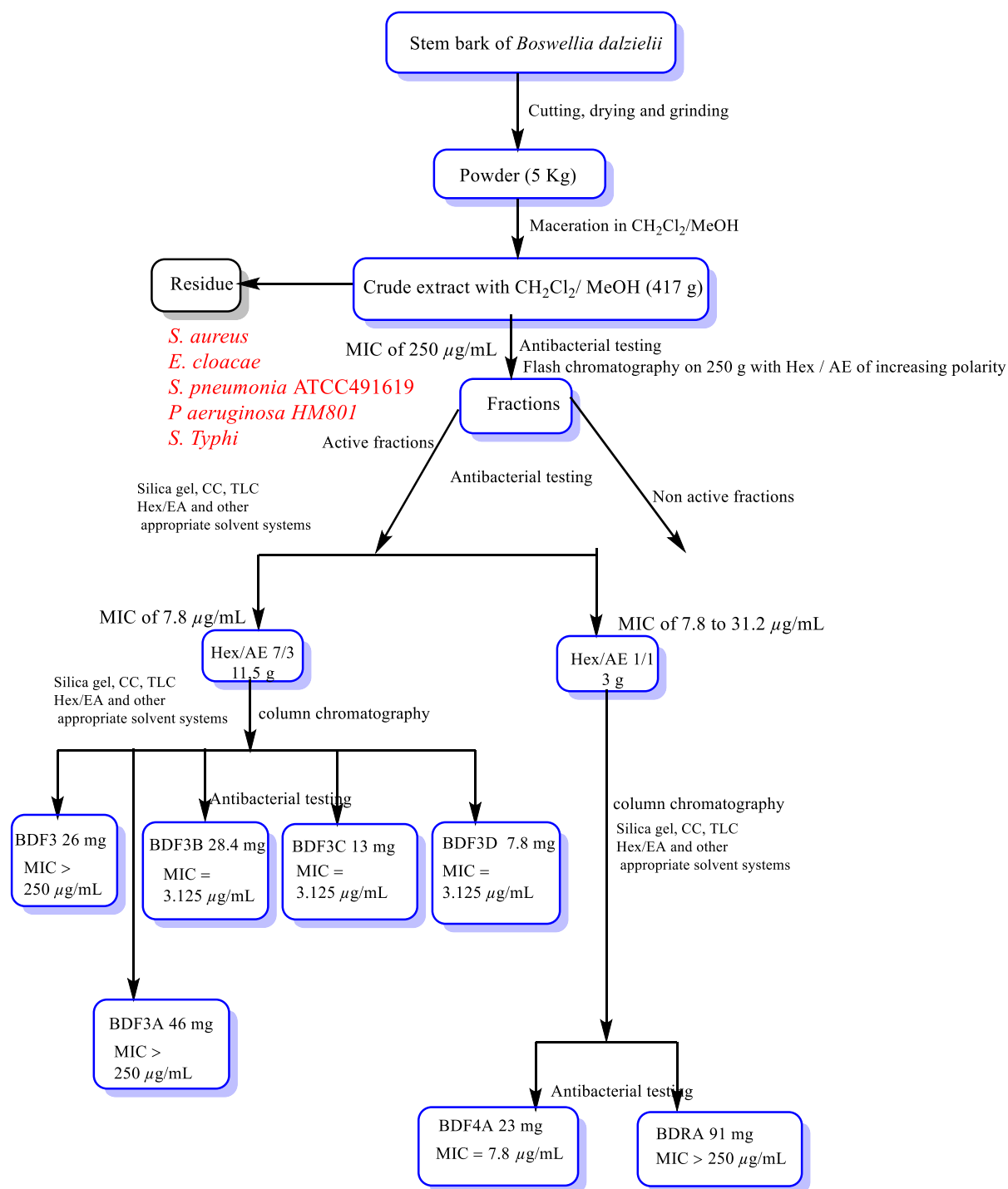
Scheme 6: Flowchart of extraction and isolation of compounds from active fractions of the stem bark extract of *B. dalzielii*

2.1.2.2. Isolation of compounds from non active fractions

The non-active fractions (Hexane-EtOAc 8:2 (14.6 g), EtOAc (13 g), EtOAc- MeOH 8:2 (72 g) of stem bark and (Hexane-EtOAc (7:3, v/v) (31.4 g), Hexane-EtOAc (1:1, v/v) (16.0 g), EtOAc (6.4 g) fractions of branches were subjected to chromatographic separations to give twenty-six compounds coded: BDF2A, BDF2B, BDF2C, BDF5A, BDRA, BDCA10, BDCA8, BDF5C, BDb1, BDb2, BDb3, BDb5, BDb6, BDb7, BDb8, BDb9, BDb10, BDb11, BDb12, BDb14, BDb16, BDb17, BDb18, BDR1, BDR3 and BDC1. These compounds were also tested on the same strains, only BDb3, BDb11, BDb16, BDb18 exhibited moderate antibacterial activities against *S. aureus, S. typhi, P. aeruginosa* HM801, *k. pneumoniae* NR41388, *k. pneumoniae*, with MICs ranging from 7.8 to 62.5 μg/ml.

Stem bark of *Boswellia dalzielii*

Cutting, drying and grinding

Powder (5 Kg)

Maceration in CH_2Cl_2/MeOH

Crude extract with CH_2Cl_2/ MeOH (417 g) → Residue

MIC = 250 μg/mL   Antibacterial testing
Flash chromatography on 250 g with Hex / AE of increasing polarity

S. aureus
E. cloacae
S. pneumonia ATCC491619
P aeruginosa HM801
S. Typhi

Fractions

Active fractions

Antibacterial testing

column chromatographySilica gel, CC, TLC
Hex/EA and other
appropriate solvent systems

Non active fractions   MIC >250 μg/mL

Silica gel, CC, TLC
Hex/EA and other
appropriate solvent systems

Silica gel, CC, TLC
Hex/EA and other
appropriate solvent systems

Hex/AE 8/2
14,6 g

AE 13 g

AE/MeOH 8/2
72 g

MeOH 117,6 g

column chromatography

MIC >100 μg/mL

Antibacterial testing

BDF2A
33 mg

BDF2B
24 mg

BDF2C
52.1 mg

BDF2C
52.1 mg

column chromatography

Silica gel, CC, TLC
Hex/EA and other
appropriate solvent systems

Silica gel, CC, TLC
Hex/EA and other
appropriate solvent systems

Antibacterial testing

column chromatography

MIC >100 μg/mL

sephadex CH_2Cl_2/ MeOH

BDF5A
73 mg

BDF5B
21 mg

Antibacterial testing

MIC >100 μg/mL

BDCA10
30 mg

BDCA12
27 mg

BDCA14
204 mg

Scheme 7: Flowchart of extraction and isolation of compounds from non-active fraction of the stem bark extract of *B. dalzielii*.
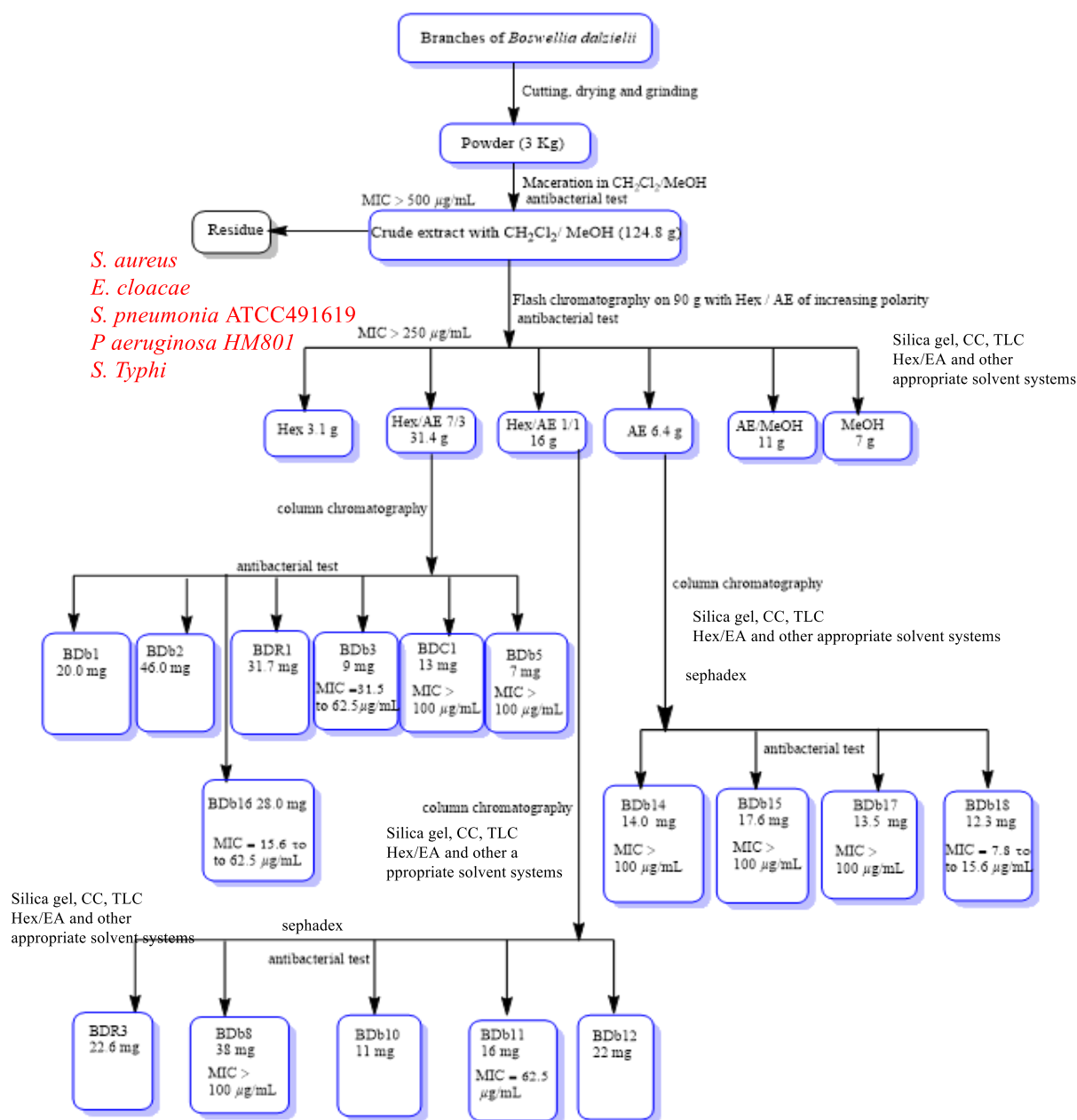
Scheme 8: Flowchart of extraction and isolation of compounds from branches extract of B. dalzielii.

The above mentioned separation and purification process led to the isolation of a total of thirty-three (**33**) compounds, the structure of twenty-eight (**28**) were elucidated. The structures of these compounds were elucidated by 1D and 2D spectroscopic techniques, MS, and by comparison with data in literature. The compounds where found to belong of triterpenes (**15**), Steroids (**03**), flavonoids (**04**), other phenolic compounds (**06**) as indicated on **Table 10** below

Table 10: Summary of compounds isolated from the different extracts

Number	Name of compound	Codes of compounds from stem bark of *B. dalzielii*	Codes of compounds from aerial part of *B. dalzieli*
Triterpenes			
1	Fridelin	BDF2A	
2	3α-acetyl-β-boswellic acid.	BDF3A	
3	β-boswelic acid	BDF3C	
4	Acetyl-11-keto-boswellic acid	BDF3d	
5	Urs-12-ene-3α,24β-diol		BDC1
6	α-amyrin		BDR1
7	α-boswellic acid	BDF3B	
8	*β*-amyrin acetate		BDb1
9	3α-acetyl-α-boswellic acid		BDb16
10	β-amyrin		BDR1
11	Lupeol	BDF2B	BDbL
12	Betulinic acid	BDF3	
13	3-O-acetyl-28-hydroxylupeolic acid	BDF4A	
14	lupenone		BDb2
15	Lanostane		BDR3
Steroids			
16+17	Stigmasterol + *β* - Sitosterol	BDF2C	BDbS
18	*β*-sitosterol-3-*O*-*β*-D-glucopyranoside	BDF5A	
Flavonoids			
19	4',5-Dihydroxy-7-methoxyflavanone		BDb3
20	Soforaflavanone B		BDb11
21	*2R,3R*-(+)-3-Acetoxy-4',5-dihydroxy-7-methoxyflavanone		BDb17
22	5,4′-Dihydroxy-7-(γ,γ-dimethylallyloxy)dihydroflavonol		BDb18
Other Phenolic compounds			
23	Angolensin	BDRA	
24	7-(3,4-Dihydroxyphenyl)-1-(4-hydroxyphenyl)-3(R)-heptanol		BDb8
25	dalzienoside	BDCA10	
26	4-methoxy-2-O-*α*-D-glucopyranosylphenyl methanol	BDCA8	
27	desoxyrhapontigenin-3-O-rutinoside	BDF5B	
Other compounds			
28	Aurantiamide acetate		BDb5

2.2. Elucidation of structures

2.2.1. Friedelane

2.2.1.1 Identification of the structure of BDF2A

Compound BDF2A was obtained as white needles in pure hexane from the Hex/EA (8/2) fraction of the stem bark of *Boswellia dalzielii*. It was soluble in chloroform and the Liebermann-Burchard test characteristic of triterpenes is positive (red-violet coloration).

The spectroscopic data led to the identification of compound **BDF2A** to following structure (**56**)
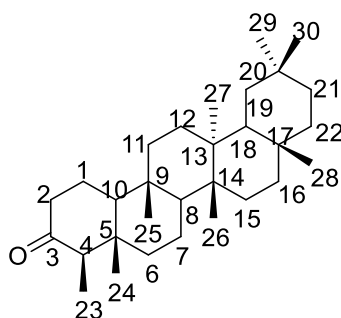
(56)

In the ^{1}H NMR spectrum (**Fig 3**) of compound BDF2A we observed:

-Eight methyl signals between δ_H 0.70 – 1.20 amongst which seven singlets and one methyl doublet at δ_H 0.87 (3H, d, J=7.0), characteristic of CH_3-23 of friedelane triterpenes (Douanla et al, 2018).

-Several signals of methylene and methine between δ_H 1.20 – 1.80 and

- A multiplet between δ_H 2.22 and 2.35 integrating for one proton and attributable to H-2b and a signal of one proton at δ_H 2.40 (d, $J = 4.8$ Hz, 1H) assignable to the H-2a both of which are α to a keto functional group.
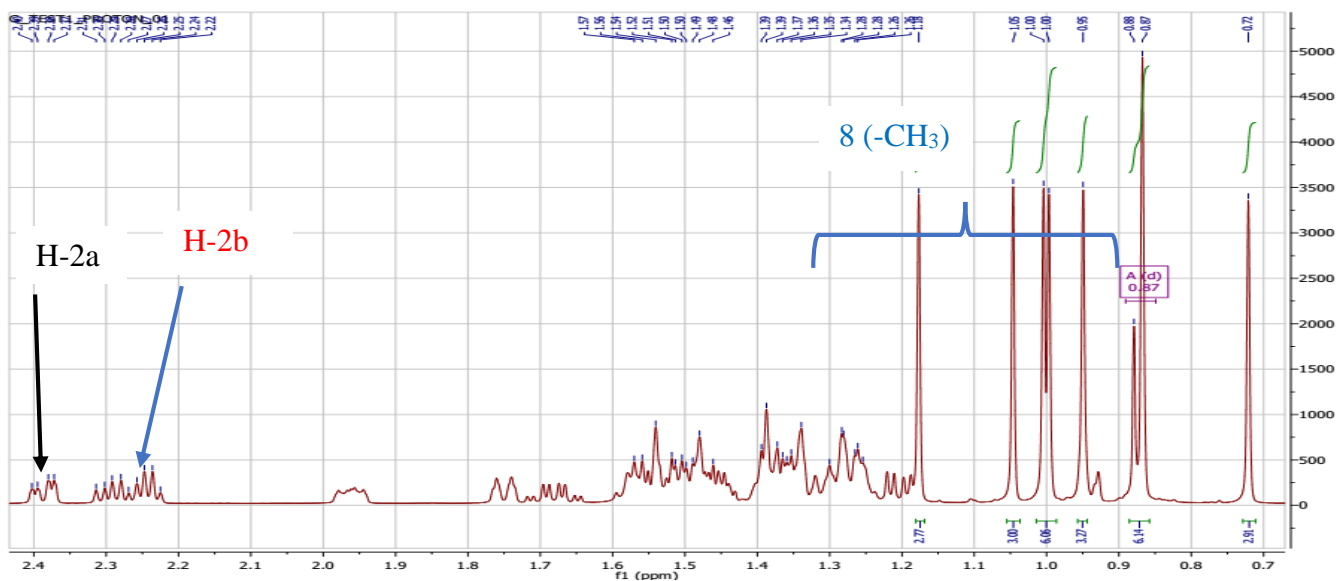
Figure 3: ^{1}H NMR (500 MHz, CDCl$_3$) spectrum of compound BDF2A

Analysis of the ^{13}C NMR spectrum (**Fig 8**) shows thirty signals amongst which;

-A signal at δ_C 6.8 attributed to C-23 that confirm the friedelane class of triterpenes (Mahato and Kundu, 1994).

-A ketone carbonyl signal at δ_C 213.2 attributable at C-3.
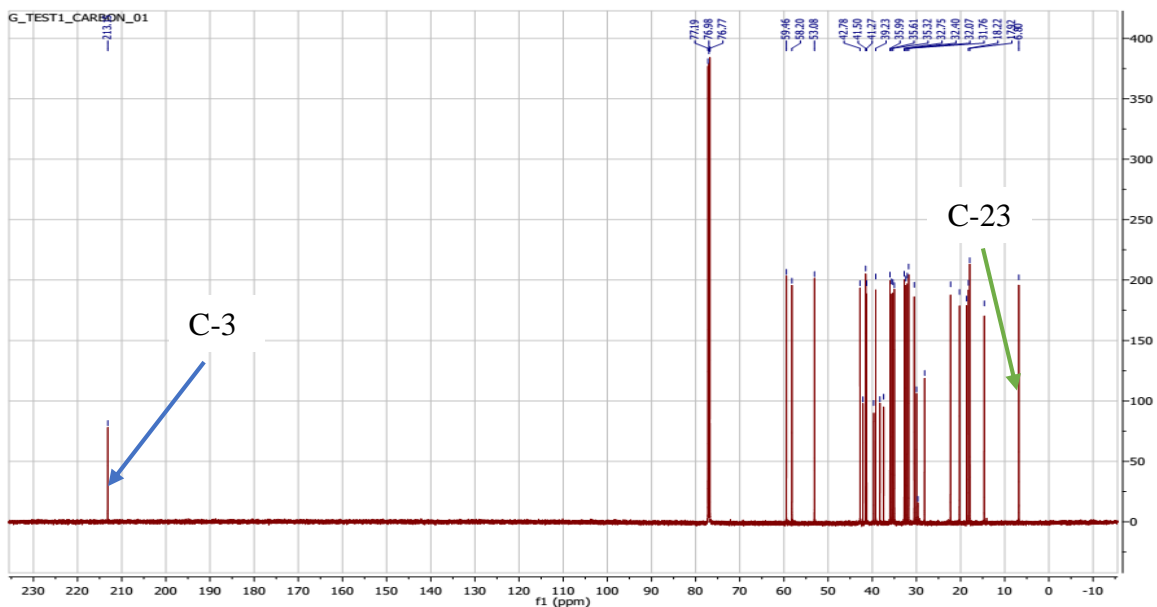
Figure 4: ^{13}C NMR (125 MHz, CDCl$_3$) spectrum of compound BDF2A

The above physical and spectroscopic data, compared to those of the literature (Mahato and Kundu, 1994) led to the identification of compound BDF2A to friedelin (**56**).

Table 11: ^{1}H NMR (500 MHz) and ^{13}C NMR (125 MHz) data of BDF2A compared to ^{13}C NMR (400 MHz) data of Friedelin in CDCl$_3$

	BDF2A		Friedelin (Mahato and Kundu, 1994)
POSITION	δ_H (m, J(Hz))	δ_C	δ_C
1	1.99 (1H,m), 1.60 (1H,m)	22.3	22.3
2a,2b	2.40 (1H,d, J= 4.8), 2.20-2.35 (1H,m)	41.5	41.5
3	-	213.2	213.2
4	2.29 (1H,q J= 6.5)	58.2	58.2
5	-	42.1	42.2
6		41.3	41.3
7		18.2	18.3
8		53.1	53.1
9	-	37.4	37.5
10		59.5	59.5
11		35.6	35.6
12		30.5	30.5
13	-	38.3	38.3
14	-	39.7	39.7
15		32.4	32.4
16		36.0	36.0
17	-	30.0	30.0
18		42.8	42.8
19		35.3	35.4
20	-	28.2	28.2
21		32.8	32.8
22		39.3	39.3
23	0.87 (3H,d, J=7.0)	6.8	6.8
24	0.75 (3H,s)	14.6	14.7
25	0.90 (3H,s)	17.9	18.0
26	1.03 (3H,s)	20.2	20.3
27	1.07 (3H,s)	18.6	18.7
28	1.20 (3H,s)	32.1	32.1
29	1.03 (3H,s)	35.0	35.0
30	0.97 (3H,s)	31.8	31.8

2.2.3. Ursanes

2.2.3.1. Identification of the structure of BDF3A

BDF3A was obtained from the stem bark of *Boswellia dalzielii* as a white powder in the mixture Hex/EA (85:15). It is soluble in DCM + MeOH (7:3) and the Liebermann-Buchard test for triterpenes is positive (red-violet coloration). The HRESI mass and spectroscopic data allowed us to allocate to BDF3A the structure (**19)** underside.
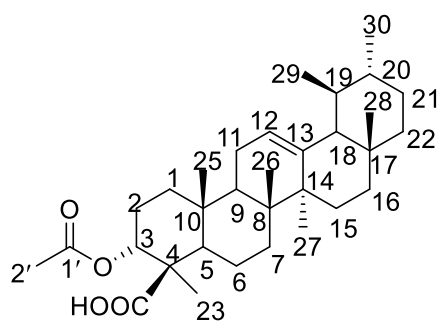
(19)

Indeed its HRESI (**Fig5**) showed the pseudo-molecular ion peak [M-H]⁻ at *m/z* 497.3635 (calcd. 497.3631): thus its molecular formula has been deduced to $C_{32}H_{50}O_4$ corresponding to eight double bond equivalent.
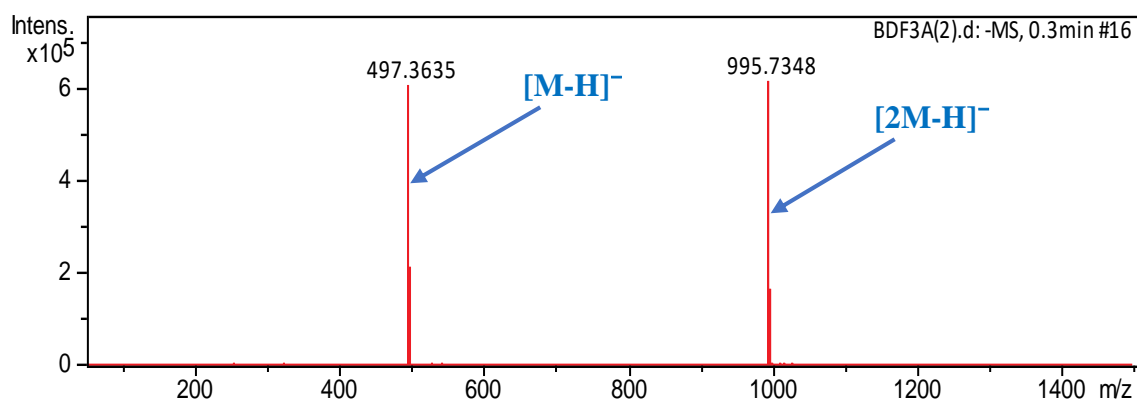
Figure 5: HRESI mass Spectrum of BDF3A

Its ^{1}H NMR spectrum (**Fig6**) displayed signals for a vinyl proton as a triplet ($J = 3.4$ Hz) at δ_H 5.17,

- An oxymethine proton acetylated at position 3 and deshieded by the carbonyl group at δ_H 5.33 (d, $J = 2.6$ Hz, 1H)
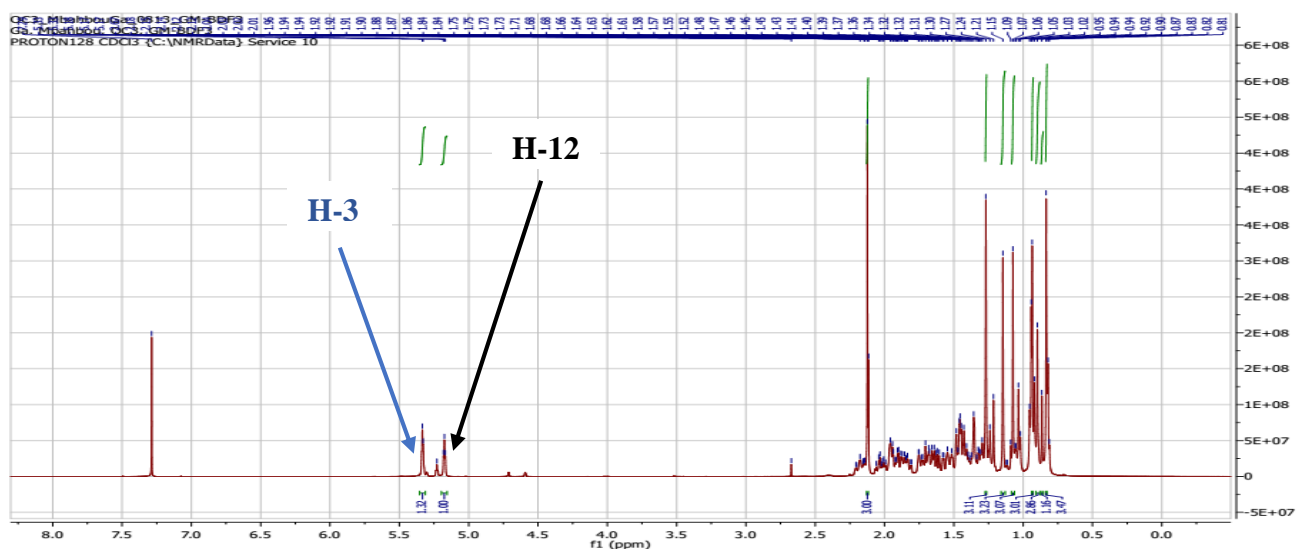
Figure 6: ^{1}H NMR (500 MHz, CDCl$_3$) spectrum of compound BDF3A

- An intense singlet of three protons at δ_H 2.12, which is attributable to one acetyl methyl group.

- Two methyl groups as doublets at δ_H 0.83(d, J = 4.8 Hz, 3H) and at δ_H 0.95 (d, J = 5.9 Hz, 3H) both suggestive of methyls 29 and 30 of Urs-12-ene skeleton. (**Mahato and Kundu, 1994**)

- Five intense angular methyl signals are also observed at $\delta_{H:}$ 0.83, 0.94, 1.07, 1.15, 1.27
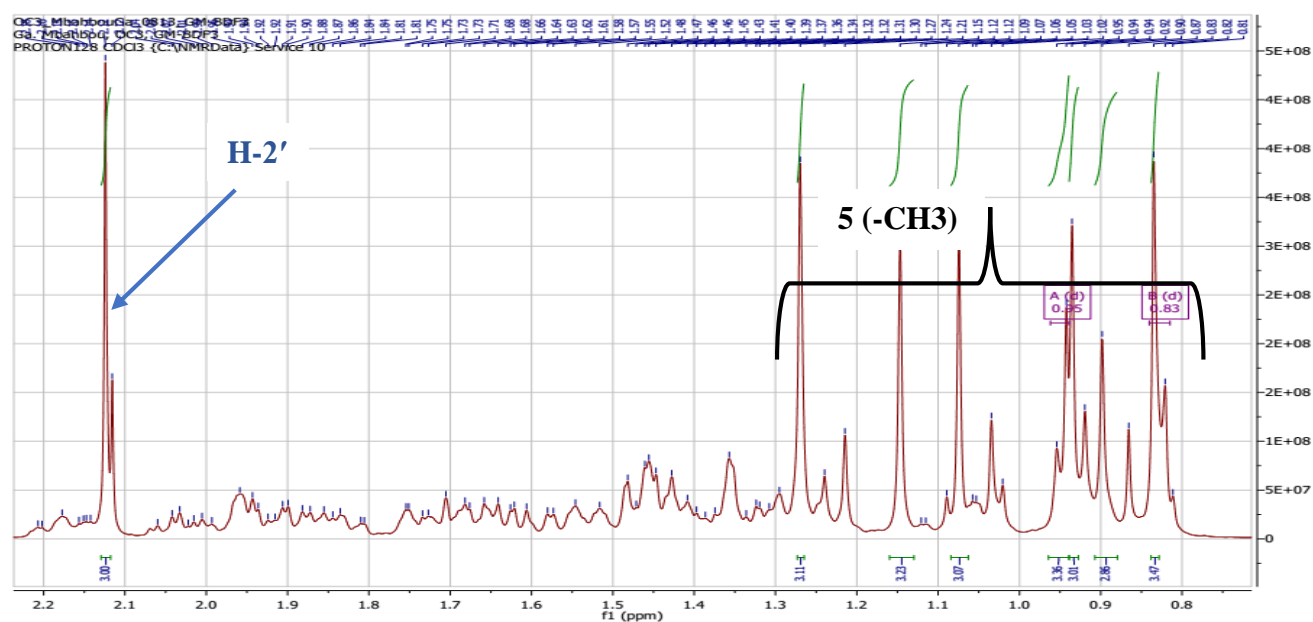
Figure 7: Expanded ^{1}H NMR (500 MHz, CDCl$_3$) spectrum of compound BDF3A

The ^{13}C NMR spectrum (**Fig9**) revealed the presence of thirty-two carbon resonances amongst which these are the Urs-12-ene diagnostic signals at δ_C 139.6(C-13) and δ_C 124.5 (C-

12) (**Lee et al, 2011**). The DEPT experiment (**Fig8**) revealed the presence of 8 quaternary carbons, 7 tertiary carbons, 9 secondary sp2 carbons, and 8 primary sp3 carbons.

The signals at δ_C 182.2 and 170.6 are ascribable to carbons of a carboxylic acid group C-24 and acetyl group C-1′ respectively (**Belsner et al., 2003**). We also observe a signal at δ_C 73.2 assignable to C-3 of triterpenes.
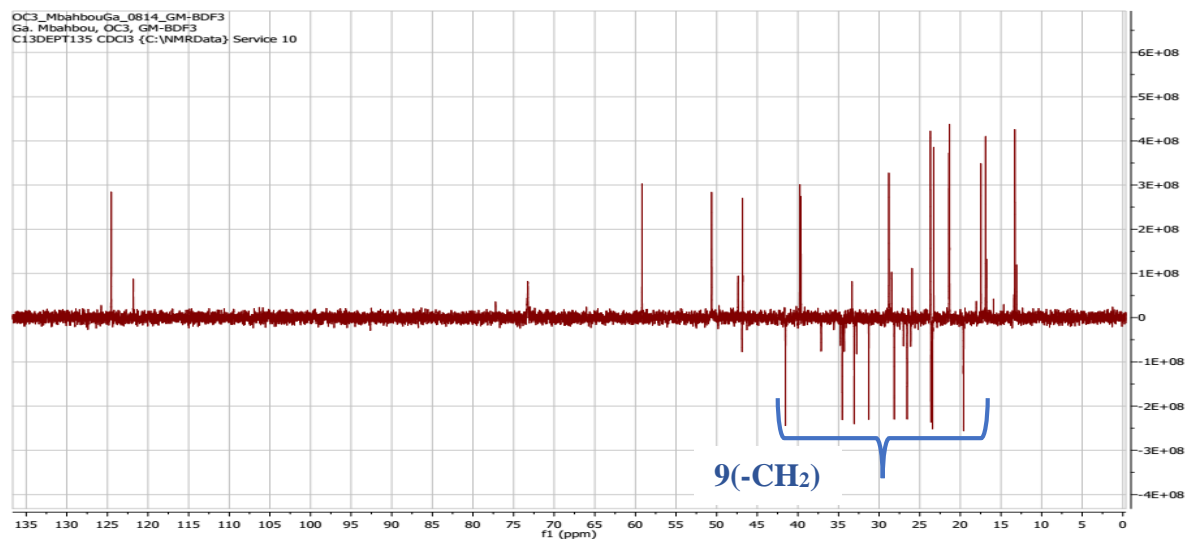
Figure 8: DEPT 135 (125 MHz, CDCl₃) spectrum of compound BDF3A
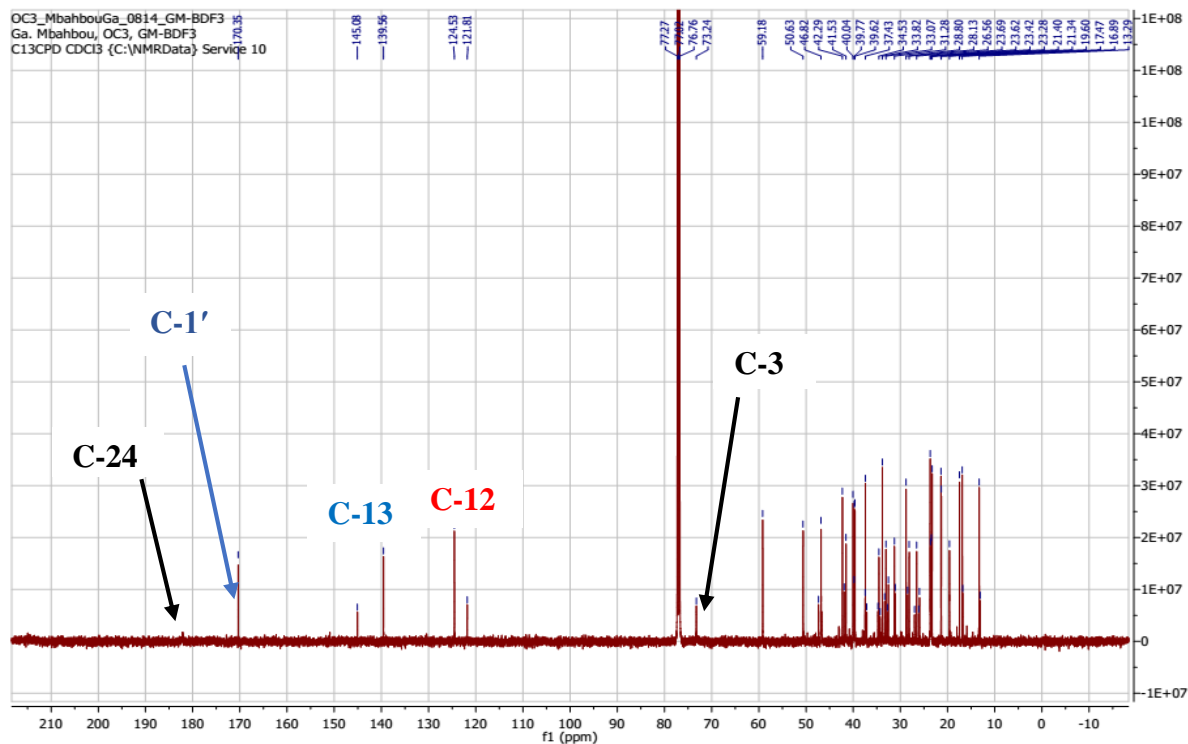
Figure 9: ¹³C NMR (125 MHz, CDCl₃) spectrum of compound BDF3A

The position of carboxylic acid group and acetyl group were confirmed by the HMBC correlation which the methyl group at position C-23 showed correlation with carboxylic acid group C-24 and the proton H-3 showed correlation with acetyl group at δ_C 170.6 (C-1′).
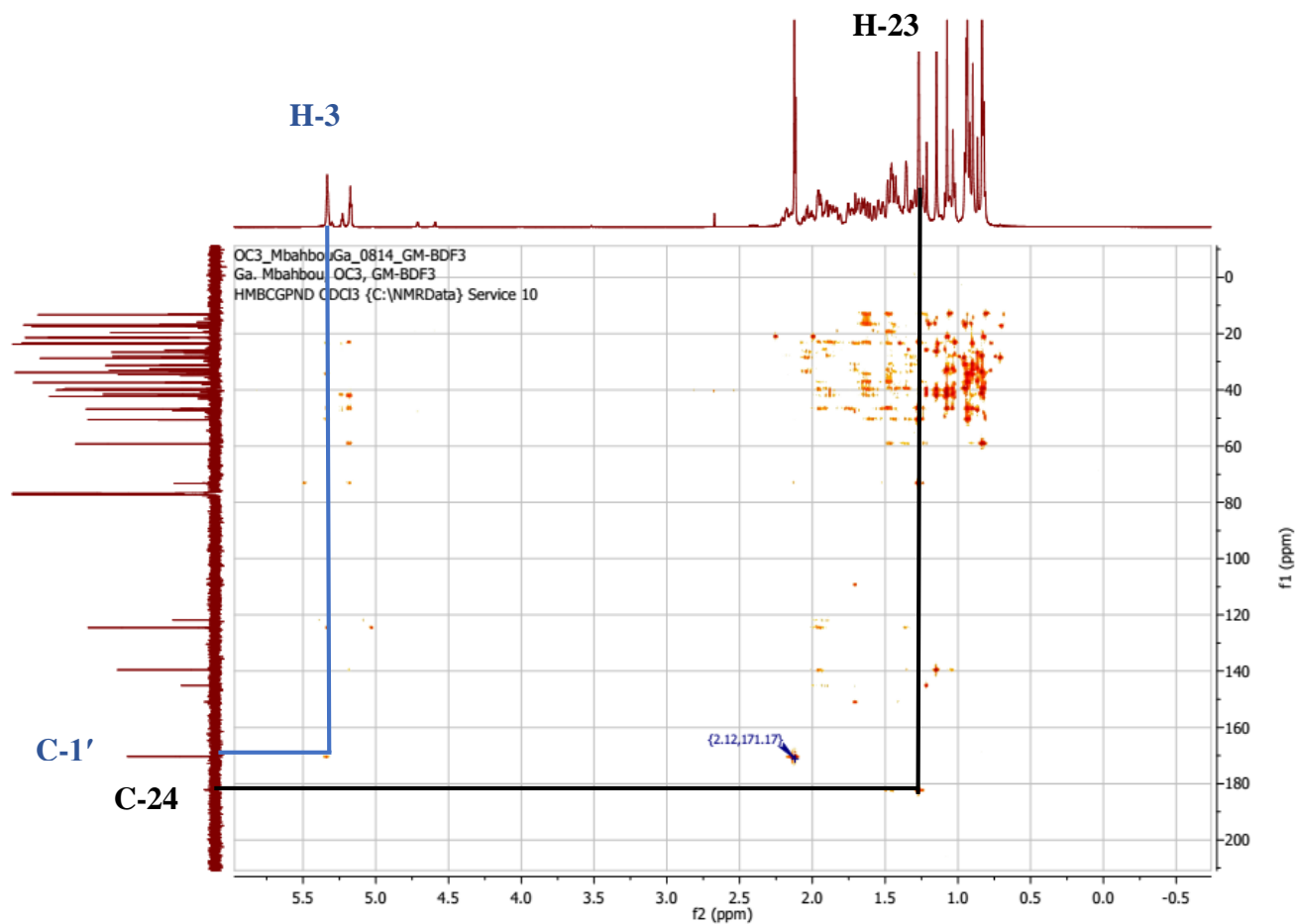
Figure 10: HMBC (CDCl₃) spectrum of compound BDF3A

By comparison of NMR data with those reported in the literature (**Belsner *et al*., 2003**) this compound has been identified as 3α-acetyl-β-boswellic acid (**19**).

Table 12: ^{1}H NMR (500 MHz) and ^{13}C NMR (125 MHz) data of BDF3A compared to ^{1}H NMR (400 MHz) and ^{13}C NMR (100 MHz) data of 3α-acetyl-β-boswellic acid in CDCl₃

POSITION	BDF3A δ_C	BDF3A δ_H	3α-acetyl-β-boswellic acid (Belsner et al., 2003) δ_C	3α-acetyl-β-boswellic acid (Belsner et al., 2003) δ_H
1	34.5	1.56 (m)	34.6	1.48 (m, β)
		1.23 (m)		1.19 (m, α)
2	23.6	2.19 (m)	23.6	2.15 (bt, J = 15.3, α)
				1.64 (bd, J = 15.4, β)
3	73.2	5.33 (1H, d, J = 2.6 Hz)	73.4	5.30 (bs, β)
4	46.7		46.7	
5	50.6	1.45 (m)	50.7	1.39 (d, J = 10.9, α)
6	19.6	1.90 (m)	19.6	1.81 (bt, J =12.2, α)
		1.73 (m)		1.71 (bd, J = 12.7, β)
7	33.1	1.56 (m, α)	33.1	1.53 (m, α)
		1.42 (m, β)		1.40 (bd, β)
8	40.0		40.1	
9	46.8	1.62 (m)	46.9	1.57 (dd, α)
10	37.4		37.4	
11	23.4	1.73 (m)	23.4	1.69 (m, α, β)
12	124.5	5.17 (1H, t, J = 3.4 Hz)	124.6	5.15 (t, J = 3.5)
13	139.6		139.6	
14	42.3		42.3	
15	26.6	1.90 (m)	26.6	1.83 (m, α)
		1.02 (m)		1.00 (m, β)
16	28.1	2.07 (m)	28.2	2.01 (td, J = 13.3, 4.3, α)
		0.90 (m)		0.85 (d, J = 13.3, β)
17	33.8		33.8	
18	59.2	1.35 (m)	59.2	1.28 (α)
19	39.6	0.91 (m)	39.6	0.87 (m, α)
20	39.7	0.95 (m)	39.8	0.9 (m, α)
21	31.3	1.41 (m)	31.3	1.37 (m)
		1.28 (m)		1.23 (m)
22	41.5	1.45 (m)	41.6	1.40 (t, α)
		1.29 (m)		1.25 (d, β)
23	23.7	1.27 (3H, s)	23.7	1.24 (s)
24	182.2		182.3	
25	13.4	0.94 (3H, s)	13.4	0.92 (s)
26	16.9	1.07 (3H, s)	16.9	1.05 (s)
27	23.3	1.15 (3H, s)	23.3	1.12 (s)
28	28.8	0.83 (3H, s)	28.8	0.81 (s)
29	17.5	0.82 (d, J = 4.8 Hz)	17.5	0.79 (d)
30	21.4	0.95 (d, J = 5.9 Hz)	21.4	0.92 (d, J = 5.8)
1'	170.6		170.3	
2'	21.3	2.12 (3H, s)	21.3	2.10 (s)

2.2.3.2. Identification of the structure of BDF3C

BDF3C was obtained from the stem bark of *Boswellia dalzielii* as a white powder in Hex/EA (7:3) fraction. It is soluble in $CHCl_3$ and the Liebermann-Buchard test for triterpenes is positive (red-violet coloration). The HRESI mass and spectroscopic data led to the identification of compound **BDF3C** to structure (**17**) following
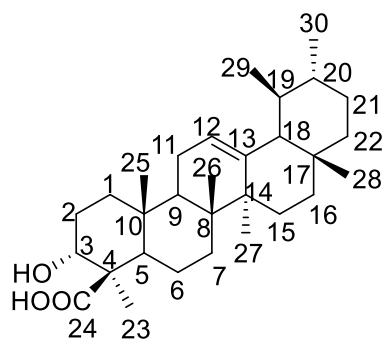
(17)

Its HRESI showed the pseudo-molecular ion peak [M-H]⁻ at *m/z* 455.3535 (calcd. 455.3525. Hence its molecular formular was deduces as ($C_{30}H_{48}O_3$), with six double bond equivalent.
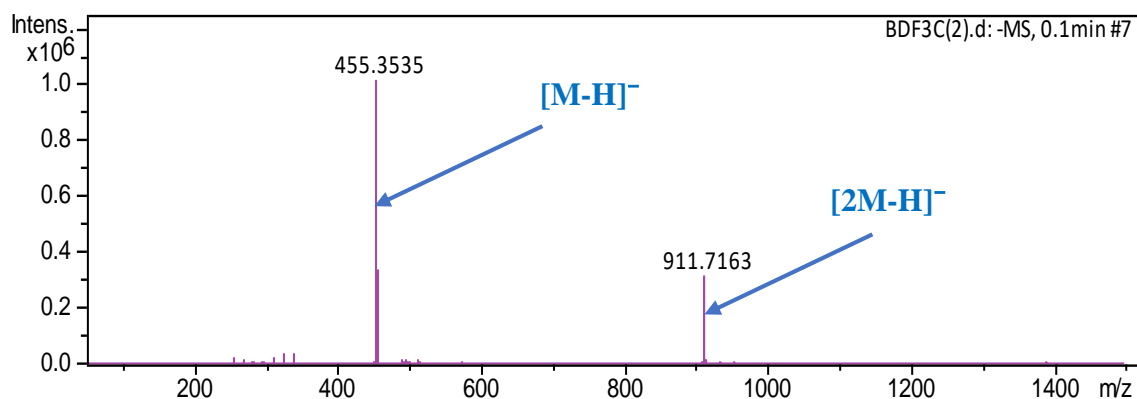
Figure 11: HRESI mass Spectrum of BDF3C

Its ^{1}H NMR spectrum **(Fig 12)** displayed a signal of multiplet for an oxygenated methine at δ_H 4.07 assignable to H-3 of triterpenes. **(Culioli *et al*. 2003)** A vinyl proton as a broad singulet at δ_H 5.14 attributed to H-12 of Urs-12-ene
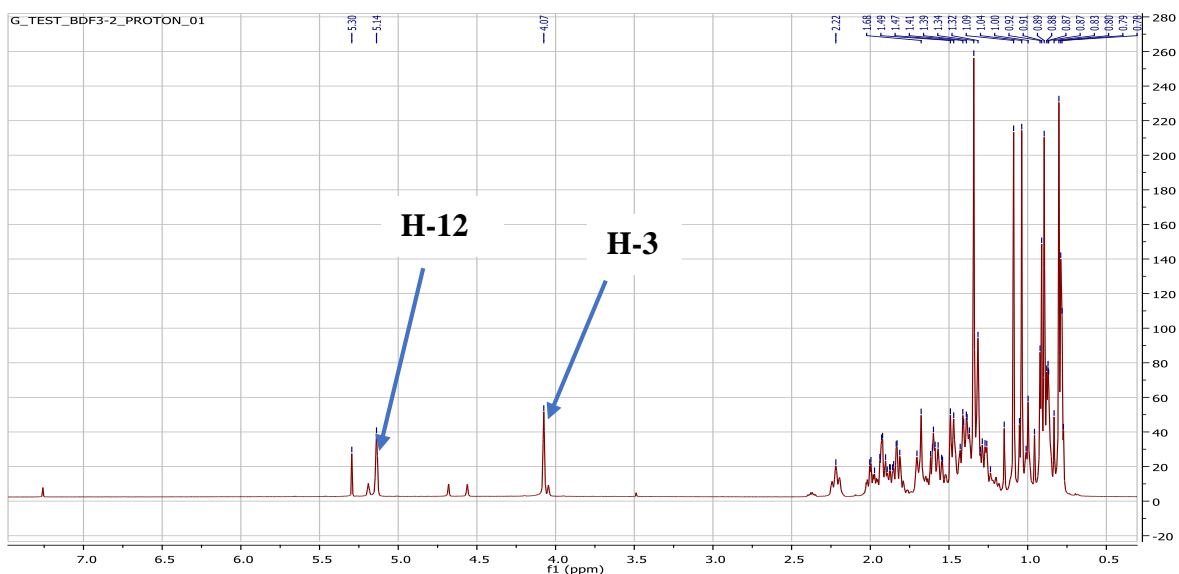
Figure 12: ^{1}H NMR (500 MHz, CDCl$_3$) spectrum of compound BDF3C

Two methyl groups as doublets at δ_H 0.80 (3H, d, J= 6.7Hz) and at δ_H 0.92 (3H, d, J= 6.3Hz), both suggestive of an Urs-12-ene skeleton (**Mahato et Kundu, 1994**).
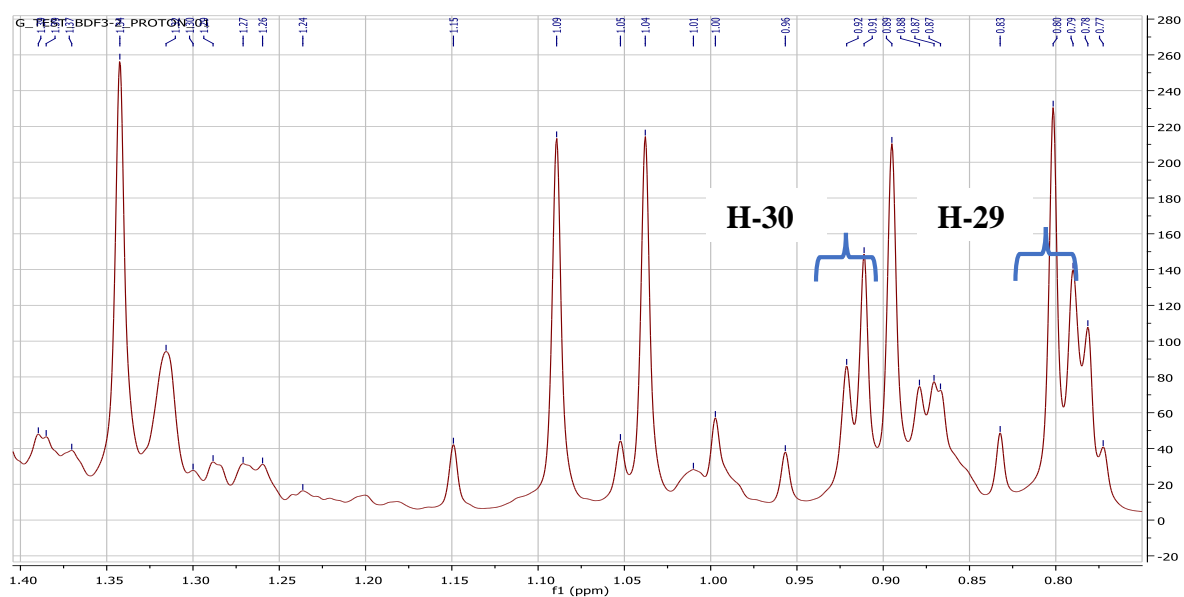
Figure 13: Expanded ^{1}H NMR (500 MHz, CDCl$_3$) spectrum of compound BDF3C

Five other intense angular methyl signals are also observed at δ_H 0.77, 0.79, 0.93, 0.98 and 1.08 attributed to methyl 29, 28, 30, 25, 26, 27 and 23 respectively.

Figure 14: Expanded (2)^{1}H NMR (500 MHz, CDCl₃) spectrum of compound BDF3C

The ^{13}C NMR spectrum **(Fig15)** showed 30 signals for 30 carbon resonances amongst which are the Urs-12-ene diagnostic signals at δ_C 139.6 (C-13) and δ_C 124.5 (C-12) **(Lee et al, 2011)** as well as oxymethine and carboxylic acid signals at δ_C 70.7 (C-3) and δ_C 183.2 (C-24).
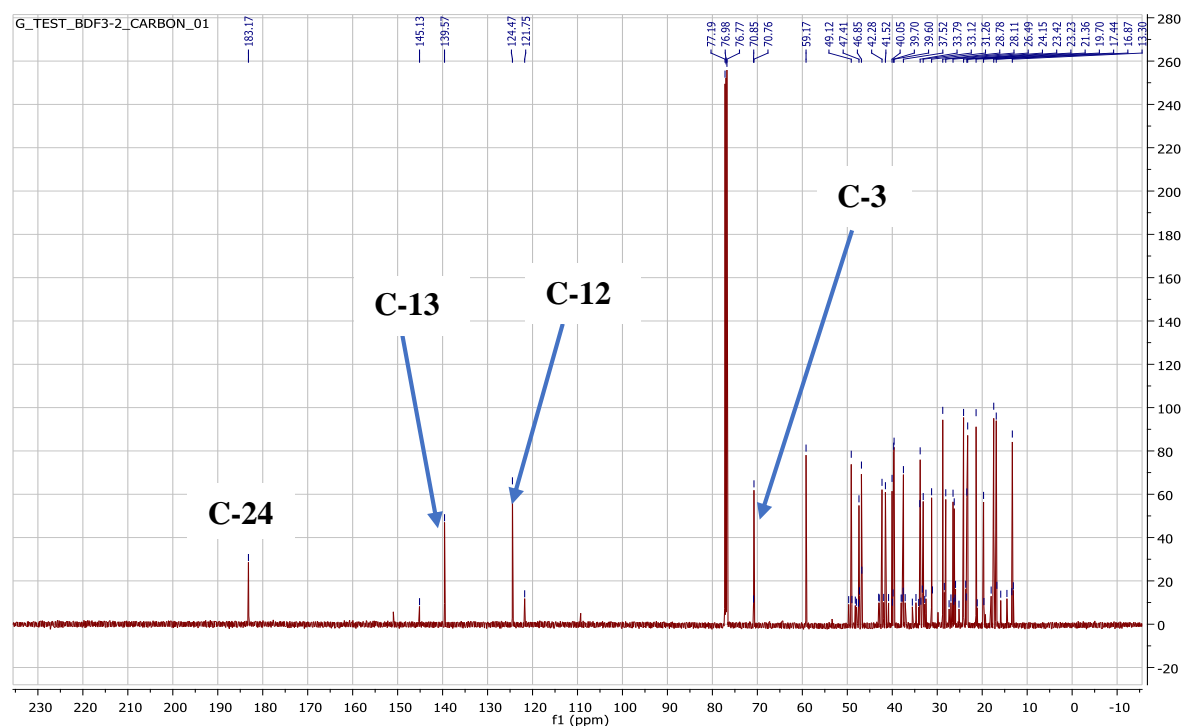
Figure 15: ^{13}C NMR (125 MHz, CDCl₃) spectrum of compound BDF3C

On the basis of the comparison with those reported in the literature **(Culioli *et al*. 2003)** but

more especially by the analysis of their NMR spectra, this compound has been identified to 3α-hydroxy-urs-12-en-24-oic acid (β-boswellic acid) (**17**).

Table 13: ^{1}H NMR (500 MHz) and ^{13}C NMR (125 MHz) data of BDF3C and ^{1}H NMR (400 MHz) and ^{13}C NMR (100 MHz) data of *β*- boswelic acid in CDCl$_3$

| POSITION | BDF3C | | *β*- boswellic acid (Culioli *et al*. 2003) | |
	δ_C (δppm)	δ_H (δppm, *J* in Hz)	δ_C (δppm)	δ_H (δppm, *J* in Hz)
1	33.9	1.49m, 1.33m	33.9	1.49 m, 1.33 m
2	26.2	2.22m	26.2	2.24 m, 1.60 m
3	70.3	4.07(1H, s)	70.8	4.08 t (2.5)
4	47.4		47.4	
5	49.1	1.50m	49.1	1.50 m
6	19.7	1.83m, 1.70m	19.7	1.83 m, 1.70 m
7	33.1	1.58m, 1.41m	33.1	1.58 m, 1.41 m
8	40.0		40.0	
9	46.8	1.63m	46.8	1.63 m
10	37.6		37.5	
11	23.4	1.92m, 1.18m	23.4	1.92 m, 1.18 m
12	124.5	5.14 (1H, s)	124.5	5.14 t (3.5)
13	139.6		139.6	
14	42.3		42.3	
15	26.5	1.86m, 1.02m	26.5	1.86 m, 1.02 m
16	28.1	2.02m, 0.88m	28.1	2.02 m, 0.88 m
17	33.8		33.8	
18	59.2	1.32 m	59.2	1.34 m
19	39.7	1.32 m	39.7	1.34 m
20	39.6	0.94m	39.6	0.94 m
21	31.3	1.41 m, 1.29 m	31.3	1.41 m, 1.29 m
22	41.6	1.45 m, 1.27 m	41.5	1.45 m, 1.27 m
23	24.2	1.34 s	24.2	1.34 (s)
24	183.2		183.1	
25	13.3	0.90 s	13.3	0.91 s
26	16.9	1.04 (s)	16.9	1.05 s
27	23.2	1.09 (s)	23.2	1.11 s
28	28.8	0.80 (s)	28.8	0.83 s
29	17.4	0.79 (2H, d, *J* = 5.1)	17.4	0.80 (d, *J* = 5.5)
30	21.3	0.92 (2H, d, *J* = 6.1)	21.4	0.94 (d, *J* = 6.0)

2.2.3.3. Identification of the structure of BDF3d

BDF3d was obtained from the stem bark of *Boswellia dalzielii* as a white powder in Hex/EA (7:3). It is soluble in $CHCl_3$ and the Liebermann-Buchard test for triterpenes is positive (red-violet coloration). The interpretation of spectroscopic data allows us to allocate the structure (**20**) following to **BDF3d**

(20)
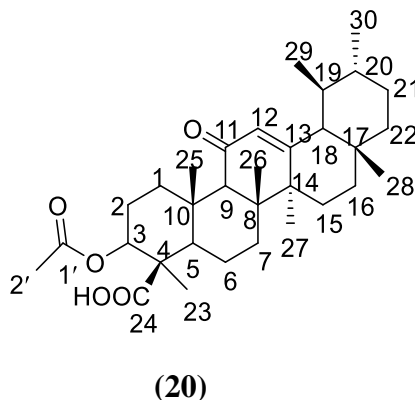
Its ESI mass showed the pseudo-molecular ion peak $[M+Na]^+$ at *m/z* 535.4, its molecular formular was deduces as $C_{32}H_{48}O_5$ with nine double bond equivalent
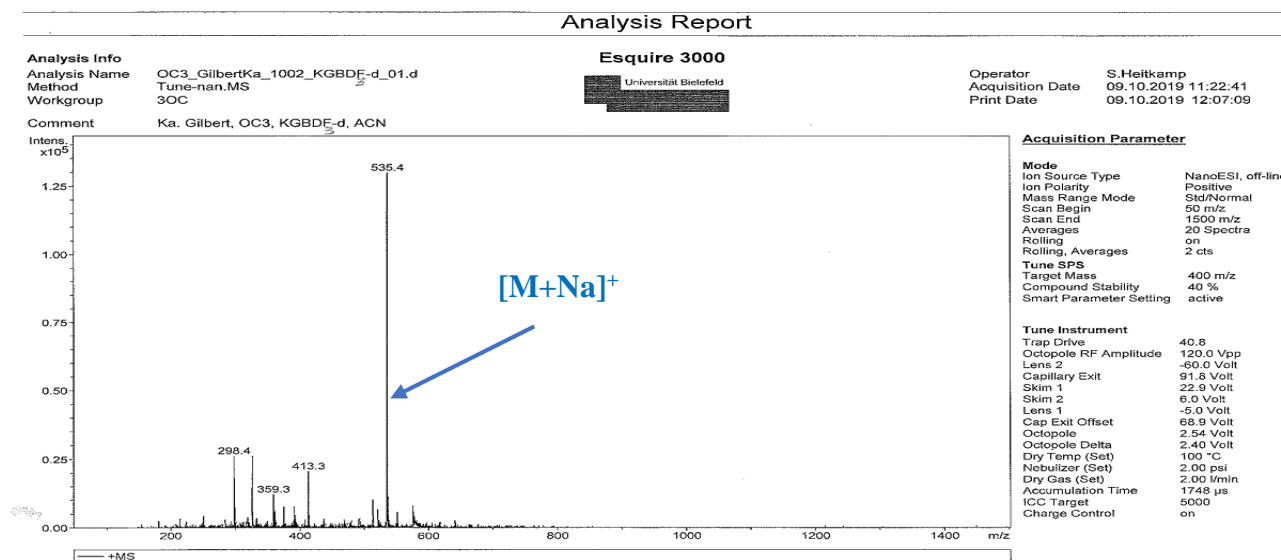
Figure 16: ESI mass Spectrum of BDF3d

The 1H NMR spectrum (**Fig 17**) showed seven methyl signals at δ_H 0.74, 0.76, 0.88, 1.07, 1.12, 1.17 and 1.28 corresponding respectively to methyl 29, 28, 30, 25, 26, 27 and 23 of triterpene (**Jinqian *et al*. 2017**).

-An intense singlet of three protons at δ_H 2.02, which is attributable to one acetyl methyl group.
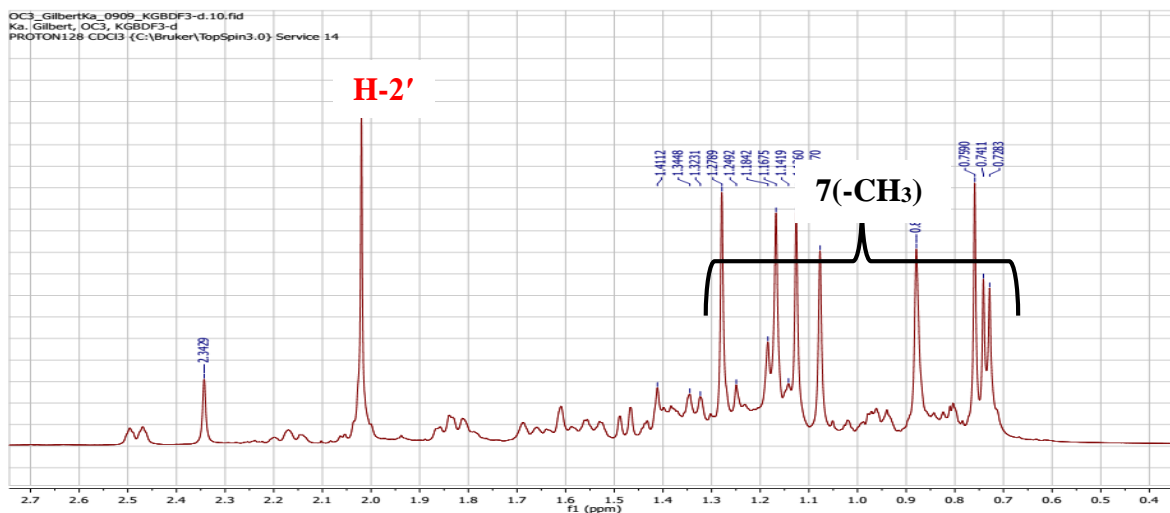
Figure 17: ¹H NMR (500 MHz, CDCl₃) spectrum of BDF3d

- A broad singulet at δ_H 5.50 attributed to H-12 of Urs-12-ene

- A downfield oxymethine proton which resonates at δ_H 5.26(1H, s).

Figure 18: ¹H NMR (500 MHz, CDCl₃) spectrum of BDF3d

The broad band decoupled ¹³C NMR spectrum of **BDF3d (Fig19)** displayed 32 carbons resonances, which were sorted by DEPT spectra into 9 quaternary carbons, 7 methine groups, 8 methylene, and 8 methyl groups.

Figure 17: ^{1}H NMR (500 MHz, CDCl$_3$) spectrum of BDF3d

- A broad singulet at δ_H 5.50 attributed to H-12 of Urs-12-ene

- A downfield oxymethine proton which resonates at δ_H 5.26(1H, s).
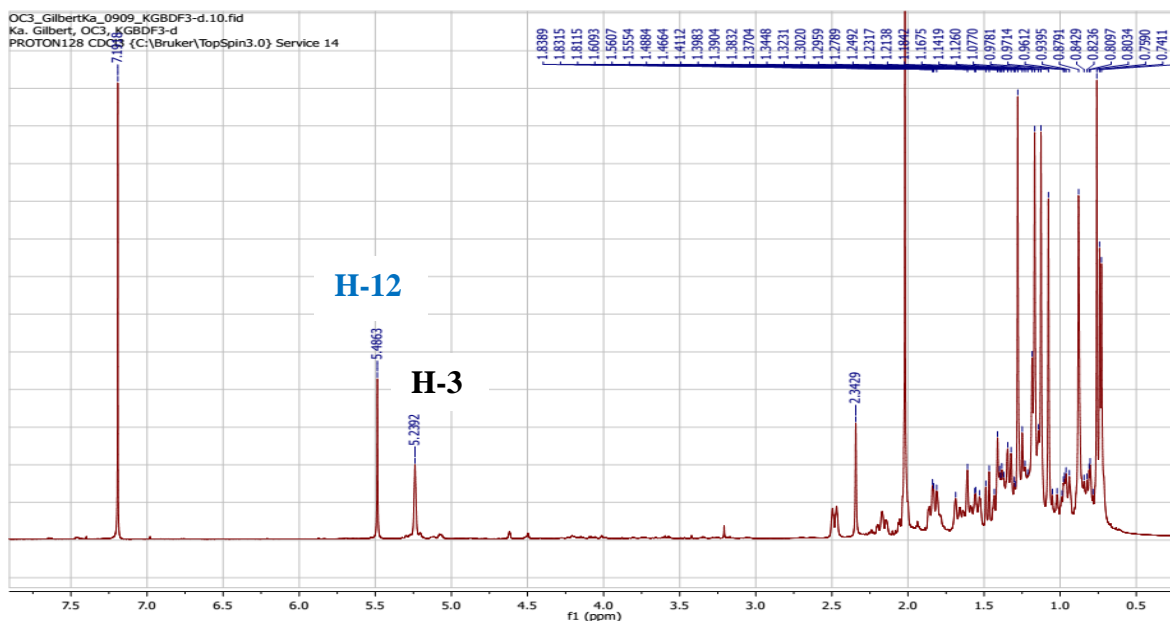
Figure 18: ^{1}H NMR (500 MHz, CDCl$_3$) spectrum of BDF3d

The broad band decoupled ^{13}C NMR spectrum of **BDF3d (Fig19)** displayed 32 carbons resonances, which were sorted by DEPT spectra into 9 quaternary carbons, 7 methine groups, 8 methylene, and 8 methyl groups.
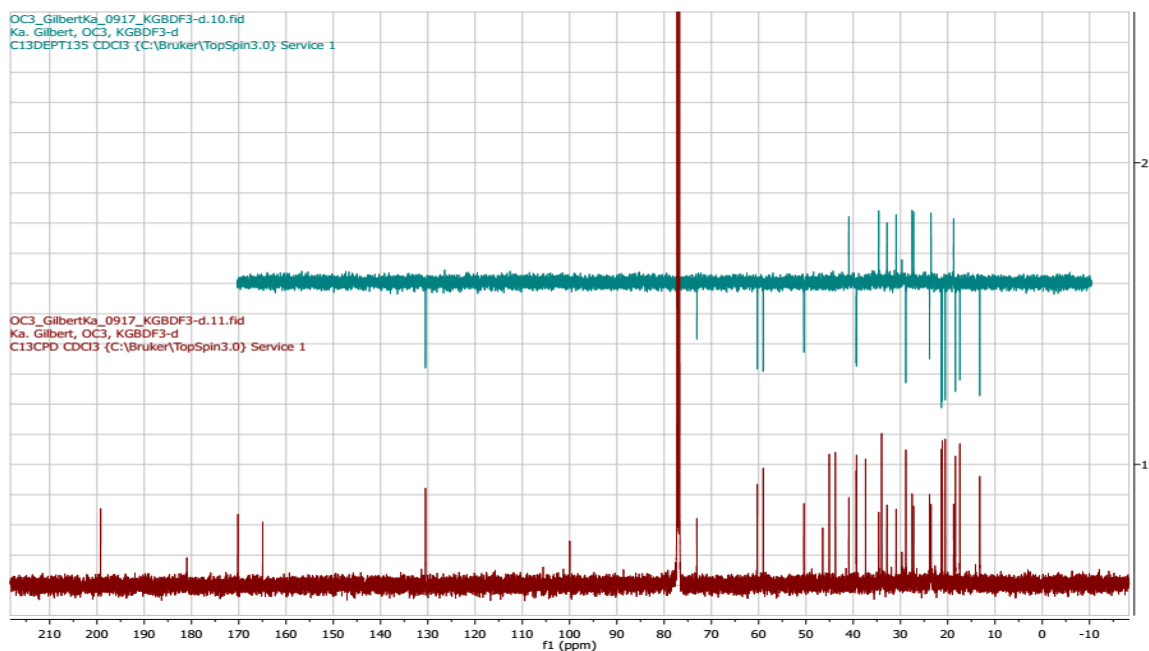
Figure 19: ¹³C NMR (125 MHz, CDCl₃) and DEPT 135 (125MHz, CDCl₃) spectra of BDF3d

The absence of methyl at position 24 suggests that the methyl was oxidized by the carboxylic acid. The signal of carbon at δ_C 199.2 is ascribable to a carbonyl (ketone) group. Moreover, the absence of signal of two protons at position H-11 suggested this ketone group is located at C-11. This suggestion was confirmed by the HMBC spectrum in which proton (H-9) at δ_H 2.35 showed correlation with the ketone group at 199.2 (C-11).

On the HMBC spectrum **(Fig21)**, we observe correlation between the proton at δ_H 5.26 (H-3) and a carbonyl group at δ_C 170.2 (C-1′), which suggests that the carbon at C-3 is linked to the acetyl group.
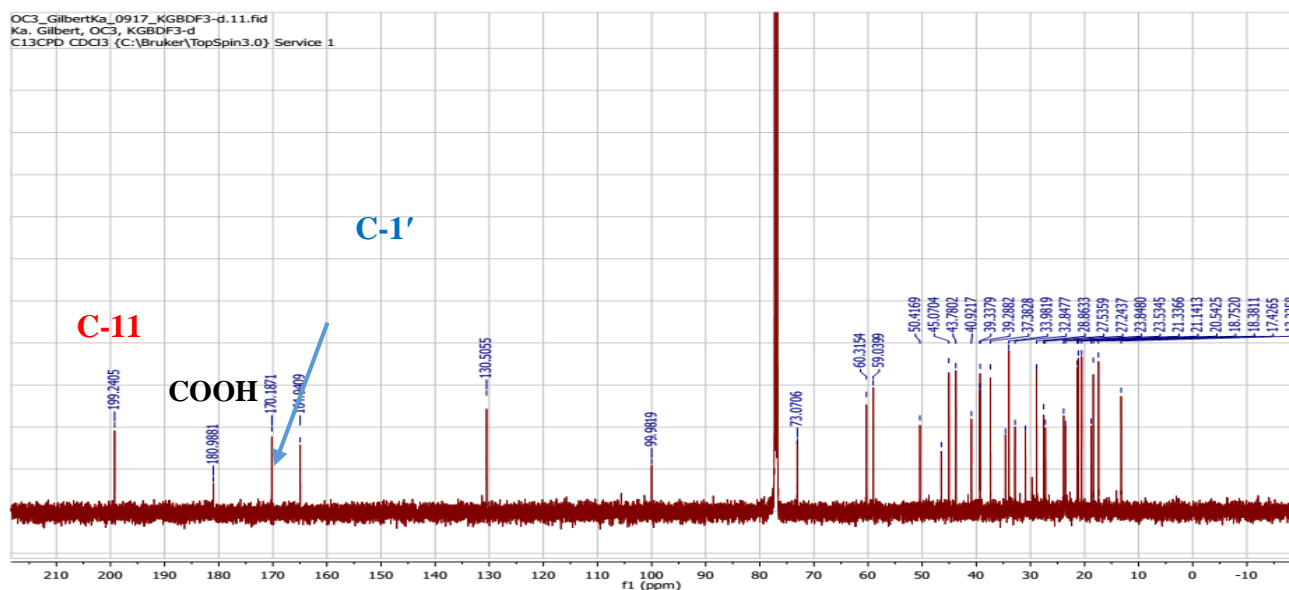
Figure 20: ^{13}C NMR (125 MHz, CDCl$_3$) spectrum of compound BDF3d
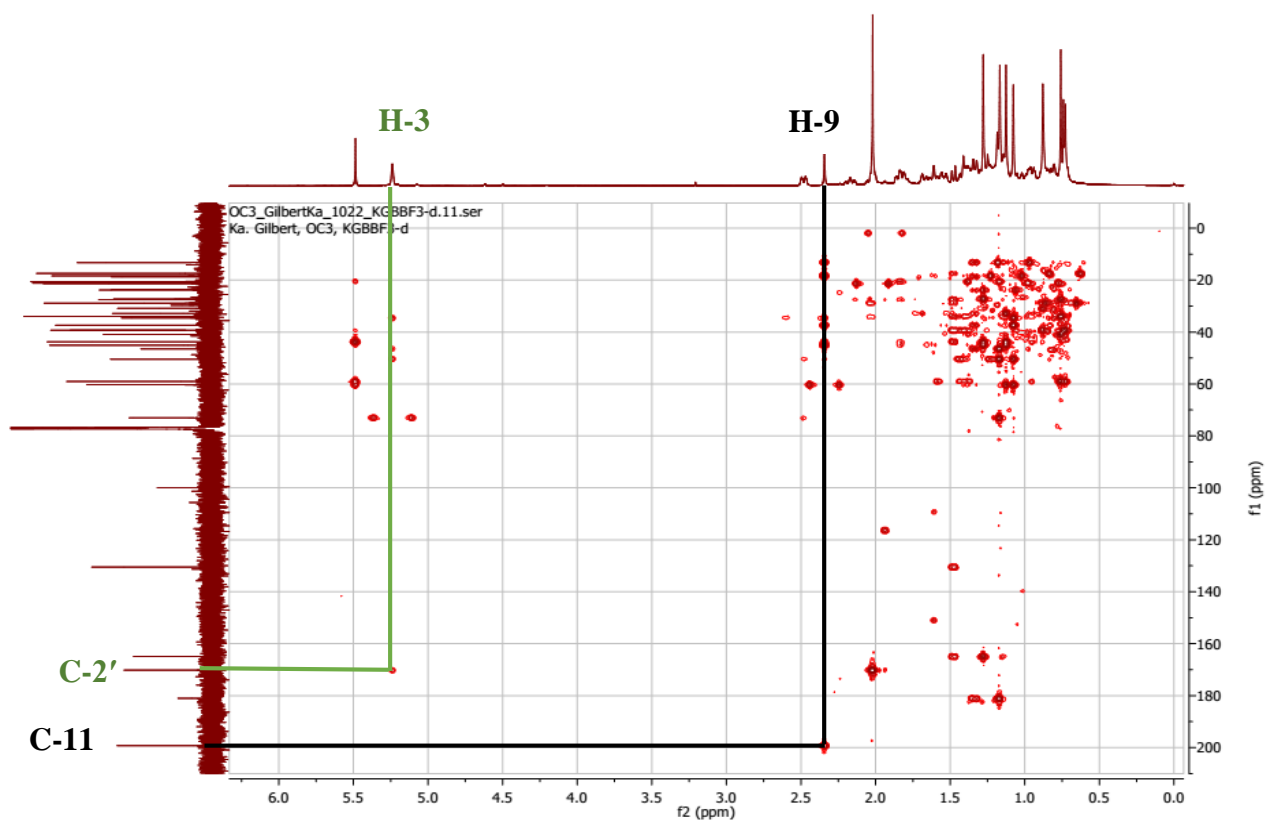
Figure 21: HMBC (CDCl$_3$) spectrum of compound BDF3d

The spectroscopic data information compared to those published by (**Belsner** *et al.* **2003**) and (**Jinqian** *et al.* **2017**), led to the identification of **BDF3d** to Acetyl-11-keto-boswellic acid (**20**).

Table 14: ^{1}H NMR (500 MHz) and ^{13}C NMR (125 MHz) data of BDF3d and ^{1}H NMR (400 MHz) and ^{13}C NMR (100 MHz,) data of Acetyl-11-keto-boswellic in CDCl₃

	BDF3d		Acetyl-11-keto-boswellic (**Jinqian** *et al.* **2017**)	
POSITION	δ_C (δppm)	δ_H (δppm, J in Hz)	δ_C (δppm)	δ_H (δppm, J in Hz)
1	34.6	2.48 (bd, J= 13.2)	34.6	2.53 (bd, J= 13.2, β)
				1.19 (d, t, α)
2	23.5	2.22 (1H, m)	23.5	2.22 (bt, J =14, α)
				1.58 (m, β)
3	73.2	5.26 (s)	73.2	5.28 (bs, β)
4	23.8		23.8	
5	50.2		50.4	1.37 (bd, J = 12.1, α)
6	18.7		18.7	1.86 (m, α)
				1.69 (d, J = 12.4, β)
7	32.8		32.8	1.65 (m, α)
				1.44 (d, β)
8	45.0		45.0	
9	60.4	2.34 (s)	60.3	2.39 (s, α)
10	37.4		37.4	
11	199.2		199.2	
12	130.5	5.55 (s)	130.5	5.53 (s)
13	165.6		164.8	
14	43.8		43.8	
15	27.3		27.3	1.89 (m, α)
				1.20 (d, J = 15.3, β)
16	27.5		27.5	2.16 (m, α)
				1.0 (bd, β)
17	34.0		34.0	
18	59.0		59.0	1.52 (d, J = 11.3, α)
19	39.3		39.3	1.40 (m, α)
20	39.3		39.3	0.93 (m, α)
21	30.9		30.9	1.44 (m)
				1.28 (m)
22	40.9		40.9	1.47 (m, β)
				1.32 (m, α)
23	23.8	1.28 (s)	23.8	1.21 (s)
24	181.0		181.7	
25	13.2	1.08 (s)	13.2	1.12 (s)
26	18.4	1.12 (s)	18.4	1.17 (s)
27	20.5	1.17 (s)	20.5	1.32 (s)
28	28.8	0.76 (s)	28.8	0.81 (s)
29	17.4	0.74 (d, J = 6.4)	17.4	0.78 (d, J = 6.5)
30	21.1	0.88 (s)	21.1	0.93 (s)
1′	170.2		170.2	
2′	21.3	2.03 (s)	21.3	2.06 (s)

2.2.3.4. Identification of the structure of BDC1

BDC1 was obtained from the extract of the arial part of *Boswellia dalzielii* as a white powder in mixture of Hex/EA (7:3). It is soluble in DCM and the Liebermann-Buchard test for triterpenes is positive (red-violet coloration). The spectroscopic data led to the identification of compound **BDC1** to structure (**57**) below.
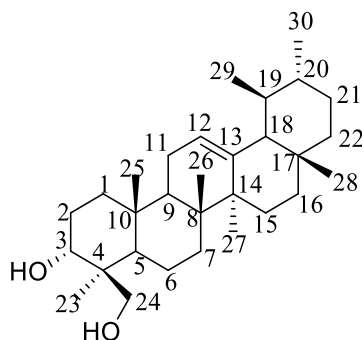
(57)

Its ^{1}H NMR spectrum (**Fig22** and **23**) displayed signals for:

- A vinyl proton as a triplet) at δ_H 5.16 (H-12) (J = 3.6 Hz)

- Two methyl groups as doublets at δ_H 0.82 (3H, d, J = 6.7 Hz) and at δ_H 0.94 (3H, d, J = 6.3 Hz), both suggestive of methyls 29 and 30 of Urs-12-ene skeleton.

- Five intense angular methyl signals are also observed at δ_H 0.83, 0.97, 1.01, 1.11 and 1.13,

- An oxygenated methine signal at δ_H 3.90 assignable to H-3 of triterpenes

- Protons of hydroxymethylene were also observed at δ_H 3.76 and 3.56 (d, J=11.1 Hz, 2H)

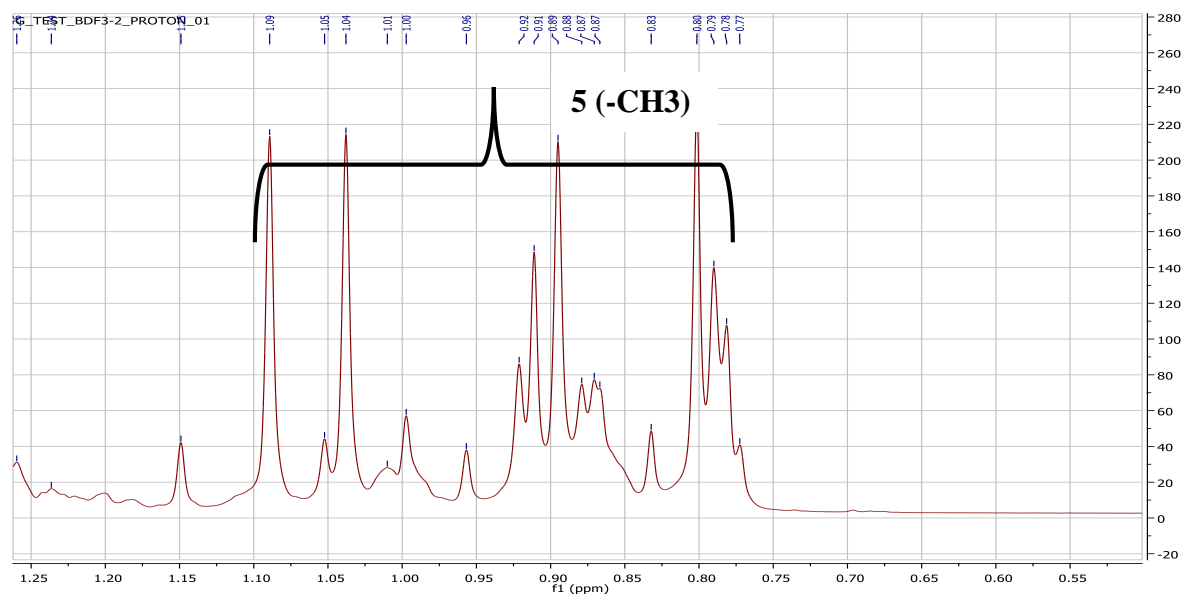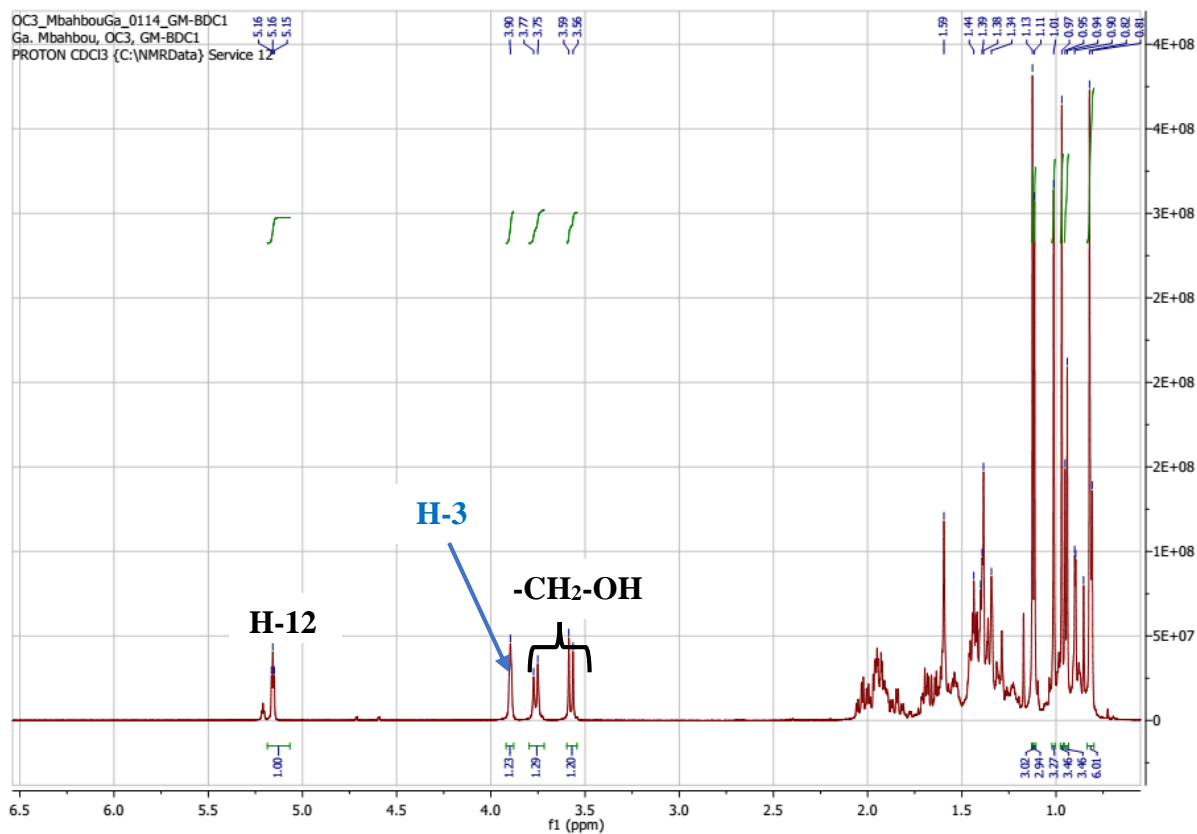**Figure 22: ¹H NMR (500 MHz, CD₃OD) spectrum of compound BDC1**

Figure 23: Expanded ¹H NMR (500 MHz, CD₃OD) spectrum of compound BDC1

The ¹³C NMR spectrum (**Fig24**) showed 30 signals for 30 carbon resonances amongst which are the Urs-12-ene diagnostic signals at δ_C 139.5(C-13) and δ_C 124.4 (C-12) as well as

oxymethine carbon signal at δ_C 70.7 and one signal of oxymethylene at δ_C 66.7 attributted respectively to carbon C-3 and C-24 (**Amarinder *et al*., 2017**)
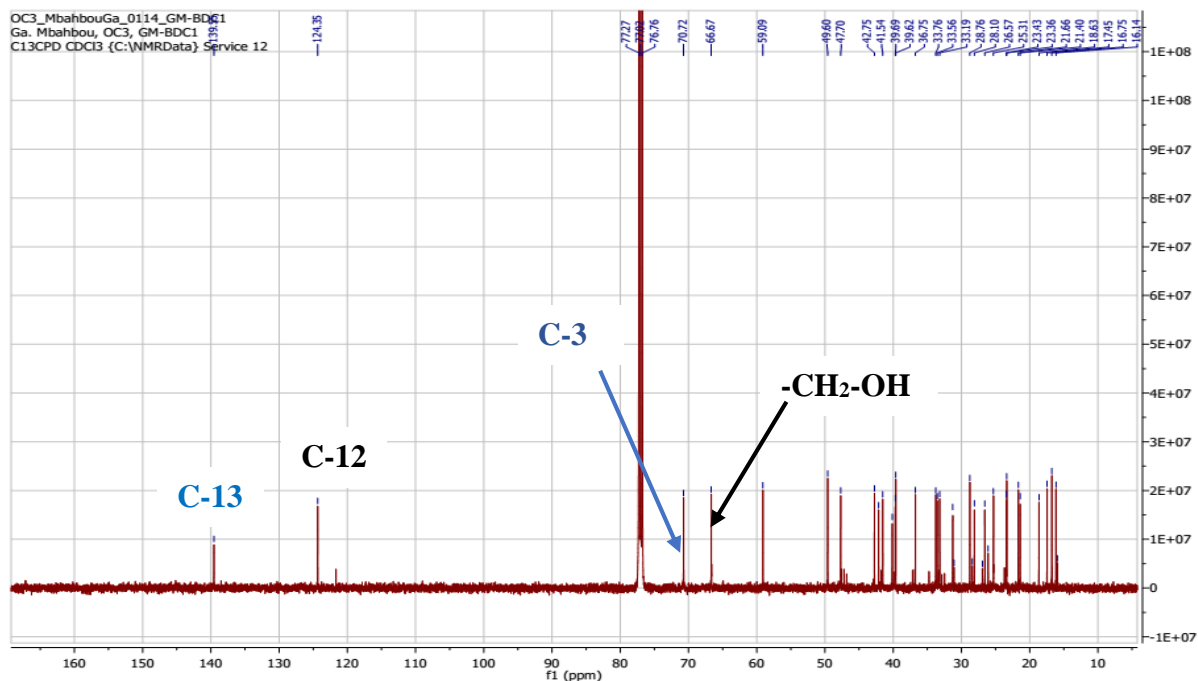
Figure 24: ^{13}C (125 MHz, CD₃OD) NMR spectrum of compound BDC1

The position of oxymethylene was confirmed by the HMBC spectrum (**Fig25**) in which protons H-24a and H-24b showed correlation with carbons at δ_C 70.7 (C-3) δ_C 42.1 (C-4) and δ_C 21.6 (C-23) respectively, this correlation demonstrated that the methyl group at position H-24 was substituted by oxymethylene.
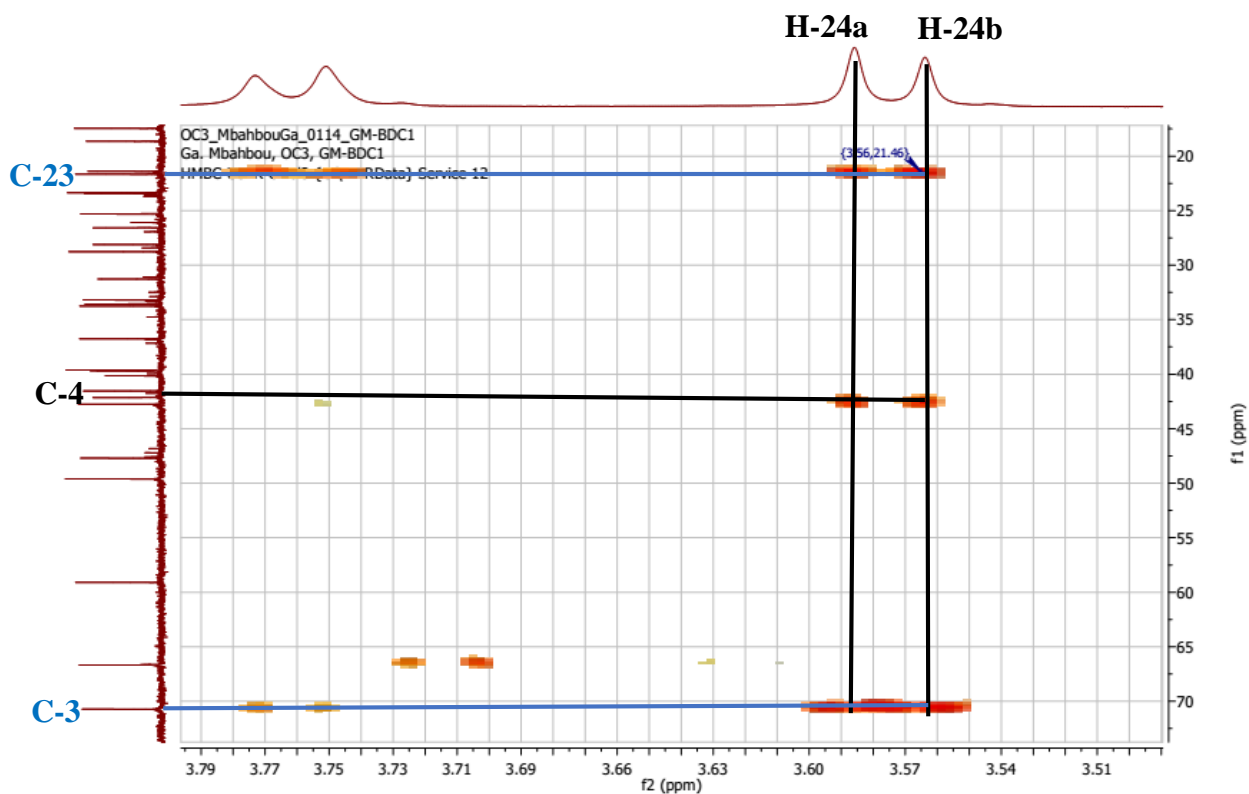
Figure 25: HMBC (125 MHz, CD₃OD) spectrum of compound BDC1

The rest of signals were assigned by comparison of the spectroscopic data with that reported by (**Amarinder** *et al*.**, 2017; Pu** *et al*.**, 2011**) which led to the attribution of the structure of Urs-12-ene-3α,24β-diol (**57**) to **BDC1**.

Table 15: ^{13}C NMR (125 MHz) data of BDC1 and ^{13}C NMR data of Urs-12-ene-3α,24β-diol (125 MHz) (Amarinder _et al._, 2017; Pu _et al._, 2011) in CD₃OD

	BDC1		Urs-12-ene-3α,24β-diol (Amarinder _et al._, 2017; Pu _et al._, 2011)	
POSITION	δ_C	δ_H	δ_C	δ_H
1	33.6		33.6	
2	25.3		25.2	
3	70.7	3.90 (s)	70.7	3.72 (br. s)
4	42.1		42.1	
5	47.7	1.59 (m)	47.7	1.65 (m)
6	18.6		18.6	
7	33.2		33.2	
8	40.1		40.1	
9	49.6	1.60 (m)	49.6	1.72 (m)
10	36.7		36.7	
11	23.3		23.4	
12	124.4	5.16(1H, t, $J = 3.6$ Hz)	124.1	5.16 (1H, t, $J = 3.5$ Hz)
13	139.5		139.6	
14	42.7		42.7	
15	28.1		28.1	
16	26.6		26.6	
17	33.7		33.7	
18	59.1	1.34 (m)	59.1	1.32 (m)
19	39.7	1.28 (m)	39.7	1.28 (m)
20	39.6	1.40 (m)	39.6	1.41 (m)
21	31.3		31.3	
22	41.5		41.5	
23	21.6	1.11 (s)	21.7	1.08 (s)
24	66.7	3.76-3.56 (2H, d, J=11.1 Hz)	66.5	3.58, 3.44 (2H, d, J=11.3 Hz)
25	16.7	0.97 (s)	16.7	0.98 (s)
26	16.1	1.01 (s)	16.2	1.04 (s)
27	23.4	1.13 (s)	23.4	1.13 (s)
28	28.8	0.83 (s)	28.8	0.83 (s)
29	17.4	0.82 (d, J=7.3)	17.5	0.82 (d, J=6.5)
30	21.4	0.94 (d, J=6.3)	21.4	0.94 (d, J=6.3)

2.2.3.5. Identification of the structure of BDR1

BDR1 was obtained from the Hexane fraction from the branches of _Boswellia dalzielii_ as a white powder soluble in CHCl₃ and the Liebermann-Buchard test for triterpenes is positive (red-violet coloration). The spectroscopic data allows us to identify compound **BDR1** to mixture of structures (**26)** and **(58)** below.
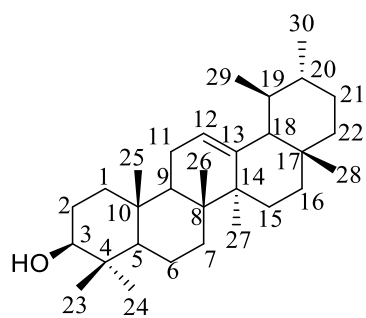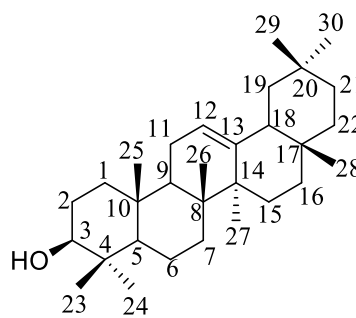
(26)   **(58)**

Its ^{1}H-NMR spectrum (**Fig26** and **27**) revealed the presence of;

- Two olefinic protons appearing as a triplet at δ_H 5.21 (H-12) and δ_H 5.15 (H-12) which are characteristic of olean-12-ene and Urs-12-ene triterpene

-A methine proton assignable to H-3 at δ_H 3.43
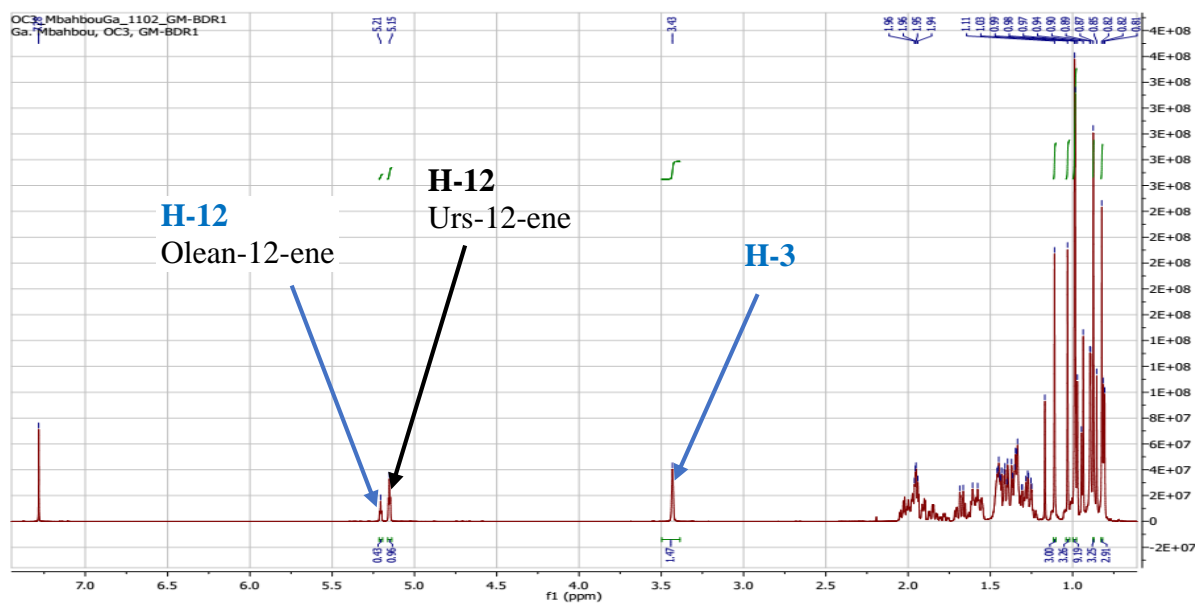
Figure 26: ^{1}H NMR (500MHz, CDCl₃) spectrum of compound BDR1

Sixteen singlets of methyl groups appearing at δ_H 0.82, 0.85, 0.87, 0.89, 0.90, 0.93, 0.95, 1.11 and 0.82, 0.94, 0.95, 0.99, 1.03, 1.11, 1.17 which are characteristic of olean-12-ene and Urs-12-ene of triterpenes respectively.
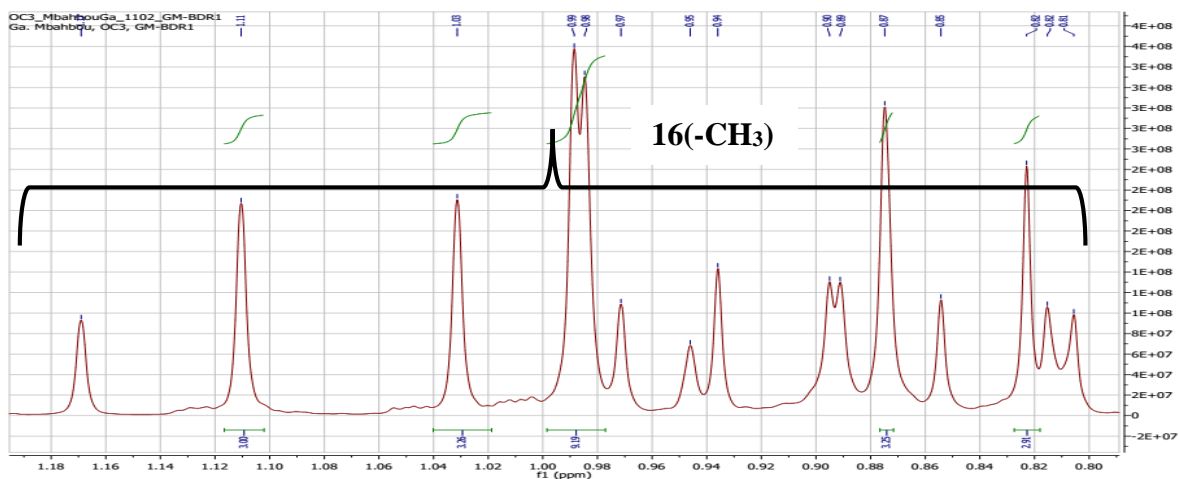
Figure 27: Expanded ^{1}H NMR (500MHz, CDCl₃) spectrum of compound BDR1

A combined analysis of a part of the ^{13}C-NMR spectrum (**Fig28**) and DEPT 135 spectrum (**Fig29**), revealed the presence of sixty signals which could be grouped into sixteen methyls, twenty-five methylenes and methines and nineteen quartenary carbons.

The ^{13}C NMR spectrum (**Fig28**) showed:

- Signals at δ_C 121.78 and 145.20 representing two olefenic carbons which are respectively characteristic of C-12 and C-13 of olean-12-ene triterpenes (**Mahato and Kundu, 1994**).

- Signals at δ_C 124.47 (C-12) and 139.56 (C-13) typical of Urs-12-ene triterpenes (**Mahato and Kundu, 1994**
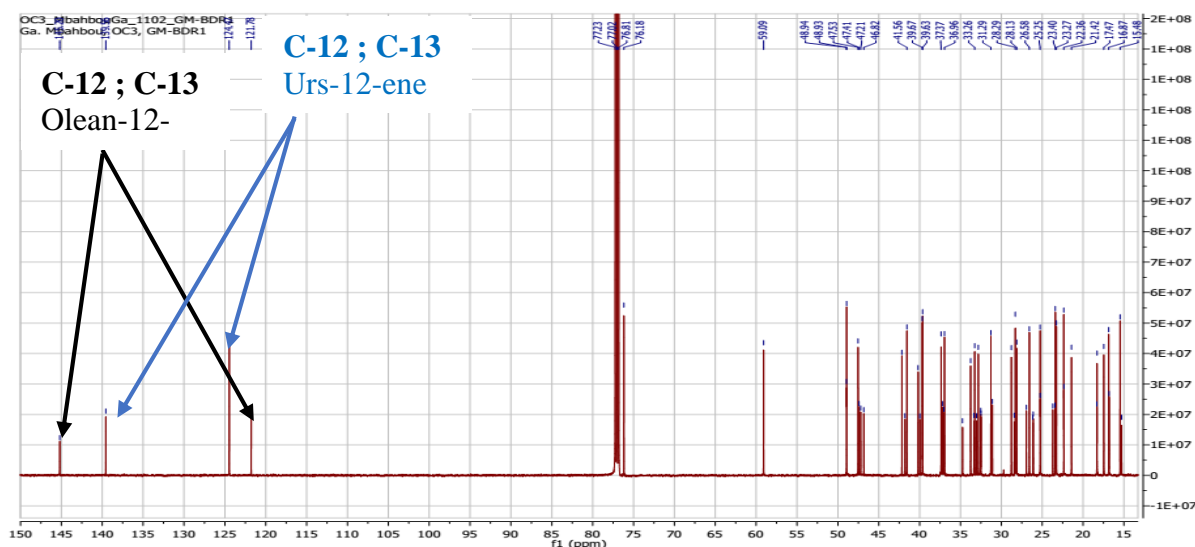
Figure 28: ^{13}C NMR (125 MHz, CDCl₃) spectrum of compound BDR1
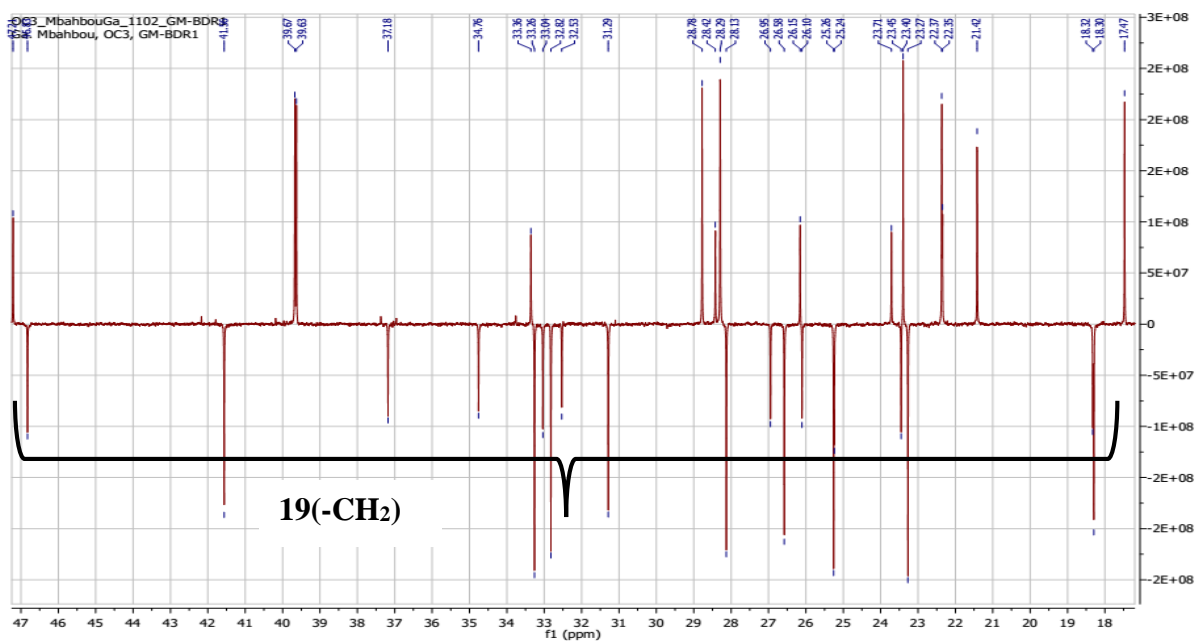
Figure 29: DEPT 135 (125 MHz, CDCl₃) spectrum of compound BDR1

The above spectroscopic data compared with the data of previous reports (**Mahato and Kundu, 1994**) helps us to conclude that, **BDR1** is a mixture of α-amyrin and β-amyrin (**26**) and (**58**).

Table 16: ^{13}C NMR (125 MHz, CD$_3$OD) data of BDR1 compared to those of α-amyrin and β-amyrin (Mahato and Kundu, 1994)

	BDR1(a)	α-amyrin (Mahato and Kundu, 1994)	BDR1(b)	β-amyrin (Mahato and Kundu, 1994)
POSITION	δ_C	δ_C	δ_C	δ_C
1	39.7	38.7	39.7	38.7
2	28.1	27.2	28.1	27.3
3	76.2	78.3	76.2	79.0
4	39.7	38.7	39.9	38.8
5	49.0	55.2	49.0	55.3
6	18.3	18.3	18.3	18.5
7	33.0	32.9	32.8	32.8
8	40.2	40.0	39.9	38.8
9	48.9	47.7	47.5	47.7
10	36.9	36.9	37.4	37.6
11	23.3	23.3	23.5	23.6
12	124.5	124.3	121.8	121.8
13	139.6	139.3	145.2	145.1
14	42.2	42.0	41.8	41.8
15	28.7	28.7	26.2	26.2
16	26.6	26.6	26.9	27.0
17	33.7	33.7	32.5	32.5
18	59.1	58.9	47.4	47.4
19	39.6	39.6	46.8	46.9
20	39.6	39.6	31.1	31.1
21	31.3	31.2	34.7	34.8
22	41.6	41.5	37.2	37.2
23	28.1	28.1	28.3	28.2
24	15.6	15.6	15.3	15.5
25	15.6	15.6	15.5	15.6
26	16.8	16.8	16.9	16.9
27	23.4	23.3	26.1	26.0
28	28.1	28.1	28.4	28.4
29	17.5	17.4	33.3	33.3
30	21.4	21.3	23.7	23.7

2.2.4. Oleananes

2.2.4.1. Identification of the structure of BDF3B

BDF3B was obtained from the Hex/EA (7:3) fraction from the stem bark of *Boswellia dalzielii* as a white powder soluble in CHCl$_3$ and the Liebermann-Buchard test for triterpenes is positive (red-violet coloration).

The spectroscopic data led to the identification of compound **BDF3B** to structure (**59**) below.
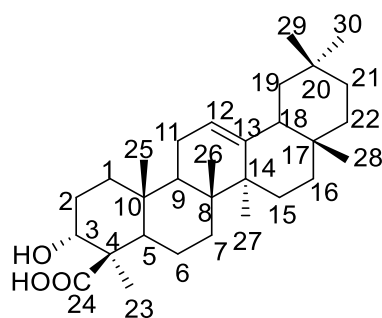
(59)

Indeed its HRESI (**Fig30**) showed the pseudo-molecular ion peak [M-H]⁻ at *m/z* 455.3536 (calcd. 456.3525); so its molecular formula was deduces as $C_{30}H_{48}O_3$ with six double bond equivalent.
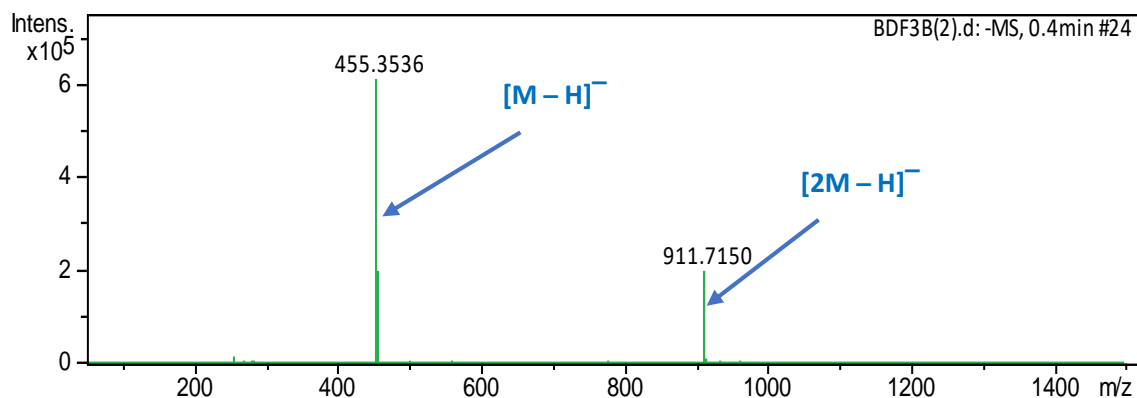
Figure 30: HRESI mass Spectrum of BDF3B

Its ¹H NMR spectrum (**Fig 31** and **32**) displayed the following signals;

-A methine proton at δ_H 4.08 (1H, t, *J*=12Hz) attributable to H-3 (**Culioli *et al*. 2003**)

-An olefenic proton at δ_H 5.19 (1H, t, *J*=3.5Hz) characteristic of H-12 of olean-12-ene triterpenes (**Mahato et Kundu, 1994**)

77
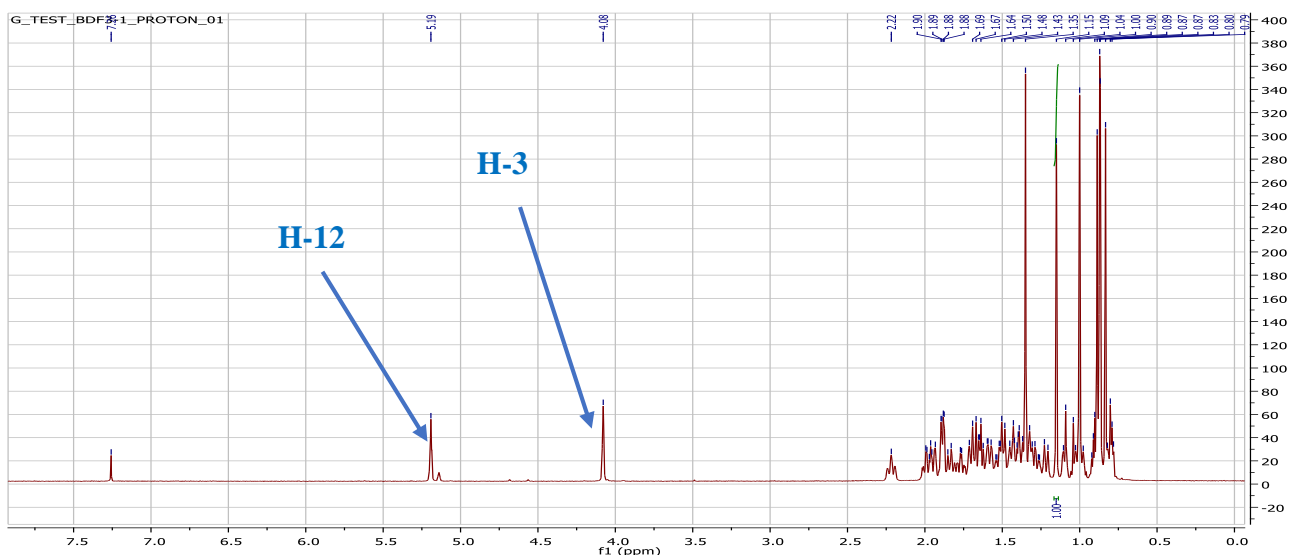
Figure 31: ^{1}H NMR (500 MHz, CDCl₃) spectrum of compound BDF3B

- Seven intense methyl singlets at δ_H 0.84, 0.87, 0.87, 0.89, 1.00, 1.15 and 1.35 typical of oleanane triterpenes and respectively attributable to protons of methyl 28, 29, 30, 25, 26, 27, and 23 (**Mahato et Kundu, 1994**)
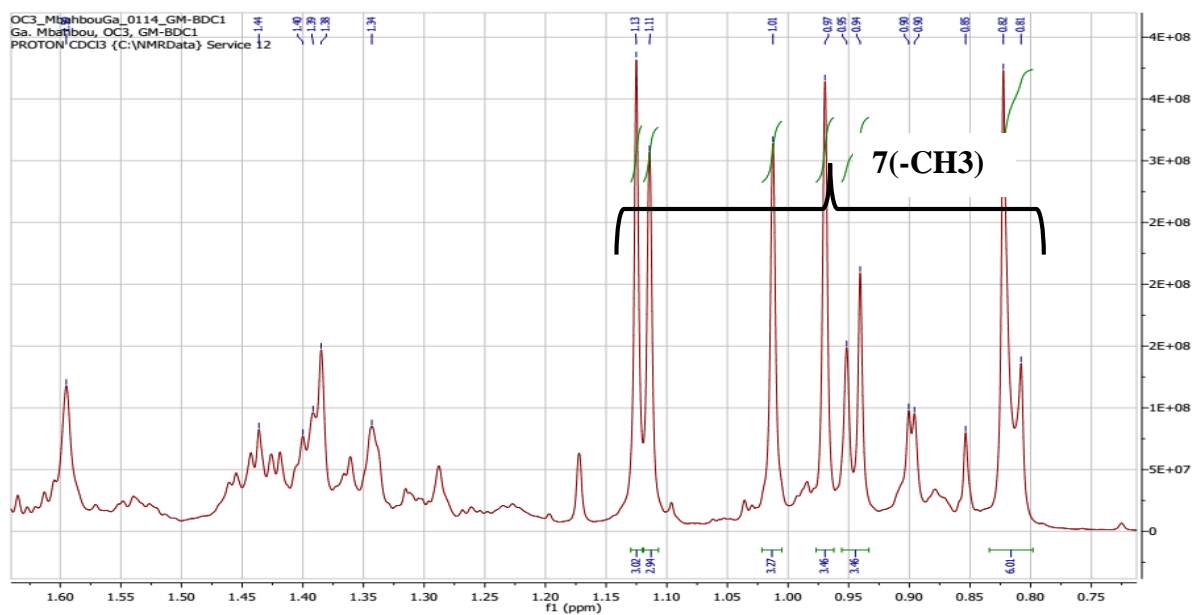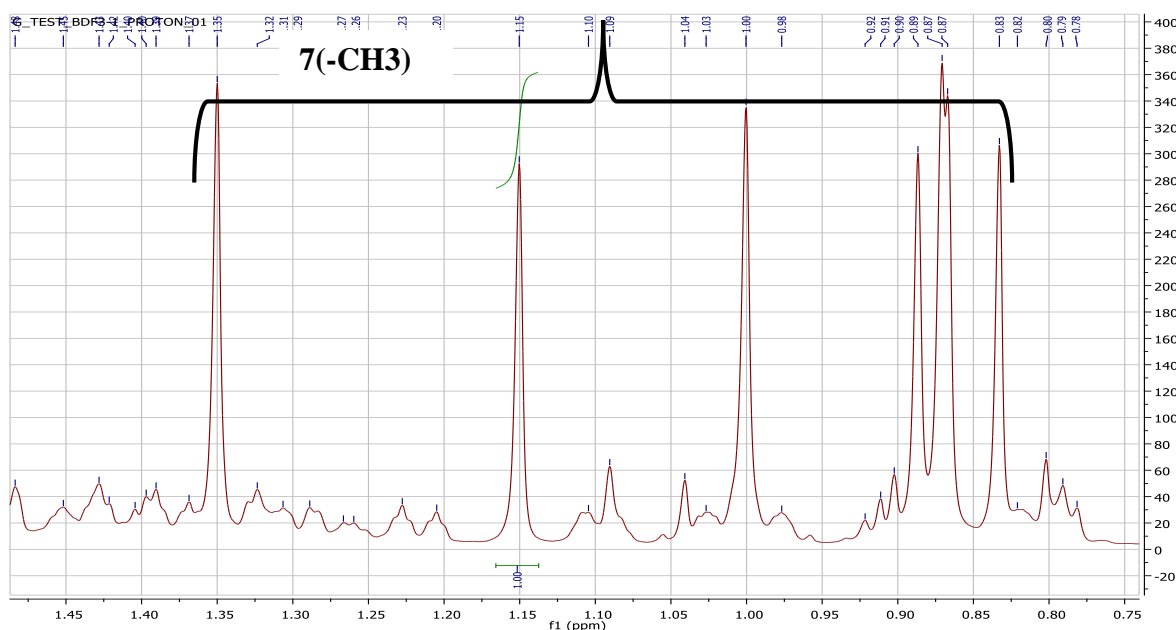

Figure 32: Expanded ^{1}H NMR (500 MHz, CDCl₃) spectrum of compound BDF3B

The ^{13}C NMR spectrum (**Fig33**) showed 30 signals for 30 carbon resonances characteristic of triterpene

- Two signals at δ_C 121.7 and 145.2 which attributed to C-12 and C-13 respectively of Olean-12-ene triterpenes (**Mahato and Kundu, 1994**),

One oxymethine and carboxylic acid signals at δ_C 70.7 and δ_C 182.2, attributable to C-3 and C-24 respectively. The rest of the signals were assigned by comparison of the spectroscopic data with those reported by Culioli *et al*. in 2003
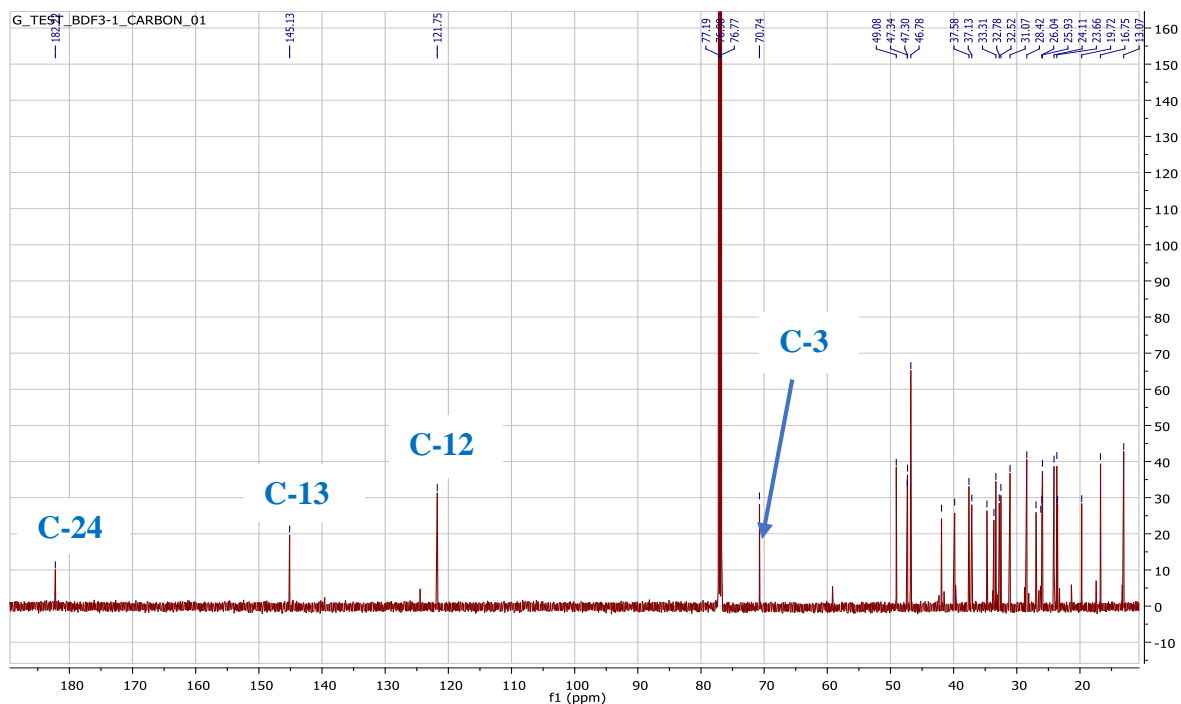
Figure 33: ^{13}C NMR (125 MHz, CDCl₃) spectrum of compound BDF3B

The above spectroscopic data compared with those of previous reports **(Culioli *et al*., 2003)** led to the identification BDF3B to 3α-hydroxy-olean-12-en-24-oic acid (α-boswellic acid) **(59)** with a molecular formular of C₃₀H₄₈O₃.

Table 17: [^1]H NMR (500 MHz) and [^13]C NMR (125 MHz) data of BDF3B and [^1]H NMR (400 MHz) and [^13]C NMR (100MHz) data of α- boswellic acid in CDCl₃

POSITION	BDF3B δ_C (δppm)	δ_H (δppm, J in Hz)	α- boswellic acid (Culioli *et al*. 2003) δ_C (δppm)	δ_H (δppm, J in Hz)
1	33.6	1.45m, 1.29m	33.6	1.45 m ,1.29 m
2	26.2	2.22m	26.2	2.22 m, 1.59 m
3	70.7	4.08 (1H, s)	70.8	4.08 t (2.5)
4	47.4		47.4	
5	49.1	1.49 (m, 1H)	49.1	1.49 m
6	19.7	1.85m, 1.70m	19.7	1.85 m, 1.70 m
7	32.7	1.52m, 1.37m	32.7	1.52 m, 1.37 m
8	39.8		39.8	
9	46.8	1.66m	46.7	1.66 m
10	37.6		37.6	
11	23.5	1.88m	23.5	1.88 m
12	121.7	5.19 (1H, s)	121.7	5.19 t (3.5)
13	145.1		145.1	
14	41.9		41.9	
15	26.0	1.77m, 1.00m	26.0	1.77 m, 1.00 m
16	26.9	2.00m, 0.81m	26.9	2.00 m, 0.81 m
17	32.5		32.5	
18	47.3	1.96m	47.3	1.96 m
19	46.8	1.70m, 1.02m	46.7	1.70 m, 1.02 m
20	31.1		31.1	
21	34.7	1.33m, 1.10m	34.7	1.33 m, 1.10 m
22	37.1	1.44m, 1.22m	37.1	1.44 m, 1.22 m
23	24.1	1.35 (s)	24.2	1.35 s
24	182.2		183.2	
25	13.0	0.89 (s)	13.1	0.89 s
26	16.7	1.00 (s)	16.7	1.00 s
27	25.9	1.15(s)	25.9	1.15 s
28	28.4	0.84 (s)	28.4	0.84 s
29	33.3	0.87 (s)	33.3	0.87 s
30	23.6	0.87 (s)	23.7	0.87 s

2.2.4.2. Identification of the structure of BDb1

Compound **BDb1** was obtained from the arial part extract of *Boswellia dalzielii* as white powder in pure hexane and it is soluble in CDCl₃. It gives a red-violet coloration to the Liebermann-Burchard test reagent, suggestive of a triterpenoid nature. The spectroscopic data led to the identification of compound **BDb1** to structure (**60)** following.
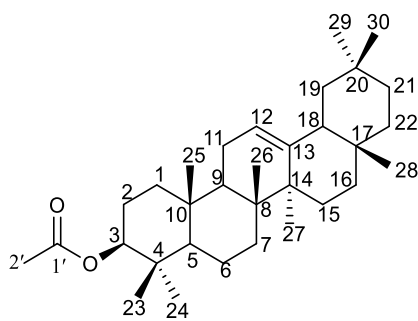
(60)

Its ^{1}H-NMR spectrum (**Fig34**) revealed the presence of;

- An olefinic proton appearing as a triplet at δ_H 5.18 (J = 5.0 Hz) and eight singlets of methyl groups appearing at δ_H 0.82, 0.85, 0.88, 0.91, 0.91, 0.93, 0.95 and 1.08 which are characteristic of olean-12-ene triterpenes, corresponding to the protons of Me-24, Me-28, Me-27, Me-30, Me-25, Me-29, Me-23 and Me-26 respectively.

-A methine proton assignable to H-3 which is shifted downfield to δ_H 4.53 suggesting the presence of a deshielding group close to it.

-An intense singlet of three protons at δ_H 2.06, which is attribuable to one acetyl methyl group.

-A cluster of signals in the region δ_H 1.09 - 2.01 ppm revealed the presence of methylene and methine protons of the pentacyclic triterpene framework.
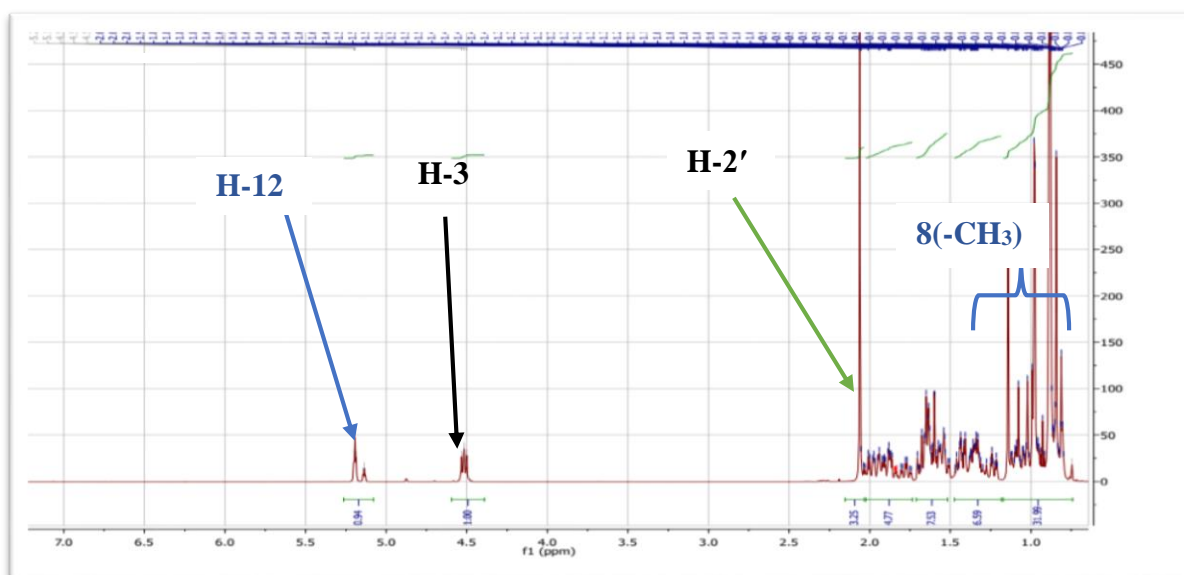
Figure 34: ^{1}H NMR (500 MHz, CDCl$_3$) spectrum of compound BDb1

Its ^{13}C-NMR spectrum (**Fig 35**) showed 32 signals of carbon atoms. The signals at δ_C 145.1 (C-13) and 121.6 (C-12) representing two olefenic carbons are characteristic of olean-12-ene triterpenes (**Mahato and Kundu, 1994**). The signal at δ_C 170.9 (C-1′) suggests the presence of the carbonyl of an ester group. The relative downfield signal at δ_C 80.92 attribuable to C-3 suggests that this carbon is linked to an acetyl group which is responsible for the deshielding effect. The other signals were assigned by comparison with the literature data (**Mahato and Kundu, 1994**).
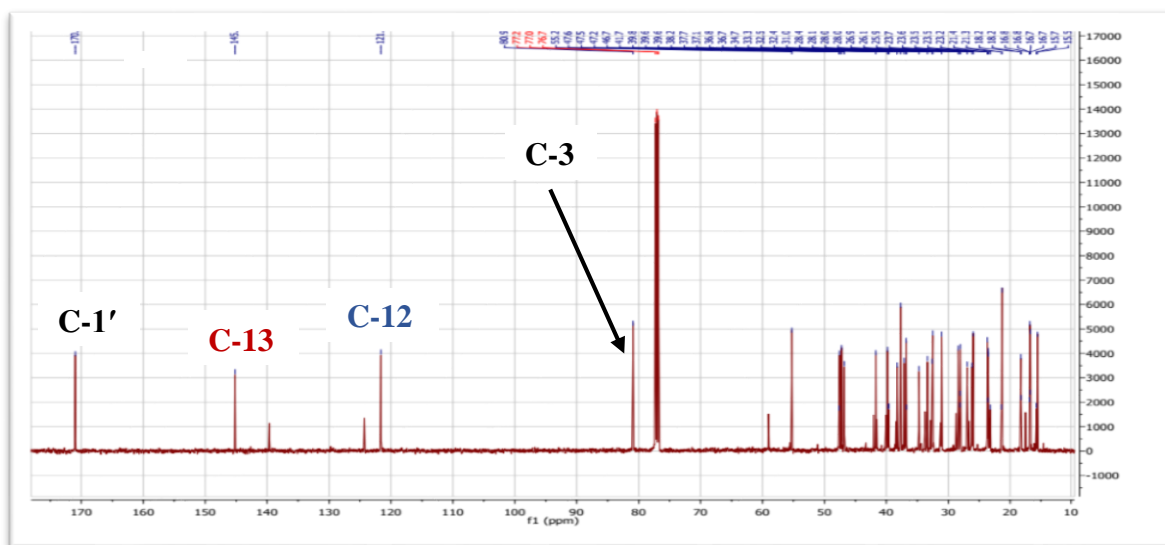
Figure 35: ^{13}C NMR (125 MHz, CDCl₃) spectrum of compound BDb1

The above spectroscopic data compared with the TLC of an authentic sample in the laboratory and the data of previous reports (**Mahato and Kundu, 1994**) led to the attribution of the structure (**60**) to β-amyrin acetate.

Table 18: ^{13}C NMR (125 MHz, CDCl$_3$) data of BDb1 and ^{13}C NMR data compared to ^{13}C NMR data of β-amyrin acetate (Mahato et Kundu, 1994)

POSITION	BDb1 δ_C	β-amyrin acetate (Mahato et Kundu, 1994)
1	38.2	38.5
2	26.1	26.9
3	80.9	81.3
4	36.7	38.3
5	55.2	55.2
6	18.2	18.2
7	32.5	32.6
8	39.6	39.8
9	47.5	47.6
10	37.7	37.1
11	16.8	23.5
12	121.6	121.6
13	145.1	145.2
14	41.7	41.7
15	28.4	28.4
16	28.0	26.1
17	32.5	32.5
18	47.2	47.2
19	46.7	46.8
20	31.0	31.0
21	34.7	34.7
22	37.7	37.7
23	28.1	28.1
24	15.5	15.5
25	15.7	15.5
26	16.8	16.8
27	25.9	25.9
28	28.1	28.0
29	33.3	33.3
30	23.5	23.7
1′	170.9	171.0
2′	21.3	21.3

2.2.4.3. Identification of the structure of BDb16

BDb16 was obtained from the extract of the branches of *Boswellia dalzielii* as a white powder in Hex/EA (7:3). It is soluble in DCM and the Liebermann-Buchard test for triterpenes is positive (red-violet coloration). The spectroscopic data led to the identification of compound **BDb16** to structures **(19)** and **(61)** below.

(19)   **(61)**
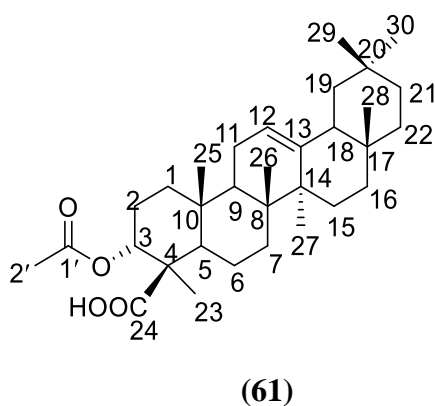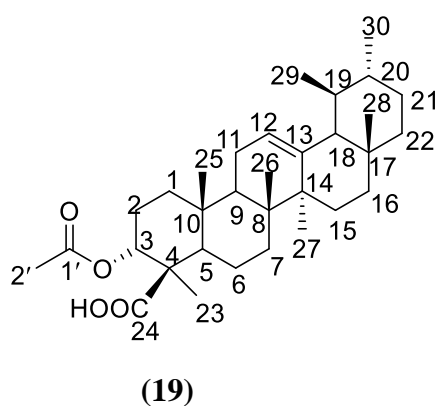
Its ^{1}H NMR spectrum (**Fig36** and **37)** displayed two signals for vinyl protons as a triplet at δ_H 5.17 (H-12) Urs-12-ene and 5.22 (H-12) olean-12-ene

- A oxymethine proton which resonates at δ_H 5.32 (d, J = 2.6 Hz, 2H) assignable to H-3 of triterpenes

- Two intense singlet of three protons at δ_H 2.12; δ_H 2.11 which is attributable to two acetyl methyl group
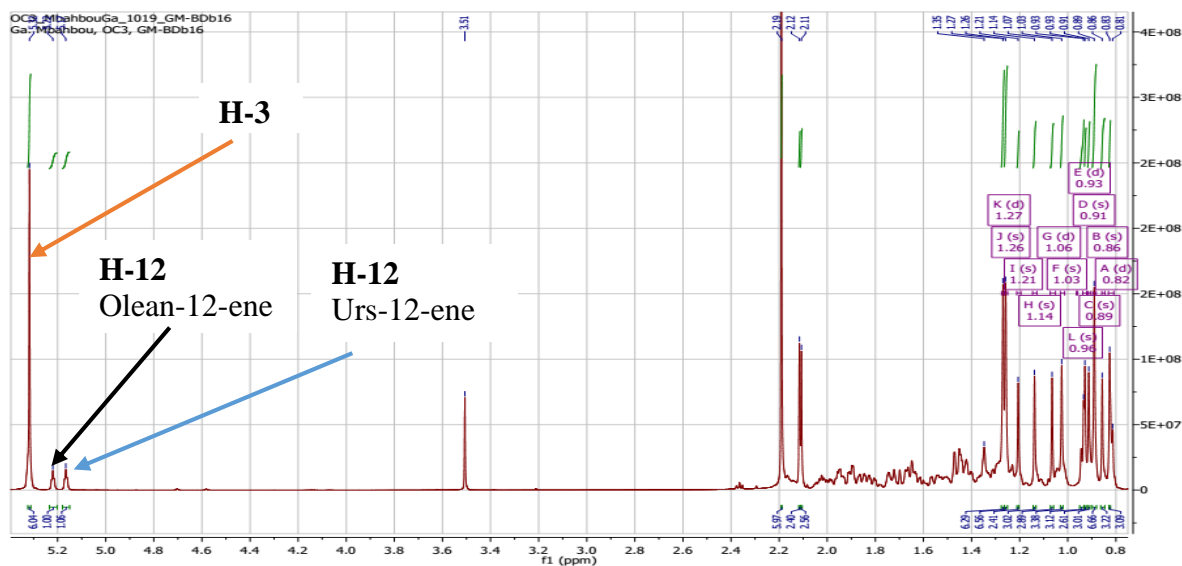
Figure 36: ^{1}H NMR (500 MHz, CDCl$_3$) spectrum of BDb16
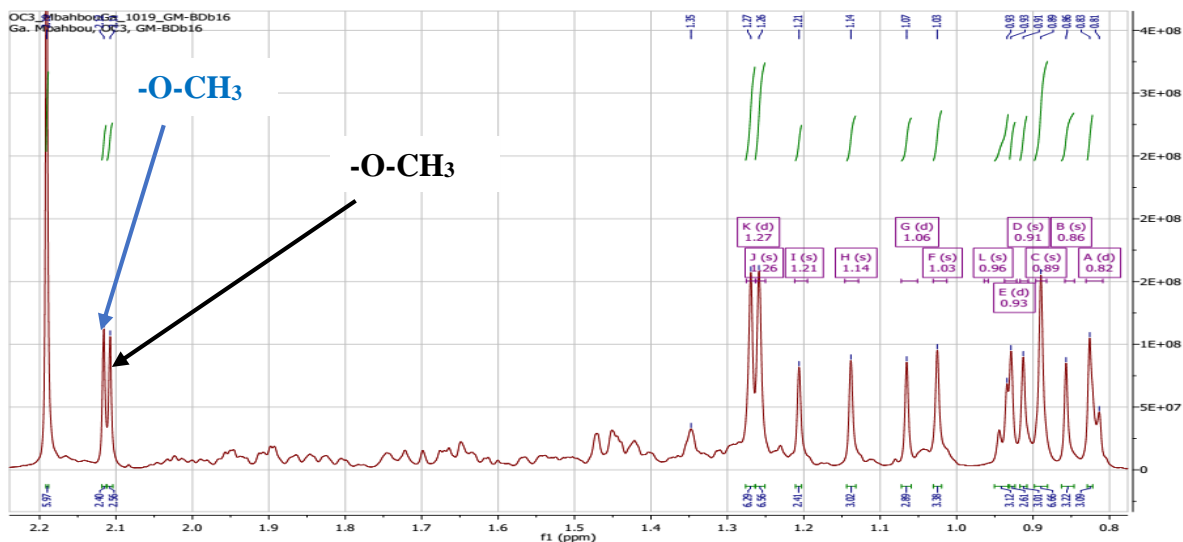
Figure 37: Expanded ^{1}H NMR (500 MHz, CDCl$_3$) spectrum of BDb16

- Two methyl groups as doublets at δ_H 0.82(d, J = 4.8 Hz, 3H) and δ_H 0.96 (d, J = 5.9 Hz, 3H) both suggestive of methyls 29 and 30 of Urs-12-ene skeleton. (**Mahato et Kundu, 1994**)

- Five intense angular methyl signals are also observed at $\delta_{H:}$ 0.86, 0.93, 1.06, 1.14, 1.26 which are characteristic of Urs-12-ene triterpenes (**Mahato et Kundu, 1994**)

- seven singlets of methyl groups appearing at δ_H 0.85, 0.89, 0.89, 0.91, 0.93, 0.96 and 1.27 which are characteristic of olean-12-ene triterpenes;
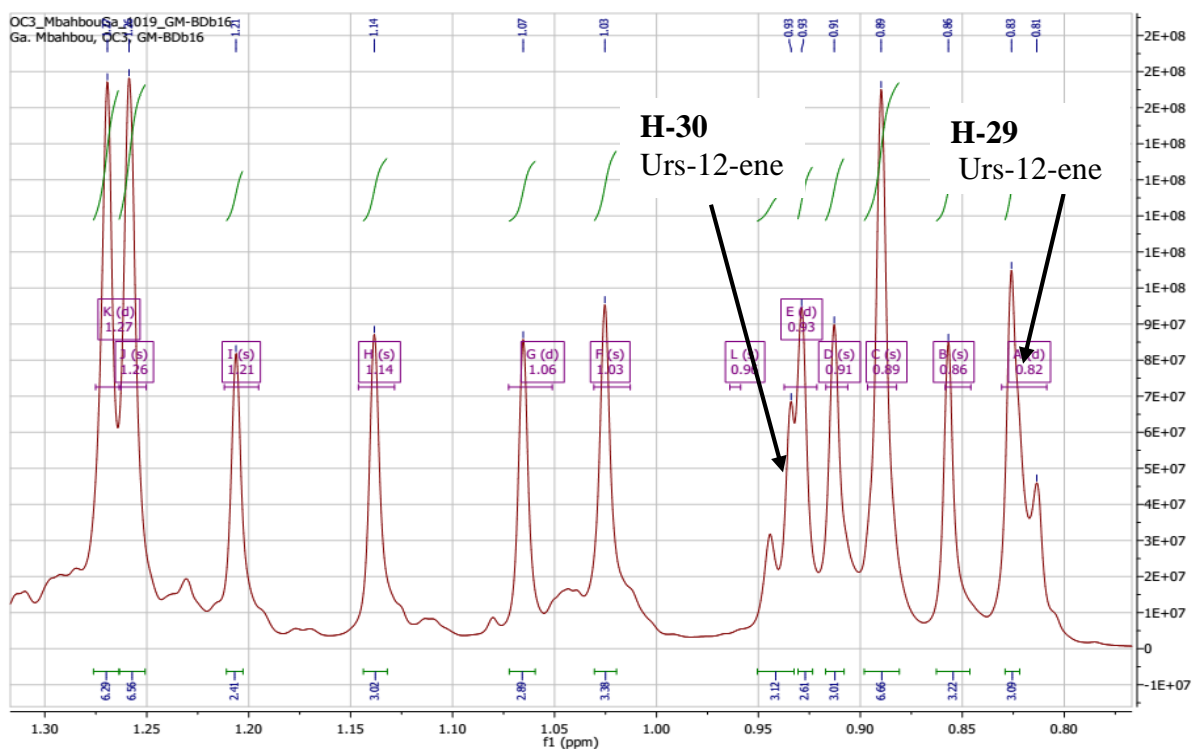
Figure 38: Expanded (2) ^{1}H NMR (500 MHz, CDCl$_3$) spectrum of compound BDB16

The ^{13}C NMR spectrum (**Fig39**) revealed the presence of sixty-four carbon resonances amongst which these are the Urs-12-ene diagnostic signals at δ_C 139.6 (C-13) and δ_C 124.5 (C-12) (**Mahato *et* Kundu, 1994**), and the olean-12-ene signals at δ_C 145.1 (C-13) and δ_C 121.8 (C-12) (**Mahato *et* Kundu, 1994**).

Two signals at δ_C 182.2, 182.1 and δ_C 170.4, 170.3 are ascribable to two carboxylic acid group and a two carbonyl of an ester group C-1′ respectively (**Belsner *et al.*, 2003**). We also observe a signal at δ_C 73.2 (2H) assignable to C-3 of triterpenes.

The DEPT 135 (**Fig41**) experiment revealed the presence of 17 quaternary carbons, 19 secondary sp2 carbons, 28 tertiary carbons and primary sp3 carbons.
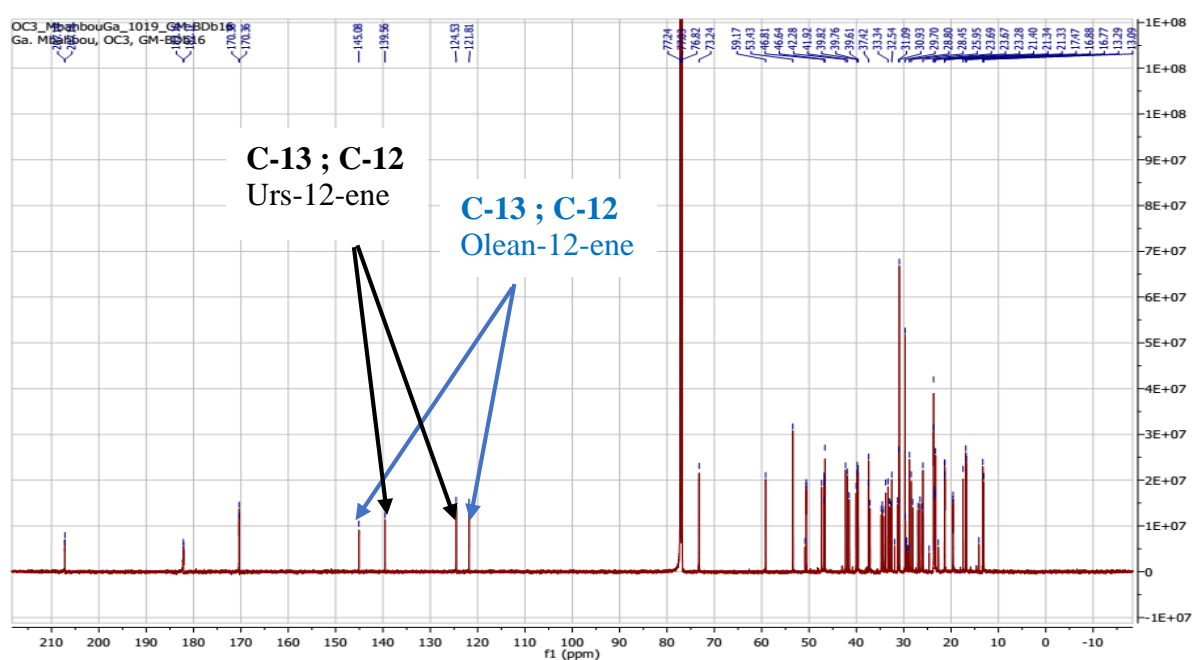
Figure 39: ^{13}C NMR (125 MHz, CDCl₃) spectrum of compound BDb16
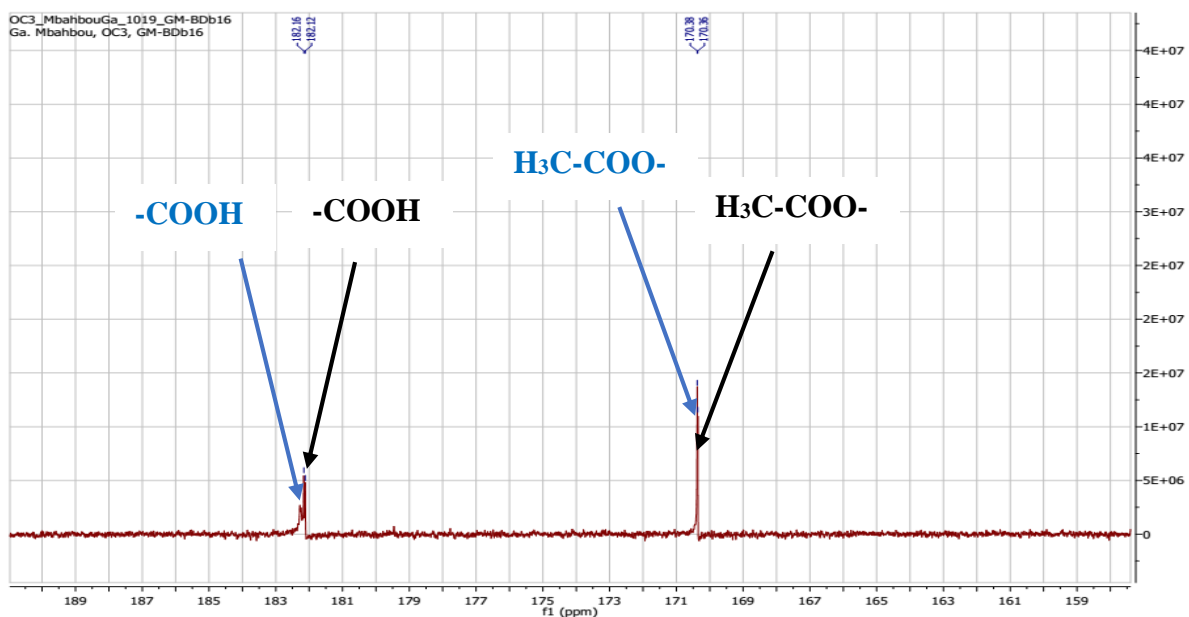
Figure 40: ^{13}C NMR (125 MHz, CDCl$_3$) spectrum of compound BDb16
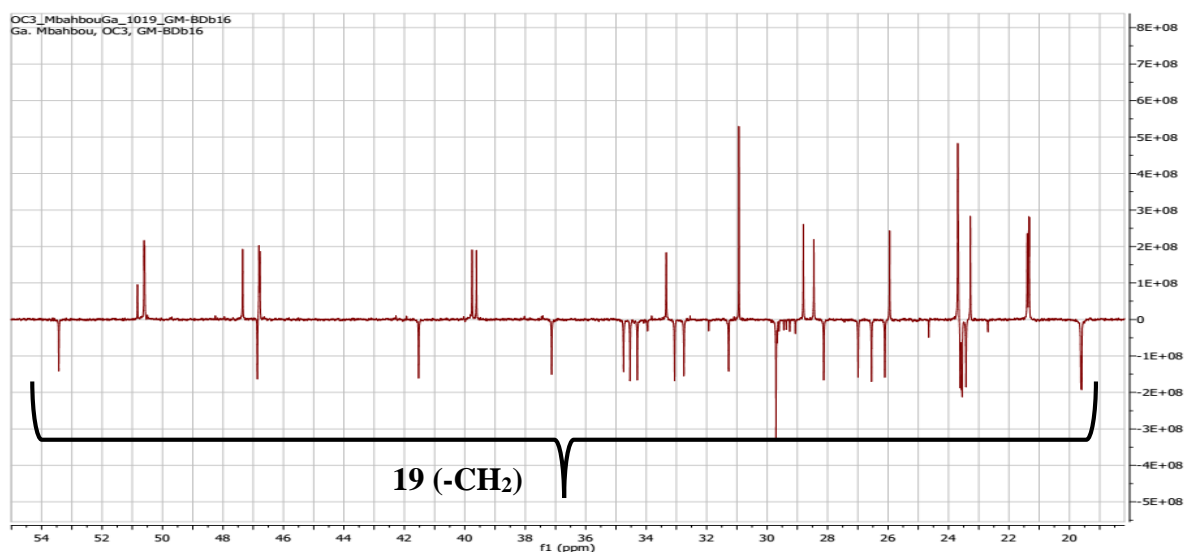
Figure 41: DEPT 135 (125 MHz, CDCl$_3$) spectrum of compound BDb16

The position of carboxylic acid group was confirmed by the HMBC (**Fig42**) correlation in which the two methyl group at position H-23 showed correlation with two carboxylic acid group δ_C 182.2, 182.1.
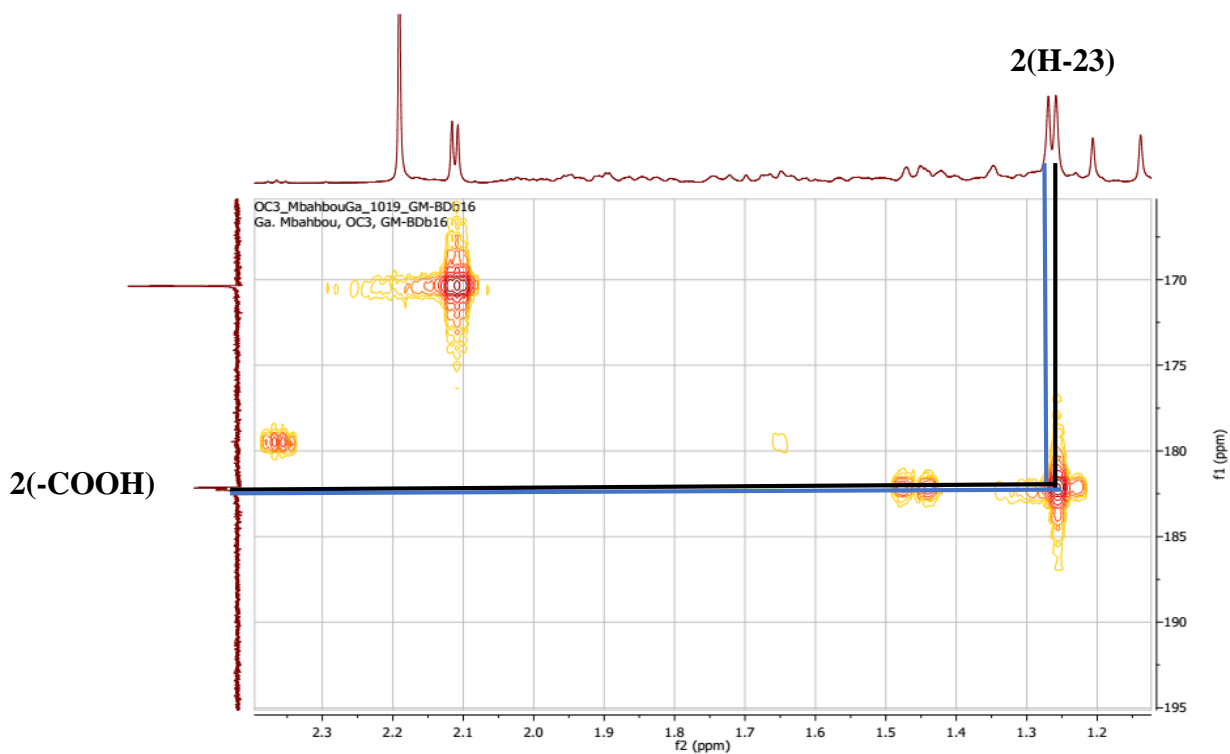
Figure 42: HMBC (CDCl₃) spectrum of compound BDb16

By the comparison of its NMR data with those reported in the literature (**Belsner *et al.*, 2003**) this **BDb16** have been identified as a mixture of 3α-acetyl-β-boswellic acid **(19)** and 3α-acetyl-α-boswellic **(61)**.

Table 19: ^{1}H NMR (500 MHz) and ^{13}C NMR (125 MHz) data of BDb16 compared to ^{1}H NMR (400 MHz) and ^{13}C NMR (100 MHz) data of 3α-acetyl-β-boswellic acid (BDb16) and 3α-acetyl-α-boswellic acid (BDF3A) in CDCl₃

POSITION	BDb16 δ_C	3α-acetyl-α-boswellic acid (Klaus et al., 2003) δ_C	BDF3A (19) δ_C	3α-acetyl-β-boswellic acid (Klaus et al., 2003) δ_C
1	34.3	34.4	34.5	34.6
2	23.6	23.6	23.6	23.6
3	73.2	73.6	73.2	73.4
4	46.7	46.7	46.7	46.7
5	50.6	50.7	50.6	50.7
6	16.7	16.7	19.6	19.6
7	32.7	32.8	33.1	33.1
8	39.8	39.9	40.0	40.1
9	46.8	46.8	46.8	46.8
10	37.4	37.5	37.4	37.4
11	23.5	23.6	23.4	23.4
12	121.8	121.9	124.5	124.6
13	145.2	145.2	139.6	139.6
14	41.9	41.9	42.3	42.3
15	26.1	26.1	26.6	26.6
16	26.9	27.0	28.1	28.2
17	32.5	32.6	33.8	33.8
18	47.3	47.4	59.2	59.2
19	46.9	46.9	39.6	39.6
20	31.1	31.1	39.7	39.8
21	34.7	34.8	31.3	31.3
22	37.1	37.2	41.5	41.6
23	23.7	23.8	23.7	23.7
24	182.1	182.2	182.2	182.3
25	13.1	13.2	13.4	13.4
26	16.7	16.8	16.9	16.9
27	25.9	25.9	23.3	23.3
28	28.4	28.4	28.8	28.8
29	23.6	23.7	17.5	17.5
30	33.1	33.3	21.4	21.4
1′	170.4	170.4	170.6	170.4
2″	21.3	21.3	21.3	21.3

2.2.5. Lupanes

2.2.5.1. Identification of the structure of BDF2B

BDF2B was obtained as a white powder from Hex/EA (8/2) fraction of the stem bark of *Boswellia dalzielii*. It is soluble in CHCl₃ and gives a red-violet coloration to the Liebermann-

Burchard test reagent indicative of a triterpenoid nature. The spectroscopic data allows us to allocate structure (**25**) to **BDF2B**.
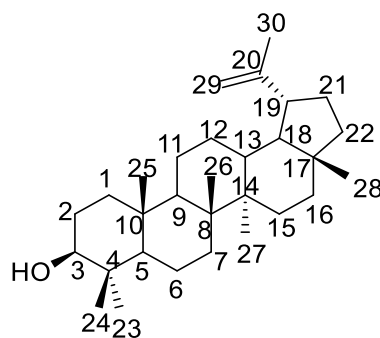
(**25**)

Its ^{1}H NMR spectrum (**Fig43**) displayed the following signals;

-Six methyl singlets at δ_H 0.77, 1.02, 0.96, 1.03, 0.81 and 0.95 corresponding to methyl 24, 23, 25, 26, 28 and 27 respectively of the lupane skeleton.

-Two intense broad singlets at δ_H 4.58 and 4.70 characteristic of the exocyclic double bond protons of the lup-20(29)-ene series triterpenes, The two information make us think this can be lup-20(29)-ene series triterpenes.

-A methyl singlet signal at δ_H 1.69 indicating the presence of a vinylic methyl group,

A methane proton at δ_H 3.23 (1H, t, $J=12$Hz) attributable to H-3 of triterpenes
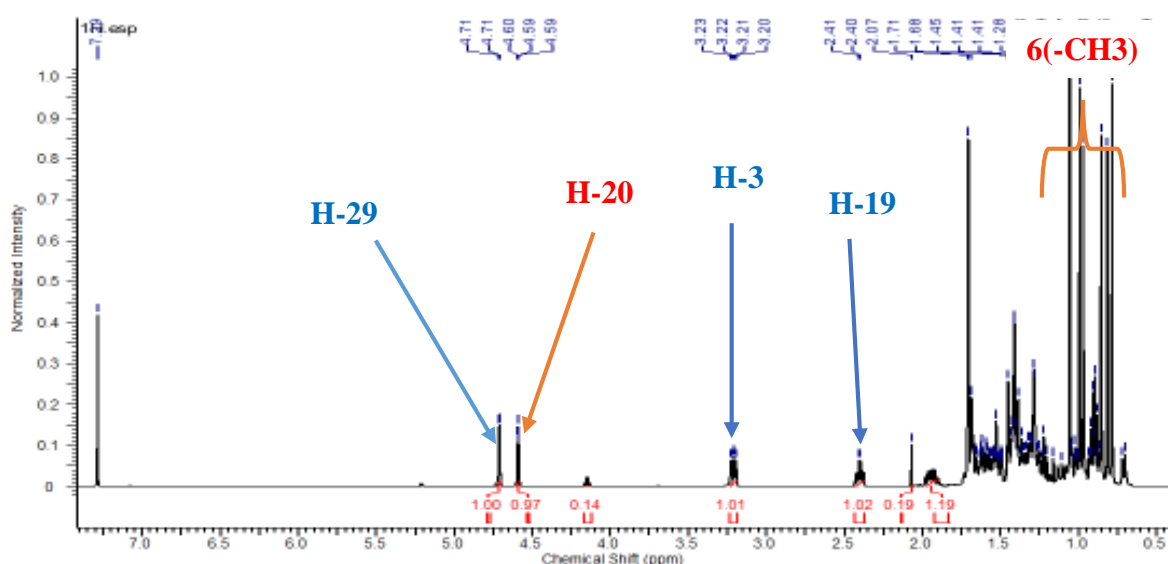
Figure 43: ^{1}H NMR (500 MHz, CDCl₃) spectrum of compound BDF2B

The ^{13}C NMR spectrum **(Fig44)** revealed signals at;

- δ_C 150.9 and 109.3 which are respectively characteristic of C-20 and C-29 of lup-20(29)-ene **(Mahato and Kundu, 1994)**,

-δ_C 79.0 assignable to C-3 hydroxylated of triterpenes.
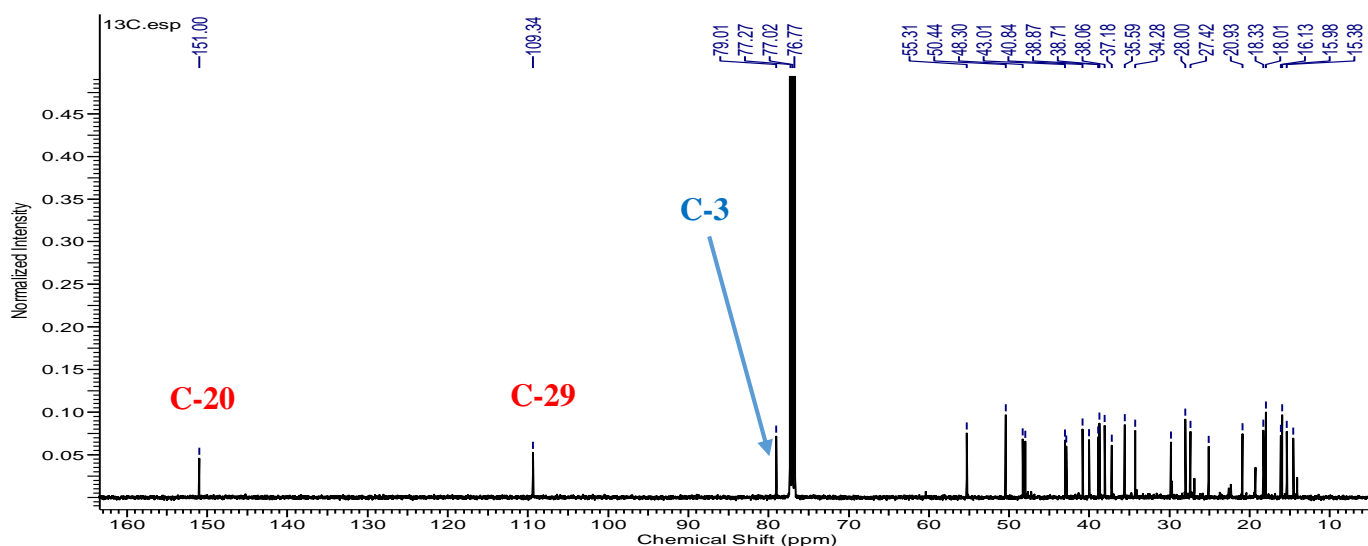
Figure 44: ^{13}C NMR (125 MHz, CDCl$_3$) spectrum of compound BDF2B

The above spectroscopic data compared with those of previous reports **(Mahato and Kundu, 1994)** led to the attribution of the structure **BDF2B (25)** to lupeol.

Table 20: ^{13}C NMR (125 MHz, CDCl₃) data of BDF2B compared to ^{13}C NMR data of lupeol

	BDF2B	lupeol (Mahato and Kundu. 1994)
POSITION	δ_C (δppm)	δ_C (δppm)
1	38.7	38.7
2	27.4	27.4
3	79.0	79.0
4	38.8	38.8
5	55.3	55.3
6	18.3	18.3
7	34.2	34.3
8	40.8	40.8
9	50.4	50.4
10	37.1	37.1
11	20.9	20.9
12	25.1	25.1
13	38.0	38.0
14	42.8	42.8
15	27.4	27.4
16	35.5	35.6
17	43.0	43.0
18	47.9	48.0
19	48.3	48.3
20	151.0	151.6
21	29.8	29.7
22	40.0	40.0
23	28.0	28.0
24	15.3	15.3
25	15.9	15.9
26	16.1	16.1
27	14.5	14.5
28	18.0	18.0
29	109.3	109.3
30	19.3	19.3

2.2.5.2. Identification of the structure of BDF3

Compound **BDF3** was obtained from the extract of the stem bark of *Boswellia dalzielii* at Hex/EA (7:3) fraction as white powder soluble in CHCl₃. It gives a red-violet coloration to the Liebermann-Burchard test for triterpenes. The HRESI and spectroscopic data led to the identification of compound BDF3 to structure **(62)** below.
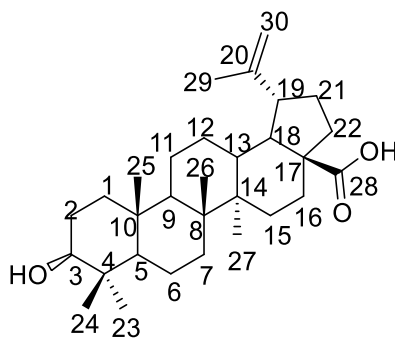
(62)

Its HRESI showed the pseudo-molecular ion peak $[M+H]^+$ at m/z 457.3673 (calcd. 457.3682) for $C_{30}H_{48}O_3$ with seven double bond equivalent. The difference in mass between (lupeol) and BDF3 is 2 oxygen suggesting oxidation of one methyl group into a carboxylic acid.
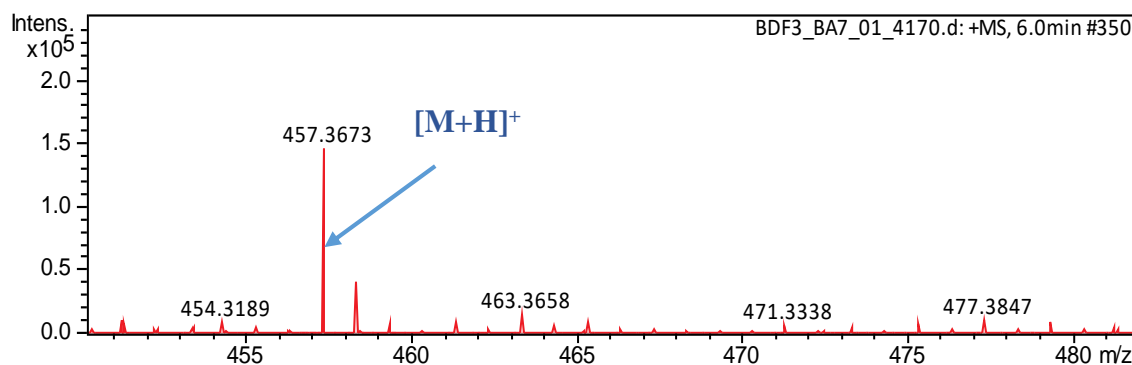
Figure 45: HRESI mass Spectrum of BDF3

Its ^1H NMR spectrum (**Fig46**) is identical to that of lupeol except for the absence of one methyl. We observe;

-Two intense broad singlets at δ_H 4.76 and 4.63 diagnostic of the exocyclic double bond protons (H-29) of the lup-20(29)-ene series triterpenes,

-A methine proton at δ_H 3.21 (dd, J = 11.4, 4.8 Hz, 1H) attributable to H-3 of triterpenes, and a multiplet at δ_H 3.02 assignable to H-19

-Five upfield methyl singlets at δ_H 0.78, 0.85, 0.96, 0.99 and 1.00 and a lowfield methyl singlet signal at δ_H 1.71 indicating the presence of a vinylic methyl group ascribable to CH_3-30 of the lupane skeleton.
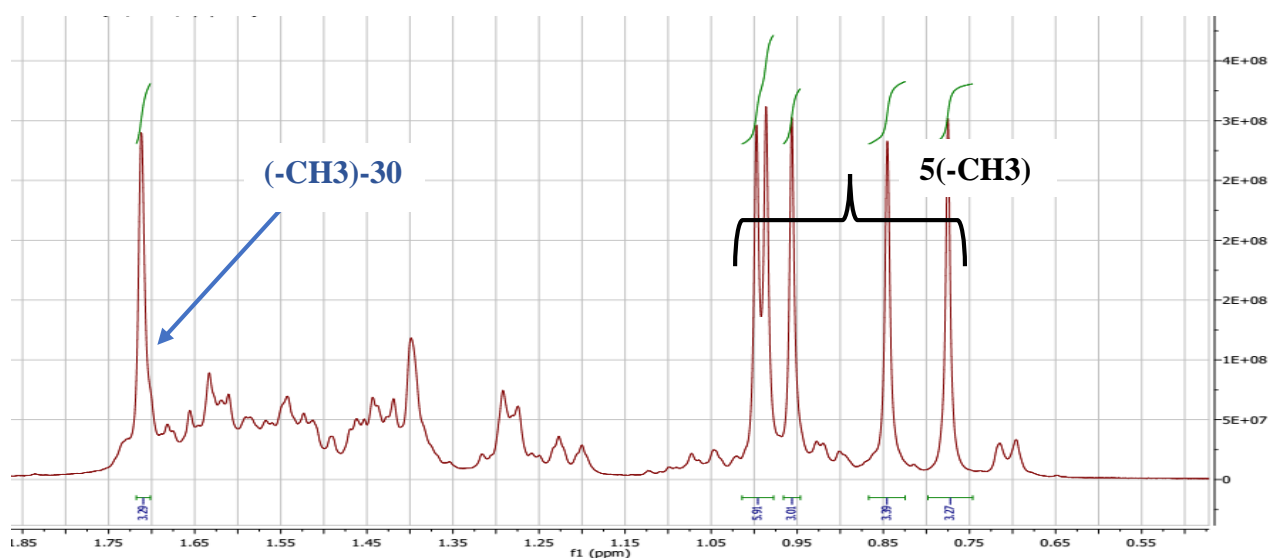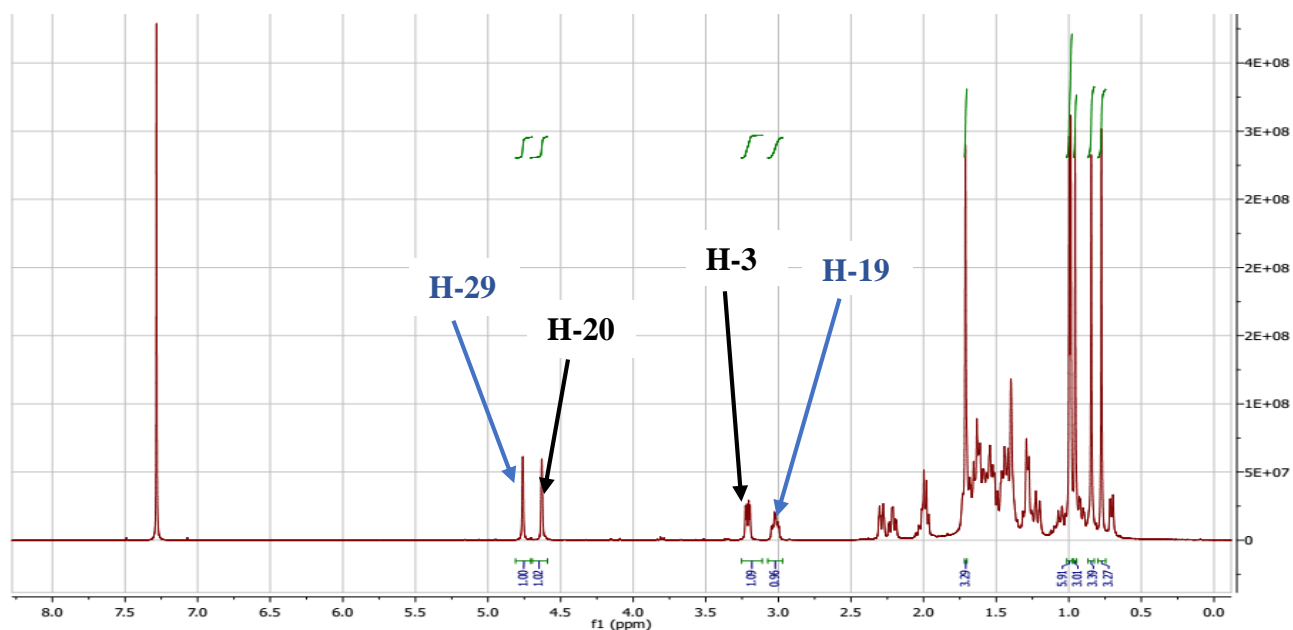
Figure 46: Expanded ¹H NMR (500 MHz, CDCl₃) spectrum of compound BDF3

The ^{13}C NMR spectrum **(Fig47)** revealed signals at;

- δ_C 150.9 and 109.3 which are characteristic of C-20 and C-29 respectively of lup-20(29)-ene triterpenes **(Mahato and Kundu, 1994)**,

- δ_C 79.0 assignable to C-3 of triterpenes.

- One carboxylic acid signals at δ_C 180.4, attributable to C-28. This position was confirmed by comparison with data reported by **Mahato and Kundu in 1994**.
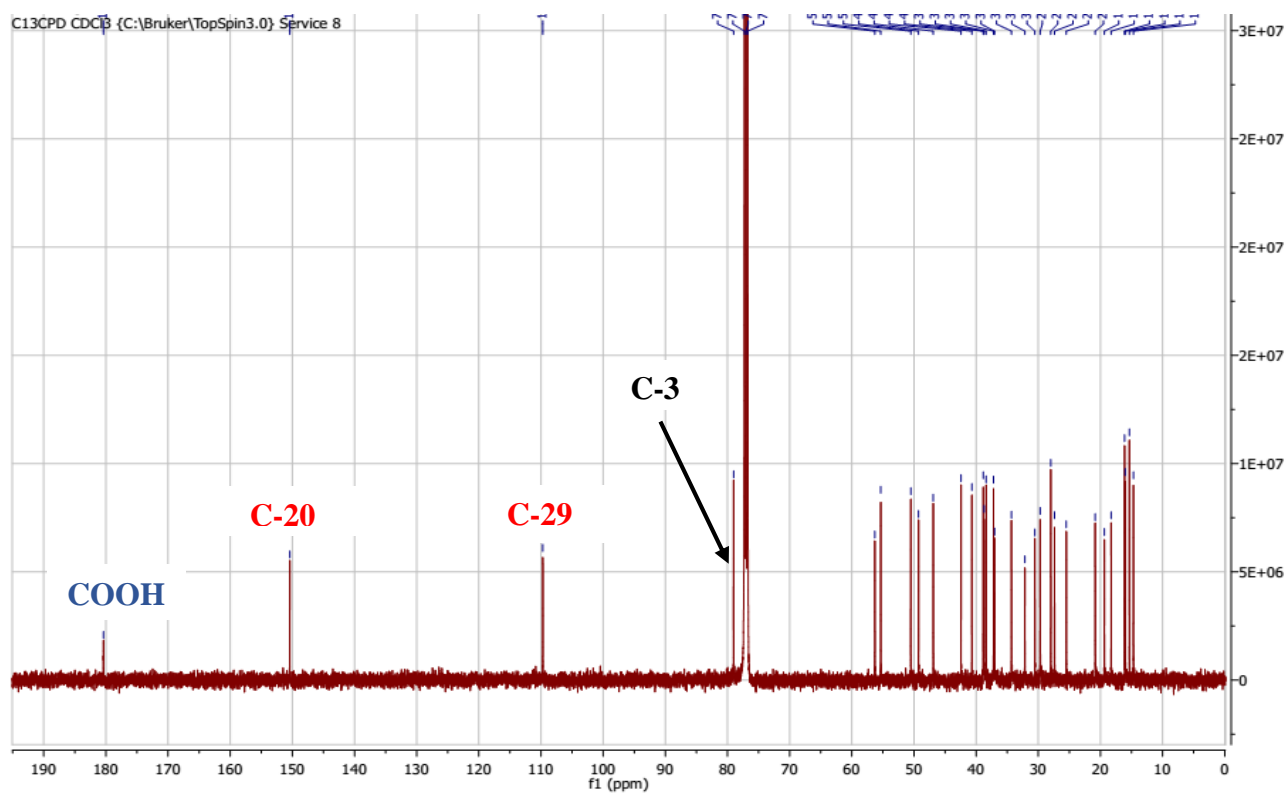
Figure 47: ^{13}**C NMR (125 MHz, CDCl₃) spectrum of compound BDF3**

The rest of the signals were assigned by comparison of the spectroscopic data with those reported by (**Mahato et Kundu, 1994**); this compound has been identified as betulinic acid (**62**).

Table 21: ^{1}H NMR (500 MHz) of BDF3 and ^{13}C NMR (125 MHz) data of BDF3 compared to ^{13}C NMR data of betulinic Acid in CDCl₃

	BDF3	betulinic Acid (Yili et *al.*, 2009)
POSITION	δC	δC
1	38.7	38.7
2	27.4	27.4
3	79.0	78.9
4	38.8	38.8
5	55.3	55.3
6	18.3	18.3
7	34.3	34.3
8	40.7	40.7
9	50.5	50.5
10	37.2	37.2
11	20.8	20.8
12	25.5	25.5
13	38.4	38.4
14	42.4	42.4
15	30.5	30.5
16	32.2	32.1
17	56.3	56.3
18	46.9	46.8
19	49.3	49.2
20	150.4	150.3
21	29.7	29.7
22	37.0	37.0
23	27.9	27.9
24	15.3	15.3
25	16.0	16.0
26	16.1	16.1
27	14.7	14.7
28	180.4	180.5
29	109.7	109.6
30	19.4	19.4

2.2.5.3. Identification of the structure of BDF4A

BDF4A was obtained as a white powder from Hex/EA (1/1) fraction from the extract of the stem bark of *Boswellia dalzielii*. It is soluble in CHCl₃ and gives a red-violet coloration to the Liebermann-Burchard test reagent indicative of a triterpenoid nature. The HRESI and spectroscopic data led to the identification of compound **BDF4A** to structure **(63)** following.
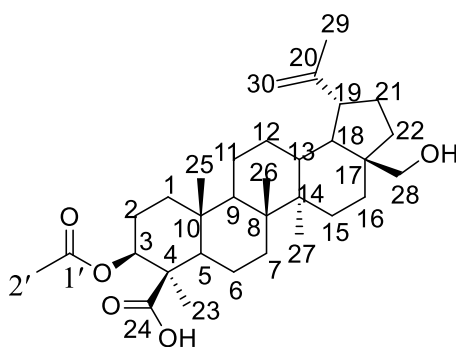
(63)

The HRESI **(Fig48)** showed the molecular ion peak at $[M-H]^-$ (calcd 513.3599), compatible with $C_{32}H_{50}O_5$ as molecular formula, which was confirmed by the NMR data.
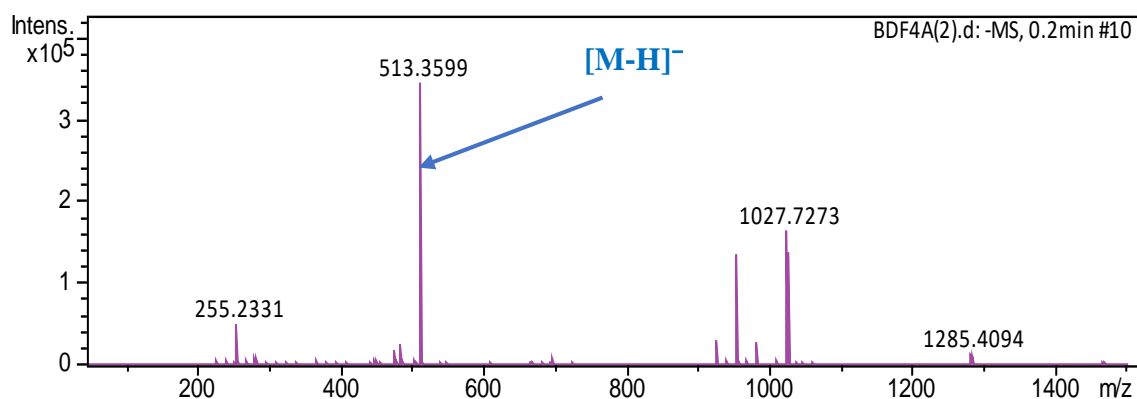
Figure 48: HRESI mass Spectrum of BDF4A

The ^1H NMR spectrum **(Fig49)** revealed the presence of five tertiary methyl groups at δ_H 0.81, 1.05, 1.09, 1.22, 1.70, and the acetate methyl at δ_H 2.11 (H-2′).
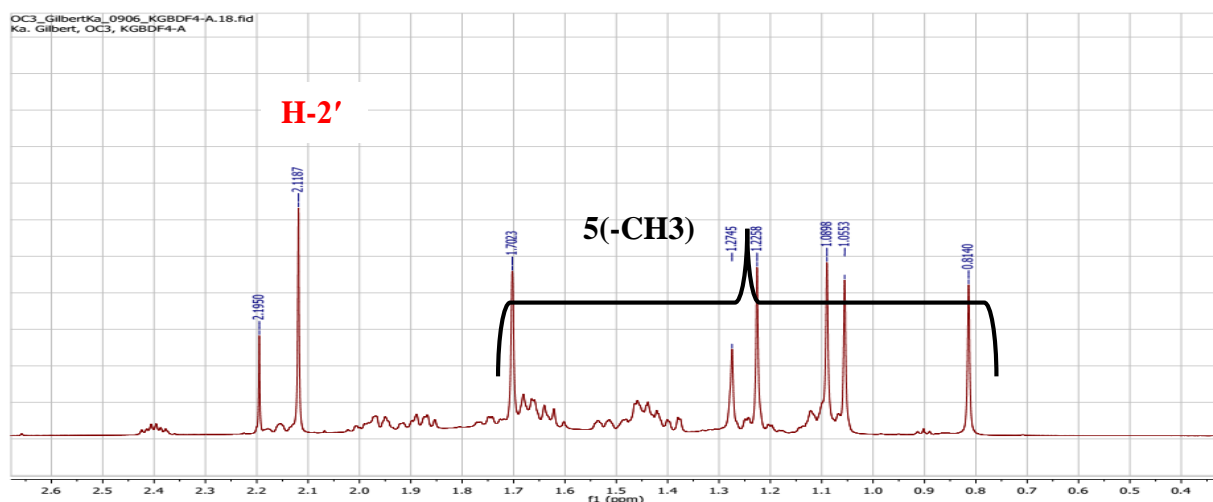
Figure 49: Expanded ^1H NMR (500 MHz, CDCl₃) spectrum of compound BDF4A

-Two intense broad singlets at δ_H 4.60 and 4.70 informative of the exocylic double bond protons of the lup-20(29)-ene series triterpenes and two others protons of hydroxymethylene were observed at δ_H 3.84 and 3.38 (H-28a and H-28b).

-A methyl singlet signal at δ_H 1.70 (H-30) indicating the presence of a vinylic methyl group,

-A methine proton at δ_H 5.29 (s, 1H) attributable to H-3
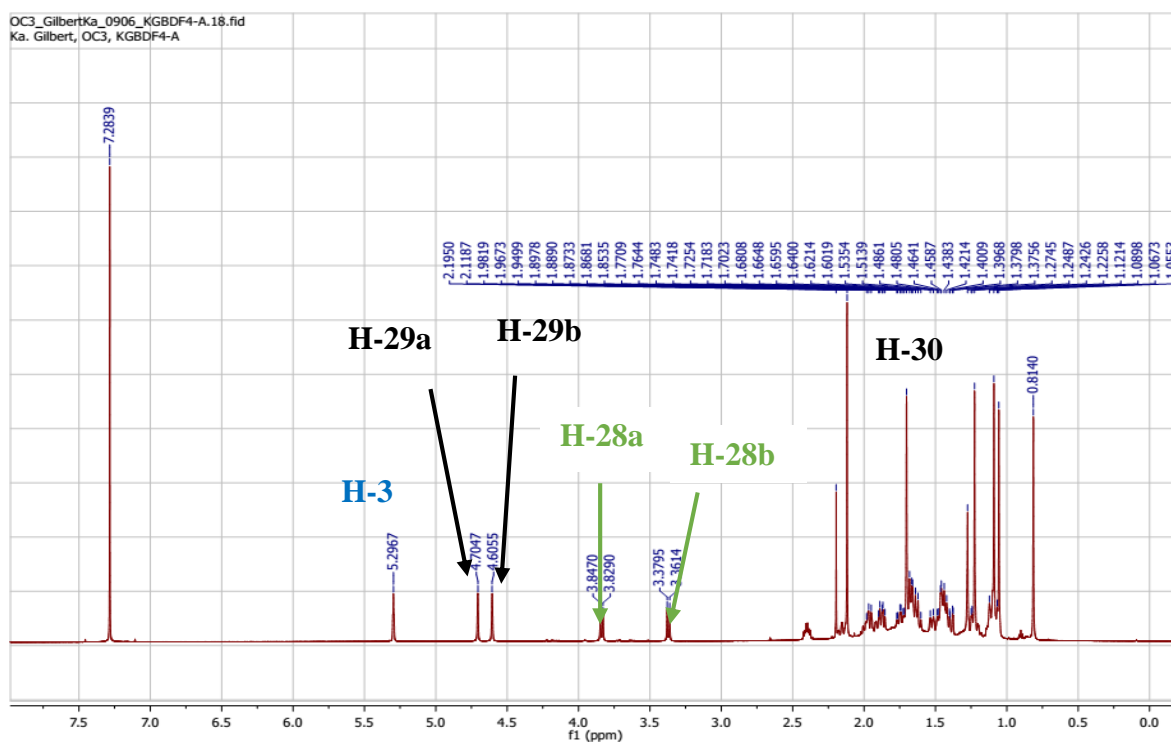
Figure 50: ^{1}H NMR (500 MHz, CDCl$_3$) spectrum of compound BDF4A

The ^{13}C NMR spectrum **(Fig51)** revealed the presence of thirty-two carbon resonances. The DEPT spectrum **(Fig52)** revealed the presence of 8 quaternary carbons, 6 tertiary carbons, 12 secondary sp2 carbons, and 6 primary sp3 carbons.

- The signals at δ_C 150.3 and 109.8 ppm indicated the presence of a lupane triterpenoid and could be assigned to the olefenic carbons C-20 and C-29 respectively **(Mahato and Kundu. 1994)**.

- The signals at δ_C 179.8 and 170.3 are ascribable to a carboxylic acid group C-24 and a carbonyl of an ester group C-1′ respectively.

The ^{13}C NMR spectrum revealed signals at;

- δ_C 73.6 assignable to C-3 of triterpenes. This value show us one proton at position H-3 is substituted by the acetyl group, this position was confirmed by the HMBC spectrum among which the proton H-3 showed correlation with carbon (C-1′) at δ_C 170.3.
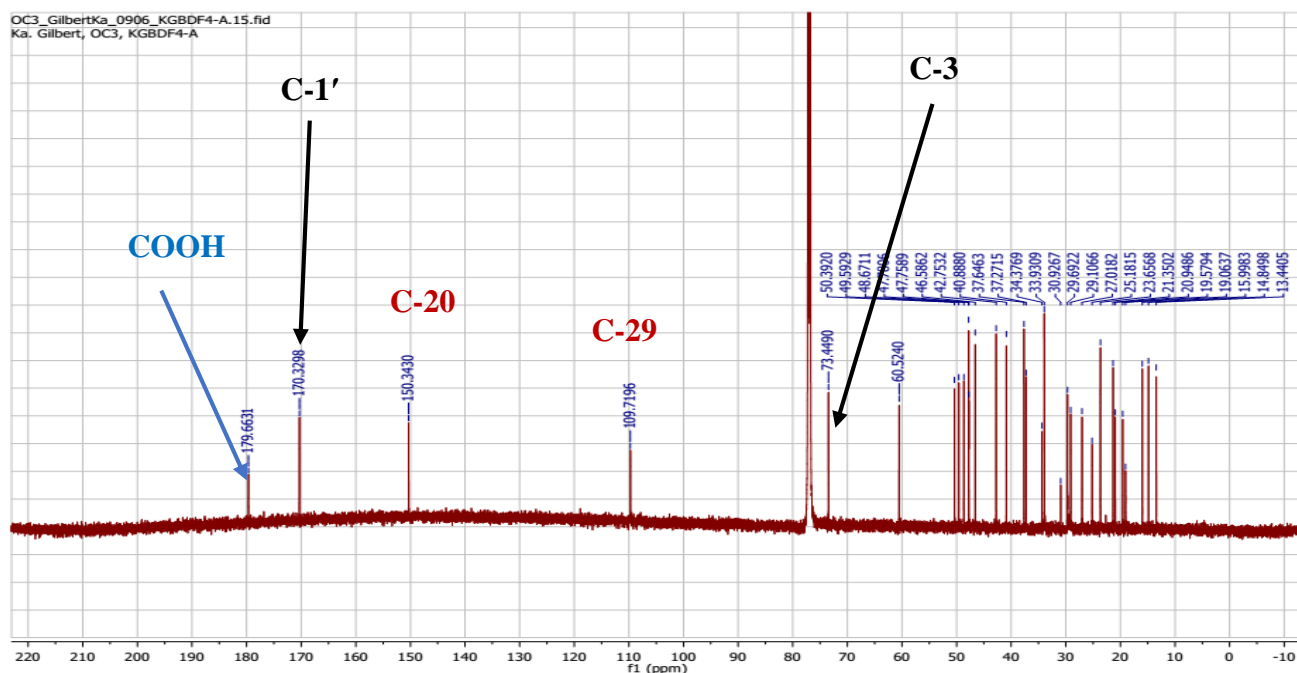
Figure 51: ^{13}C NMR (125 MHz, CDCl$_3$) spectrum of compound BDF4A
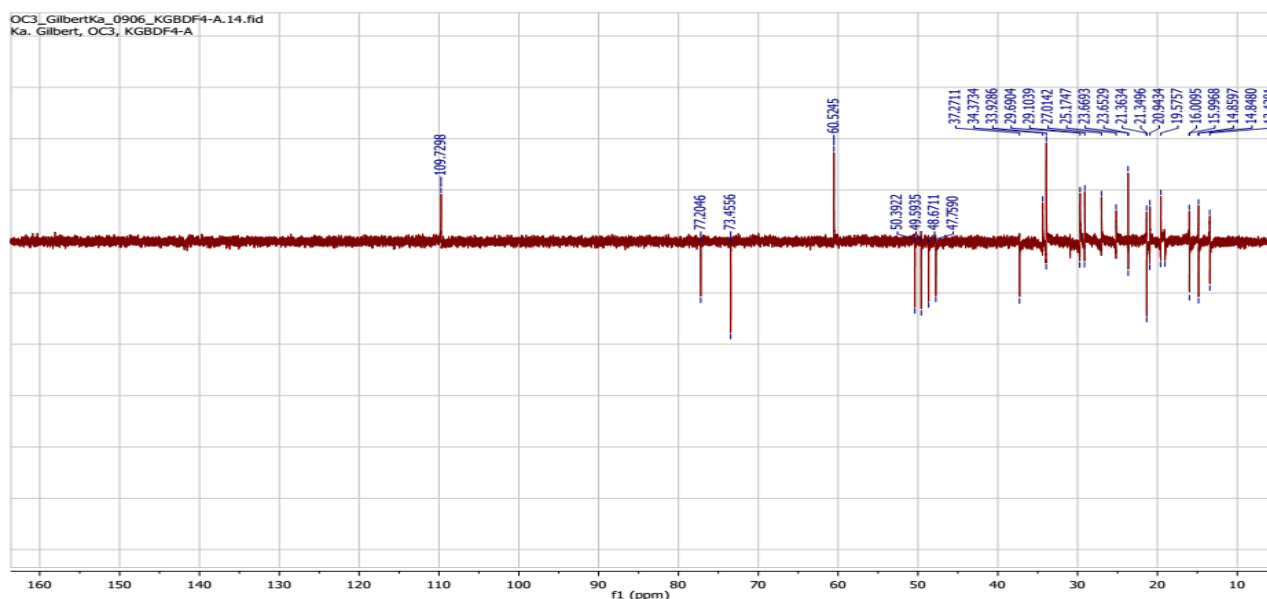
Figure 52: DEPT (125 MHz, CDCl$_3$) spectrum of compound BDF4A

The HMBC spectrum **(Fig 53)** shows correlation between Proton H-3 and carbon (C-1′) at δ_C 170.3. In the same HMBC spectrum **(Fig 54)** Protons of methyl group at position H-23 showed correlation with the carboxylic acid group at δ_C 179.8 (C-24).

The methyl group at position 28 was substituted by oxymethylene group **(Verhoffa et al. 2012)**. This suggestion was confirmed by the HMBC spectrum **(Fig 53)** in which Protons H-28a and H-28b showed correlation with (C-22) at δ_C 34.4 and (C-16) at δ_C 29.7 respectively.
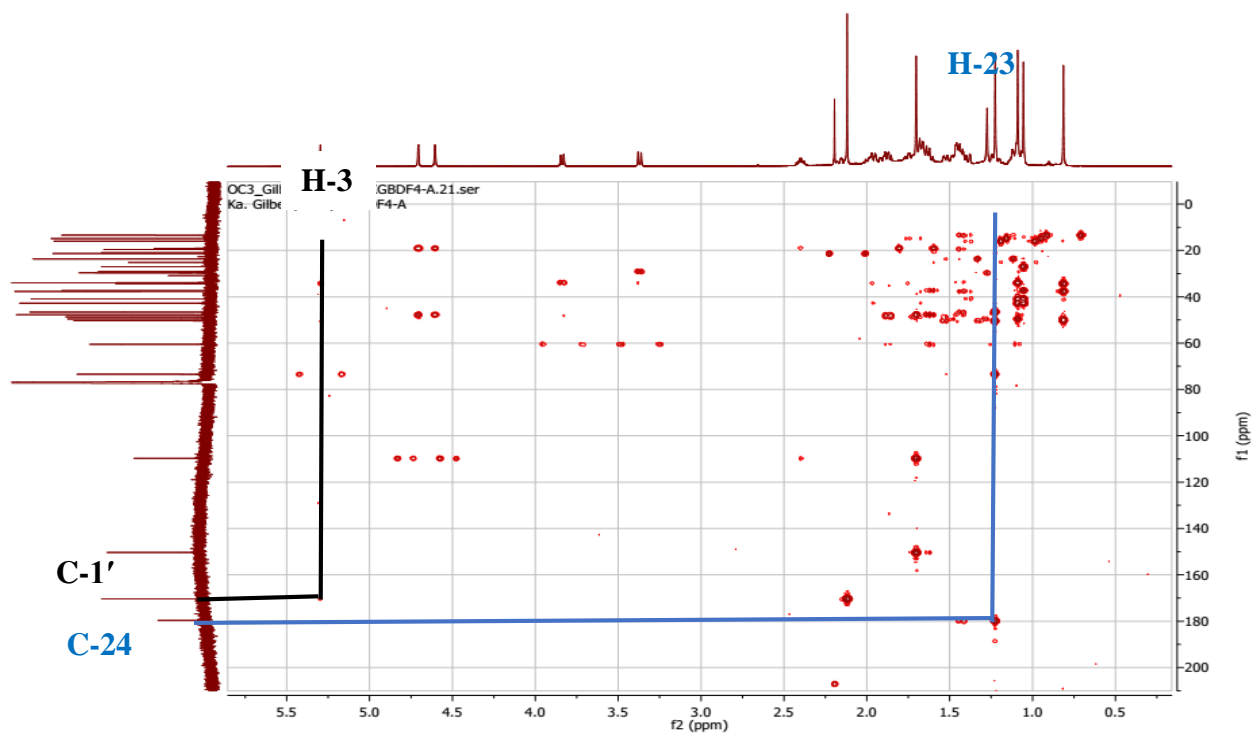
Figure 53: HMBC (CDCl₃) spectrum of compound BDF4A
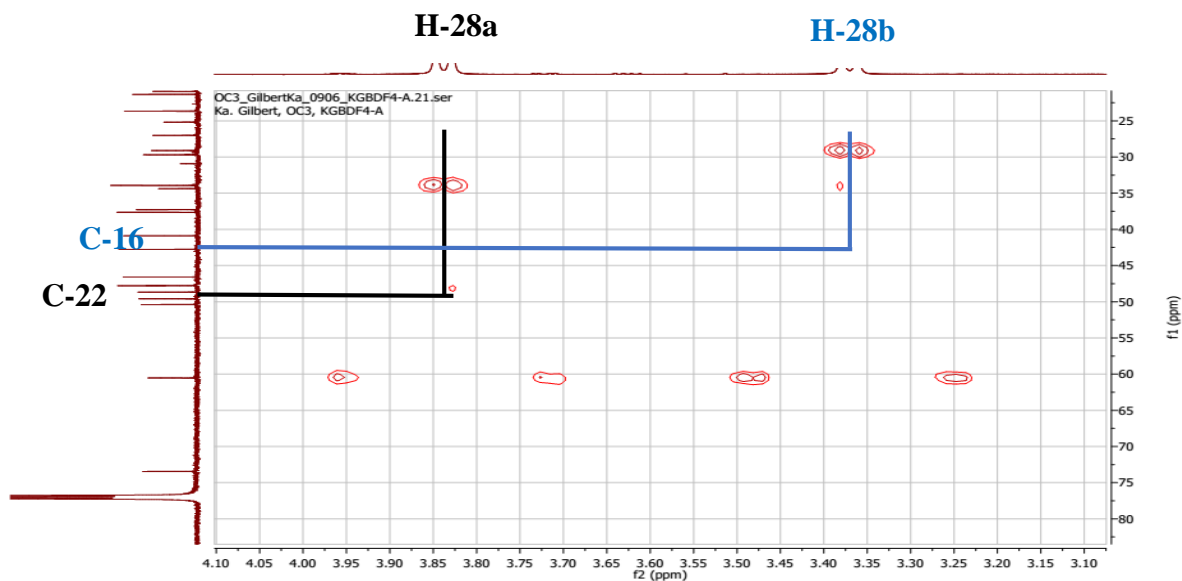
Figure 54: Expanded HMBC (CDCl₃) spectrum of compound BDF4A

These spectroscopic data compared with with those from the literature (**Verhoffa** *et al.* **2012**) allowed us to identified **BDF4A (63)** to 3-*O*-acetyl-28-hydroxylupeolic acid.

Table 22: ^{1}H NMR (500 MHz) data of BDF4A and ^{13}C NMR (125 MHz) data of BDF4A in CDCl$_3$ compared to those of ^{1}H NMR (500 MHz) and ^{13}C NMR (125 MHz) data of 3-*O*-acetyl-28-hydroxylupeolic acid in CD$_3$OD

POSITION	BDF4A		3-*O*-acetyl-28-hydroxylupeolic acid (Verhoffa *et al*. 2012)	
	δ_C (δppm)	δ_H (δppm, *J* in Hz)	δ_C (δppm)	δ_H (δppm, *J* in Hz)
1	34.5	1.57 – 1.36 (m, H-1)	35.8	1.66–1.37 (m, H-1b)
				1.16–1.13 (m, H-1a)
2	23.8	2.21 – 2.18 (m, H-2)	24.8	2.21–2.13 (m, H-2b)
				1.66–1.37 (m, H-2a)
3	73.6	5.29 (1H, s)	75.3	5.24 (1H, t, J = 2.7 Hz)
4	46.7		47.8	
5	50.5	1.66 – 1.37 (m, H-5)	51.8	1.66–1.37 (m, H-5)
6	19.7	2.02 – 1.73 (m, H-6)	20.8	1.99–1.90 (m, H-6b)
				1.83–1.70 (m, H-6a)
7	34.1	1.57 – 1.36 (m, H-7)	35.4	1.66–1.37 (m, H-7a, H-7b)
8	41.0		42.2	
9	49.7	1.57 – 1.36 (m, H-9)	51.1	1.66–1.37 (m, H-9)
10	37.8		38.9	
11	21.5	1.57 – 1.36 (m, H-11)	22.2	1.26–1.20 (m, H-11a)
				1.66–1.37 (m, H-11b)
12	25.3	1.10 – 1.06 (m, H-12)	26.7	1.83–1.70 (m, H-12b)
				1.10–1.06 (m, H-12a)
13	37.4		38.8	1.83–1.70 (m, H-13)
14	42.9		43.9	
15	27.2	2.02 – 1.73 (m, H-15)	28.2	1.83–1.70 (m, H-15b)
				1.10–1.06 (m, H-15a)
16	29.3	2.02 – 1.73 (m, H-16)	30.4	1.99–1.90 (m, H-16b)
				1.26–1.20 (m, H-16a)
17	29.8		30.7	
18	48.8	1.57 – 1.36 (m, H1-8)	50.0	1.66–1.37 (m, H-18)
19	47.9	2.40 (1H, td, *J* = 11.0, 5.8 Hz)	48.7	2.43 (1H, dt, J = 5.9 Hz, 11.1 Hz)
20	150.5		151.9	
21	29.8	2.02 – 1.73 (m, H-21)	30.9	1.99–1.90 (m, H-21b)
				1.66–1.37 (m, H-21a)
22	34.4	2.02 – 1.73 (m, H-22)	35.1	1.99–1.90 (m, H-22b)
				1.03–1.00 (m, H-22a)
23	23.8	1.22 (3H, s)	24.3	1.17 (3H, s)
24	179.8		179.8	
25	13.6	0.81 (s)	14.1	0.84 (3H, s)
26	16.1	1.09 (s)	16.5	1.11 (3H, s)
27	15.0	1.05 (s)	15.2	1.05 (3H, s)
28	60.7	3.84 (1H, d, *J* = 10.8 Hz)	60.4	3.77–3.74 (1H, dd, J = 1.3 Hz, 11.1 Hz)
		3.37 (1H, d, *J* = 10.9 Hz)		3.29 (1H, s)
29	109.8	4.70 (1H, s) – 4,60 (1H, s)	110.3	4.69 (1H, dd, J = 2.2 Hz)

					4.58 (1H, dd, J = 2.2 Hz, 1.4 Hz)
30	19.7	1.70 (3H, s)		19.3	1.70 (3H, s)
1′	170.7			172.4	
2′	21.4	2.08 (3H, s)		21.1	2.08 (3H, s)

2.2.5.4. Identification of the structure of BDb2

Compound **BDb2** was obtained from the extract of the branches of *Boswellia dalzielii* at Hex/EA (95:5) as cream white flakes and is soluble in CDCl₃. The Liebermann-Buchard test for triterpenes is positive (red-violet coloration). The spectroscopic data allows us to allocate structure **(22)** below to **BDb2**.
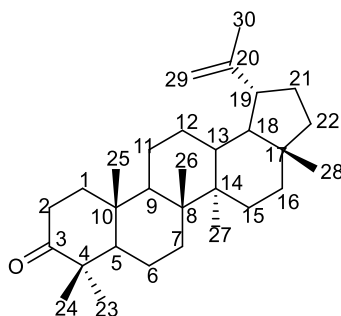
(22)

Indeed, the ¹H NMR (500 MHz, CDCl₃) spectrum (**Fig55)** of **BDb2** revealed the presence of;

-Two broad singlets at δ_H 4.59 and 4.70 corresponding to exocyclic double bond protons (H-29) of lup-20(29)-ene.

- A signal at δ_H 1.69 integrated for three protons, indicating the presence of a vinylic methyl group and six methyl singlets at δ_H 1.45, 1.09, 0.96, 1.03, 0.81 and 0.94, both diagnostic of lup-20(29)-ene series triterpenes.

- Two downfield multiplets at δ_H 2.40 and 2.49 attributable to methylene protons in α position of a carbonyl group and another multiplet at δ_H 2.40 attributable to the proton H-19.

-The absence of a multiplet signal in the area 3.30-3.50.
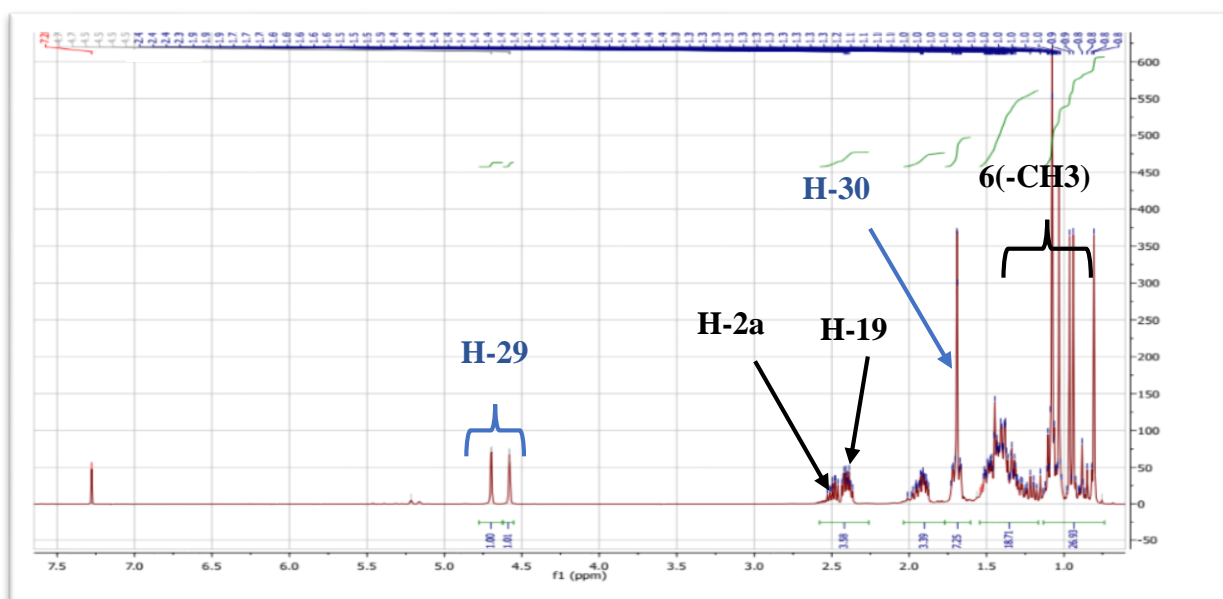
Figure 55: ^{1}H NMR (500 MHz, CDCl$_3$) spectrum of compound BDb2

The ^{13}C NMR (125MHz, CDCl$_3$) spectrum (**Fig56**) revealed the presence of thirty carbon resonances. The signals at δ_C 150.8 and 109.4 ppm indicated the presence of a lup-20(29)-ene series triterpenes and could be assigned to the olefenic carbons C-20 and C-29 respectively (**Mahato and Kundu, 1994**). The signal at δ_C 218.1 is ascribable to a carbonyl (ketone) carbon. Moreover, the absence of a signal between δ_C 76 and 80 for C-3 hydroxylated triterpenes suggests that the ketone group is on C-3.
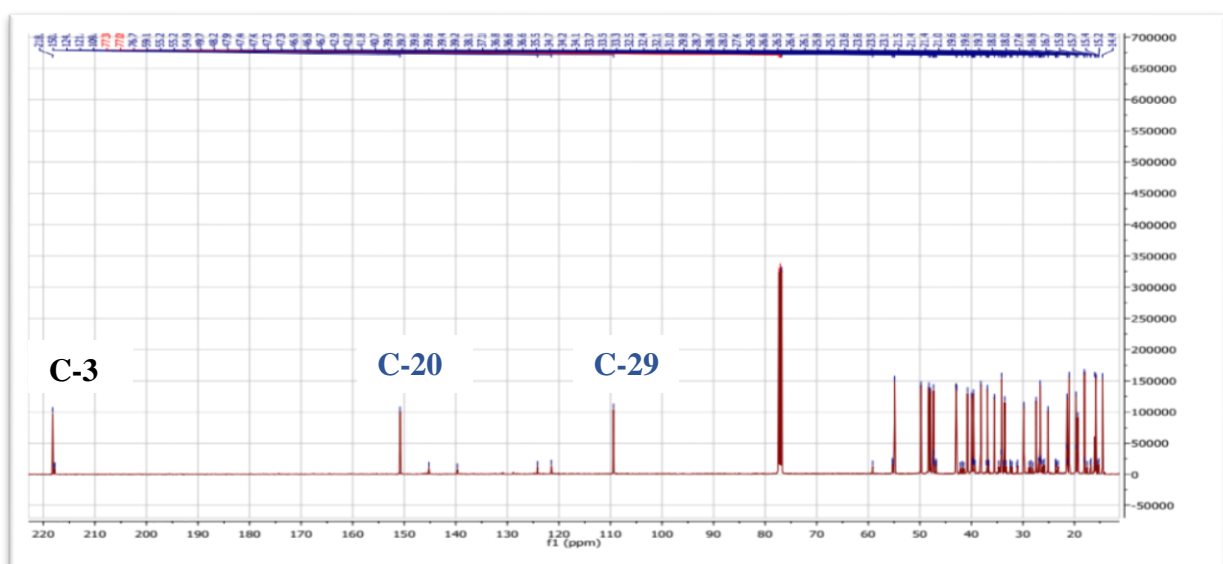
Figure 56: ^{13}C NMR (125 MHz, CDCl$_3$) spectrum of compound BDb2

The above spectroscopic data compared with data from literature (**Mahato and Kundu, 1994**) led to the attribution of lupenone to **BDb2**.

Table 23: ^{13}C NMR (125 MHz) data of BDb2 compared to ^{13}C NMR (400 MHz) data of lupenone (Yili et *al*., 2009) in CDCl₃

POSITION	BDb2	Lupenone (Yili et *al*., 2009)
	δ_C	δ_C
1	39.6	39.9
2	34.2	34.1
3	218.1	218.1
4	47.4	47.2
5	54.9	54.8
6	19.6	19.6
7	33.7	33.5
8	40.7	40.7
9	49.7	49.9
10	36.8	36.8
11	21.5	21.4
12	25.8	25.1
13	38.1	38.1
14	42.8	42.9
15	27.4	27.3
16	35.5	35.4
17	42.9	42.8
18	48.2	48.1
19	47.9	47.2
20	150.8	150.8
21	29.8	29.7
22	39.9	39.6
23	26.6	26.6
24	21.0	21.2
25	15.7	15.9
26	15.9	15.8
27	14.4	14.4
28	18.0	18.0
29	109.4	109.3
30	19.3	19.2

2.2.6. Tirucalane

2.2.6.1. Identification of the structure of BDR3

BDR3 was isolated as white powder from the Hexane fraction of the branches of *Boswellia dalzielii*. It is soluble in CHCl₃ and showed a positive Liebermann-Buchard test for tirucallane (blue-green coloration). The spectroscopic data allows us to identify compound **BDR3** to structure **64** below
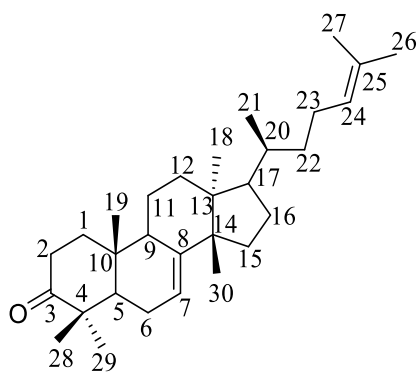
(64)

Its ^{1}H-NMR spectrum (**Fig57**) indicated the presence of eight methyl groups at δ_H 0.82, 0.92, 0.83, 1.61, 1.57, 0.92, 0.95 and 0.98 which are respectively attributable to Me-18, Me-19, Me-21, Me-26, Me-27, Me-28, Me-29, Me-30 of tirucallane (**Carla *et al*; 2009**) Two olefenic-proton resonances at δ_H 5.25 (d, *J* = 2.8 Hz, 1H) and δ_H 5.02 (m) which are attributable to the trans protons H-7 and H-24 respectively. spectrum (**Fig58**)
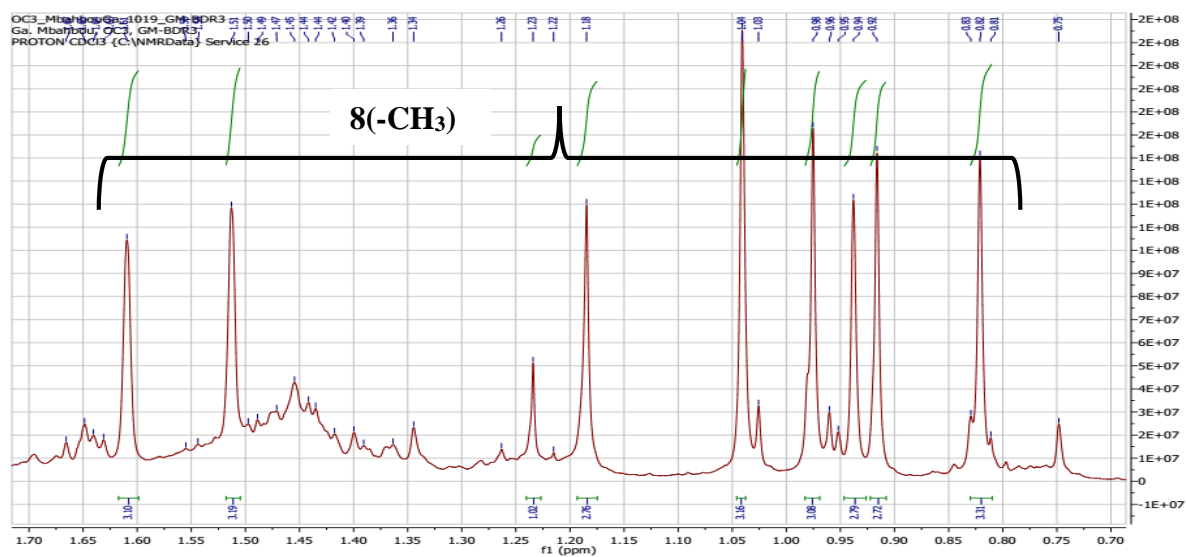
Figure 57: Expanded ^{1}H NMR (500 MHz, CDCl₃) spectrum of compound BDR3
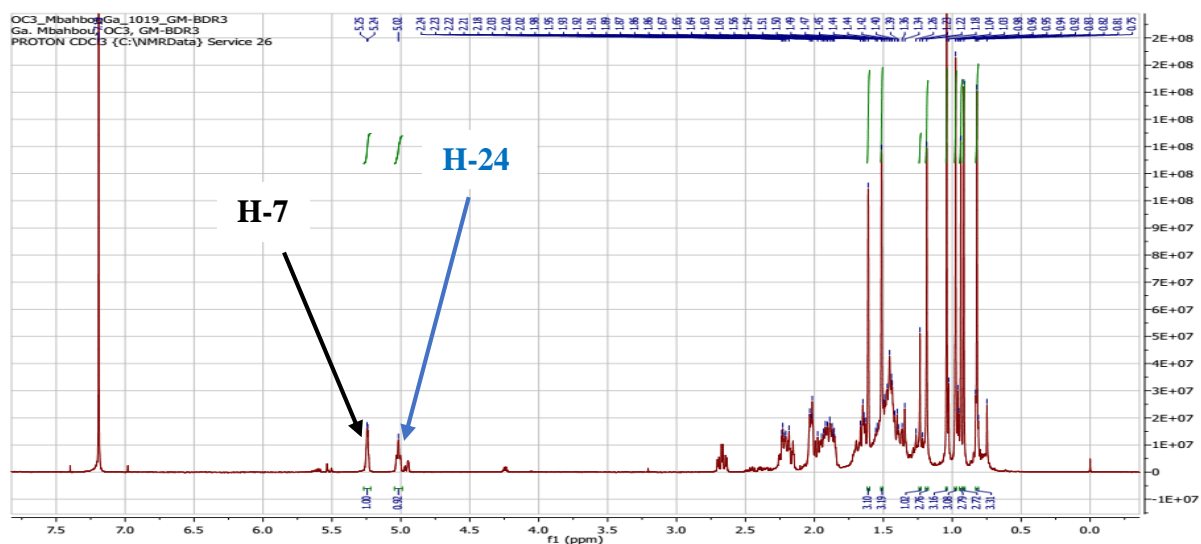
Figure 58: ¹H NMR (500 MHz, CDCl₃) spectrum of compound BDR3

The ^{13}C NMR spectrum (**Fig59**) showed 30 signals for 30 carbon atoms. Analysis of the ^{13}C NMR and DEPT 135 spectrum **(Fig60)** revealed the presence of two olefenic carbon signals at δ_C 118.2 and 145.8 which are characteristic of tirucala-7-ene nucleus. The signals of two other olefinic carbons were observed at δ_C 123.5 and 132.3, attributable to C-24 and C-25 respectively. In addition, the signal at δ_C 217.2 is ascribable to a carbonyl (ketone) carbon. Moreover, the absence of a signal between δ_C 76 and 80 for C-3 hydroxylated triterpenes suggests that the ketone group is on C-3.
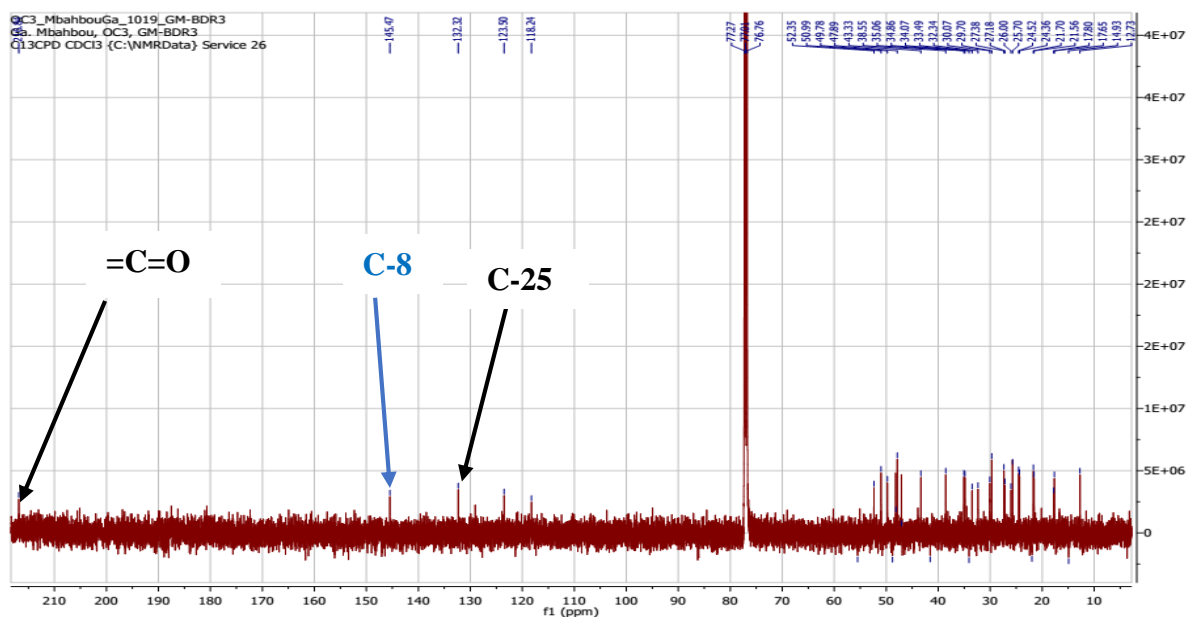
Figure 59: ¹³C NMR (125 MHz, CDCl₃) spectrum of compound BDR3
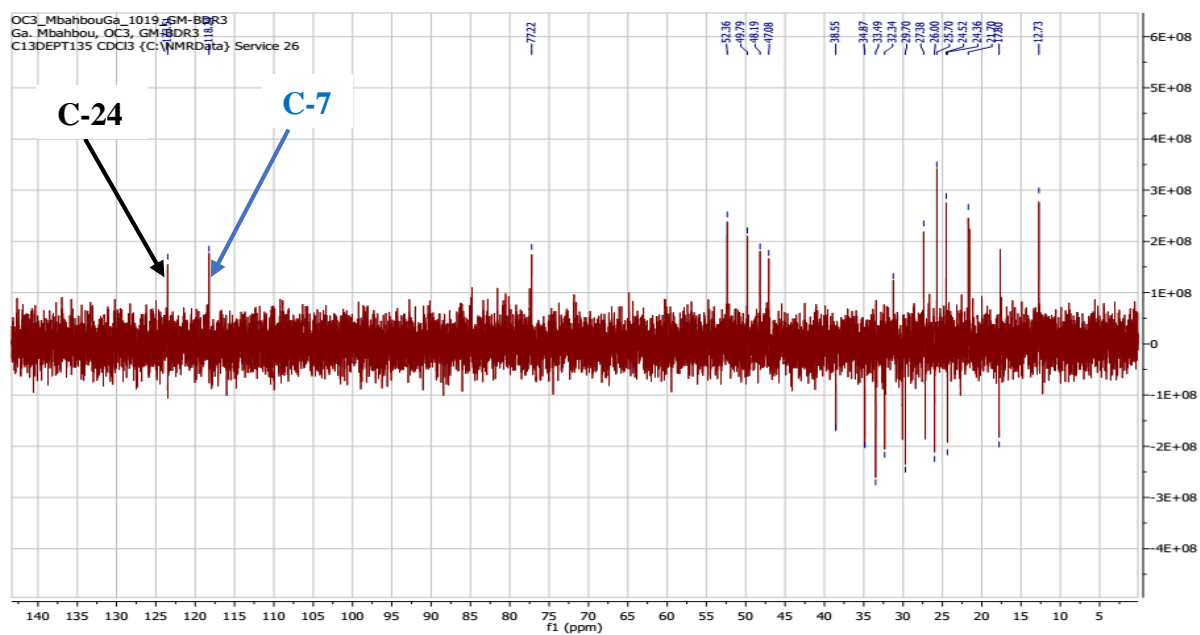
Figure 60: DEPT 135 (125 MHz, CDCl₃) spectrum of compound BDR3

By comparison of NMR data with those reported in the literature (**Toshihiro *et al***; **2016**) and (**Carla *et al*; 2009**), **BDR3** have been identified as lanosta-7,24-dien-3-one (**64**)

Table 24: ^{13}C NMR (125 MHz, CDCl$_3$) data of BDR3 compared to those ^{13}C NMR data of lanosta-7,24-dien-3-one (Toshihiro *et al*; 2016; Carla *et al*; 2009)

POSITION	BDR3 δ_C	δ_H	lanosta-7,24-dien-3-ol (Toshihiro *et al*; 2016 ; Carla *et al*; 2009) δ_C	δ_H
1	35.1		36.8	
2	22.5		24.2	
3	217.2		81.1	
4	38.5		37.8	
5	49.8		50.8	
6	24.4		23.8	
7	118.2	5.25 (m)	117.6	5.63 m
8	145.8		146.0	
9	48.8		48.9	
10	34.8		34.8	
11	17.6		18.1	
12	32.3		33.7	
13	43.3		43.5	
14	51.0		51.2	
15	33.5		34.0	
16	27.4		28.2	
17	52.3		52.9	
18	21.9	0.92 (3H, s)	21.9	0.96 (3H, s)
19	13.7	0.98 (3H, s)	13.2	0.99 (3H, s)
20	34.8		35.9	
21	17.8	0.83 (3H, s)	18.3	0.87 (3H, s)
22	36.1		36.2	
23	25.7		25.0	
24	123.5	5.02 (1H, s)	125.2	5.11 (s, br)
25	132.3		131.0	
26	26.0	1.57 (3H, s)	25.7	1.61 (3H, s)
27	17.6	1.61 (3H, s)	17.7	1.68 (3H, s)
28	27.4	1.04 (3H, s)	27.6	1.09 (3H, s)
29	15.8	1.04 (3H, s)	15.9	1.09 (3H, s)
30	27.3	0.96 (3H, s)	27.3	1.02 (3H, s)
			171.0	
			21.3	

2.2.7. Steroids

2.2.7.1. Identification of the structure of BDF2C

Compound **BDF2C** was obtained from the Hex/EA (8:2) fraction from the extract of stem bark of *Boswellia dalzielii* as white powder. It was soluble in dichloromethane and reacted positively to Lieberman Burchard test, characteristic of steroids by given a blue colour which turns quickly to dark green. **BDF2C** was identified as mixture of stigmasterol (**65**) and *β*-

sitosterol (**66**) (Habib *et al.*, 2007) thanks to its NMR data and its TLC profile compared to a sample kept in the laboratory.

Stigmasterol

(65)
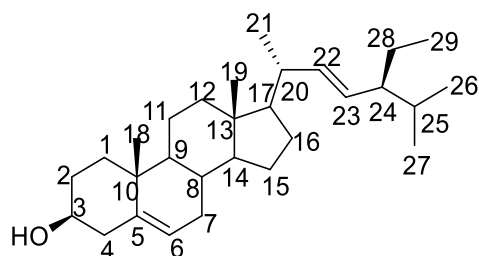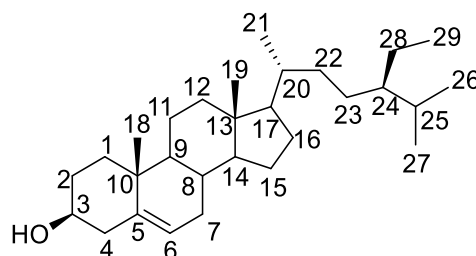
β-**Sitosterol**

(66)

Its proton spectrum (**Fig 61**), showed characteristic resonances of protons of steroids at *δ*$_H$ 5.28 (1H, m, H-6), 3.46 (1H, m, H-3), 5.09 (1H, dd, *J* = 15.2, 8.6 Hz, H-22) and 4.94 (1H, dd, *J* = 15.1, 8.7 Hz, H-23).
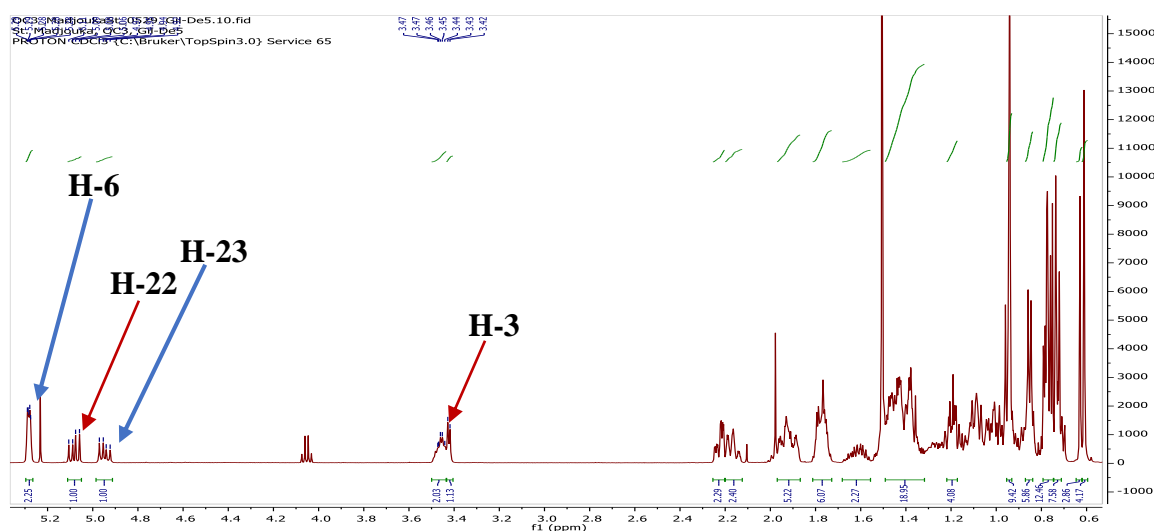
Figure 61: ¹H NMR spectrum (CDCl₃, 500 MHz) of BDF2C

2.2.7.2. Identification of the structure of BDF5A

BDF5A was obtained from EtOAc 100% fraction from the stem bark of *Boswellia dalzielii* as white powder soluble in pyridine. It reacted positively to the Liebermann-Burchard test for steroids (blue -violet colour). The HRESI mass spectrum associated to the comparison on TLC with an authentic sample led to the identification of compound **BDF5A** to following structure (**67**)
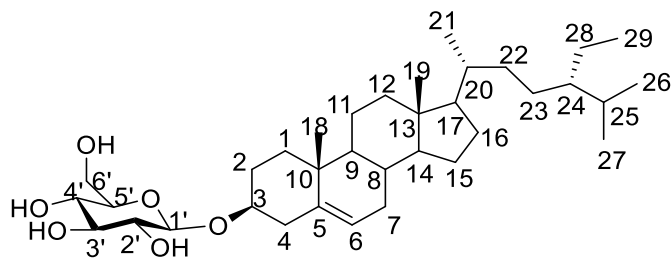
(67)

The HRESI mass spectrum, showed a pseudomolecular ion peak [M+Na]$^+$ at *m/z* 599.4530 with molecular formula $C_{35}H_{60}O_6$, implying six double bond equivalent which suggested that compound **BDF5A** contains a *β*-sitosterol moiety together with sugar moiety.
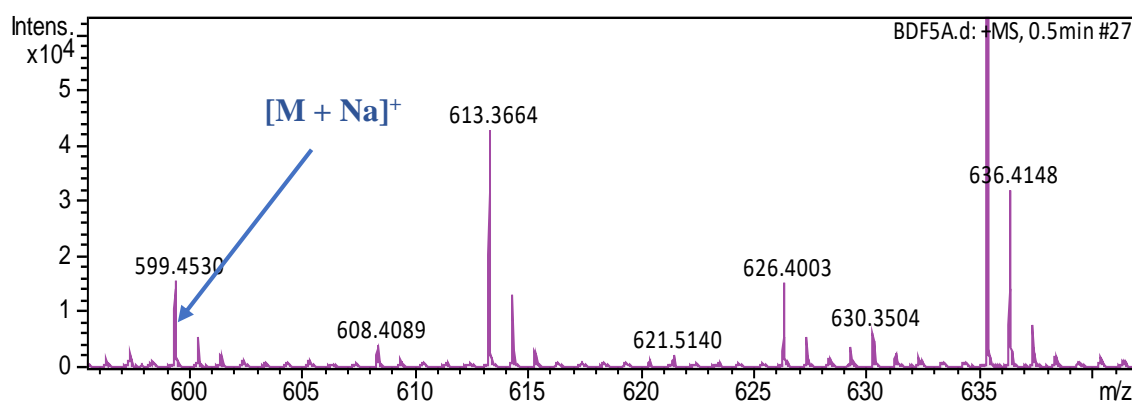
Figure 62: HRESI mass Spectrum of BDF5A

These observations prompted us to identify **BDF5A** as ***β*-sitosterol-3-*O*-*β*-D-glucopyranoside** (**67**).

2.2.8. Flavonoids

2.2.8.1. Identification of the structure of BDb3

BDb3 was obtained as a pale white powder from the aerial part of *Boswellia dalzielii* in Hex/EA

(8/2). It is soluble in CDCl$_3$ and reacted positively with alcoholic ferric chloride (deep purple coloration), suggesting a phenolic nature. The HRESI Mass and spectroscopic data led to the identification of compound **BDb3** to structure (**68**) following
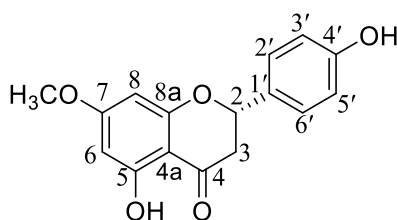
(68)

The High resolution mass spectra (HRESI) showing [M−1]⁻ ion peak at *m/z* 285.0743 corresponding to a molecular formula of ($C_{16}H_{14}O_5$) which accounted for ten double bond equivalent.
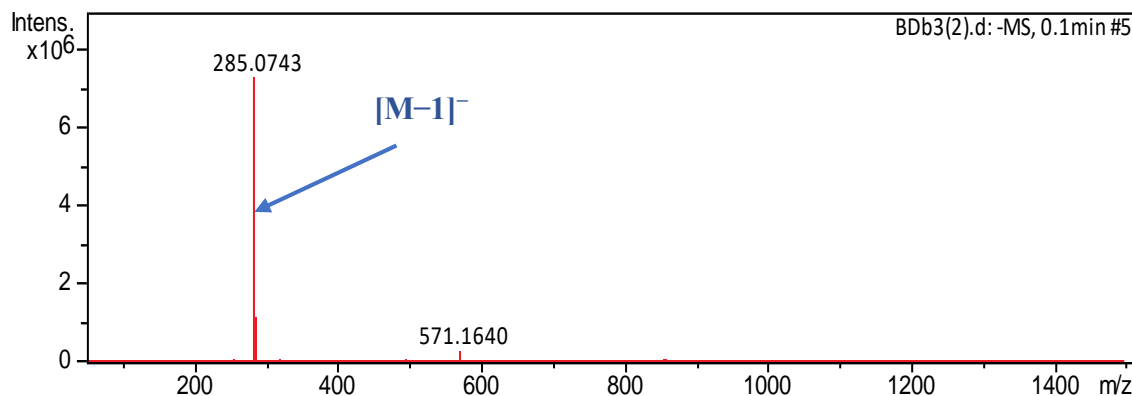
Figure 63: HRESI mass Spectrum of BDb3

The ^{1}H NMR spectrum (**Fig64**), showed two family of aromatic protons signals: the first one is materialised by two doublets of one proton each at 6.04 (d, *J* = 2.3 Hz, 1H) and 6.03 (d, *J* = 2.3 Hz, 1H) corresponding to ring A proton while the second family of proton is represented by the signals of AA′BB′ type aromatic protons signals at δ_H 7.30 (d, *J* = 8.5 Hz, 1H) and δ_H 6.87 (d, *J* = 8.5 Hz, 1H) due to ring B protons.). One methoxy proton signal which appeared as a singlet at δ_H 3.80.
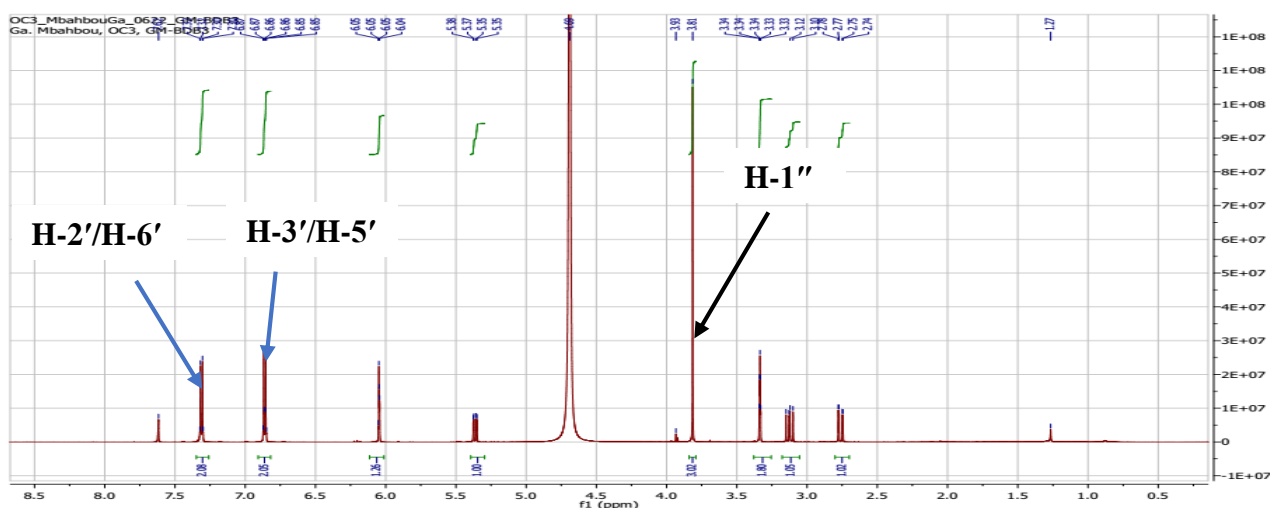
Figure 64: ^{1}H NMR (500MHz, CDCl₃ + CD₃OD) spectrum of compound BDb3

The broad band decoupled ^{13}C NMR (**Fig 64**) and DEPT (**Fig 65**) spectra revealed the presence of one methyl, one methylene, seven methine and seven quaternary carbons.

The ^{13}C NMR spectrum (**Fig65),** showed the characteristic dihydroflavanone signals at δ_C 196.6 (C-4), 79.1 (C-2), 42.8 (C-3), **(Markham, 1982),** it also showed signals for AA′BB′ system at δ_C 127.7 (C-2′/C-6′), 115.3 (C-3′/C-5′) which should be located in ring B. the position of methoxy group δ_C 55.2 is confirmed by the HMBC spectrum (**Fig 67)** in which proton of methoxy at δ_H 3.80 showed correlation with carbon (C-7) at δ_C 168.1 located in ring A.
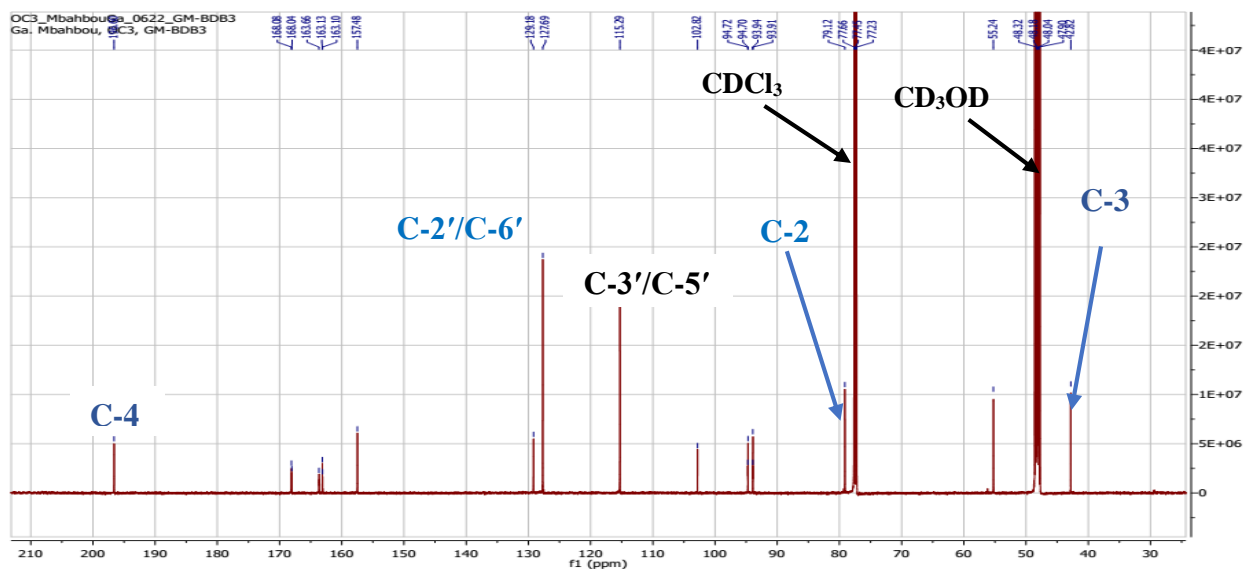
Figure 65: ^{13}C NMR (125 MHz, CDCl$_3$ + CD$_3$OD) spectrum of compound BDb3
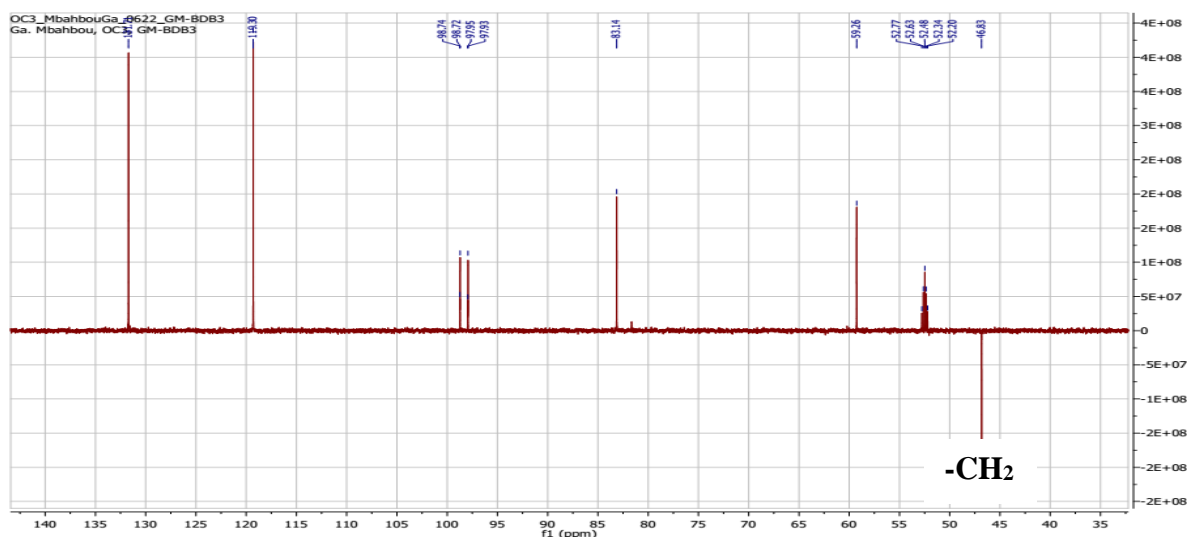
Figure 66: DEPT 135 (125 MHz, CDCl$_3$ + CD$_3$OD) spectrum of compound BDb3
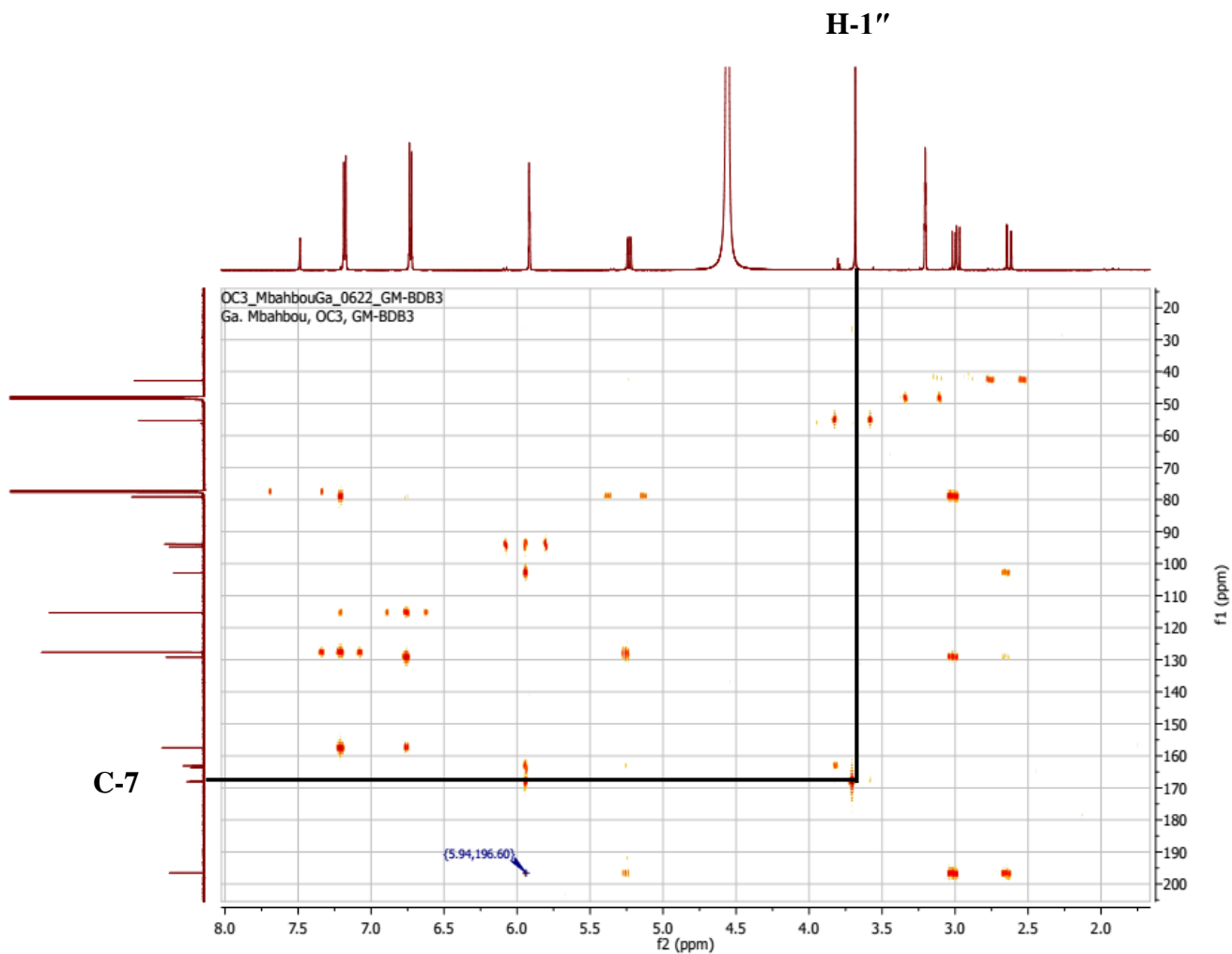
Figure 67: HMBC (CDCl₃ + CD₃OD) spectrum of compound BDb3

On the basis of the comparison of NMR data with reported in the literature (**Motahareh**
et al., 2014), **BDb3** compound have been identified as 4',5-dihydroxy-7-methoxyflavanone (**68**)

Table 25: ^{1}H NMR (500 MHz) data and ^{13}C NMR (125 MHz) data of BDb3 in (CD$_3$OD + CDCl$_3$) compared to those ^{1}H NMR (500 MHz) data and ^{13}C NMR (125 MHz) data of 4',5-dihydroxy-7-methoxyflavanone in CDCl$_3$

POSITION	BDb3 δ_C	δ_H	4',5-dihydroxy-7-methoxyflavanone (Motahareh *et al.*, 2014) δ_C	δ_H
2	79.1	5.35 (1H, dd, *J* = 13.0, 2.9 Hz)	79.0 (CH)	5.34 (dd, 13.0, 3.0)
3	42.8	3.08 (1H, dd, *J* = 17.2, 13.0 Hz)	43.2 (CH2)	A 3.08 (dd, 17.3, 13.0)
		2.75 (1H, dd, *J* = 17.2, 3.0 Hz)		B 2.78 (dd, 17.3, 3.0)
4	196.6		196.2 (C)	
4a	102.8		103.9 (C)	
5	163.7		164.5 (C)	
6	94.7	6.04 (1H, d, *J* = 2.3 Hz)	95.1 (CH)	6.06 (d, 2.4)
7	168.1		168.1 (C)	
1″	55.2	3.80 (3H, s)	55.7 (CH3)	3.79 (s)
8	93.9	6.03 (1H, d, *J* = 2.3 Hz)	94.2 (CH)	6.03 (d, 2.4)
8a	163.1		163.2(C)	
1'	127.3		127.7(C	
2'/6'	127.7	7.30 (2H, d, *J* = 8.5 Hz)	127.9 (CH)	7.31 (d, 8.6)
3'/5'	115.7	6.85 (2H, d, *J* = 8.5 Hz)	115.7 (CH)	6.88 (d, 8.6)
4'	157.4		156.5 (C)	

2.2.8.2. Identification of the structure of BDb11

BDb11 was obtained as a white powder from the extract of the branches of *Boswellia dalzielii* in Hex/EtOAc 7:3. It is soluble in chloroform. It reacted positively both with ferric chloride (blue colour) and the mixture of magnesium with hydrochloride acid (red colour), indicating its phenolic nature and suggest that **BDb11** is a flavonoid. The spectroscopic data led to the identification of compound **BDb11** to structure (**69**) bellow.
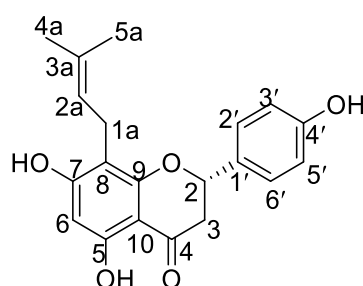
(69)

The 1H NMR spectrum (**Fig 68**) exhibites signals fo aromatic protons with AA′/BB′ spin system at δ_H 7.57 (d, *J* = 8.4 Hz, 2H), and 7.23 (d, *J* = 8.4 Hz, 2H) assigned to *para*-substituted benzene ring.

- A signal at δ_H 12.80 for a chelated hydroxyl group probably at C-4

- One aromatic protons at δ_H 6.46 (s, 1H)

- Signals observed at δ_H 1.65 (s, 3H), 1.75 (s, 3H), 3.61 (m, 2H), and the olefinic proton at δ_H 5.64 (m, 1H) were typical for a 3-methylbut-2-enyl chain.
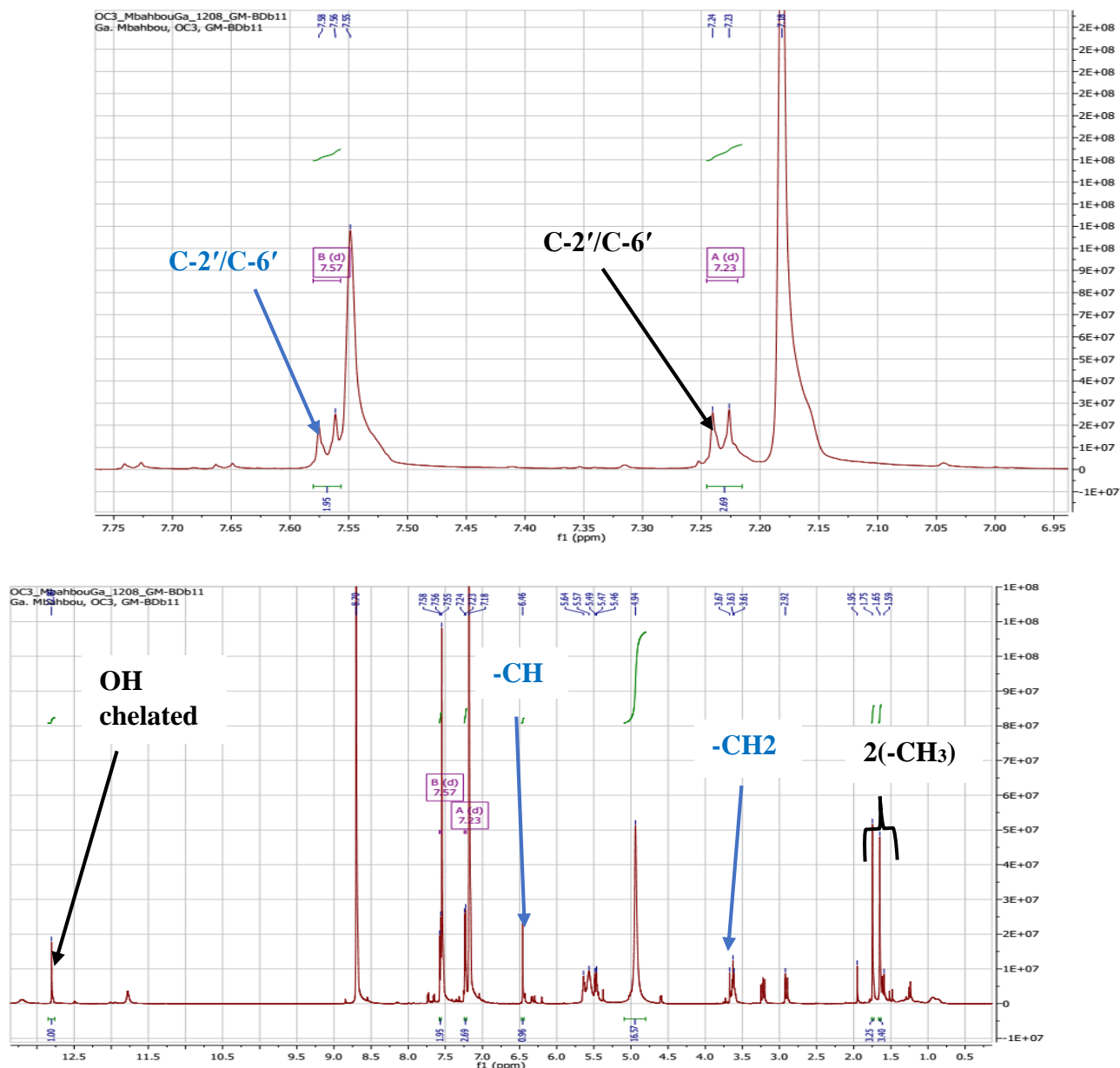
Figure 68: ^{1}H NMR (500 MHz, CDCl$_3$) spectrum of compound BDb11

The broad band decoupled 13C NMR (**Fig 70**) and DEPT (**Fig 69**) spectra revealed the presence of two methyl, two methylene, eight methine and nine quaternary carbons. The 13C NMR spectrum (**Fig 70**) shows the presence of the flavanone skeleton suggested by the characteristic signal of C-2 at δ_C 79.1, C-3 at δ_C 42.9, C-4 at δ_C 196.6 (Agrawal, 1989). It shows also signals for AA′BB′ system at δ_C 128.4 (C-2′/C-6′), 116.2 (C-3′/C-5′) which should be located in ring B.
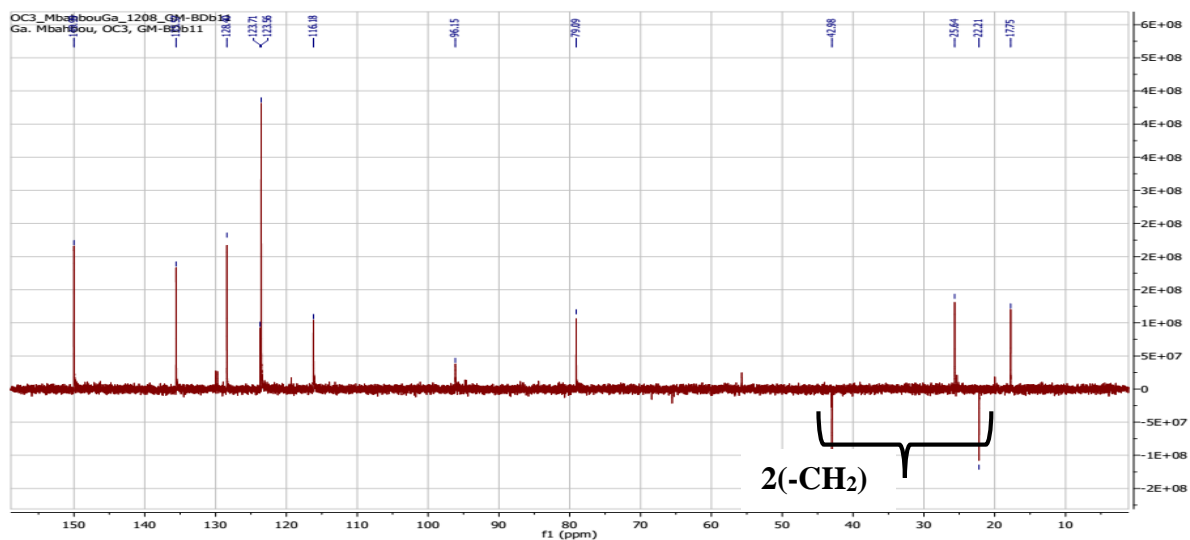
Figure 69: DEPT 135 (CDCl₃) spectrum of compound BDb11
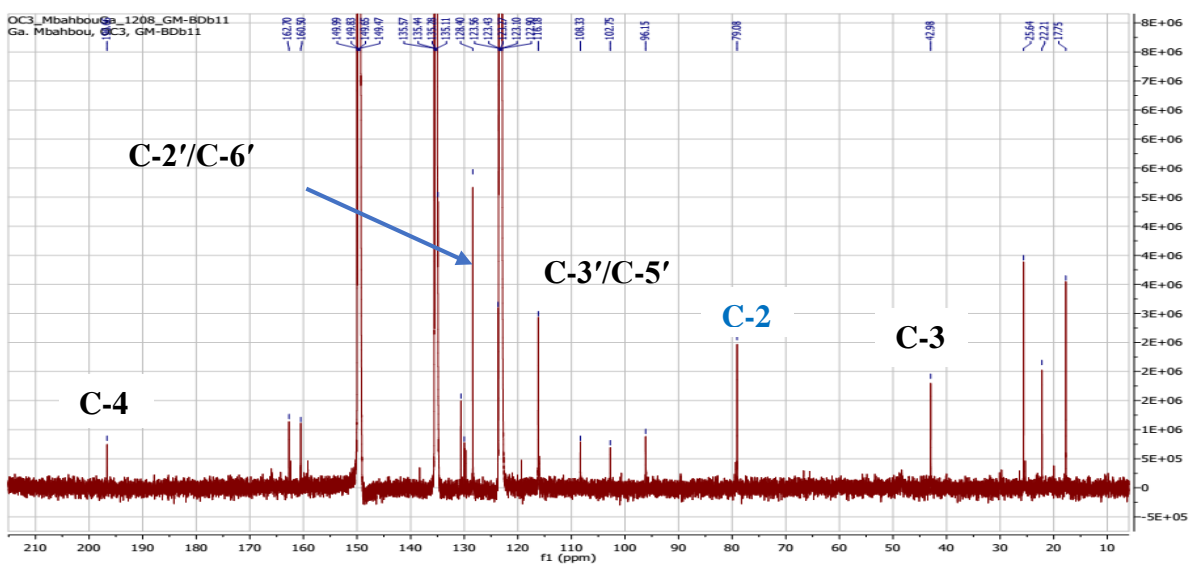
Figure 70: ¹³C NMR (125 MHz, CDCl₃) spectrum of compound BDb11

The position of 3-methylbut-2-enyl chain is confirmed by the HMBC spectrum (**Fig71**) in which methylene protons at δ_H 3.61 showed correlation with carbons (C-8) at δ_C 108.3, (C-9) at δ_C 160.5, (C-7) at δ_C 165.7 located in ring A.
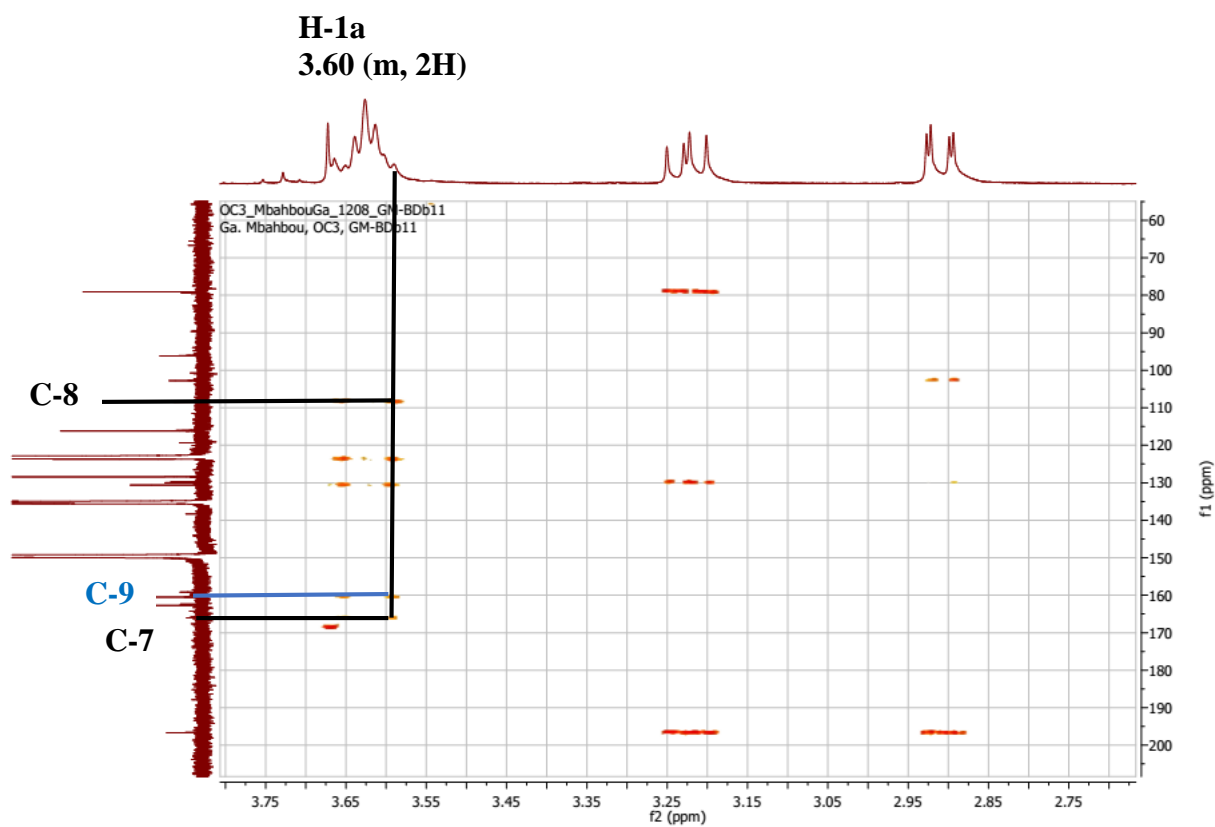
Figure 71: HMBC (CDCl₃) spectrum of compound BDb11

Based on these spectroscopic and by comparison with the literature (**Agrawal, 1989;**
Shi *et al*; 1997), the structure of compound **BDb11** was identified as Soforaflavanone B (**69**).

Table 26: ^{13}C NMR (125 MHz, CD$_3$OD and CDCl$_3$) data of BDb11 compared to ^{13}C NMR data of Soforaflavanone B (Agrawal, 1989; Shi *et al*; 1997)

POSITION	BDb11 δ_C	δ_H	Soforaflavanone B (Agrawal, 1989 ; Shi *et al*; 1997) δ_C
2	79.1	5.47 (1H, s)	78.3
3	42.9	3.21- 2.90 m	42.0
4	196.6		197.1
5	162.7		161.6
6	96.2	6.46 (1H, s)	95.4
7	165.7		164.7
8	108.3		107.1
9	160.5		160.1
10	102.7		102.0
1′	129.9		129.5
2′	128.4	7.57 (1H d, J = 8.4 Hz)	128.3
3′	116.2	7.23 (1H d, J = 8.4 Hz)	115.4
4′	159.2		157.9
5′	116.2	7.23 (1H d, J = 8.4 Hz)	115.4
6′	128.4	7.57 (1H d, J = 8.4 Hz)	128.3
1a	22.2	3.61 (2H, m)	21.6
2a	123.4	5.63 (1H, s)	122.8
3a	130.6		130.2
4a	25.6	1.65 (3H, s)	25.6
5a	17.7	1.75 (3H, s)	17.6

2.2.8.3. Identification of the structure of BDb18

BDb18 was obtained as a white powder from the extract of the branches of *Boswellia dalzielii* in Hex/EtOAc 1:1. It is soluble in chloroform. It reacted positively both with ferric chloride (blue colour) and the mixture of magnesium with hydrochloride acid (red colour), indicating its phenolic nature and suggest that **BDb18** is a flavonoid. The spectroscopic data allows us to identify **BDb18** to structure (**70**) bellow.
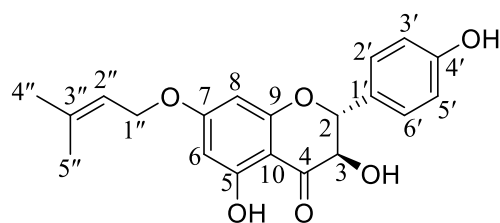
(70)

Indeed, the ^{1}H NMR spectrum (**Fig72**), shows two family of aromatic protons signals like **BDb3**: one proton at δ_H 6.05 (d, J = 2.1 Hz, 1H) and the other at δ_H 5.99 (d, J = 2.1 Hz, 1H) corresponding to ring A proton while the second family of protons is represented by the

signals of AA′BB′ type aromatic protons signal at δ_H 7.37 (d, J = 8.5 Hz, 2H) and δ_H 6.84 (d, J = 8.5 Hz, 2H) belonging to ring B.

- Two methyls protons signals which appeare as a singlet at δ_H 1.73 (s, 3H), 1.66 (s, 3H),

- A signal at δ_H 11.11 for a chelated hydroxyl group probably at C-4 for flavonoids (**Agrawal, 1989**)

-A doublet of 2 protons at δ_H 4.47 (2H, d, J = 6.7 Hz) which on the COSY spectrum (**Fig 73**) correlate with an olefenic proton appearing as a triplet at δ_H 5.37 (1H, t, J = 6.7 Hz,) and 2 methyl singlet signals at δ_H 1.66 (s, 3H) and 1.73 (s, 3H) suggesting the existence of an isoprenyl moiety in the molecule
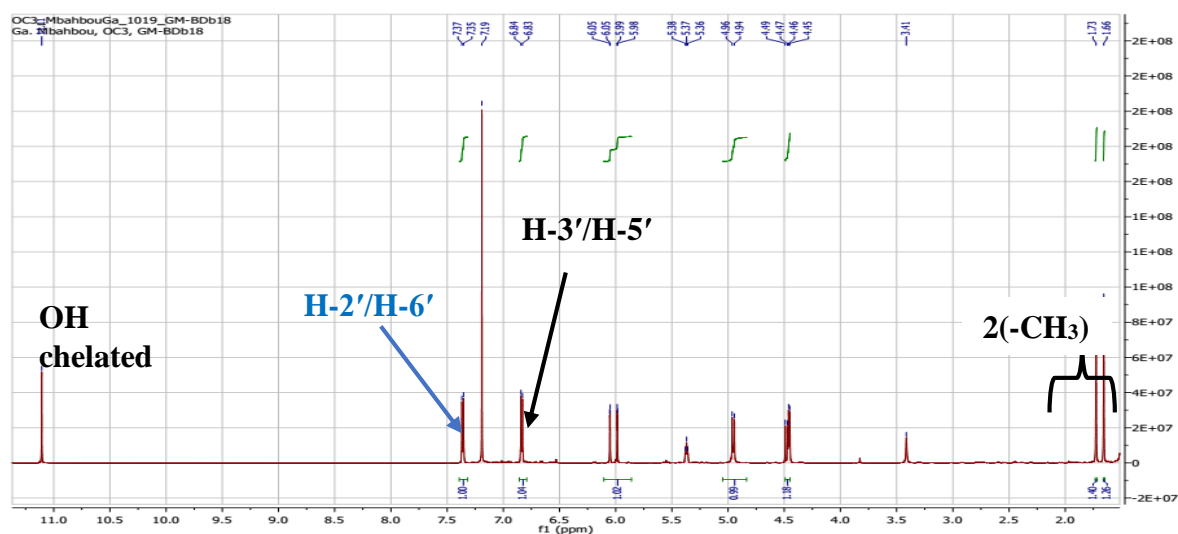
Figure 72: ^{1}H NMR (500 MHz, CDCl$_3$) spectrum of compound BDb18
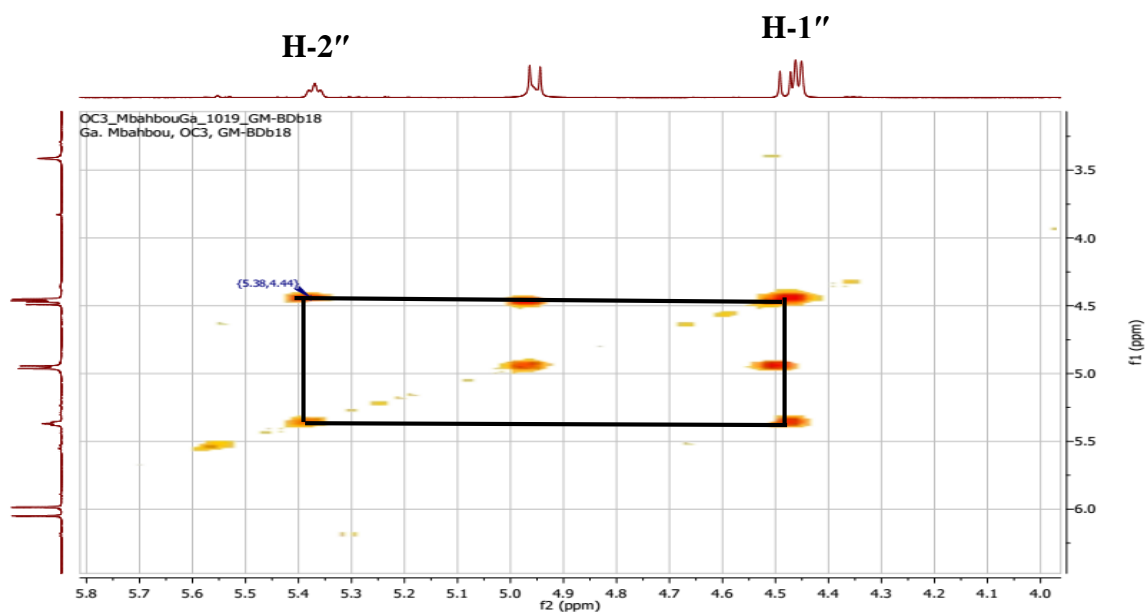
Figure 73: COSY (CDCl$_3$) spectrum of compound BDb18

The ^{13}C NMR spectrum (**Fig 74**) displays a total of 21 signals, with those at δ_C 195.8, 83.1, 72.3 attributable to C-4, C-2, C-3 of flavanonols derivative. Signals of an isoprenyl fragment are observed at δ_C 18.5 and 25.8 (1 CH$_3$ each), 118.3 and 139.4 (C=C) and at δ_C 65.2.
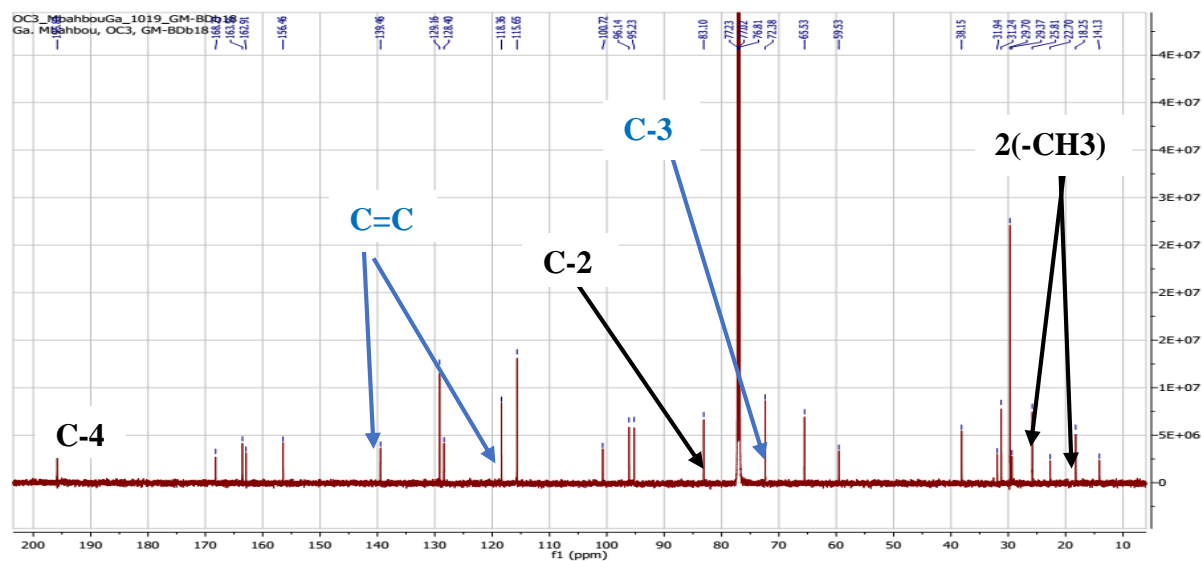
Figure 74: ^{13}C NMR (125 MHz, CDCl$_3$) spectrum of compound BDb18

The HMBC spectrum (**Fig 75**) was used to locate the O-prenyl group at C-7 of the ring A through correlations between proton δ_H 4.46 (H-1″) and carbon δ_C 168.2 (C-7), δ_H 6.05 (H-6) and 168.2 (C-7), δ_H 5.99 (H-8) and 168.2 (C-7).
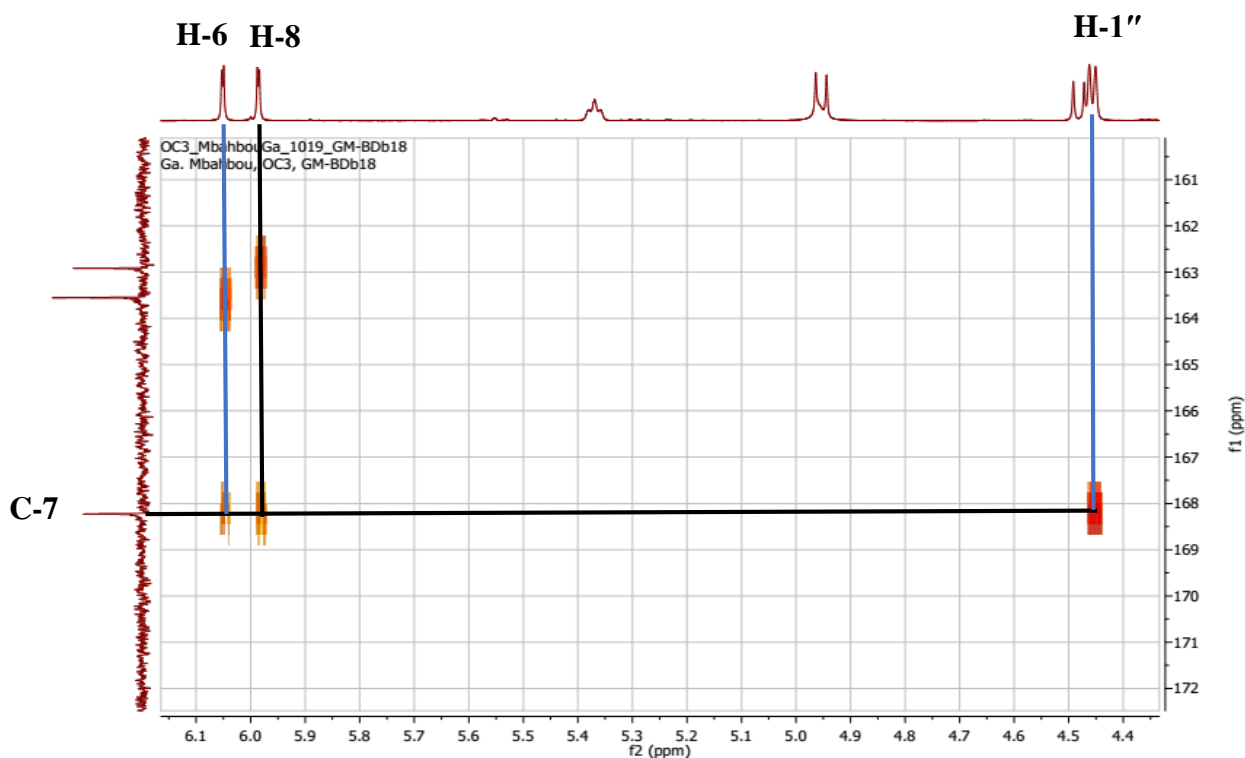
Figure 75: HMBC (CDCl$_3$) spectrum of compound BDb18

The spectroscopic data was in harmony with that published (**Alarcón *et al*., 2008; Bohlmann *et al*., 1981**) for 5,4′-Dihydroxy-7-(γ,γ-dimethylallyloxy)dihydroflavonol (**70**)

Table 27: ^{13}C NMR (125 MHz) data of BDb18 and ^{1}H NMR (500 MHz) data of BDb18 in (CD₃OD + CDCl₃) compared to ^{13}C NMR (75 MHz) data and ^{1}H NMR (300 MHz) data of 5,4′-Dihydroxy-7-(*γ,γ*-dimethylallyloxy)dihydroflavonol in CDCl₃

	BDb18		5,4′-Dihydroxy-7-(*γ,γ*-dimethylallyloxy)dihydroflavonol (Alarcón *et al*., 2008 ; Bohlmann *et al*., 1981)	
POSITION	δ_C	δ_H	δ_C	δ_H
2	83.1	4.95 (1H, d, J = 11.9 Hz)	83.2	5.03 (1H, d, J = 11.5 Hz)
3	72.3	4.48 (1H, d, J = 11.9 Hz)	72.3	4.56 (1H, d, J = 11.5 Hz
4	195.8		196.0	
5	163.5		163.0	
6	96.1	6.05 (1H, d, J = 2.1 Hz)	96.0	6.13 (1H, d, J = 2.3 Hz)
7	168.2		168.1	
8	95.2	5.99 (1H, d, J = 2.1 Hz)	95.1	6.06 (1H, d, J = 2.3 Hz)
9	162.9		162.9	
10	100.7		100.8	
1′	128.4		127.5	
2′	129.1	7.37 (1H, d, J = 8.5 Hz)	129.1	7.43 (d, J = 8.0 Hz, 1H)
3′	115.6	6.84 (1H, d, J = 8.5 Hz)	115.6	6.91 (d, J = 8.0 Hz, 1H)
4′	156.4		157.3	
5′	115.6	6.84 (1H, d, J = 8.5 Hz)	115.6	6.91 (1H, d, J = 8.0 Hz)
6′	129.1	7.37 (1H, d, J = 8.5 Hz)	129.1	7.43 (1H, d, J = 8.0 Hz)
1″	65.2	4,46 (1H, d, J = 8.5 Hz)	65.5	4.53 (1H, d, J = 7.0 Hz)
2″	118.3	5.37 (1H, t, J = 6.7 Hz)	118.4	5.44 (1H, t, J = 7.0 Hz)
3″	139.4		139.3	
4″	25.8	1.73 (3H, s)	25.7	1.73 s
5″	18.5	1.66 (3H, s)	18.2	1.80 s

2.2.8.4. Identification of the structure of BDb17

BDb17 was obtained as a white powder from the extract of the branches of *Boswellia dalzielii* in Hex/EtOAc 1:1. It is soluble in chloroform. It reacted positively both with ferric chloride (blue colour) and the mixture of magnesium with hydrochloride acid (red colour), indicating its phenolic nature and suggest that **BDb17** is a flavonoid. The spectroscopic data led to the identification of **BDb17** to structure (**71**) bellow.
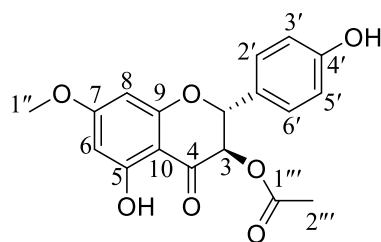
(71)

The ^{1}H NMR spectrum (**Fig76**), shows two family of aromatic protons signals like **BDb18**: one proton at δ_H 6.14 (d, J = 1.4 Hz, 1H) and the other at δ_H 6.08 (d, J = 2.0 Hz, 1H) corresponding to ring A protons while the second family of proton is represented by the signals of AA′BB′ type aromatic proton signal at δ_H 7.37 (d, J = 8.3 Hz, 2H) and δ_H 6.89 (d, J = 8.4 Hz, 2H) belonging to ring B.

- One methoxy proton signals which appeares as a singlet at δ_H 3.84 (s, 3H) and one methyl group at 2.06 (s, 3H);

- A signal at δ_H 11.51 for a chelated hydroxyl group probably at C-4 for flavonoids (**Agrawal, 1989**)
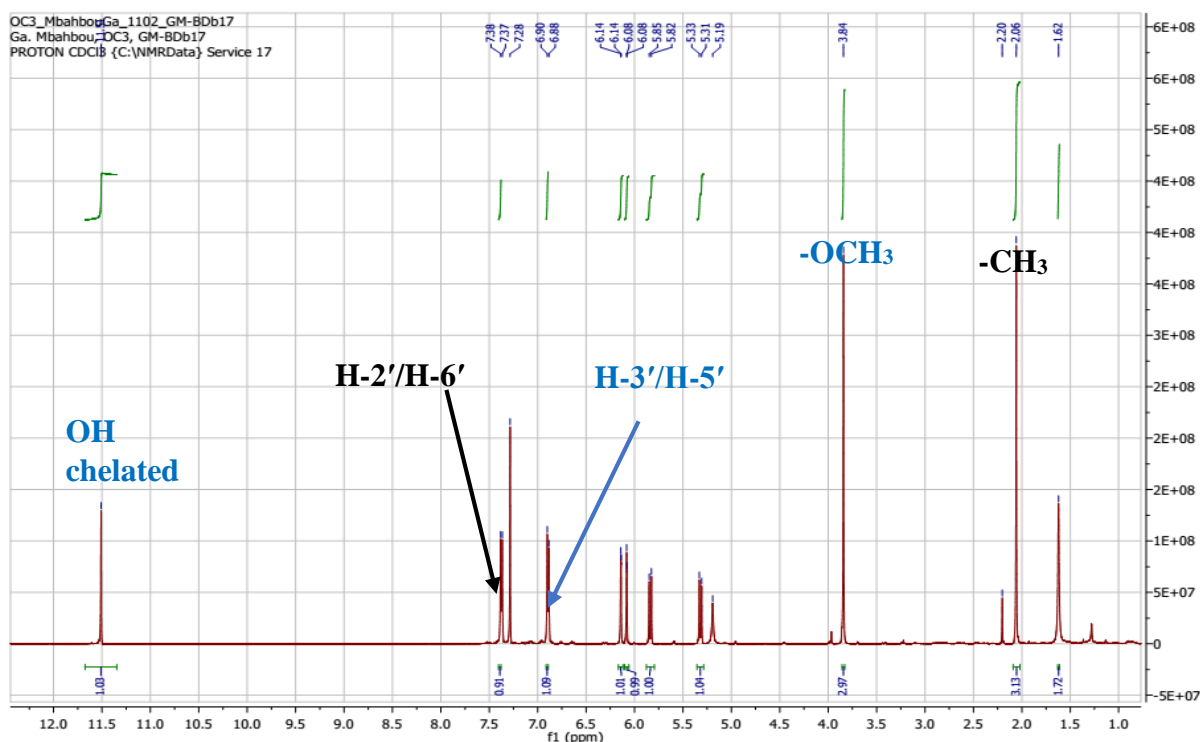
Figure 76: ^{1}H NMR (500 MHz, CDCl₃) spectrum of compound BDb17

The ^{13}C NMR spectrum (**Fig77**) displayed a total of eighteen carbon signals, which in conjunction with the DEPT 135 spectrum (**Fig78**) were repartitioned into 2 CH₃, 8 CH and 08 quartenary carbons. The signals include;

- Typical signals for a 3-acetyl flavanone at δ_C 191.9 (C-4), 81.1 (C-2) and 72.4 (C-3) **(Agrawal, 1989)**

The methoxy group at δ_C 55.8 established that one OH group in the ring was substituted by methoxy group.
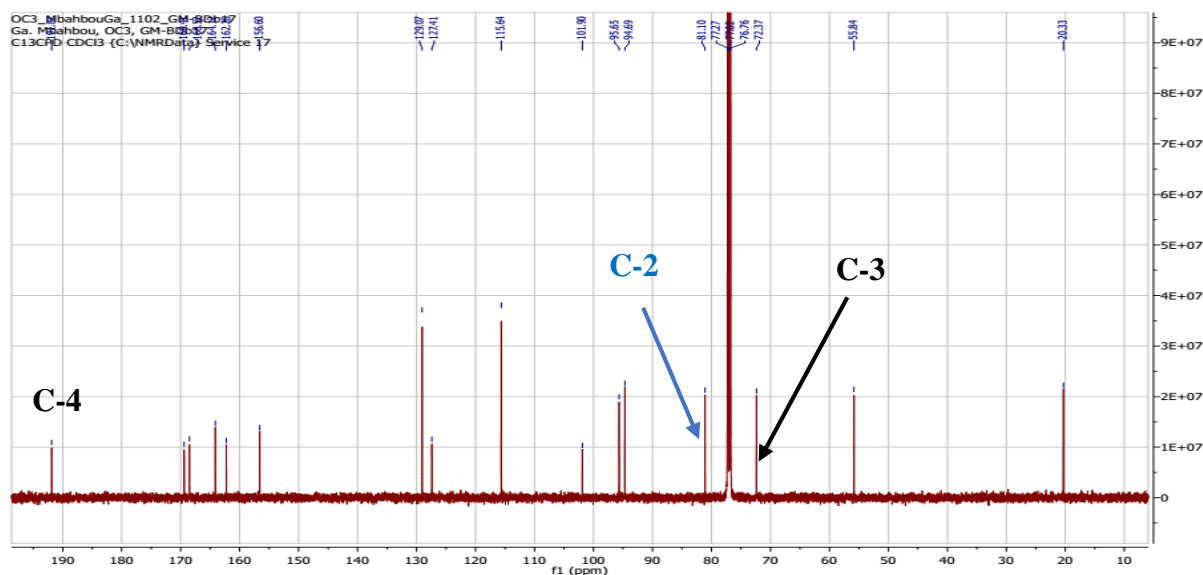
Figure 77: ^{13}C NMR (125 MHz, CDCl$_3$) spectrum of compound BDb17
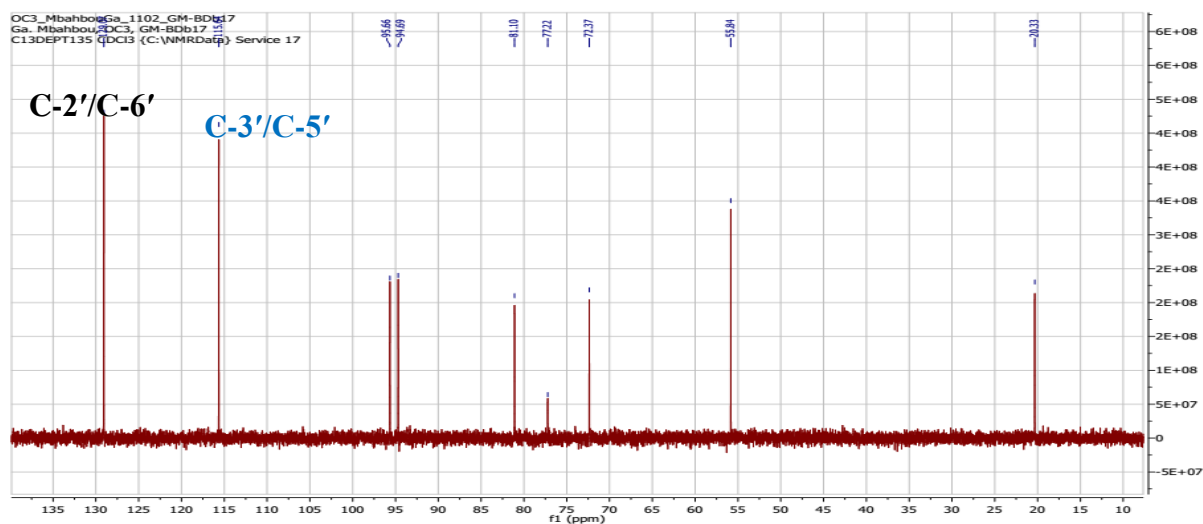
Figure 78: DEPT 135 (CDCl$_3$) spectrum of compound BDb17

The position of methoxy and methyl group was confirming by the help of HMBC **(Fig79)** correlation in which protons of methoxy at δ_H 3.84, H-1″ showed correlation with the C-7 carbon at δ_C 168.5 and protons of methy group at δ_H 2.06, H-2‴ showed correlation with the C-1‴ at δ_C 169.4
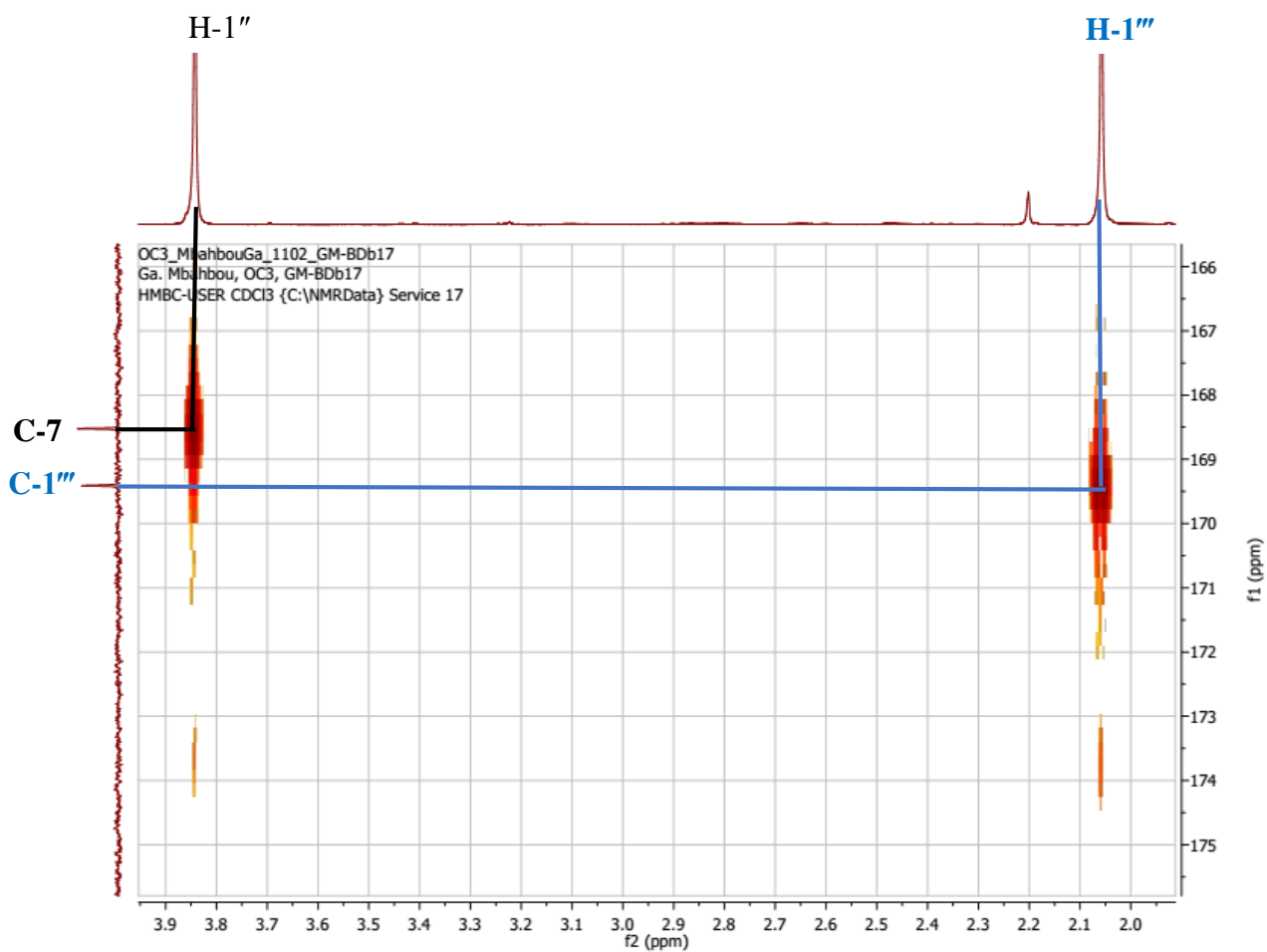
Figure 79: HMBC (CDCl₃) spectrum of compound BDb17

On the basis of these spectroscopic data and by comparaison with those published by **(Ayafor *et al*., 1981) BDb17** was attributed the structure of **3-Acetoxy-4',5-dihydroxy-7-methoxyflavanone (71)**

Table 28: ^{13}C NMR (125 MHz) data and ^{1}H NMR (500 MHz) data of BDb17 compared with ^{13}C NMR (75 MHz) data of 3-Acetoxy-4', 5-dihydroxy-7-methoxyflavanone in CDCl$_3$

	BDb17		3-Acetoxy-4',5-dihydroxy-7-methoxyflavanone (Ayafor *et al.*, 1981)
POSITION	δ_C	δ_H	δ_C
2	81.1	5.32 (1H, d, *J* = 11.8 Hz)	81.7
3	72.4	5.84 (1H, d, *J* = 11.8 Hz)	72.9
4	191.9		192.6
5	164.1		164.2
6	95.6	6.14 (1H, d, *J* = 1.4 Hz)	95.9
7	168.5		169.1
8	94.7	6.08 (1H, d, *J* = 2.0 Hz)	95.0
9	162.3		162.9
10	101.9		102.2
1′	127.4		126.5
2′	129.1	7.37 (1H, d, *J* = 8.3 Hz)	129.3
3′	115.6	6.89 (1H, d, *J* = 8.4 Hz)	115.9
4′	156.6		158.5
5′	115.6	6.89 (1H, d, *J* = 8.4 Hz)	115.9
6′	129.1	7.37 (1H, d, *J* = 8.3 Hz)	129.3
1″	55.8	3.84 (3H, s)	
1‴	169.4		170.3
2‴	20.3	2.06 (3H, s)	20.3

2.2.9. Other Phenolic compounds

2.2.9.1. Identification of the structure of BDRA

Compound **BDRA** was isolated as a brown paste soluble in CDCl$_3$ and MeOH. The spectroscopic data led to the identification of **BDRA** to structure (**72**) bellow.
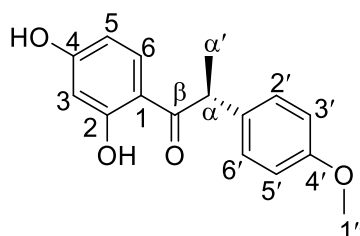
(**72**)

The negative-ion HRESI (**Fig 80**) of **BDRA** exhibited the pseudo-molecular ion peak [M-H]$^-$ at *m/z* 271.0952 (calcd. 271.0970 for C$_{16}$H$_{16}$O$_4$), containing nine double bond equivalent.
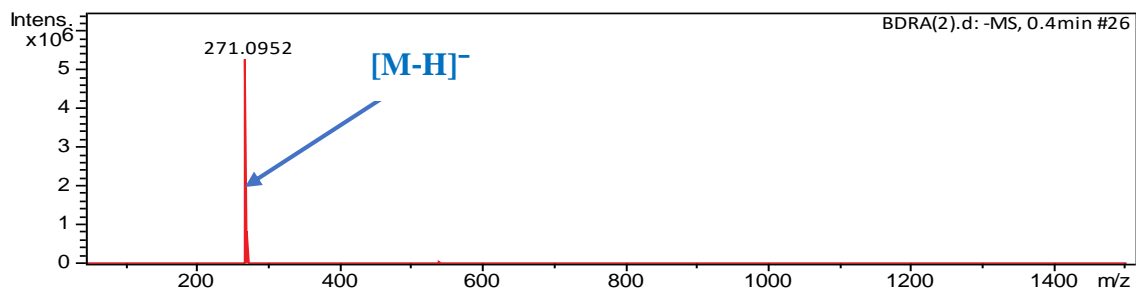
Figure 80: HRESI mass Spectrum of BDRA

The 1H NMR spectrum (**Fig 81**) of **BDRA** shows the presence of two aromatic rings: one trisubstituted phenyl with ABX system at δ_H 7.68 (1H, d, J=7.0 Hz) H-6, 6.31 (1H, d, J=2.5 Hz) H-3 and 6.28 (1H, d, J=12Hz) H-5 and one AA′BB′ system at 7.21 (2H, d, J=8.1 Hz) and 6.85 (2H, d, J=8.1 Hz).

Two signal of singlet protons at δ_H 3.74 (3H, s), 1.49 (3H, s) attributed to the methoxy and methyl group.

One chelated proton at δ_H 12.92 (s, 1H) suggesting the presence of an hydroxyl chelated into the molecule.
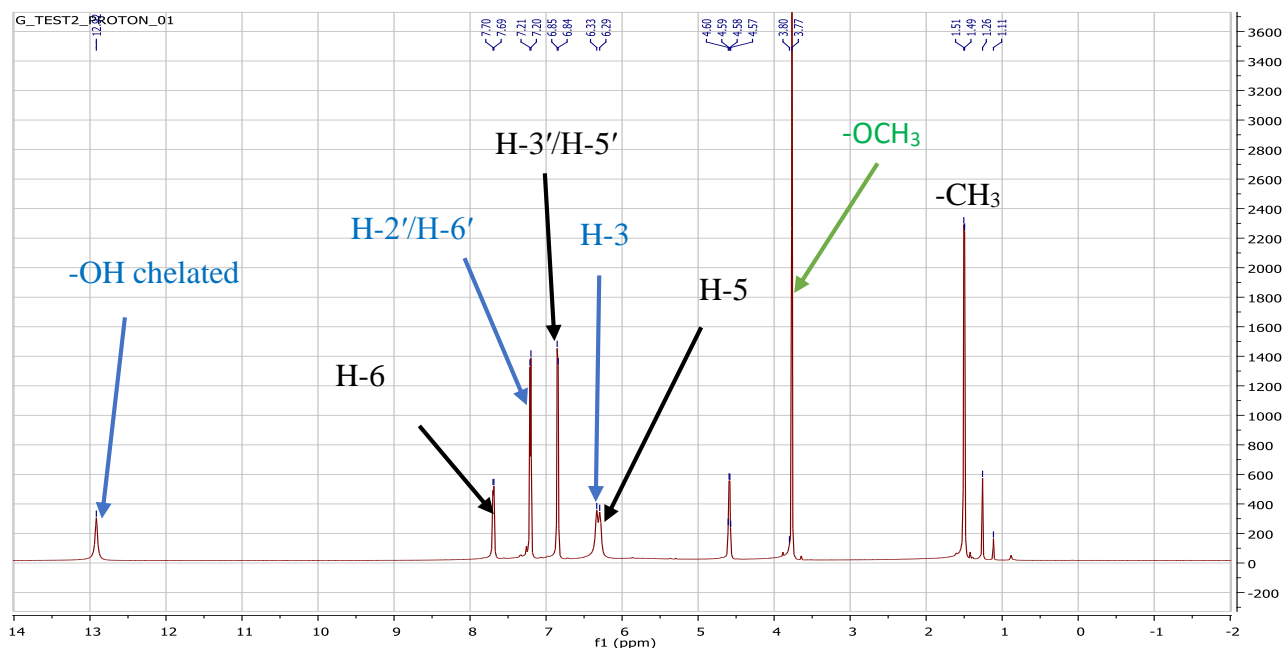
Figure 81: ^{1}H NMR (500 MHz, CDCl₃) spectrum of compound BDRA

The ^{13}C NMR spectrum (**Fig 82**) reveals the presence of sixteen carbon resonances amongst which: two intense signal of two carbons at δ_C 128.5 and 114.4 attributed to AA′BB′ aromatic ring.   One carbonyl of ketone group at δ_C 203.8. Attachment of this carbonyl to the ring A is illustrated by the presence of a hydrogen-bonded hydroxy-group. This attachment was

confirmed by the HMBC spectrum which showed long range correlation between proton H-6 of ring A and carbonyl of ketone group.
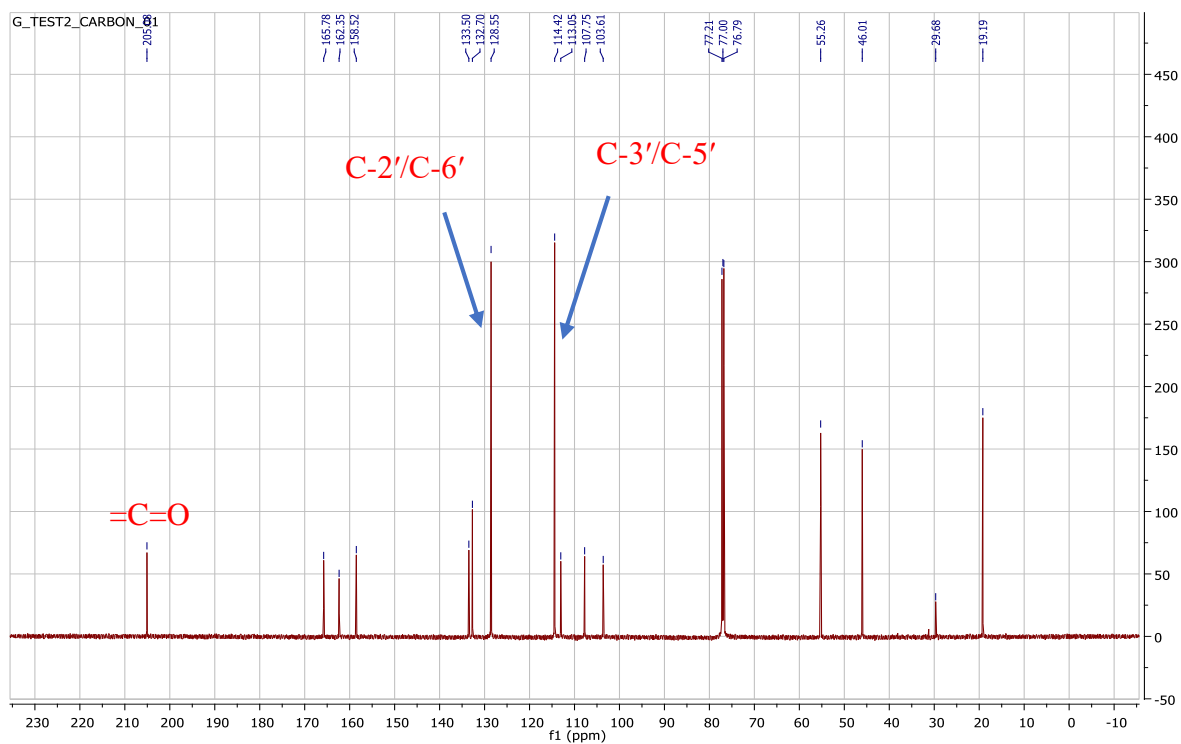
Figure 82: ^{13}C NMR (125 MHz, CDCl$_3$) spectrum of compound BDRA

The linkage of ring B to C-α was done by the help of HMBC spectrum **(Fig 83)** in which proton at δ_H 7.21(2H, d, J=8.1 Hz) (H-2′/H-6′) shows correlation with δ_C 46.6 (C-α) and proton at δ_H 4.59 (dd, J=12.9; 6.2Hz, 1H) (H-α) shows also correlation with δ_C 133.5 (C-1′)

The position of methoxy group was determined by the correlation between δ_H 3.75 of H (-OCH$_3$) with δ_C 158.5 (C-4′).

We also observe correlation between proton H-6 at δ_H 7.68 (d, J=7Hz, 1H) with carbonyl group at δ_C 205.3
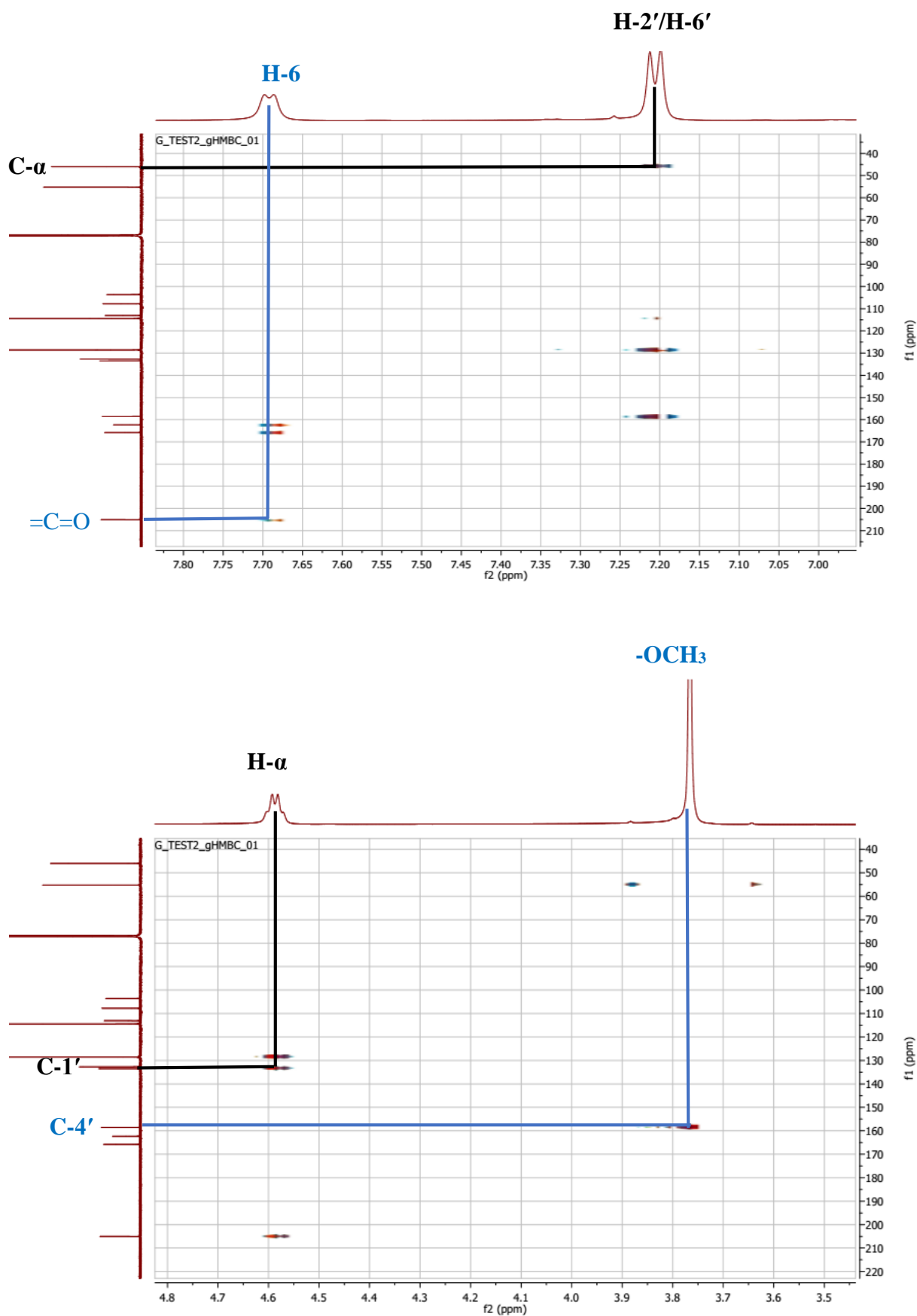
Figure 83: HMBC (CDCl₃) spectrum of compound BDRA

Based on these spectroscopic data and by comparison with the literature (Bezuidenhoudt *et al*. 1980), **BDRA (72)** was identified as **Angolensin** isolated for the first time in 1980.

Table 29: ^{1}H NMR (500 MHz) and ^{13}C NMR (125 MHz) data of BDRA compared to ^{1}H NMR (300 MHz) and ^{13}C NMR (75 MHz) data of angolensin in CDCl$_3$

	BDRA		angolensin (Bezuidenhoudt *et al*. 1980)	
POSITION	δ_C (δppm)	δ_H (δppm, *J* in Hz)	δ_C (δppm)	δ_H (δppm, *J* in Hz)
1	113		111.3	
2	162.4		161.3	
3	103.6	6.31(1H, d, *J*=9Hz)	102.5	6.30 (1H, d, *J*=8.7Hz)
4	166		164.4	
5	107.7	6.28 (1H, d, *J*=9Hz)	106.3	6.23 (1H, d, *J*=8.8Hz)
6	132.7	7.68 (1H, d, *J*=7Hz)	131.3	7.63 (1H, d, *J*=7Hz)
A	46.6	4.59 (1H, dd, *J*=12.9 ; 6.2Hz)	45	4.57 (1H, dd, *J*=12.3 ; 6.1Hz)
B	205.3		203.8	
1′	133.5		132.5	
2′	128.5	7.21 (1H, d, *J*=8.1Hz)	127	7.17 (1H, d, *J*=8.4Hz)
3′	114.4	6.85 (1H, d, *J*=8.1Hz)	113.1	6.77 (1H, d, *J*=8.2Hz)
4′	158.5		157	
5′	114.4	6.85 (1H, d, *J*=8.1Hz)	113.1	6.77 (1H, d, *J*=8.2Hz)
6′	128.5	7.21 (1H, d, *J*=8.1Hz)	127	7.17 (1H, d, *J*=8.4Hz)
α′	19.5	1.49 (3H, s)	18.1	1.47 (3H, s)
1″	55.3	3.74 (3H, s)	54.1	3.73 (3H, s)

2.2.9.2. Identification of the structure of BDb8

BDb8 was obtained as a white powder from the aerial part of *Boswellia dalzielii* in Hex/EA (7/3). It is soluble in DCM and reacted positively with alcoholic ferric chloride (deep purple coloration), suggesting a phenolic nature. The spectroscopic data allows us to identify **BDb8** to structure (**73**) folowing.
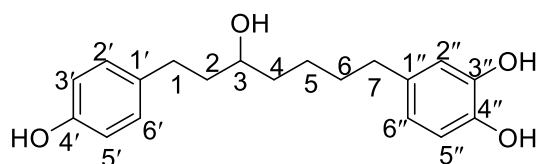
(73)

The High resolution mass spectrum (HRESI) **(Fig 84)** shows [M + Na−H2O]$^+$ ion peak at *m/z* 321.1467 corresponding to a molecular formula of (C$_{19}$H$_{24}$O$_4$) which accounted for 8 unsaturation sites.
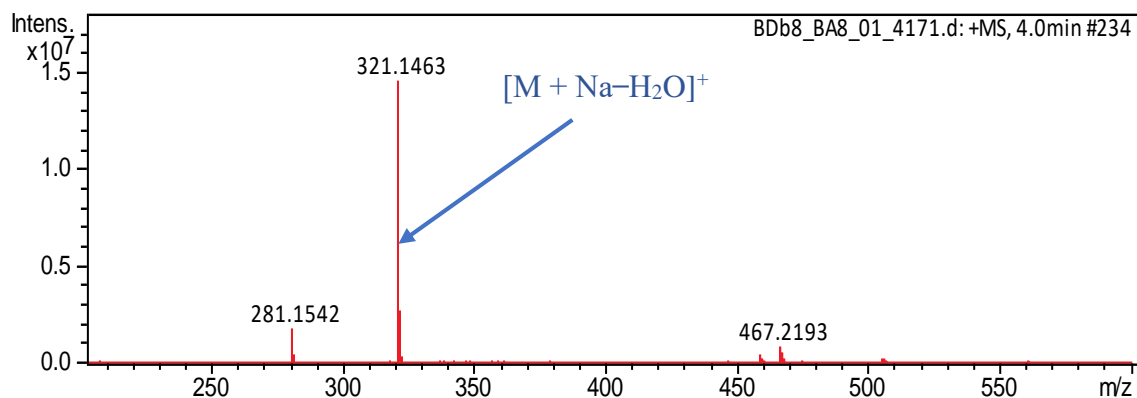
Figure 84: HRESI mass Spectrum of BDb8

The ^{1}H NMR spectrum (**Fig 85**) shows an AA′BB′ and an ABX system in the aromatic region, indicating the 1, 7-diaryl groups to be composed of one 4-hydroxyl- and one 3, 4-dihydroxy- phenyl groups. Still on the ^{1}H NMR spectrum (**Fig 85**) we have six aliphatic protons between 0.70 and 3.10 belongings to long chain.
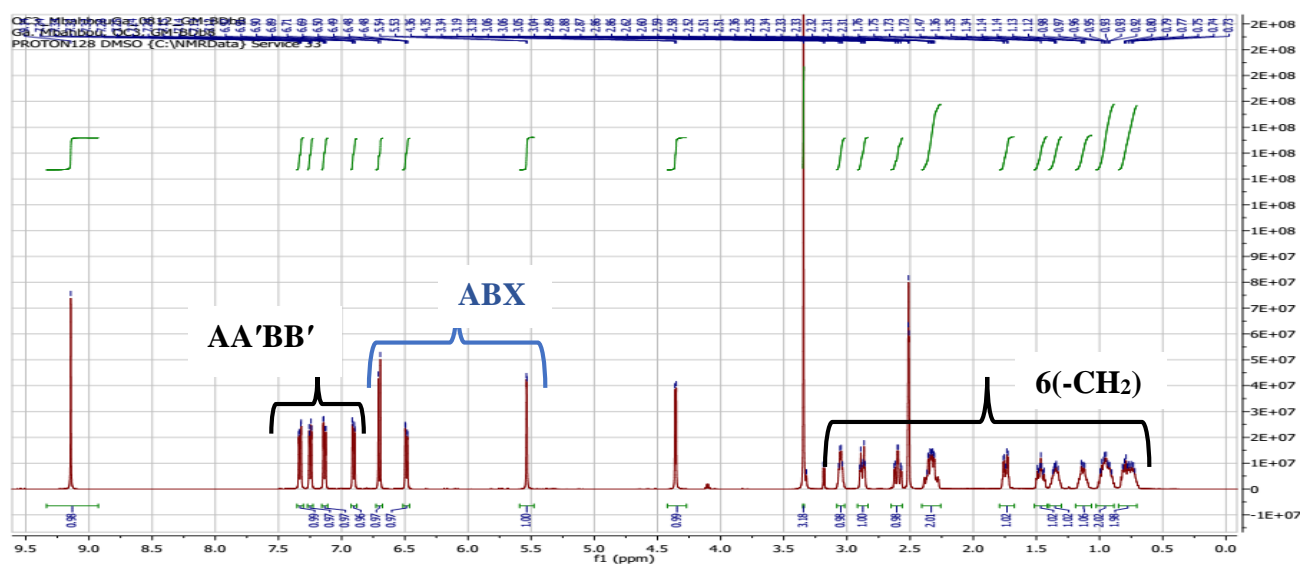
Figure 85: ^{1}H NMR (500 MHz, CDCl$_3$) spectrum of compound BDb8

The proton signals of the aromatic regions were confirmed by analysis of the COSY spectrum (**Fig 86**) in which proton at δ_H 7.25 (dd, $J = 8.2$, 2.0 Hz, H-2′) shows correlation with δ_H 6.91 (dd, $J = 8.2$, 2.5 Hz, H-3′), proton at δ_H 7.33 (dd, $J = 8.3$, 1.9 Hz, H-6′) with δ_H 7.14 (dd, $J = 8.3$, 2.5 Hz, H-5′), this confirms the AA′BB′ system. Also the proton at δ_H 6.49 (dd, $J = 8.1$, 1.6 Hz, H-6″) shows correlation with δ_H 6.70 (d, $J = 8.1$ Hz, H-5″) and δ_H 5.54 (d, $J = 1.6$ Hz, H-2″) confirming ABX system.
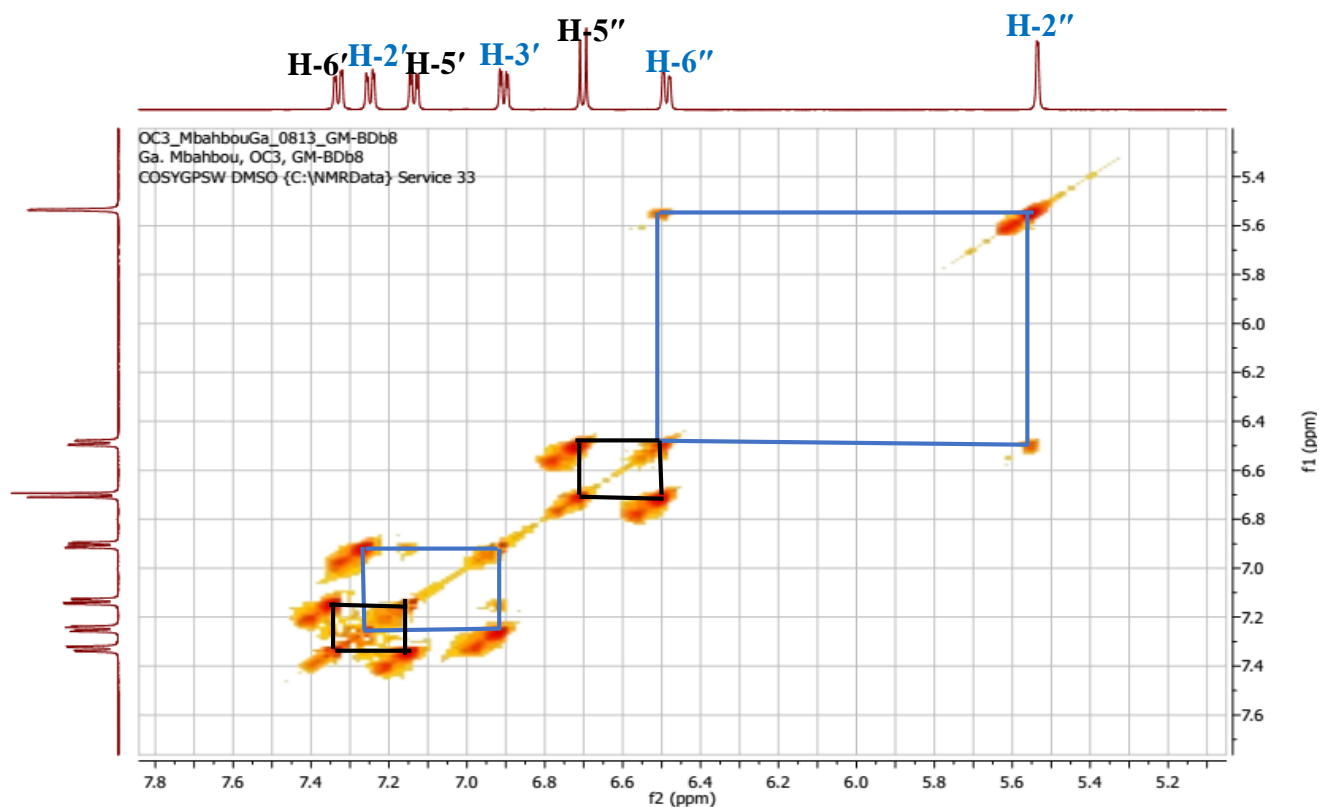
Figure 86: COSY (CDCl₃) spectrum of compound BDb8

The ^{13}C NMR (**Fig87**), and DEPT 135(**Fig88**) spectra indicated the presence of nineteen carbons among which 5 quaternary carbons, eight tertiary carbons and six secondary carbons belongings to aliphatic region.

The ^{13}C NMR spectrum (**Fig87**), showS signals of AA′BB′ system at δ_C 132.1 (C-2′), δ_C 130.6 (C-6′), δ_C 123.2 (C-3′) and δ_C 124.3 (C-5′), signals of ABX system at δ_C 122.2 (C-6″), δ_C 116.7 (C-5″) and δ_C 116.3. (C-2″).
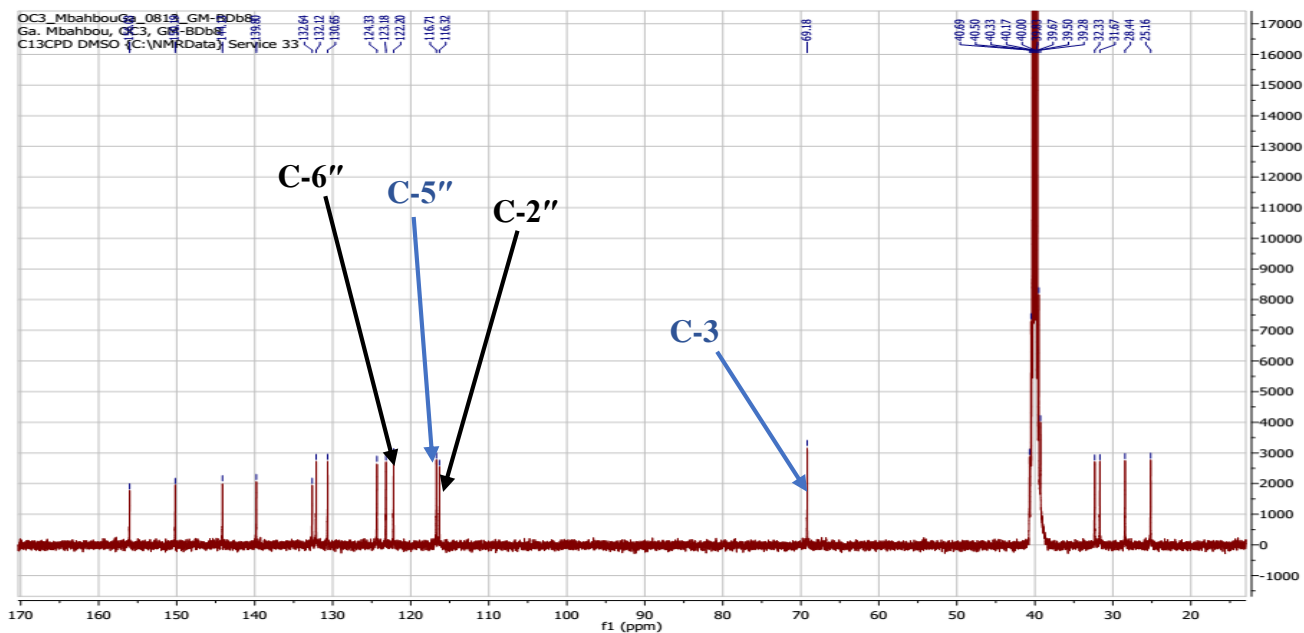
Figure 87: ^{13}C NMR (125 MHz, CDCl$_3$) spectrum of compound BDb8
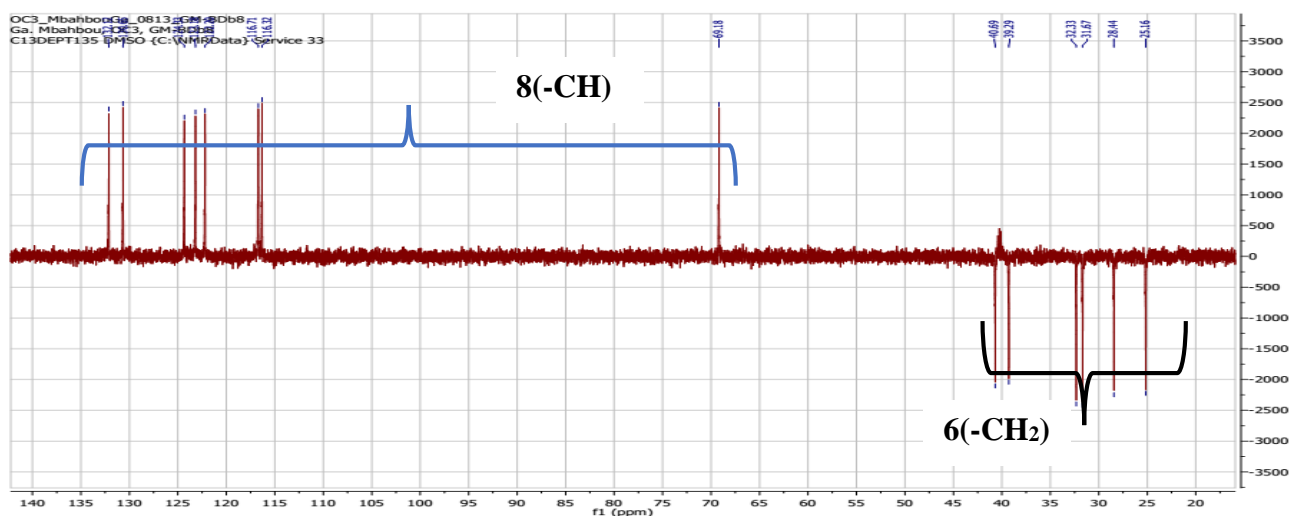
Figure 88: DEPT 135 (125 MHz, CDCl$_3$) spectrum of compound BDb8

The linkage of two aromatics rings with the long chain was done by the HMBC spectrum (**Fig 89**) in which the proton H-1 of aliphatic region shows correlation with (C-1′), (C-2′) and (C-6′) of AA′BB′ system and the proton H-7 with (C-1″), (C-2″) and (C-6″) of ABX system.

The OH group was positioned at C-3 by the HMBC spectrum (**Fig90**) in which the OH proton shows correlation with δ_C 69.1 (C-3), δ_C 40.6 (C-2) and δ_C 39.2 (C-4).
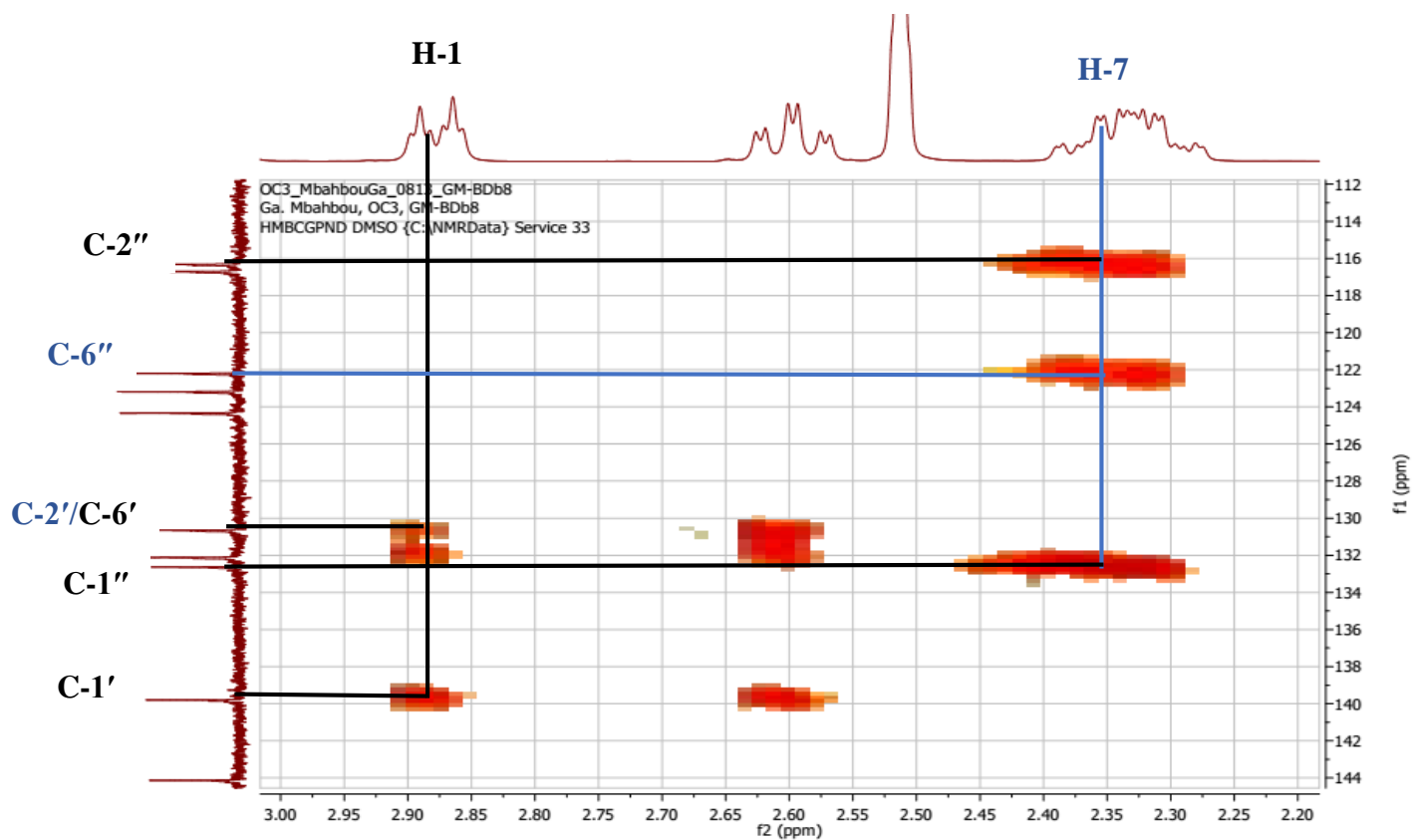
Figure 89: HMBC (CDCl₃) spectrum of compound BDb8
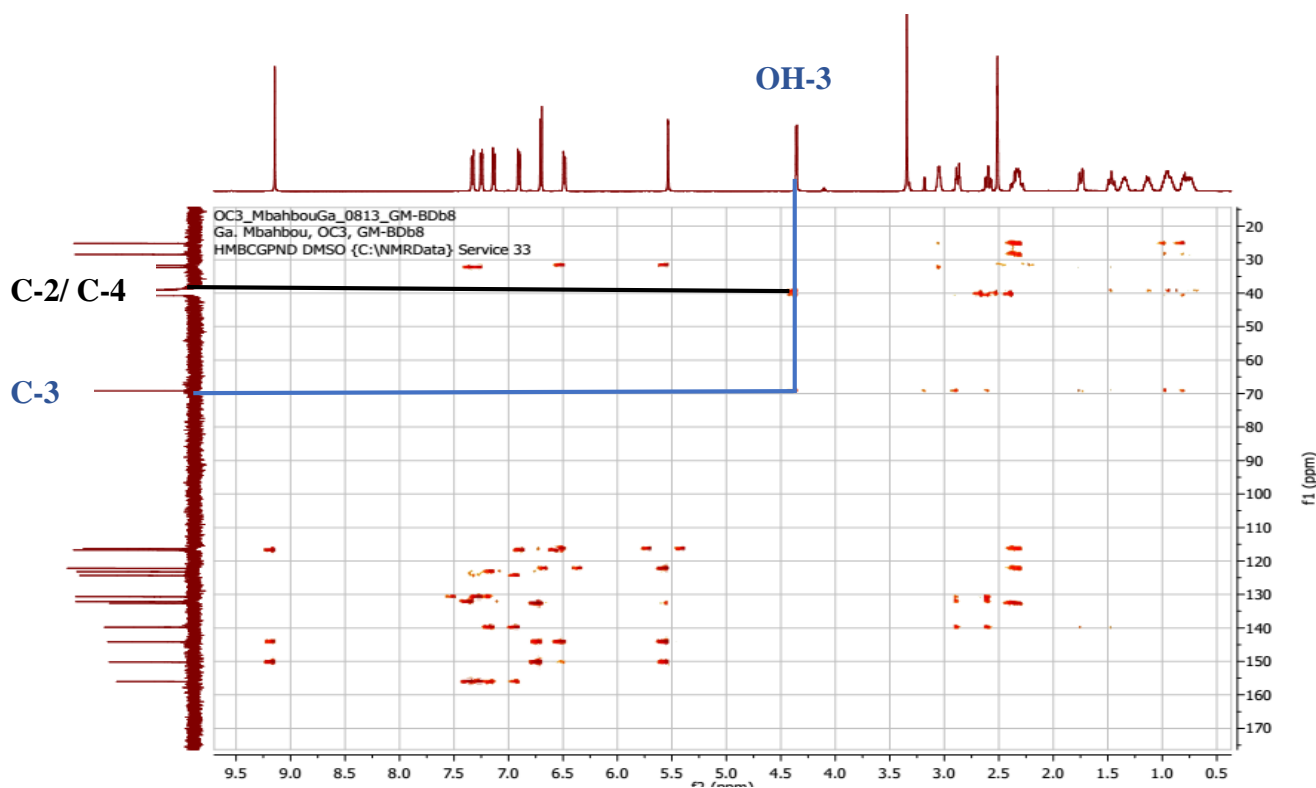
Figure 90: Expanded HMBC (CDCl₃) spectrum of compound BDb8

The above spectroscopic data compared with data from literature (**Yi-Chun *et al*, 1994**; **Jiang-Bo *et al*., 2011**) led to the attribution the name of 7-(3,4-Dihydroxyphenyl)-1-(4-hydroxyphenyl)-3-heptanol **(73)** to **BDb8**.

Table 30: ^{1}H NMR (500 MHz) and ^{13}C NMR (125 MHz) data of BDb8 and ^{1}H NMR (400 MHz) and ^{13}C NMR (100 MHz) data of 7-(3,4-Dihydroxyphenyl)-1-(4-hydroxyphenyl)-3-heptanol in CDCl₃

POSITION	BDb8 δ_C	δ_H	7-(3,4-Dihydroxyphenyl)-1-(4-hydroxyphenyl)-3(*R*)-heptanol (Yi-Chun *et al*, 1994; Jiang-Bo *et al*., 2011) δ_C	δ_H
1	32.3	2.88 (1H, dt, *J* = 12.7, 3.6 Hz) 2.60 (1H, td, *J* = 12.7, 3.7 Hz)	32.1	2.64 (1H, ddd, 5.7, 9.5, 13.8) 2.51 (1H, ddd, 7.0, 9.5, 13.8)
2	40.7	1.74 -1 .45 (2H, m)	40.6	1.70–1.59 (2H, m)
3	69.2	3.05 (1H, dd, *J* = 9.9, 4.9 Hz)	71.7	3.49 (m)
4	39.3	0.99-0.80 (2H, m)	38.2	1.50–1.40 (2H, m)
5	25.4	0.94-0.74(2H, m)	26.3	1.50–1.28 (2H, m)
6	28.4	135-1.13 (2H, m)	32.9	1.57–1.51 (2H, m)
7	31.7	2.39 (2H, m)	36.2	2.44 (t, 7.5)
1′	139.8		134.6	
2′	132.1	7.25 (1H, dd, *J* = 8.2, 2.0 Hz)	130.3	6.98 (1H, br d, *J* = 8.2 Hz)
3′	123.1	6.91 (1H, dd, *J* = 8.2, 2.5 Hz)	116.1	6.67 (1H, br d, *J* = 8.2 Hz)
4′	156.0		156.3	
5′	124.3	7.14 (1H, dd, *J* = 8.3, 2.5 Hz)	116.1	6.67 (1H, br d, *J* = 8.5 Hz)
6′	130.6	7.33 (1H, dd, *J* = 8.3, 1.9 Hz)	120.6	6.98 (1H, br d, *J* = 8.5 Hz)
1″	132.6		135.6	
2″	116.3	5.54 (1H, d, *J* = 1.6 Hz)	116.2	6.59 (1H, d, *J* = 2.0 Hz)
3″	150.2		146.0	
4″	144.1		144.1	
5″	116.7	6.70 (1H, d, *J* = 8.1 Hz)	116.5	6.64 (1H, d, *J* = 8.0 Hz)
6″	122.2	6.49 (1H, dd, *J* = 8.1, 1.6 Hz)	120.6	6.46 (1H, dd, *J* = 8.0, 2.0 Hz)

2.2.9.3. Elucidation of the structure of BDCA10

BDCA10 was isolated from the EtOAc/MeOH (8/2, v/v) fraction as brown paste soluble in acetone. The spectroscopic data allows us to identify **BDCA10** to structure (**74)** folowing.

(74)
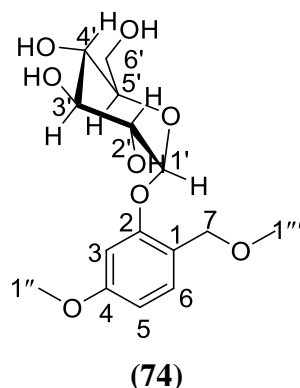
Indeed the High resolution mass spectrum (HRESI) (**Fig 91**) shows [M+Na]$^+$ ion peak at *m/z* 353.1203 (calcd. 353.1212) compatible with molecular formula ($C_{15}H_{22}O_8Na$), with five double bond equivalent
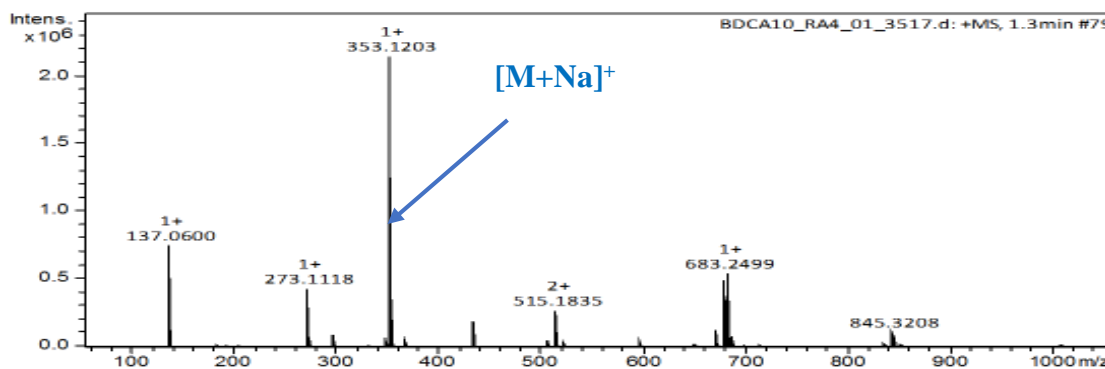
Figure 91: HRESI mass Spectrum of BDCA10

The ^{1}H NMR spectrum (**Fig 92**) shows the presence of one trisubstituted benzene ring with ABX system at δ_H 7.23 (1H, d, *J*=8.4 Hz; H-6), 6.84 (1H, d, *J*=2.5 Hz; H-3) and 6.60 (1H, dd, *J*=8.4 and 2.5 Hz; H-5). Two signal of three singlet protons at δ_H 3.30 (3H, s, H-1‴), 3.79 (3H, s, H-1″) attributed to two methoxy group. The ^{1}H NMR spectrum (**Fig 92**) shows one anomeric proton at δ_H 4.87 (1H, d, *J* = 5.1, H-1″) suggesting the presence of sugar unit. The analysis of coupling constants and chemical shifts allowed to identify the presence of the α-*D*-glucopyranoside moiety in the molecule. Two protons of hydroxymethylenes were observed at 4.60 (1H, d, *J*=11.8 Hz, H-7a) and 4.35 (1H, d, *J*=11.8 Hz, H-7b) attributed to aglycone unit and two others at 3.90 (1H, m, H-6a′) and 3.71 (1H, m, H-6b′) attributed to sugar moiety.
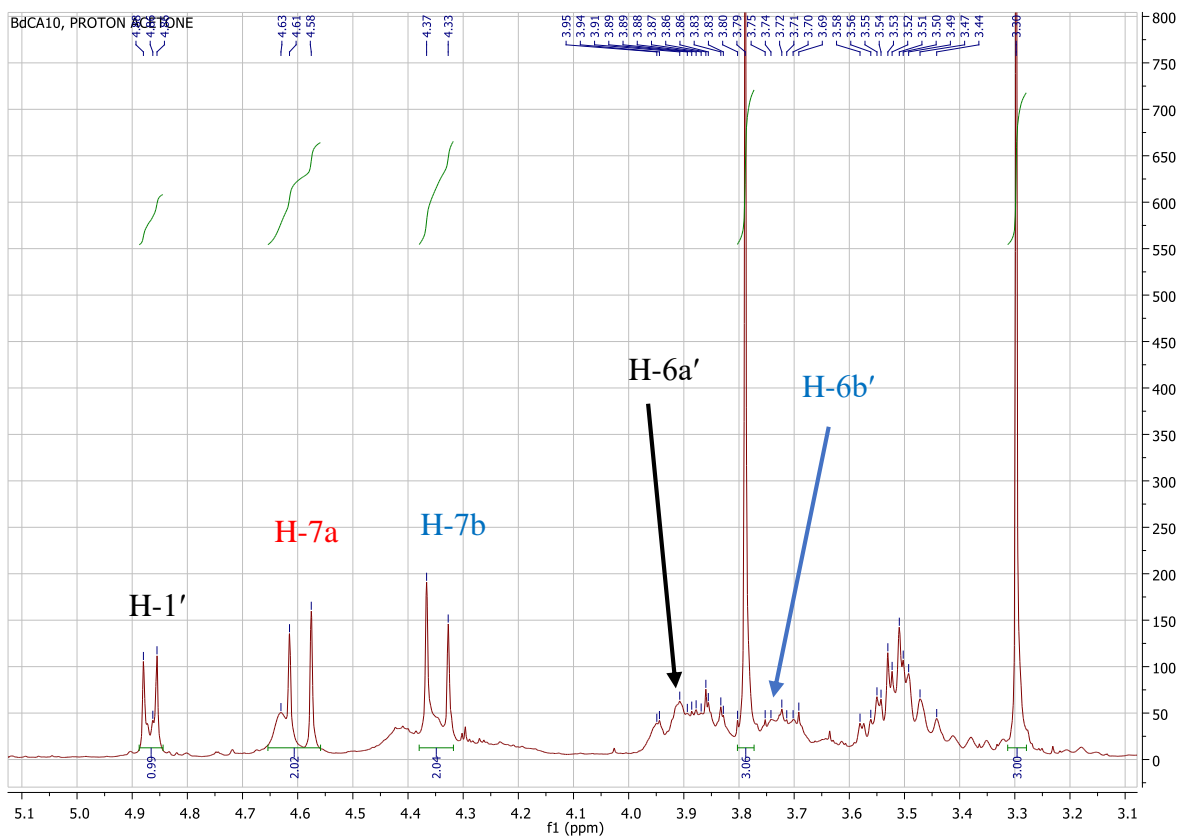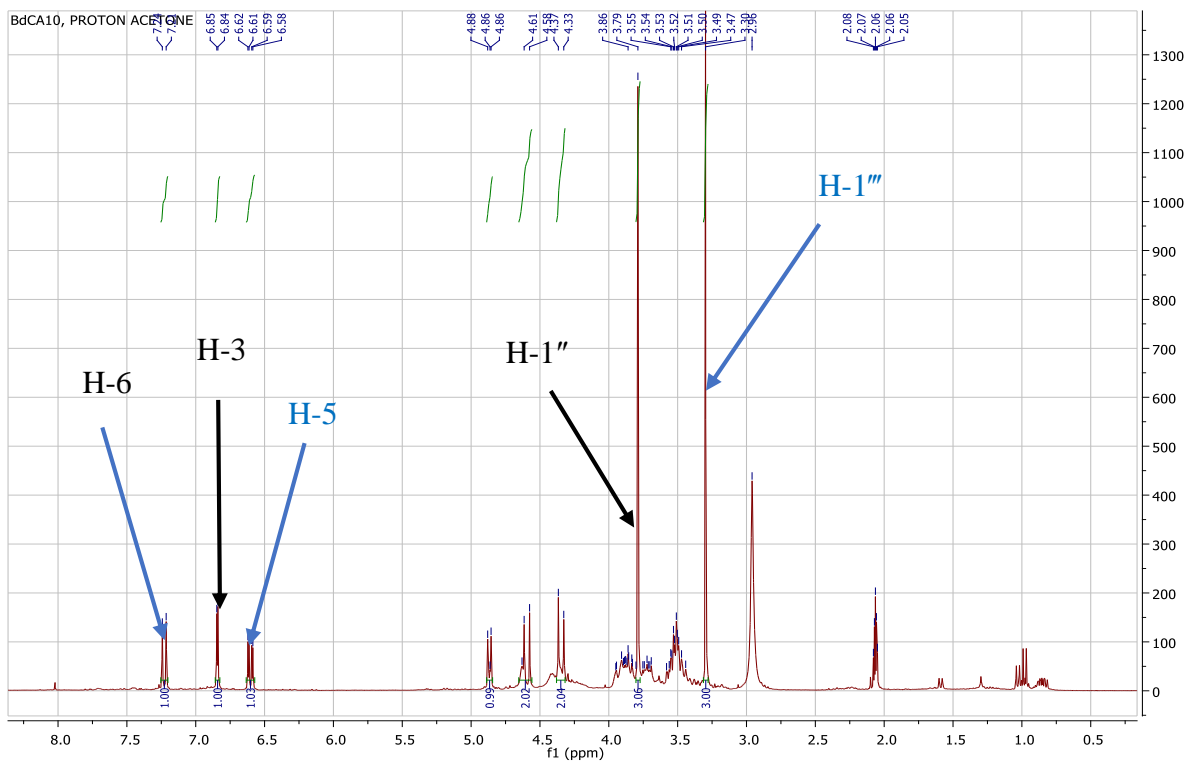
Figure 92: ^{1}H NMR (300 MHz, acetone) spectrum of compound BDCA10

The broad band decoupled ^{13}C NMR (**Fig 93)** and DEPT spectrum (**Fig 99)** reveals the presence of two oxymethyls, two methylenes, eight methines and three quaternary carbons.

Four signal of methine appeared between δ_C 71.4 and 78 attributed to glucose unit. The anomeric carbon appearing at δ_C 103.6 was assigned to C-1′ indicating the *α-D*-conformation for glucose.
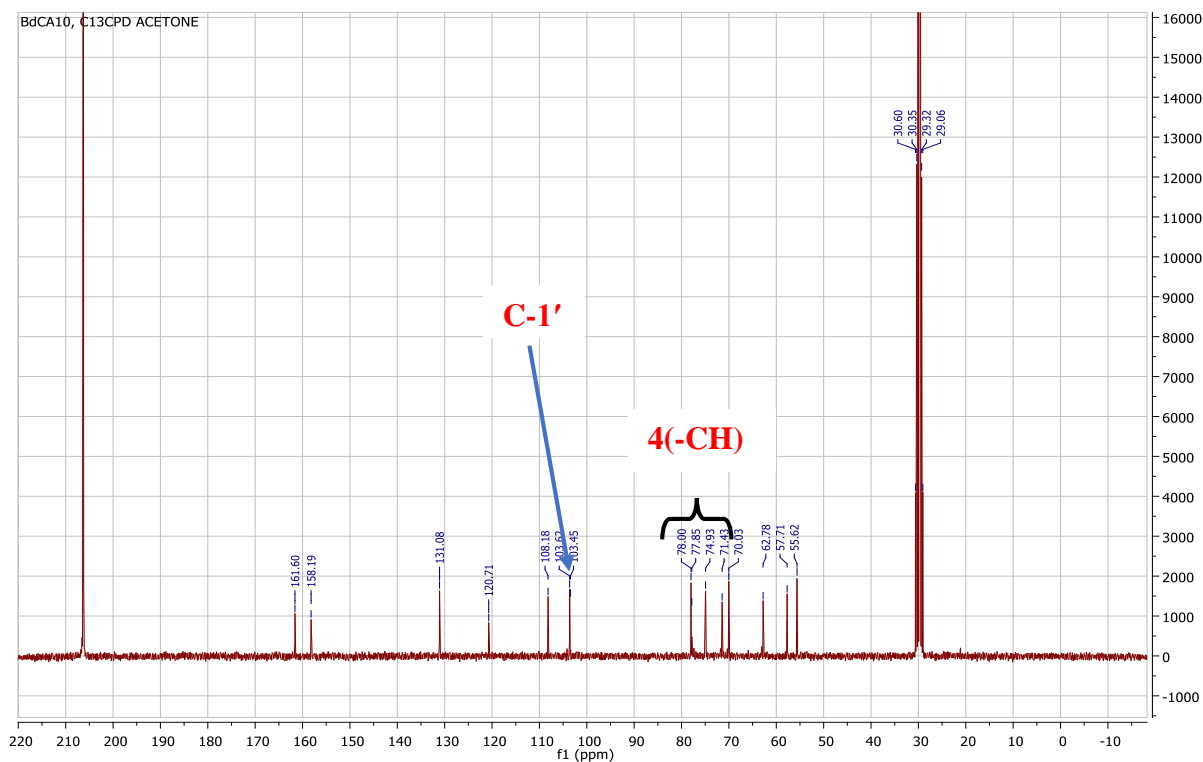
Figure 93: ^{13}C NMR (75 MHz, acetone) spectrum of compound BDCA10

The DEPT spectrum (**Fig 94)** shows carbon of hydroxymethylene at δ_C 70.0 (C-7) attributed to the aglycone, the confirmation of hydroxymethylene of benzyl was established by the help of HMBC spectrum in which these protons at δ_C 4.60 and δ_C 4.35 showed correlation with the C-2, C-6, C-1, C-1‴ at δ_C 158.2, 131, 120.7, 57.7 respectively.

The position of methoxy group have also done with the HMBC correlation in which protons of methoxy at (δ_H 3.79) showed correlation with the C-4 carbon at δ_C 161.6. The linkage between the glucose unit and the aglycone were established by the help of HMBC spectrum (**Fig 95)** in which the anomeric proton (δ_H 4.87) of glucose showed correlation with the C-2 quaternary carbon at δ_C 158.2 of the aglycone.
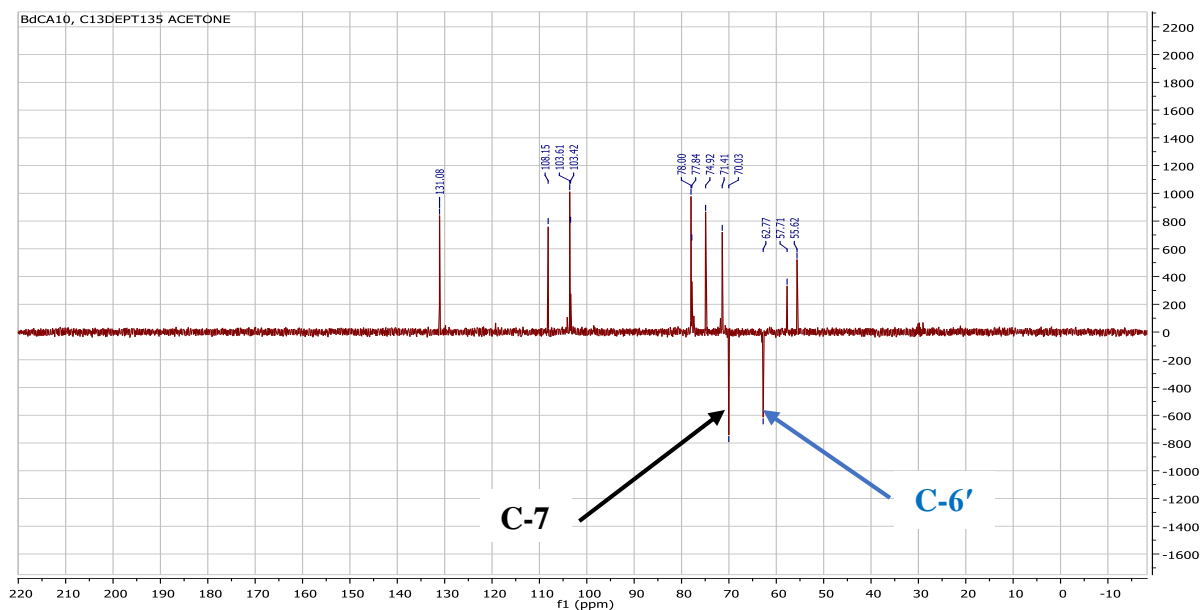
Figure 94: ^{13}C NMR (acetone) spectrum of compound BDCA10
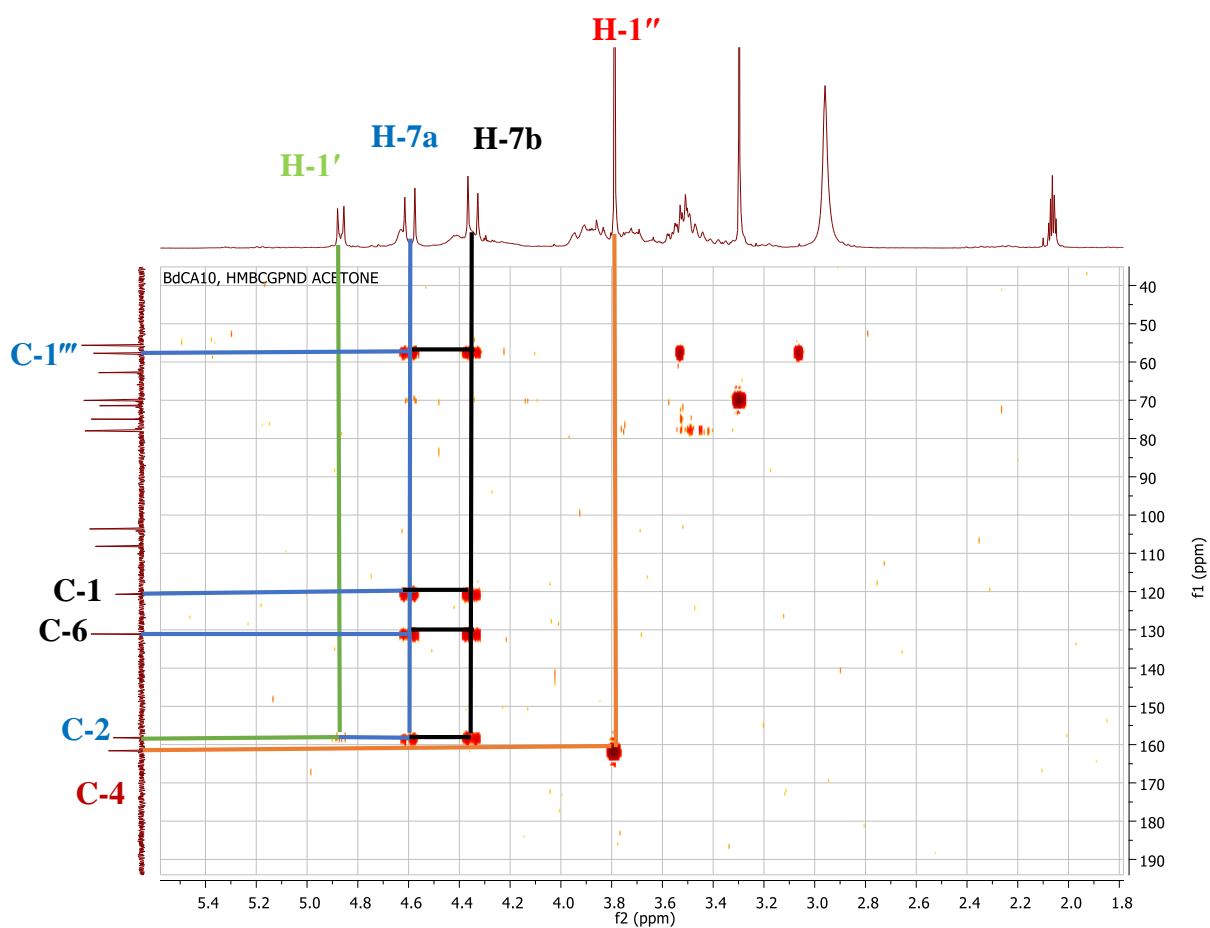
Figure 95: HMBC (acetone) spectrum of compound BDCA10

The spectroscopic data of **BDCA10** was similar to **BDCA8 (González et al. 2019)**, (**Chun-Yan et al. 2007**), the main difference between **BDCA10** and **BDCA8** is the methoxy group at position 1‴. Based on this evidence compound **BDCA10** was concluded to be 4-methoxy-1-(methoxymethyl)-2-O-α-D-Glucopyranosyl benzene namely dalzienoside **(74)** characterised for the first time.
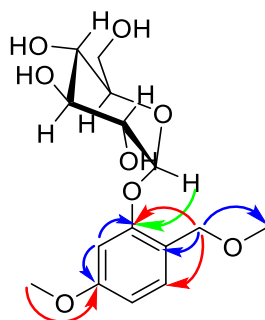
(74)

Table 31: ^{1}H NMR (300 MHz, acetone) and ^{13}C NMR (75 MHz, acetone) data of BDCA10

		BDCA10		
Position	**δ_H (δppm, J in Hz)**	**δ_C (δppm)**	**HMBC**	**COSY**
1	-	120.7		
2	-	158.2		
3	6.84 (1H, d, *J*=2.5 Hz)	103.5	C-5, C-1, C-2, C-4	H-3→ H-5
4	-	161.6		
5	6.60 (1H, dd, J=8.4, 2.5 Hz)	108.2	C-3, C-1	H-5→ H-6
6	7.23 (1H, d, *J*=8.4 Hz,)	131	C-7, C-2, C-4	H-6→H-5
7	4.60 (1H, d, *J*=11.8 Hz, 7a)	70.1	C-1‴, C-1, C-6,C-2	a→b
	4.35 (1H, d, *J*=11.8 Hz, 7b)			
Glucopyranoside				
1′	4.87 (1H, d, *J*=5.1 Hz,)	103.6	C-2	H-1′→H-2′
2′	3.48 m	74.9		
3′	3.52 m	77.8		
4′	3.46 m	71.4		
5′	3.53 m	78		
6′	3.90 m, 6a′	62.8		a′→b′
	3.71 m, 6b′			
1″	3.79 (3H, s)	55.6	C-4	
1‴	3.30 (3H, s)	57.7	C-7	

2.2.9.4. Identification of the structure of BDCA8

BDCA8 was isolated from the EtOAc/MeOH (8/2, v/v) fraction as brown paste soluble in acetone. On the basis of NMR data, its molecular formula was deduces as $C_{14}H_{20}O_8$ with five double bond equivalent. The spectroscopic data allows us to identify **BDb8** to structure (**75**) following.
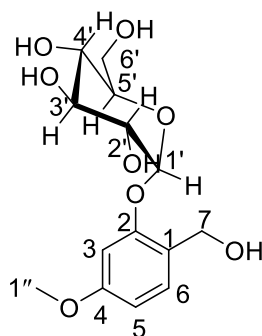
(75)

The ^1H NMR **(Fig 96)** and ^{13}C NMR **(Fig 97)** spectra data are very similar to those of **BDCA10**. The difference was the absence of the one methoxy group which appeared as singlet at δ_H 3.30 (3H, s, H-1‴) and the carbon of this methoxy group at δ_C 57.7 (C-1‴)

The DEPT spectrum **(Fig 98)** reveals also the absence of one methyl at δ_C 57.7 (C-1‴)
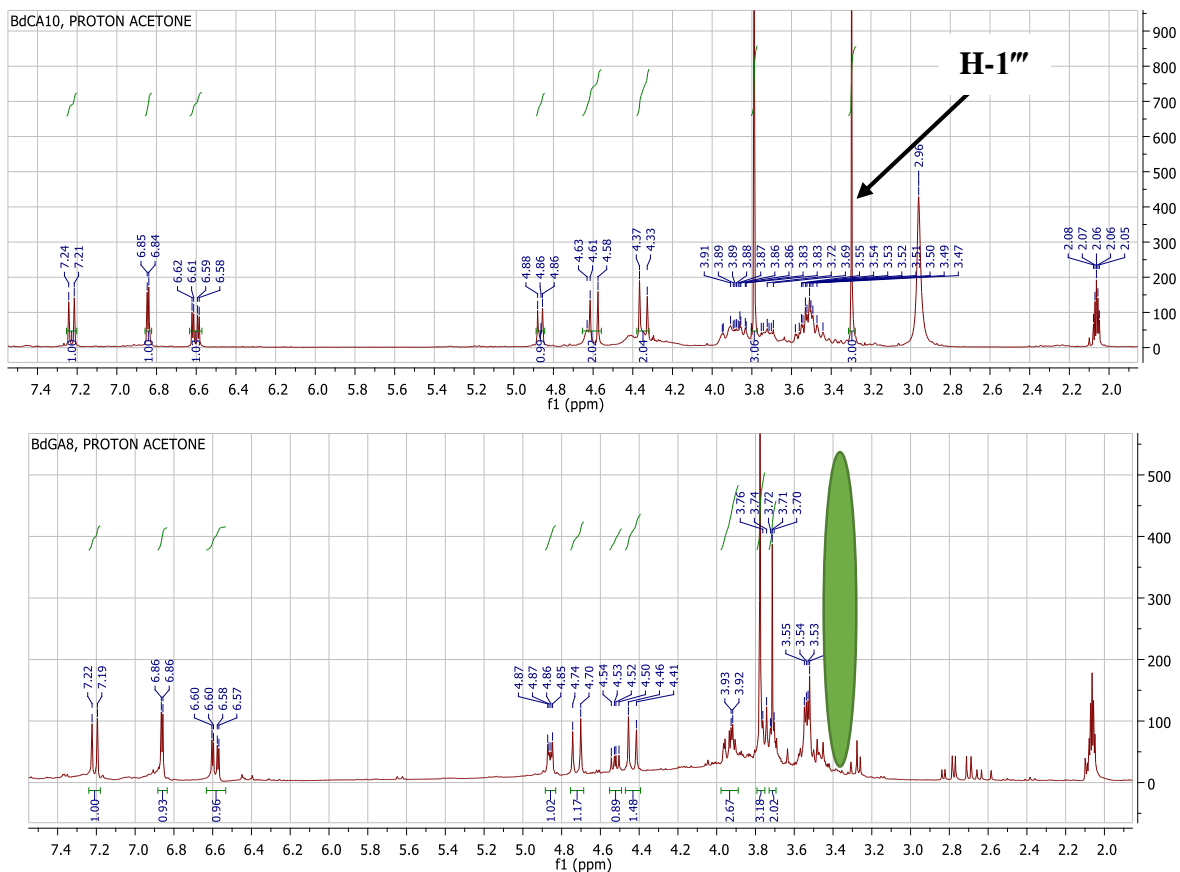
Figure 96: ^{1}H NMR (300 MHz, acetone) spectrum of compound BDCA10 and BDCA8
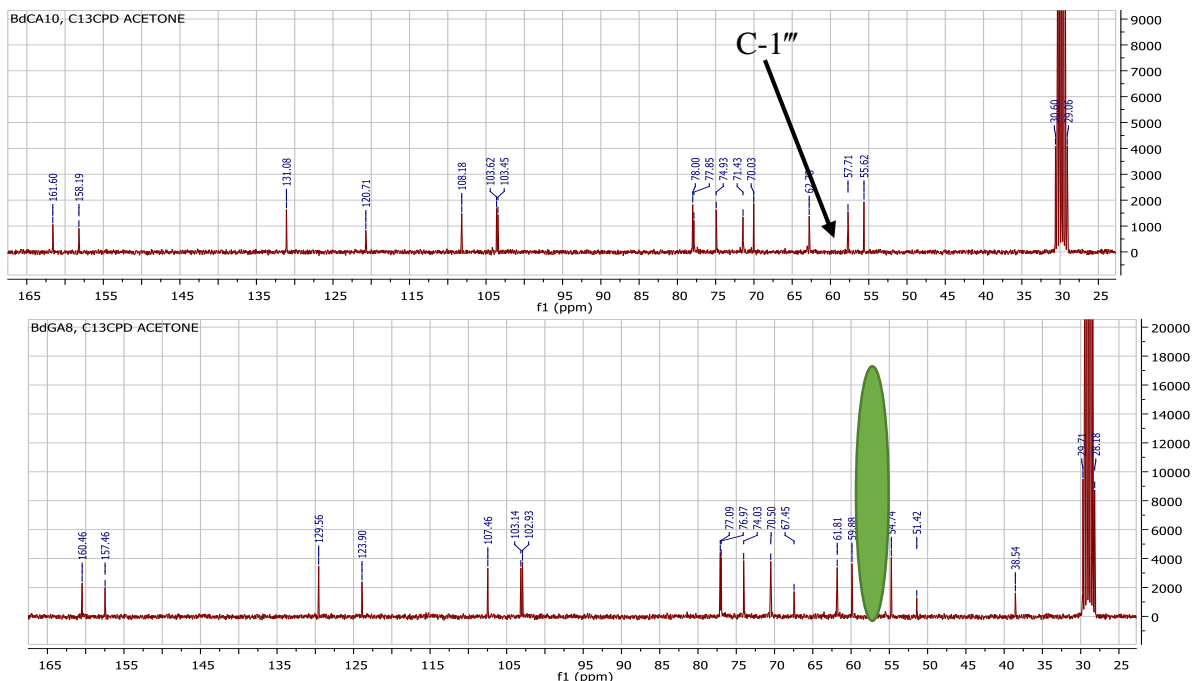
Figure 97: ^{13}C NMR (75 MHz, acetone) spectrum of compound BDCA10 and BDCA8
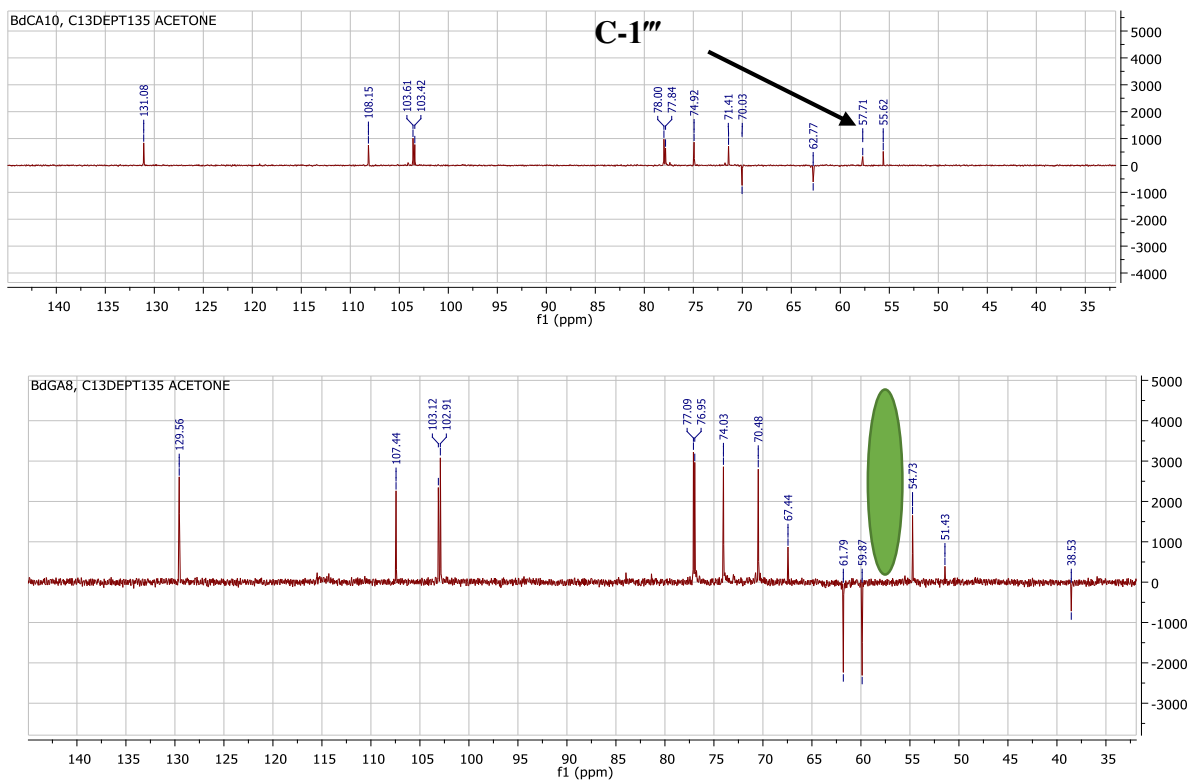
Figure 98: DEPT (acetone) spectrum of compound BDCA10 and BDCA8

On the basis of the above data and by comparison with the data of the literature **(Chun-Yan et al. 2007)**, **BDCA8** was concluded to be 4-methoxy-2-*O*-α-*D*-glucopyranosylphenyl methanol (**75**) **(Chun-Yan et al. 2007)**.

Table 32: ^{1}H NMR (300 MHz) and ^{13}C NMR (75 MHz) data of BDCA8 in acetone compared with ^{1}H NMR (400 MHz) and ^{13}C NMR (100 MHz) data of 4-Hydroxymethylphenyl-*β-D*-glucopyranoside

	BDCA8		4-Hydroxymethylphenyl-*β-D*-glucopyranoside (González *et al*. 2019)	
POSITION	δ_C (δppm)	δ_H (δppm, J in Hz)	δ_C (δppm)	δ_H (δppm, J in Hz)
1	123.9		158.5	
2	157.5		129.4	7.06 (2H, d, J = 8.6Hz)
3	102.9	6.84 (1H, d, J=2.4 Hz)	117.7	7.26 (2H, d, J = 8.6 Hz)
4	160.5		136.7	
5	107.5	6.59 (1H, dd, J = 8.3, 2.5 Hz)	117.7	7.26 (2H, d, J = 8.6 Hz, H-3, H-5)
6	129.6	7.21 (1H, d, J=8.3 Hz)	129.4	7.06 (2H, d, J= 8.6Hz)
7	61.8	4.43 (1H, d, J = 12.4 Hz, H-7b)	64.8	3.70 (1H, dd, J = 5.2, 12.0 Hz, H-7b)
		4.72 (1H, d, J = 12.4 Hz, H-7a)		3.88 (1H, dd, J = 2.0, 12.0 Hz, H-7a)
Glucopyranoside				
1′	103.1	4.86 (1H, d, J=5.3 Hz)	102.5	4.88 (1H, d, J = 7.5 Hz, H-1')
2′	74	3.45-3.52 (4H, m)	75.0	3.40–3.45 (4H, m)
3′	76.9	3.45-3.52 (4H, m)	78.2	3.40–3.45 (4H, m)
4′	70.9	3.45-3.52 (4H, m)	71.4	3.40–3.45 (4H, m)
5′	77.1	3.45-3.52 (4H, m)	78.0	3.40–3.45 (4H, m)
6′	60		62.5	
1″	54.7	3.76 (s, 3H)	-	-

2.2.9.5. Identification of the structure of BDF5B

BDF5B was isolated from the EtOAc/MeOH (8/2, v/v) fraction from the extract of stem bark of *Boswellia dalzielii* as a light brown gummy material soluble in MeOH. The High resolution mass spectrum and spectroscopic data allows us to allocate **BDF5B** tothe structure (**76**) below.
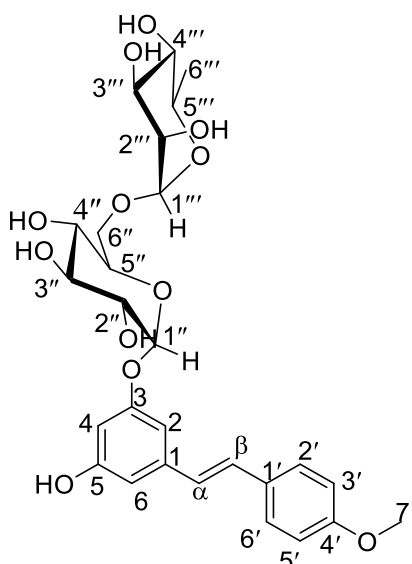
(76)

The High resolution mass spectra (HRESI) **(Fig 99)** showing [M+Na]$^+$ ion peak at *m/z* 573.1949 corresponding to the molecular formula ($C_{27}H_{34}O_{12}$), which indicated 11 double bond equivalent.
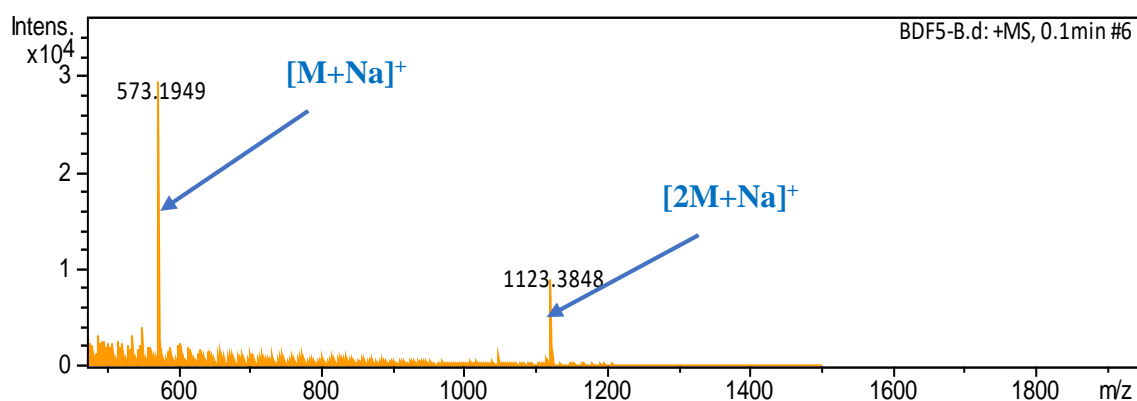
Figure 99: HRESI mass Spectrum of BDF5B

The ^{1}H NMR spectrum **(Fig 100)** of **BDF5B**, shows two anomeric protons at δ_H 4.75 (s) and 4.90 (d, *J* =7.3 Hz, 1H) and a methyl doublet at δ_H 1.22 (d, *J* =6.2 Hz, 3H), suggesting the presence of two sugars, *α-L*-rhamnopyranose and *β-D*-glucopyranose **(Atta-ur-Rahman et al. 2005)**;

-One methoxy group at δ_H 3.80 (3H, s)
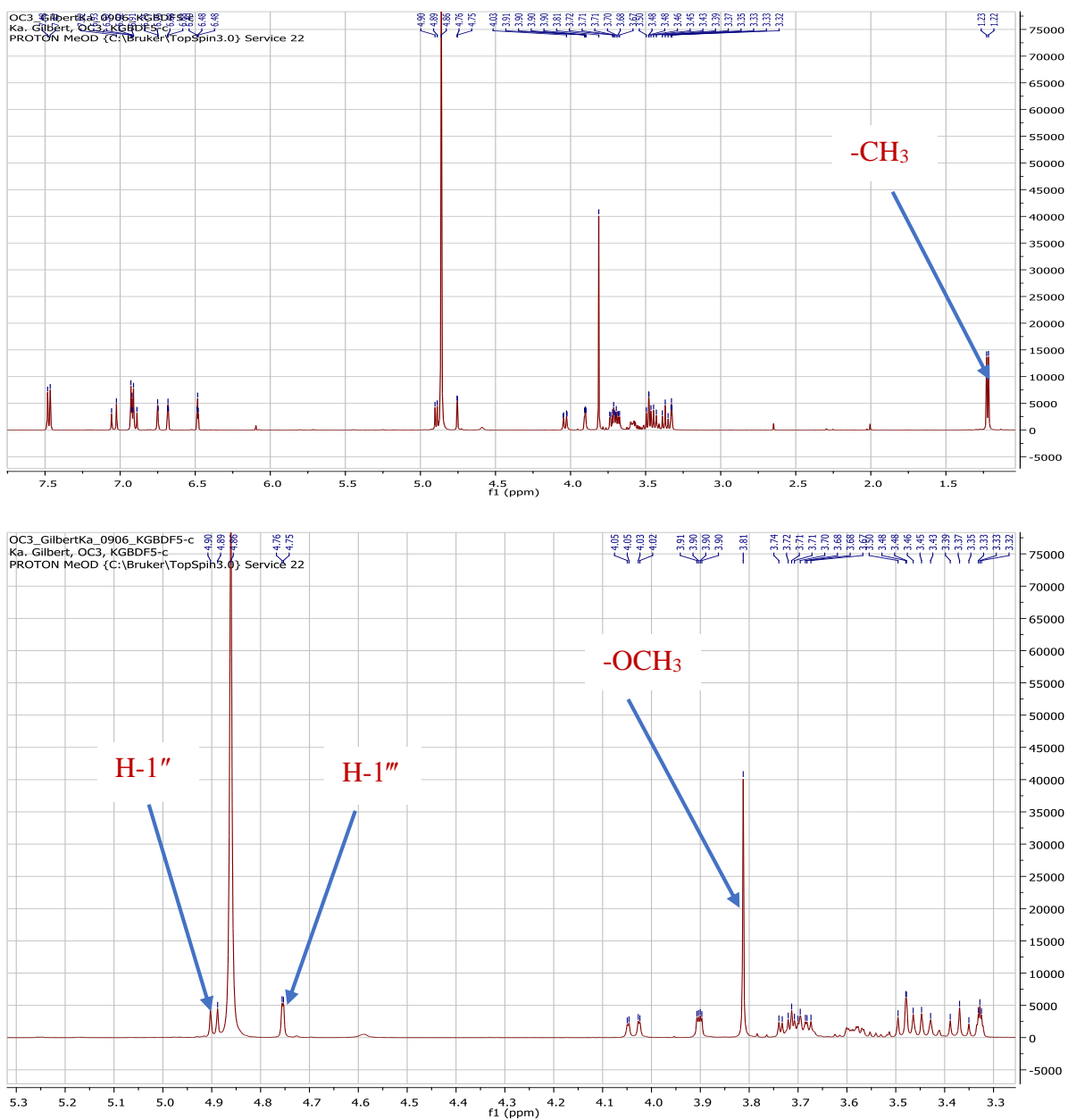
Figure 100: ¹H NMR (500 MHz, CD₃OD) spectrum of compound BDF5B

Still on the ¹H NMR spectrum (**Fig 101**) we observe the signals for a 1, 3, 5-trisubstituted aromatic ring at δ_H 6.48 (br, s), 6.68 (br, s), and 6.74 (br, s) and a *para*-disubstituted aromatic ring at δ_H 7.47 (d, J =8.5 Hz, 2H) and 6.91 (d, J =8.5 Hz, 2H)

- Two olefinic protons at δ_H 7.04 (d, J =16.0 Hz, 1H) and 6.89 (d, J =16.0 Hz, 1H). The large coupling constant (16.0 Hz) indicated the presence of *trans*-olefinic coupling.

- The anomeric proton at δ_H 4.90 shows a coupling constant of 7.3 Hz, indicating the presence of a *β-D*-glucosidic linkage.
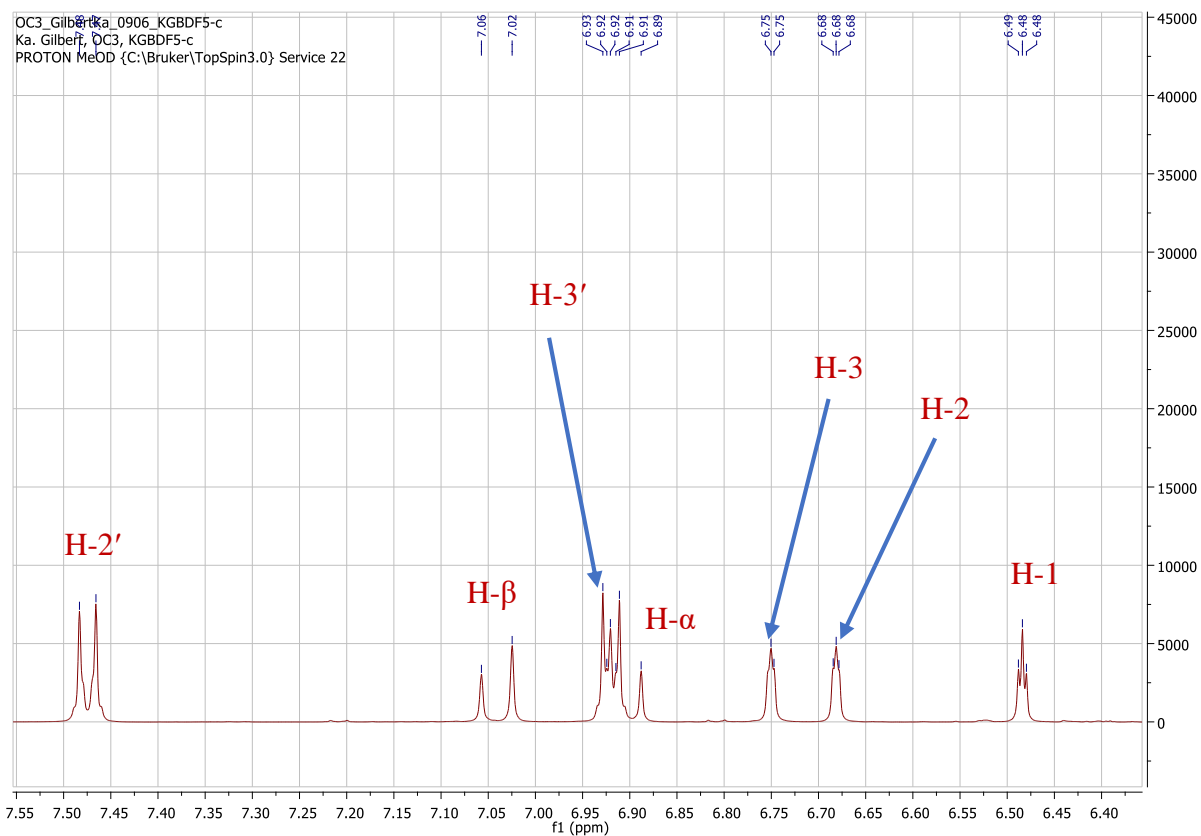
Figure 101: Expanded ^{1}H NMR (500 MHz, CD$_3$OD) spectrum of compound BDF5B

The ^{13}C NMR spectrum **(Fig 102)** reveals the presence of twenty-seven carbon resonances and exhibited two anomeric carbon signals at δ_C 100.8, 101.0 attributed respectively to C-1″ and C-1‴. Five signals of methine appeared between δ_C 71.0 - 76.6 attributed to glucopyranoside unit and three others methine between δ_C 70.0 -72.7 and one signal of methyl at δ_C 16.4 (C-6‴) attributed to rhamnopyranoside unit.

- Two olefinics carbons at δ_C 128.3 (C-β) and δ_C 126.5 (C-α). The AA′BB′ system at δ_C 127.4 (C-2′/C-6′) and δ_C 114.0 (C-3′/C-5′) and the ABX system at 106.4 (C-2), (106.8) (C-6) and (102.8) (C-4). These observations suggested that the aglycone unit could be a *trans*-stilbene **(Atta-ur-Rahman et al. 2005)**.
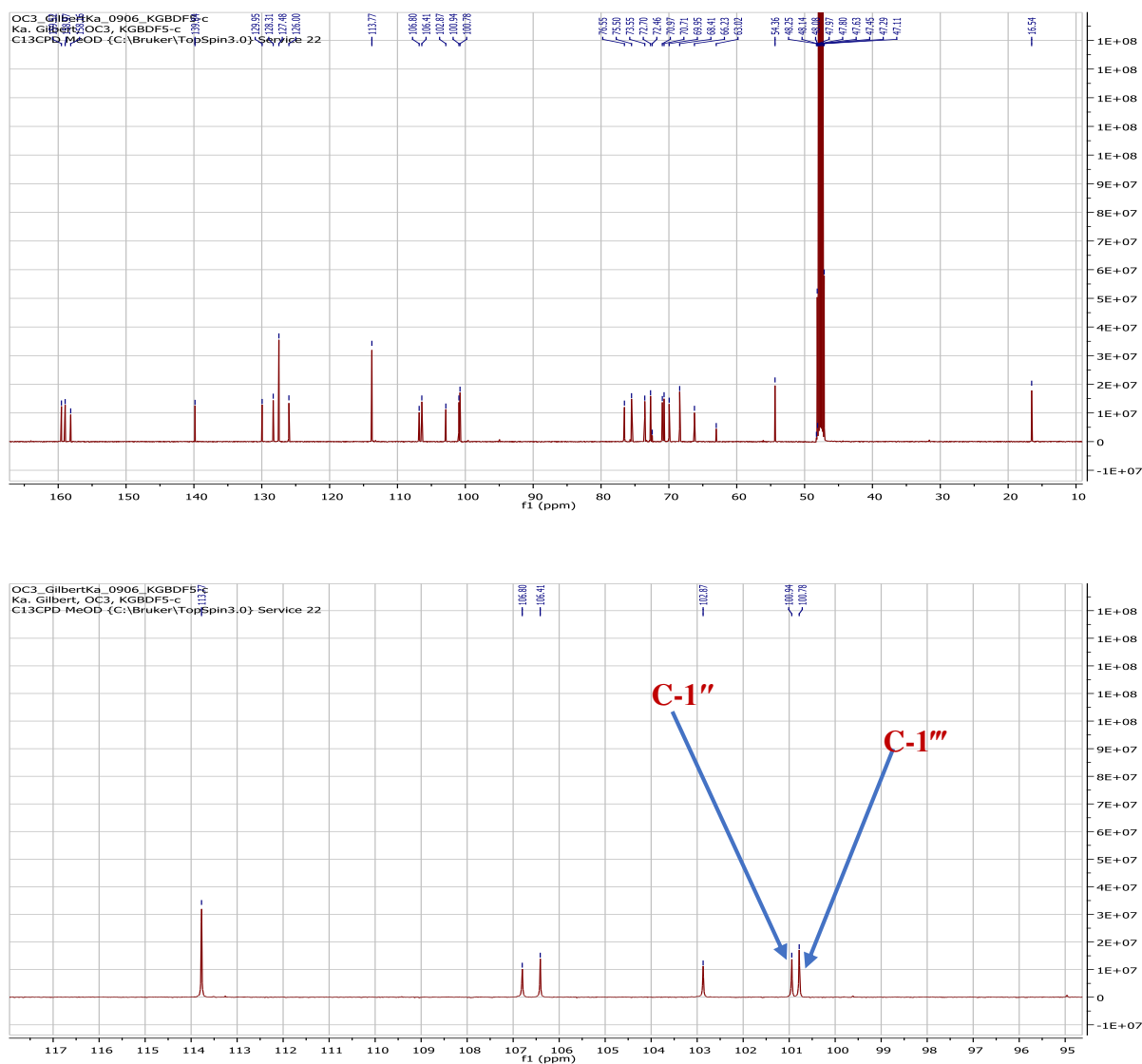
Figure 102: ^{13}C NMR (125 MHz, CD₃OD) spectrum of compound BDF5B

The HMBC spectrum **(Fig 103)** shows correlation between proton at δ_H 4.90 (H-1″) with carbon at δ_C 158.2 (C-5), indicating the attachment of β-D-glucose at C-5 of the aglycone. The anomeric proton of the rhamnose moiety at δ_H 4.75 (H-1‴) shows correlation with C-6″ at δ_C 66.4 of the glucose moiety indicating the attachment of the α-L-rhamnose moiety with C-6″ of β-D-glucose unit.

Still in HMBC spectrum **(Fig 103)** we also observe:

- Correlation between proton at δ_H 7.04 (H-β) with carbon C-1′ and C-2′ of ring B of the aglycone and correlation between proton at δ_H 6.89 (H-α) with carbon at δ_C 158.2 (C-1) and δ_C 106.4 (C-2) of ring A of the aglycone.

Correlation between proton H-7′ at δ_H 3.80 with carbon at δ_C 159.5 (C-4′) confirming the

- position of methoxy group to ring B.
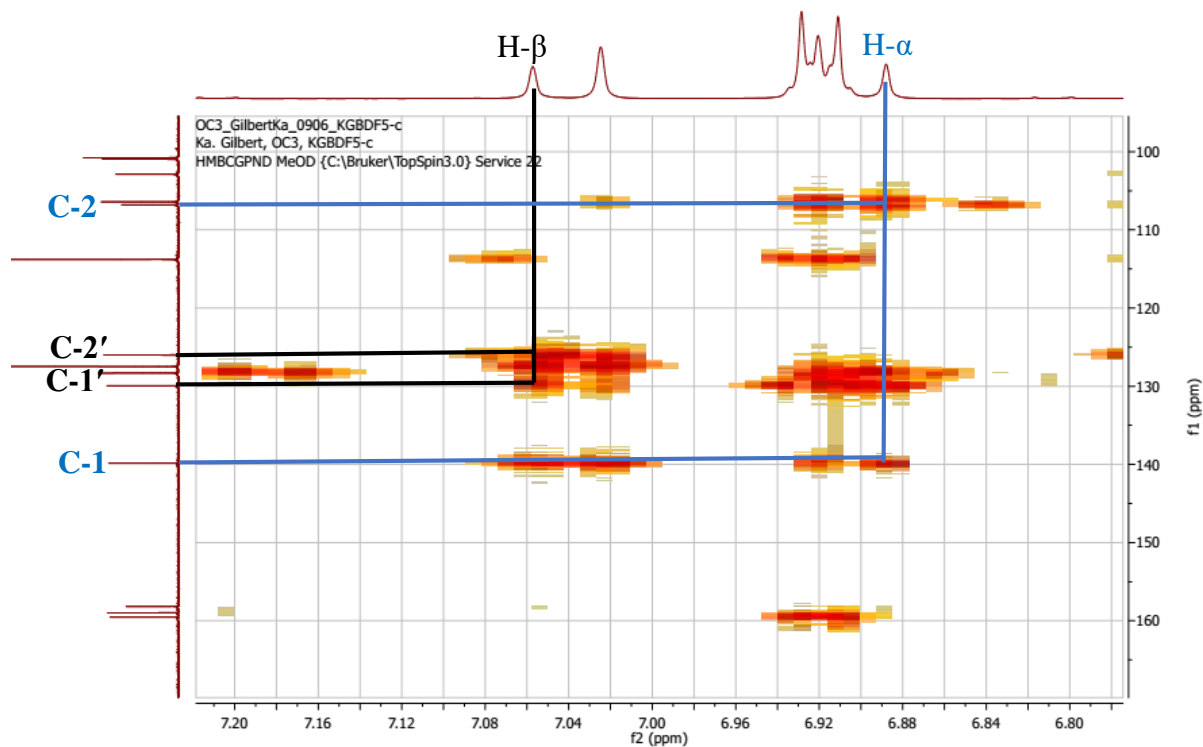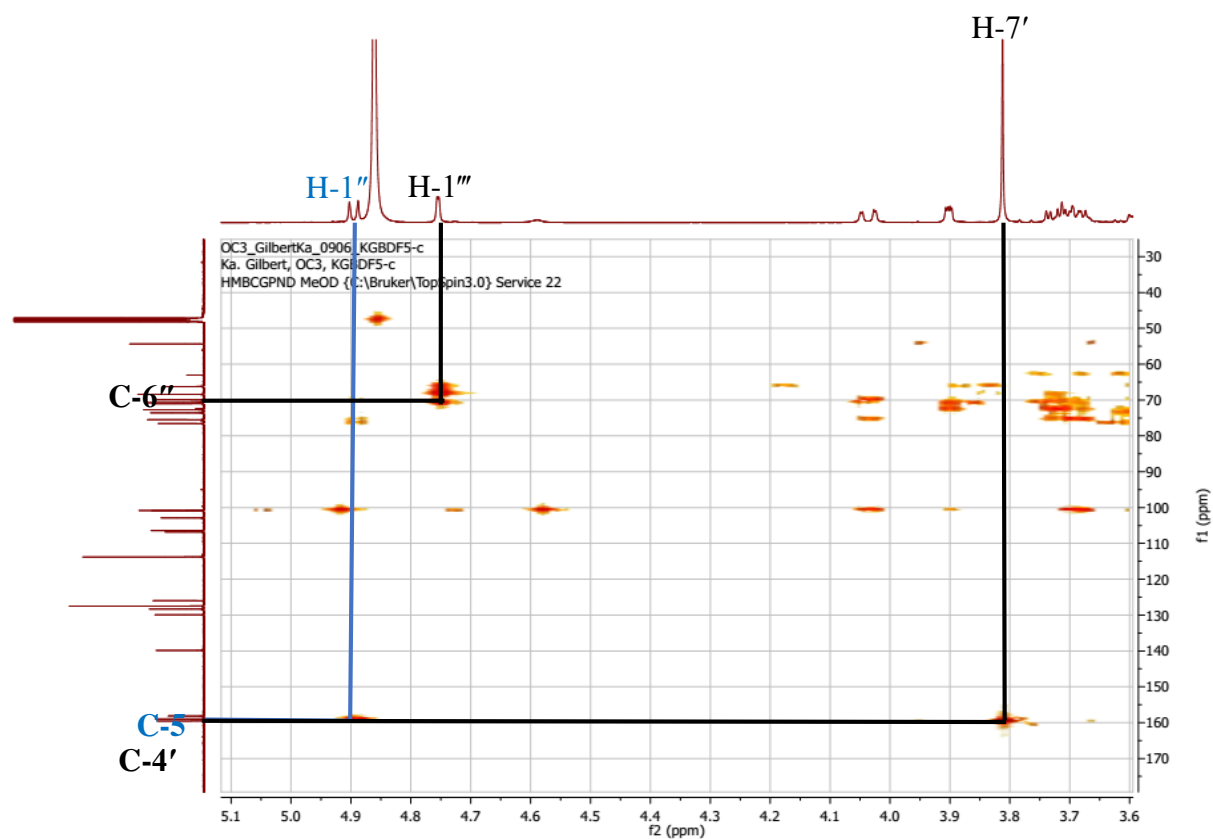
Figure 103: HMBC (CD₃OD) spectrum of compound BDF5B

On the basis of the spectroscopic data and by comparison with the literature (**Atta-ur-Rahman** *et al.* **2005**), the structure of compound **BDF5B** was identified to be desoxyrhapontigenin-3-O-rutinoside **(76)**

Table 33: ^{1}H NMR (500 MHz) and ^{13}C NMR (125 MHz) data of BDF5B in CD$_3$OD and ^{1}H NMR (400 MHz,) and ^{13}C NMR (100 MHz) data of desoxyrhapontigenin-3-*O*-rutinoside in MeOD

POSITION	δ_C (δppm)	δ_H (δppm, *J* in Hz)	δ_C (δppm)	δ_H (δppm, *J* in Hz)
	BDF5B		**desoxyrhapontigenin-3-*O*-rutinoside (Atta-ur-Rahman *et al*. 2005)**	
1	140.0		141.2	
2	106.4	6.74 (s)	107.8	6.72 (s)
3	159.0		160.4	
4	102.8	6.43 (s)	104.3	6.45 (s)
5	158.2		159.7	
6	106.8	6.68 (s)	108.2	6.65 (s)
1′	130.0		131.4	
2′	127.4	7.47 (1H, d, *J*=8,5Hz)	128.9	7.45 (1H, d, *J*=8.8Hz)
3′	114.0	6.90 (1H, d, *J*=8,5Hz)	115.2	6.90 (1H, d, *J*=8.8Hz)
4′	159.5		160.9	
5′	114.0	6.90 (1H, d, *J*=8,5Hz)	115.2	6.90 (1H, d, *J*=8,5Hz)
6′	127.4	7.47 (1H, d, *J*=8,5Hz)	128.9	7.45 (1H, d, *J*=8,5Hz)
7′	54.4	3.80 (s)	55.7	3.79 (s)
A	126.5	6.89 (d, *J*=16,2Hz, 1H)	127.4	6.88 (1H, d, *J*=16.8 Hz)
B	128,3	7.04 (d, *J*=16,2Hz, 1H)	129.7	7.02 (1H, d, *J*=16,4Hz)
Glucopyranoside unit				
1″	101.0	4.90 (1H, d, *J*=7,3Hz)	102.4	4.86 (1H, d, *J*=9.0Hz)
2″	73.5	3.49 (m)	74.9	3.43 (*m*)
3″	76.6	3.50 (m)	77.9	3.46 (m)
4″	71.0	3.42 (m)	71.4	3.38 (m)
5″	75.5	3.59 (m)	76.9	3.55 (*m*)
6″	66.4	4.01 (dd, *J* = 11.2, 1.7 Hz, Ha)	67.6	3.66 (m, Ha)
		4.05 (dd, *J* = 11.2, 1.7 Hz, Hb)		4.00 (dd, *J* = 13.5, 1.5 Hz, Hb)
Rhamnopyranoside unit				
1‴	100.8	4.75 (1H, d, *J* = 1.4 Hz)	102.2	4.72 (1H, d, *J* = 0.8 Hz)
2‴	70.7	3.90 (1H, dd, *J* = 3.4, 1.6 Hz)	72.1	3.86 (1H, dd, *J* = 3.2, 1.6 Hz)
3‴	70.0	3.73 (m)	71.3	3.68 (1H, dd, *J* = 3.2, 9.2 Hz)
4‴	72.7	3.38 (m)	74.1	3.34 (1H, dd, *J* = 3.2, 9.2 Hz)
5‴	68.4	3.68 (m)	69.8	3.65 (*m*)
6‴	16.4	1.22 1.22 (3H, d, *J* = 6.2 Hz)	17.9	1.18 (3H, d, *J* = 6.2 Hz)

2.2.10. Other compound

2.2.10.1 Identification of the structure of BDb5

Compound **BDb5** was obtained from the Hex/EtOAc (7/3, v/v) as a white amorphous solid soluble in CDCl$_3$. The spectroscopic data allows us to identify **BDb5** to structure 77 bellow
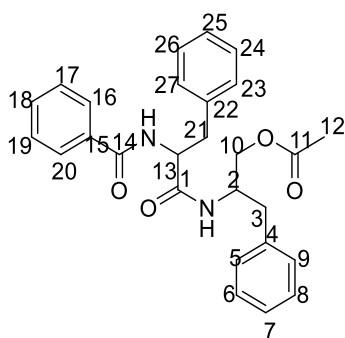
(77)

The High resolution mass spectra HRESI **Fig104** shows [M+Na]$^+$ ion peak at *m/z* 467.2051 compatible to the molecular formula (C$_{27}$H$_{28}$N$_2$O$_4$Na), with fifteen double bond equivalent
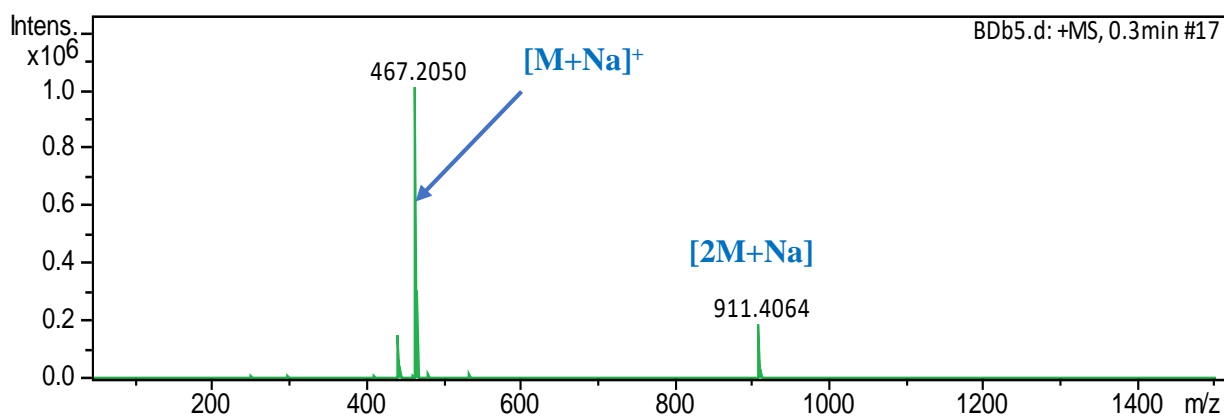
Figure 104: HRESI mass Spectrum of BDb5

Analysis of the ^{1}H NMR **Fig105** and ^{1}H COSY **Fig106** spectra of this compound identified two ABX coupling systems at δ_H 4.78 (1H, d, *J* = 6.4 Hz, H-13), δ_H 3.25 (1H, dd, *J* = 13.6, 5.6 Hz, H-21b), δ_H 3.07 (1H, dd, *J* = 13.6, 8.4 Hz, H-21a) and δ_H 4.37 (1H, m, H-2), δ_H 3.95 (1H, dd, *J* = 11.3, 4.8 Hz, H-10b), δ_H 3.84 (1H, dd, *J* = 11.3, 4.1 Hz, H-10a).

In the cosy **Fig107** spectrum we observe a correlation between the proton at δ_H 4.78 (1H, d, *J* = 6.4 Hz, H-13) and an N-Hb group at δ_H 6.75 (1H, d, *J* = 7.1 Hz, N-Hb).

We also observe correlation between the proton at δ_H 4.37 (1H, m, H-2) with two other groups of protons at δ_H 2.77 (2H, m, H-3) and δ_H 5.94 (1H, d, *J* = 8.4 Hz, N-Ha).

Analysis of the aromatic proton regions of the ^{1}H-NMR and ^{1}H-^{1}H-COSY spectra revealed the presence of three AA'BB'C coupling systems, each corresponding to a monosubstituted benzene nucleus.

The presence of an acetoxymethyl was confirmed by a 3H singlet at δ_H 2.05 in the 1H-NMR spectrum
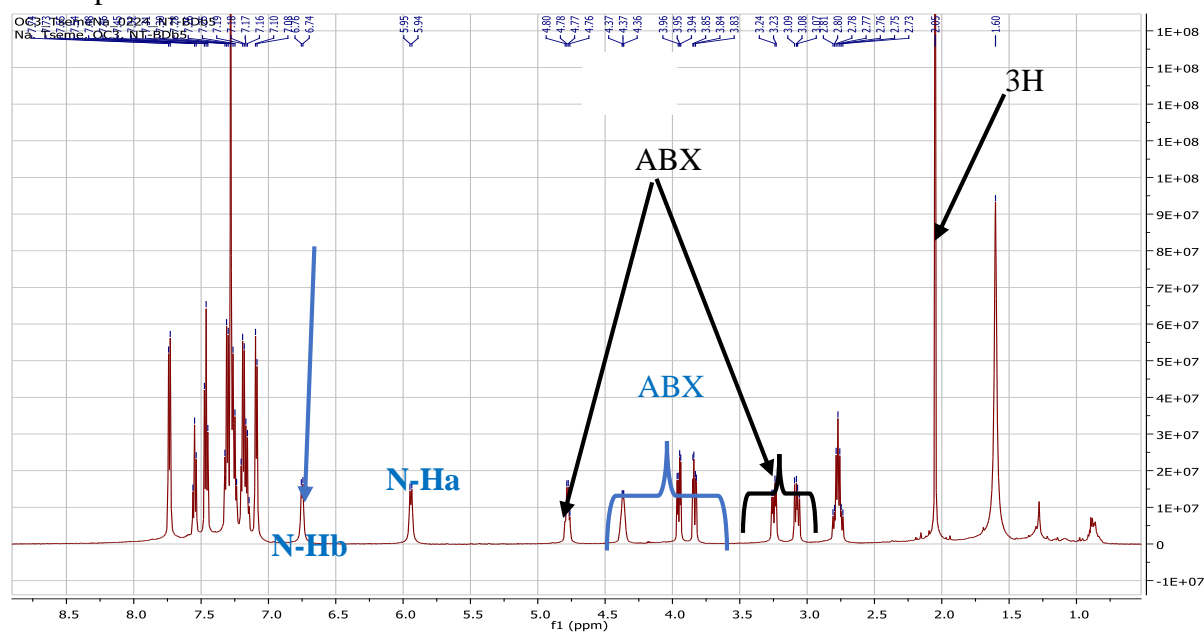
Figure 105: ^{1}H NMR (500 MHz, CDCl$_3$) spectrum of compound BDb5
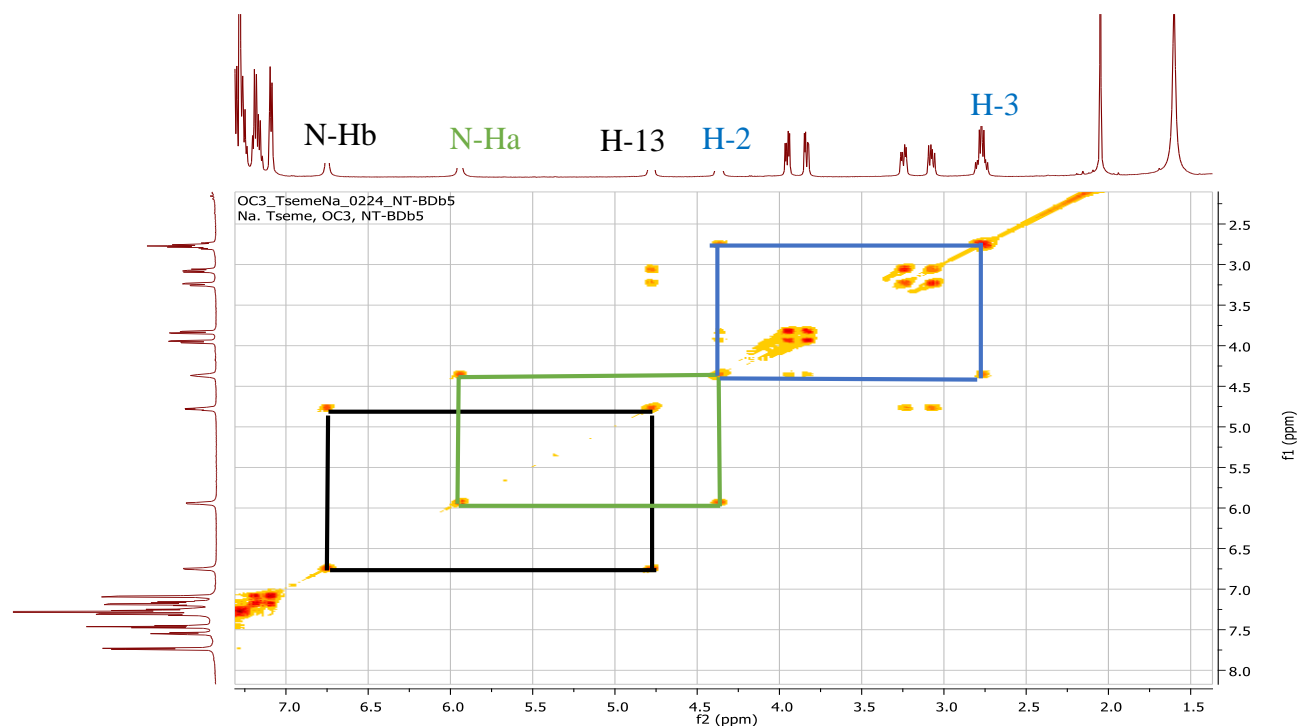
Figure 106: COSY (CDCl$_3$) spectrum of compound BDb5
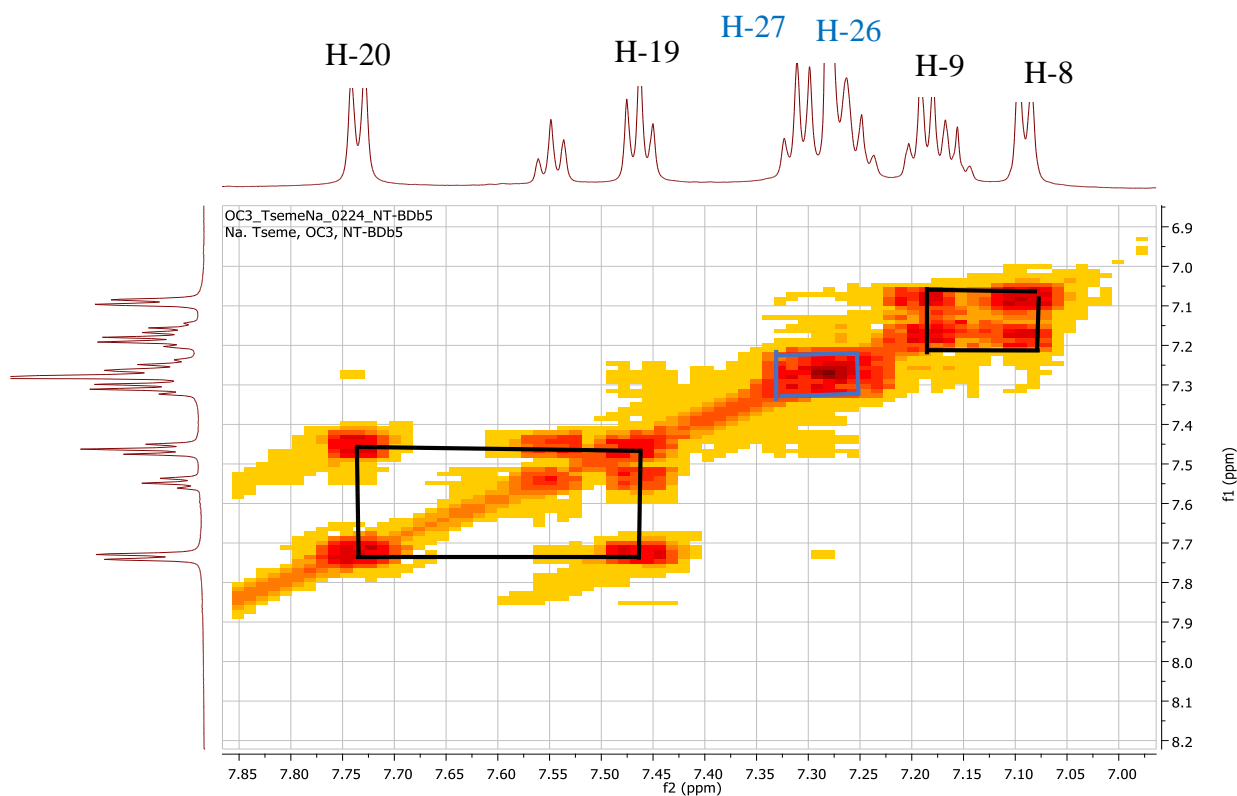
Figure 107: Expanded COSY (CDCl₃) spectrum of compound BDb5

The ^{13}C NMR **Fig108** and DEPT 135 **Fig109** spectra provided evidence that compound **BDb5** has two amide functions δ_C 170.2 (C-1) and 167.1 (C-14) and ester function at δ_C 170.8 (C-11), two benzylic methylenes δC 38.4 (C-21) and 37.5 (C-3), an oxymethylene δ_C 64.4 (C-10), a methyl group δ_C 20.7 (C-12), seventeen methines and three other quaternary carbons.
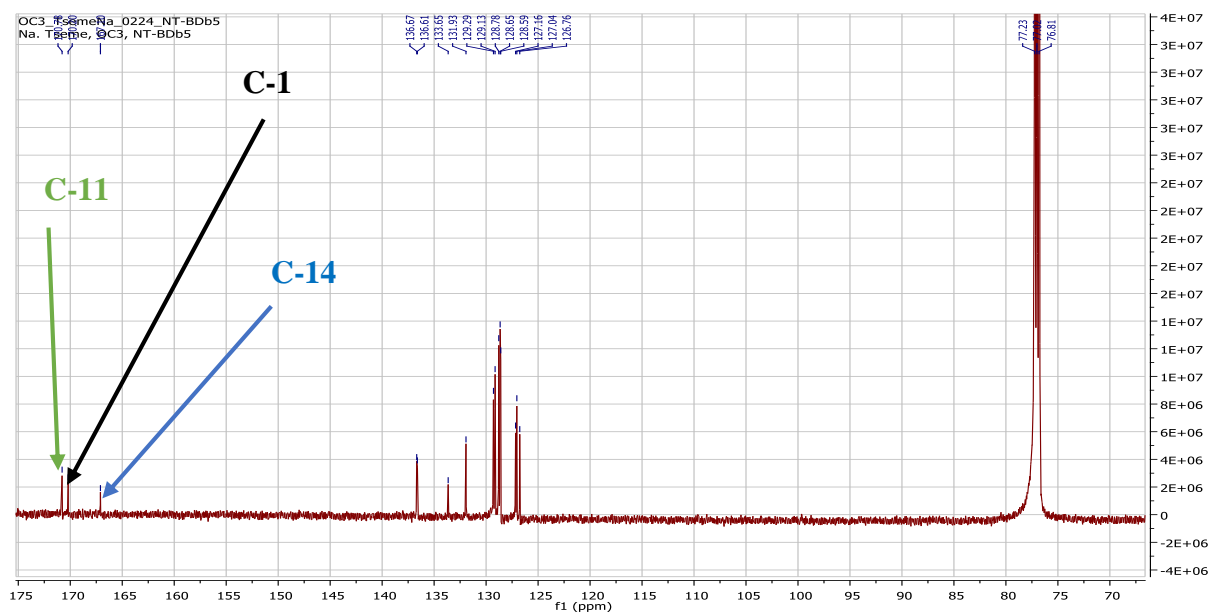
Figure 108: ^{13}C NMR (125MHz, CDCl$_3$) spectrum of compound BDb5
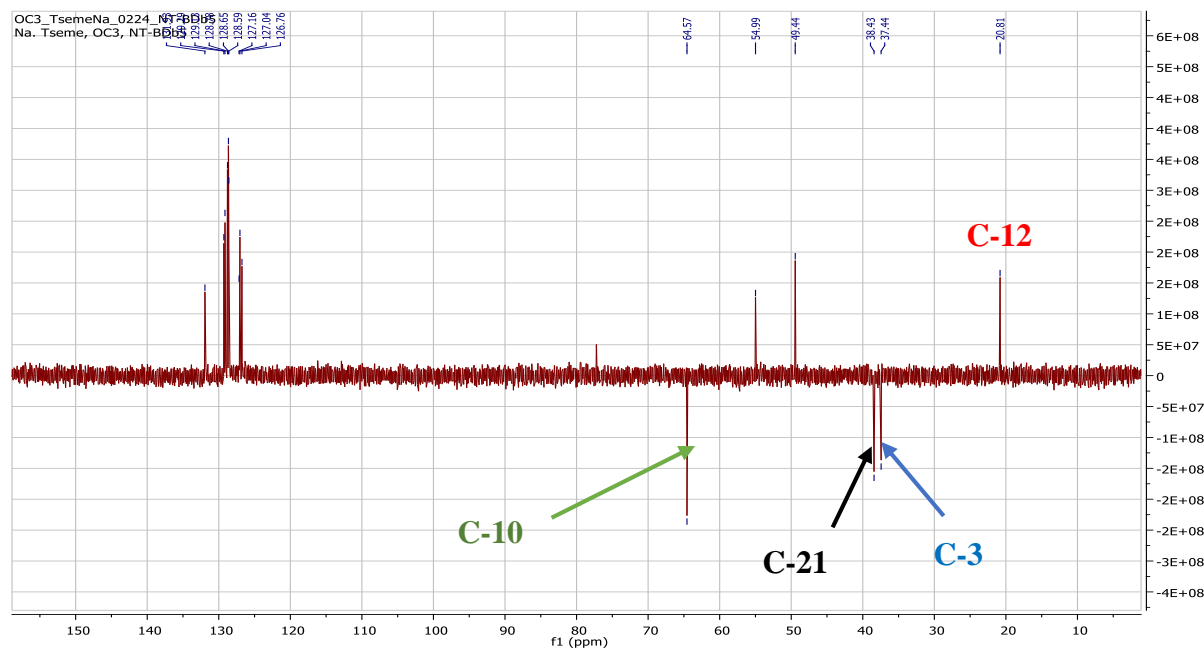
Figure 109: DEPT 135 (125MHz, CDCl$_3$) spectrum of compound BDb5

Comparison of these spectroscopy data with literature values led to the identification of compound **BDb5** as a peptide derivative, aurantiamide acetate **77 (Songue et al. 2012)**. Aurantiamide acetate has been isolated previously from *Aspergillus flavipes* (**Clark *et al*. 1977).**

Table 34: ^{1}H NMR (500 MHz) and ^{13}C NMR (125 MHz) data of BDb5 and ^{1}H NMR (700 MHz) and ^{13}C NMR (175 MHz) data of Aurantiamide acetate in CDCl₃

	BDb5		Aurantiamide acetate (Songue *et al*.2012).	
POSITION	δ_C	δ_H	δ_C	δ_H
1	170.2		171.2	
2	49.4	4.37 (1H, m)	50.4	4.37 (1H, dddd, *J* = 8.4, 7, 4.9, 4.2 Hz)
3	37.5	2.80 (1H, m, Hb)	38.4	2.80(1H, dd, *J* = 13.3, 8.4 Hz, H-b)
		2.77 (1H, m, Ha)		2.77 (1H, dd, *J* = 13.3, 7 Hz, H-a)
4	136.7		137.6	
5	128.7	7.18 (2H, d, *J* = 7.3 Hz)	129.7	7.20 (2H, d, *J* = 7 Hz)
6	128.8	7.09 (2H, d, *J* = 6.9 Hz)	129.8	7.09 (2H, d, *J* = 7 Hz)
7	126.8	7.16 (1H, t, *J* = 6.9 Hz)	127.8	7.16 (1H, t, *J* = 7 Hz)
8	128.8	7.09 (2H, d, *J* = 6.9 Hz)	129.8	7.09 (2H, d, *J* = 7 Hz)
9	128.7	7.18 (2H, d, *J* = 7.3 Hz)	129.7	7.20 (2H, d, *J* = 7 Hz)
10	64.4	3.95 (1H, dd, *J* = 11.3, 4.8 Hz)	65.5	3.95 (1H, dd, *J* = 11.9, 4.9 Hz, H-b)
		3.83 (1H, dd, *J* = 11.3, 4.1 Hz)		3.83 (1H,dd, *J* = 11.9, 4.2 Hz, H-a)
11	170.8		171.8	
12	20.7	2.05 (3H, s)	21.8	2.05 (3H, s)
13	54.6	4.78 (d, *J* = 6.4 Hz, 1H)	55.9	4.79 (1H, q, *J* = 5.6 Hz)
14	167.1		168.1	
15	133.7		134.6	
16	127	7.74 (2H, d, *J* = 7.4 Hz)	128.0	7.74 (2H, d, *J* = 7.7 Hz)
17	128.6	7.46 (2H, t, *J* = 7.6 Hz)	129.6	7.47 (2H, t, *J* = 7.7 Hz)
18	131.9	7.55 (1H, t, *J* = 7.4 Hz)	132.9	7.55 (1H, t, *J* = 7.7 Hz)
19	128.6	7.46 (2H, t, *J* = 7.6 Hz)	129.6	7.47 (2H, t, *J* = 7.7 Hz)
20	127	7.74 (2H, d, *J* = 7.4 Hz)	128.0	7.74 (2H, d, *J* = 7.7 Hz)
21	38.4	3.25 (1H, dd, *J* = 13.6, 5.6 Hz)	39.4	3.25 (1H, dd, *J* = 13.3, 6.3 Hz, H-b)
		3.07 (1H, dd, *J* = 13.6, 8.4 Hz)		3.08 (1H, dd, *J* = 13.3, 8.4 Hz, H-a)
22	136.7		137.7	
23	129.1	7.31 (2H, d, *J* = 7.3 Hz)	130.1	7.31 (2H, d, *J* = 7 Hz)
24	129.3	7.28 (2H, m)	130.3	7.28 (2H, d, *J* = 7 Hz)
25	127.2	7.25 (1H, t, *J* = 7.1 Hz)	128.2	7.25 (1H, t, *J* = 7 Hz)
26	129.3	7.28 (2H, m)	130.3	7.28 (2H, d, *J* = 7 Hz)
27	129.1	7.31 (2H, d, *J* = 7.3 Hz)	130.1	7.31 (2H, d, *J* = 7 Hz)
		6.75 (1H, d, *J* = 7.1 Hz)		6.76 (1H, d, *J* = 7.7 Hz, N-Hb)
		5.94 (1H, d, *J* = 8.4 Hz)		5.95 (1H, d, *J* = 8.4 Hz, N-Ha)

2.3. Discussion: chemophenetic significance

The bio guided study of the stem barks and branches of *Boswellia dalzielii* led to the isolation of twenty-eight compounds belonging to four classes including fifteen triterpenes, three steroids, four flavonoids and six other phenolic compounds.

One phenolic compounds dalzienoside **(74)** is isolated and characterised for the first time from the stem bark of *Boswellia dalzielii* including fourteen know compounds as friedelin **(56)**, *β*-Sitosterol and stigmasterol **(66)** and **(65)**, *β*-sitosterol-3-*O*-*β*-D-glucopyranoside **(67)**, *α*-Boswellic acid **(59)**, *β*-Boswellic acid **(17),** 3-*O*-acetyl-11-keto-*β*-boswellic acid **(20)**, 3*α*-acetyl-*β*-boswellic acid (**19**), 3-*O*-acetyl-28-hydroxylupeolic acid **(63)**, lupeol **(25)**, betulinic acid **(62)**, Angolensin **(72)**, 4-methoxy-*2*-*O*-*α*-*D*-glucopyranosylphenyl methanol **(75)**, desoxyrhapontigenin-3-*O*-rutinoside **(76)**. While *α*-amyrin (**26**), *β*-amyrin (**58**), *β*-amyrin acetate **(60)**, lupenone **(22)**, 3*α*-acetyl-*α*-boswellic acid **(61)**, lanosta-7,24-dien-3-one **(64)**, Urs-12-ene-3*α*,24*β*-diol **(57)**, Soforaflavanone B **(69)**, 4',5-dihydroxy-7-methoxyflavanone **(68)**, 5,4′-Dihydroxy-7-(*γ,γ* dimethylallyloxy)dihydroflavonol **(70)** 3-Acetoxy-4',5-dihydroxy-7-methoxyflavanone **(71)**, aurantiamide acetate **(77)** 7-(3,4-Dihydroxyphenyl)-1-(4-hydroxyphenyl)-3-heptanol **(73)** were isolated from branches of *Boswellia dalzielii*.

Plants belonging to genus *Boswellia* are reported to contain many triterpenoids like pentacyclics triterpenes, tirucalanes, diterpenes (Belsner *et al*., 2003; Culioli *et al*. 2003; Jinqian *et al*., 2017; Verhoffa et al., 2012;Carla *et al*., 2009; Manguro *et al*., 2009; Aksamija, 2012). Among them, Boswellic acid and their derivatives were frequently characterized in the different plant parts.

α-Boswellic acid **(59)**, *β*-Boswellic acid **(17),** 3-*O*-acetyl-11-keto-*β*-boswellic acid **(20)**, 3α-acetyl-*β*-boswellic acid (**19**), 3*α*-acetyl-*α*-boswellic acid (**61**), were already isolated from the gum resin of *Boswellia serrata* (Belsner *et al*., 2003; Culioli *et al*. 2003), 3-*O*- acetyl-28-hydroxylupeolic acid **(63)** was isolated from the gum resin of *Boswellia carterii* (Verhoff *et al*., 2012). In the same way *α*-amyrin (**26**), *β*-amyrin (**58**), lupeol **(25)** and desoxyrhapontigenin-3-*O*-rutinoside **(76)** were also isolated from the root of *Boswellia dalzielii* (Atta-ur-Rahman *et al*. 2005; Talom *et al*., 2019). All these compounds isolated from the *Boswellia* genus confirms the chemotaxonomic markers of the *Boswellia* genus

Six compounds isolated from the branches Soforaflavanone B **(69)** (Agrawal, 1989 ; Shi *et al*; 1997), 4',5-dihydroxy-7-methoxyflavanone **(68) (**Motahareh *et al*., 2014), 5,4′-Dihydroxy-7-(*γ,γ* dimethylallyloxy)dihydroflavonol) **(70)** (Alarcón *et al*., 2008 ; Bohlmann *et al*., 1981), 3-Acetoxy-4',5-dihydroxy-7-methoxyflavanone **(71)** (Ayafor *et al*., 1981), (Bezuidenhoudt *et al*. 1980), aurantiamide acetate **(77)** (Songue *et al*.2012), 7-(3,4-Dihydroxyphenyl)-1-(4-hydroxyphenyl)-3-heptanol **(73)** (Yi-Chun *et al*, 1994; Jiang-Bo *et al*., 2011) and two from the stem bark Angolensin **(72)** and 4-methoxy-2-*O*-*α*-*D*-glucopyranosylphenyl methanol **(75)** (González *et al*. 2019) are reported here for the first time

from the genus *Boswellia* and contribute to the chemotaxonomic significance of this genus. These results are not surprising because phenolic compounds like desoxyrhapontigenin-3-*O*-rutinoside **(76)** was already isolated from *Boswellia papyrifera* and *Boswellia dalzielii* (Atta-ur-Rahman *et al*. 2005; Talom *et al*., 2019)

2.4. Chemical Transformation

During our work Some Chemical transformation was also done. We have undertaken the acetylation of 3-*O*-acetyl-28-hydroxylupeolic in view to know the site of activity in the molecule.

2.4.1. Acetylation of 3-O-acetyl-28-hydroxylupeolic acid (BDF4A)

A mixture constituting of 10.0mg of 3-*O*-acetyl-28-hydroxylupeolic, 1.0ml of acetic anhydride and 1.0ml of pyridine were stirred at room temperature for 12 hours. The progress of the reaction was monitored by TLC. After 12 hours, the reaction mixture was partitioned between 1% H_2SO_4 and distilled water. The organic phase was evaporated and purified by column chromatography to obtain the acetylated product (7.0 mg) whose structure was confirmed by its mass and ^{1}H-NMR spectra.

(63)   **(78)**
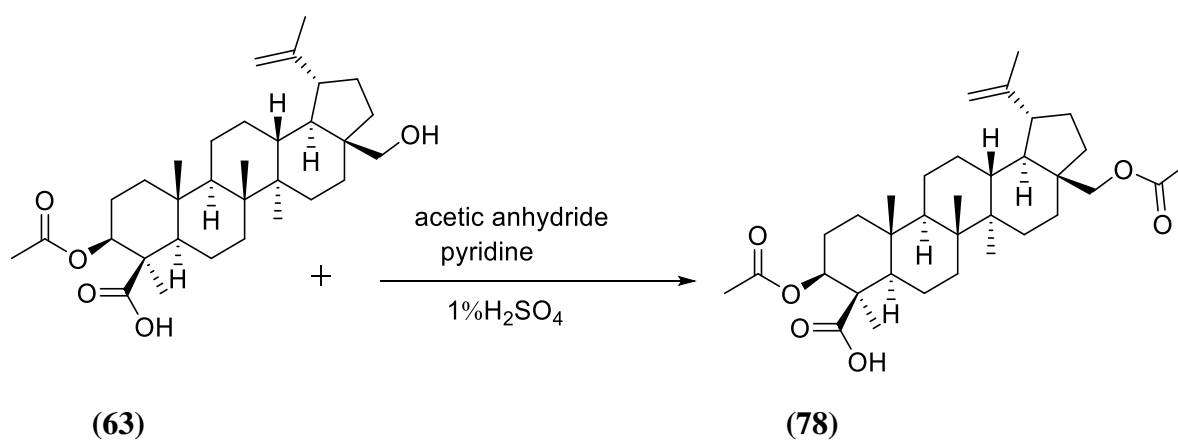
On its ^{1}H NMR spectrum we observe one major change compared to that of the starting material (3-*O*-acetyl-28-hydroxylupeolic). The ^{1}H NMR spectrum of 3-*O*-acetyl-28-hydroxylupeolic **(63)** **(Fig50)** revealed the presence of one acetate methyl at δ_H 2.11 (H-2′) when The ^{1}H NMR spectrum **(Fig113)** of 3, 28-diacetyllupeolic acid **(BDF4P)** shows the presence of two acetate methyl at δ_H 2.03 and 2.00 suggesting that acetylation of OH at position 28 have been done.
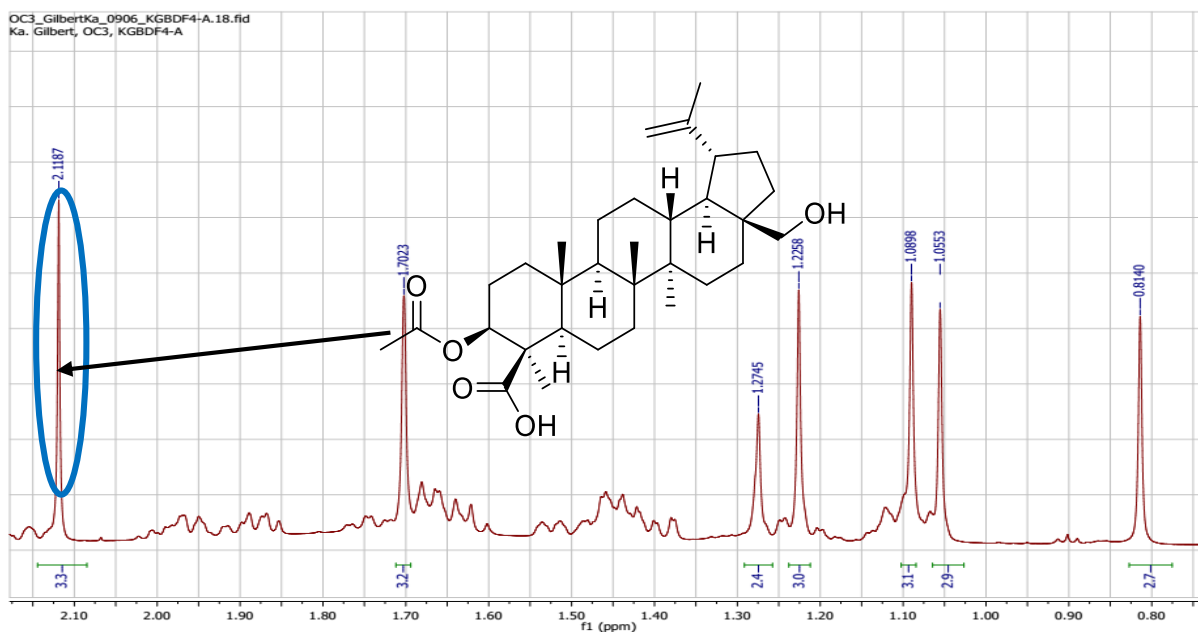
Figure 110: ^{1}H NMR (500MHz, CDCl$_3$) spectrum of BDF4
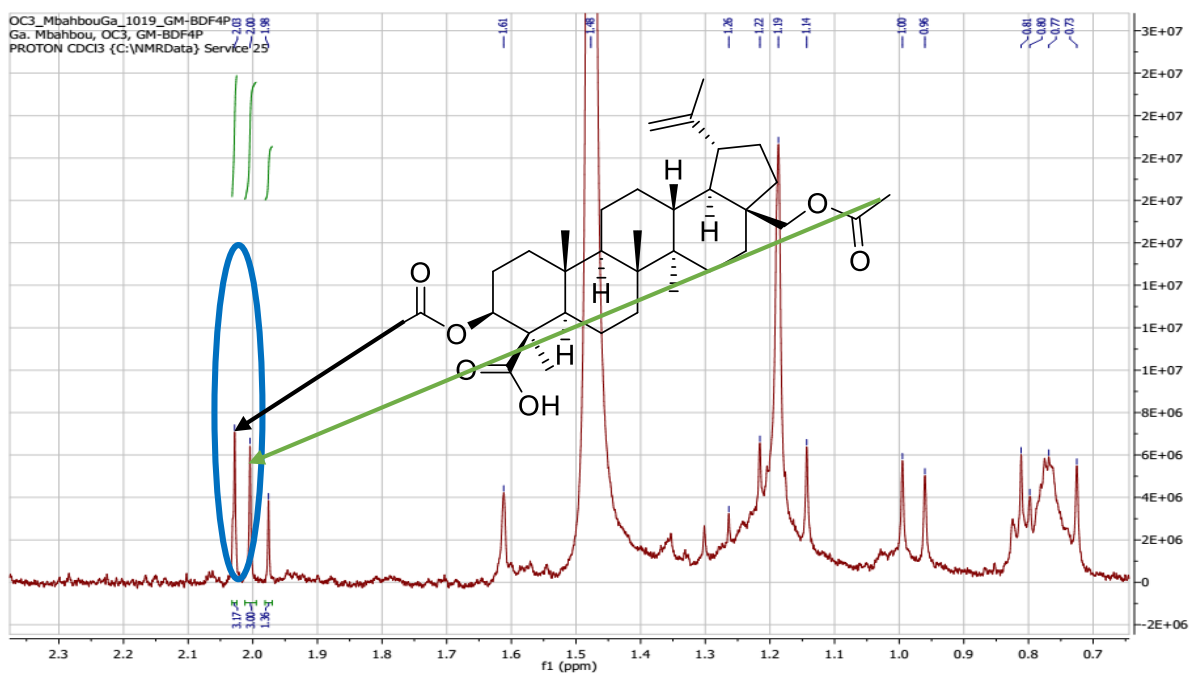
Figure 111: ^{1}H NMR (500MHz, CDCl$_3$) spectrum of BDF4P

2.5. Biological tests

The antibacterial activity of extracts, fractions and pure compounds of *B. dalzielii* were determined to ascertain their therapeutic utility and valorise the plant.

2.5.1. Antimicrobial tests

Crude extract (01), fractions (06) and isolated compounds of *Boswellia dalzielii* were tested on 08 microbial strains namely; S1 = *S. typhi,* S2 = *S. aureus* ATCC43300, S3 = *E. cloacae*, S4 = *P. aeruginosa* HM801, S5 = *S. pneumonia* ATCC491619 and S6 = *E. coli* ATCC25322 *S7= K. pneumoniae* NR41388 *and S8= K. pneumoniae clinical isolate* using ciprofloxacin as reference. The MICs were measured at eigth (08) different concentrations ranging from < 3.9 to 500 μg/ml. The minimum inhibitory concentration (MIC) was defined as the lowest concentration of the sample that prevented bacterial growth. The antibacterial activity of compounds isolated from plants was strong, moderate or weak if the MIC of the plants was ≤ 10 *μ*g/mL, 10<MIC≤100 *μ*g/mL or >100 *μ*g/mL, respectively. However, the activity of plant extracts will be classified as significant (MIC < 100 *μ*g/mL), moderate (100 < MIC ≤ 625 *μ*g/mL) or weak (MIC > 625 *μ*g/mL) (**Kuete, 2010**). The name of compounds, fractions and extract tested are shown on the table below.

Table 35: Codes of compounds, extract and fractions for antibacterial assays

Code	Number	Name of compound/Extract/Fraction
BDF3	62	Betulinic acid
BDF3A	19	3α-acetyl-β-boswellic acid
BDF3B	59	α- boswelic acid
BDF3C	17	β-boswellic acid
BDF3d	20	Acetyl-11-keto-boswellic acid
BDF4A	63	3-*O*-acetyl-28-hydroxylupeolic acid
BDRA	72	Angolensin
BDCA10	74	Dalzienoside
BDCA8	75	4-methoxy-2-*O*-α-*D*-glucopyranosylphenyl methanol
BDF5B	76	desoxyrhapontigenin-3-*O*-rutinoside
BDb3	68	4',5-Dihydroxy-7-methoxyflavanone
BDb5	77	Aurantiamide acetate
BDb8	73	7-(3,4-Dihydroxyphenyl)-1-(4-hydroxyphenyl)-3(*R*)-heptanol
BDb11	69	Soforaflavanone B
BDb16	61 and 19	3α-acetyl-α-boswellic acid and 3α-acetyl-β-boswellic acid
BDb17	71	3-Acetoxy-4',5-dihydroxy-7-methoxyflavanone
BDb18	70	5,4′-Dihydroxy-7-(γ,γ-dimethylallyloxy)dihydroflavonol
BDC1	57	Urs-12-ene-3α,24-β-diol
BDR3	64	lanosta-7,24-dien-3-ol
BDBE	/	Stem bark extract of *Boswellia dalzielii*
BDB1	/	hexane-ethyl acetate fraction (9:1, v/v)
BDB2	/	hexane ethyl acetate fraction (8:2, v/v)
BDB3	/	hexane-ethyl acetate fraction (7:3, v/v)
BDB4	/	hexane-ethyl acetate fraction (1:1, v/v)
BDB5	/	ethyl acetate fraction
BDB6	/	ethyl acetate/MeOH fraction (8:2, v/v).

2.5.1.1. Antibacterial activity of the methanolic extracts and fractions of *Boswellia dalzielii*

Extracts of stem barks and branches of *B. dalzielii* including all fractions were evaluated for antibacterial activity using six strains and the results are presented on the table below. The MIC in μg/mL for the extracts and fractions and the number of extracts and fractions active per strain are sorted out.

Table 36: Minimal inhibitory concentration of crude extract and fractions (μg/ml)

Tested samples	Bacterial strains and MIC (μg/ml)					
Strains	*S. Typhi*	*S. aureus*	*E. cloacae*	*S. Pneumoniae* ATCC 491619	*E. Coli* ATCC 25322	*P. aeruginosa* HM 801
BDBE	>500	250	250	250	>500	>500
BDB1	>500	>500	>500	>500	>500	>500
BDB2	>500	>500	>500	>500	>500	>500
BDB3	125	7.8	7.8	7.8	250	7.8
BDB4	125	31.2	7.8	31.2	>500	7.8
BDB5	>500	>500	>500	>500	>500	>500
BDB6	>500	>500	>500	>500	>500	>500
Ciprofloxacin	0.03	0.15	0.03	0.03	0.03	0.07

S. typhi: *Salmonella typhi; S. aureus*: *Staphylococcus aureus; E. cloacae*: *Enterobacter cloacae; S. pneumonia* ATCC491619: *Streptococcus pneumonia* ATCC491619*; E. coli* ATCC25322: *Escherichia coli* ATCC25322;

P. aeruginosa HM801: *Pseudomonas aeruginosa* HM801. BDBE: (Methanolic extract); BDB1: hexane-ethyl acetate fraction (9:1, v/v); BDB2: hexane ethyl acetate fraction (8:2, v/v); BDB3: hexane-ethyl acetate fraction (7:3, v/v); BDB4: hexane-ethyl acetate fraction (1:1, v/v) BDB5: ethyl acetate fraction; BDB6: ethyl acetate/MeOH fraction (8:2, v/v).

From the table above, the MeOH extract of the stem barks of *Boswellia dalzielii* exhibits moderate antibacterial activity against *S. aureus, E. cloacae, S. pneumonia* ATCC491619 with MIC of 250 μg/ml. The hexane-ethyl acetate (7:3, v/v) and hexane-ethyl acetate (1:1, v/v) fractions show significant to moderate activities against *S. aureus, S. typhi, E. cloacae, S.*

pneumonia ATCC491619, *P. aeruginosa* HM801. The results of the MIC determinations (Table 47) showed that the hexane-ethyl acetate (7:3, v/v) and hexane-ethyl acetate (1:1, v/v) fractions were the most active compare to other fractions and exhibit significant activities against *E. cloacae, S. pneumoniae* ATCC491619, *P. aeruginosa* HM801 with the same MIC value of 7.8 *μ*g/ml.

2.5.1.2. Antimicrobial activity of pure compounds

Isolated compounds were also tested against eight strains: *S. typhi, S. aureus* ATCC43300, *E. cloacae*, *P. aeruginosa* HM801, *S. pneumoniae* ATCC491619, *E. coli* ATCC25322*, K. pneumoniae* NR41388 and *K. pneumoniae clinical isolate*. Only (08) compounds mentioned on the table **37** showed significant or moderate activity on some of the strains.

Table 37: Minimal inhibitory concentration of isolated compounds (*μ*g/ml)

Tested samples	Bacterial strains and MIC (*μg/ml*)							
Strains	S. Typhi	S. aureus	E. cloacae	S.pneumoniae ATCC491619	E. Coli ATCC25322	P aeruginosa HM801	KP NR41388	KP clinical isolate
3α-acetyl-β-boswellic acid (19)	7.8	250	7.8	15.6	7.8	7.8	-	-
α-boswellic acid (59)	3.125	250	3.125	3.125	3.125	3.125	-	-
β-boswellic acid (17)	3.125	15.6	3.125	3.125	3.125	3.125	-	-
acetyl-11-keto-boswellic (20)	3.125	15.6	3.125	3.125	3.125	3.125	-	-
3-O-acetyl-28-hydroxylupeolic acid (63)	15.6	62.5	7.8	15.6	15.6	7.8	-	-
4',5-Dihydroxy-7-methoxyflavanone (68)	31.5	-	-	-	-	31.5	62.5	31.5
Soforaflavanone (69)	-	62.5	-	-	-	-	-	62.5
5,4′-Dihydroxy-7- (γ, γ-dimethylallyloxy) dihydroflavonol (70)	15.6	7.8	-	-	-	15.6	15.6	15.6
Ciprofloxacin	0.031	0.015	0.031	0.031	0.031	0.031	0.015	0.015

S. typhi: *Salmonella typhi; S. aureus*: *Staphylococcus aureus; E. cloacae*: *Enterobacter cloacae; S. pneumoniae*
ATCC491619: *Streptococcus pneumoniae* ATCC491619; *E. coli* ATCC25322: *Escherichia coli* ATCC25322; *P.*

aeruginosa HM801: *Pseudomonas aeruginosa* HM801. KPNR41388 : *Klebsiella pneumoniae NR41388,* KP clinical isolate : *Klebsiella pneumoniae clinical isolate*, BDF3A :

2.5.2. Acute oral toxicity study on aqueous extract of stem bark of *boswellia dalzielii*

2.5.2.1. Effects on some clinical parameters

Table **38** shows the effects of administration in rats of aqueuous extract of stem bark of *B. dalzielii* at doses of 2000 and 5000 mg / kg on some clinical parameters. From this table, it is noted that the plant extract was not harmless or showed no signs of toxicity with regard to the clinical parameters evaluated during the first 30 minutes and throughout the duration of the test. Animals given the aqueous plant extract did not show aggression and chills. In addition, animals that received the plant extract in the same way as normal animals that received distilled water showed normal stool appearance, sensitivity to sound and touch, and mobility. The extract also shows zero lethality below the maximum dose of 5000 mg / kg / bw.

Table 38: effects of administration in rats of aqueuous extract of stem bark of *B dalzielii*

Parameter	Witness			Extract 2000 mg/kg			Extract 5000 mg/kg		
	30 min	4 Hours	14 days	30 min	4 Hours	14 days	30 min	4 Hours	14 days
Number of deaths	0	0	0	0	0	0	0	0	0
Thrill	-	-	-	-	-	-	-	-	-
Aggressiveness	-	-	-	-	-	-	-	-	-
Mobility	+	+	+	+	+	+	+	+	+
Appearance of faeces	N	N	N	N	N	N	N	N	N
Horripilation	-	-	-	-	-	-	-	-	-
Touch sensitivity	+	+	+	+	+	+	+	+	+
Noise sensitivity	+	+	+	+	+	+	+	+	+

N= normal, + = Présent, - = Absent

2.5.2.2 Effects on weight gain

Figure **114** summarizes the weight change of animals that received a single dose of the aqueous extract of BDF and followed for 14 days. It emerges that after administration of the aqueous extract of BDF, no significant difference was observed in the body weight of the rats having received the 2000 and 5000 mg / kg doses during 14 days of experimentation compared to the control
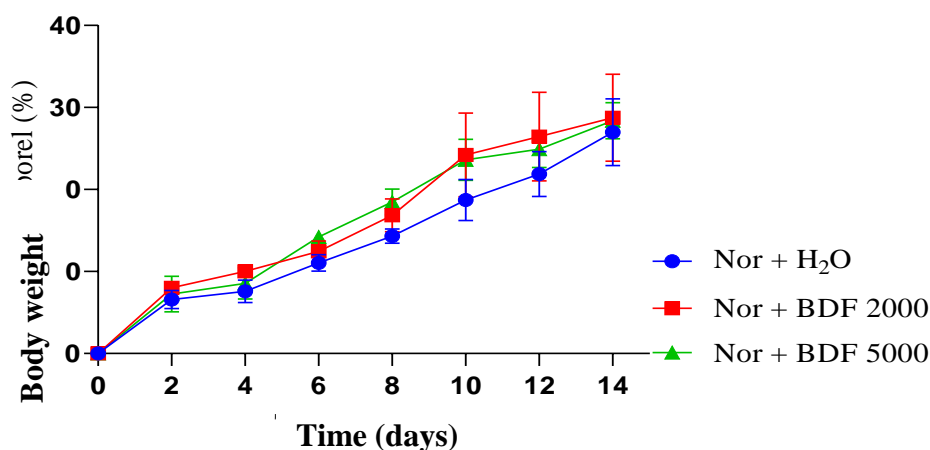
Each value represents the mean ± ESM; n = 3; Nor + H2O: healthy rats treated with distilled water; Nor + BDF 2000, Nor + BDF 5000: rats treated with aqueous extract of BDF at the respective doses of 2000 and 5000 mg / kg.

Figure 112: Effects of the aqueous extract on the weight development of rats in acute toxicity

2.5.2.3. Effects on the relative weight of certain organs

The figure below is an illustration of the effects of administration of the extract on the relative weight of the liver, kidney, heart and lung during the 14 days of testing. According to this figure, the administration for 14 days of the plant extract did not cause any significant variation in the relative weight of the various organs mentioned above compared to normal animals given distilled water.
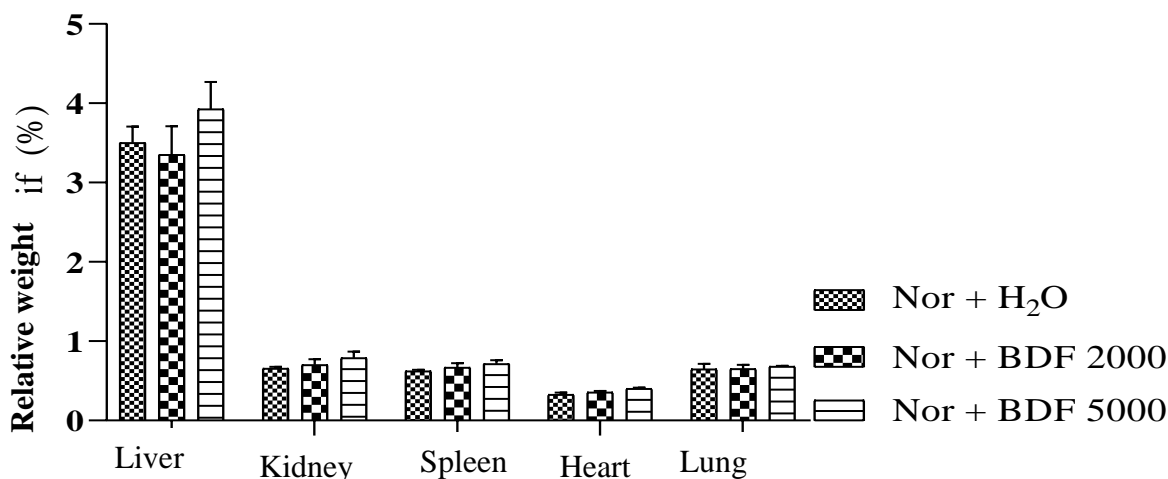
n = 3; Nor + H2O: healthy rats treated with distilled water; Nor + BDF 2000, Nor + BDF 5000: rats treated with aqueous extract of BDF at the respective doses of 2000 and 5000 mg / kg

Figure 113: Effects of aqueous BDF extract on the relative weight of acutely toxic organs

2.6. Discussion of biological part

The MeOH extract of the stem barks of *B. dalzielii* exhibits moderate antibacterial activity against *S. aureus, E. cloacae and S. pneumoniae* ATCC 491619 with MIC of 250

μg/ml. Fractions and compounds tested exhibit antibacterial activity with MICs ranging between 7.8 and 3.125 μg/ml against *S. typhi, E. cloacae, S. pneumoniae* ATCC491619, *E. coli* ATCC25322*, P. aeruginosa* HM801.

The minimum inhibitory concentration (MIC) was defined as the lowest concentration of the sample that prevents bacterial growth. The antibacterial activity of compound is strong, moderate or weak if the MIC is 10 mg/mL, 10 < MIC <100 mg/mL or > 100 mg/mL, respectively. Whereas, the activity of plant extracts is classified as significant if (MIC < 100 mg/mL), moderate if (100 < MIC < 625 mg/mL) or weak if (MIC > 625 mg/mL) (Kuete et al. 2011)

According to this criterion, the results of the MIC determinations showed that the hexane-ethyl acetate (7:3, v/v) and hexane-ethyl acetate (1:1, v/v) fractions were the most active compare to other fractions and exhibit significant activities against *S. typhi, E. cloacae, S. pneumoniae* ATCC491619, *E. coli* ATCC25322*, P. aeruginosa HM801* with the same MIC value of 7.8 μg/mL. Pure compounds such as: α-boswellic acid, β-boswellic acid and acetyl-11-keto-boswellic *acid* showed significant activity on *S. typhi, E. cloacae, S. pneumonia* ATCC491619, *E. coli* ATCC25322*, and P. aeruginosa HM 801* with a MIC value equal to 3.125 μg/mL. 3α-acetyl-β-boswellic acid and 3-O-acetyl-28-hydroxylupeolic acid showed also activity on the same strains with a MIC value ranging between 7.8 and 62.5 μg /mL, which is in agreement with previously reported antibacterial activity on *S. albus* and *S. aureus* with MIC values of 15.7 μg/ml. (**Manguro and Wagai, 2016**).

In literature, there are numerous reports available on the antibacterial activity of oleo - gum resin extracts and oleo - gum resin essential oils from *Boswellia* spp. (Burseraceae) (Abdallah *et al*., 2009; Camarda *et al*., 2007; Kasali *et al*., 2002; Weckessera *et al*., 2007) reported the antibacterial activity of *Boswellia* dry extract and keto-β-boswellic acid (KBA). Their findings revealed that the extract was highly effective against selected aerobic and anaerobic bacteria such as *Streptococcus, Coryne bacteria, Coryne perfringens and Pseudomonas acnes;* whereas KBA was not effective against these pathogens, suggesting that the effective components are other boswellic acids or essential oils contained in the extract. Also the in vitro antibacterial activity results of four boswellic acid compounds revealed AKBA (acetyl ketone boswellic acid) to be the most potent antibacterial compound against Gram-positive pathogens, but it showed no significant antibacterial activity (MIC >128 μg/ml) against the Gram negative bacteria.

In this study, we extensively evaluated the extract, fractions and boswellic acids for the antibacterial activity and further established that hexane-ethyl acetate (7:3, v/v) and hexane-ethyl acetate (1:1, v/v) fractions are the most potent antibacterial fractions between the others fractions from methanolic extract of *Boswellia dalziel*ii. This research work provides the evidence that hexane-ethyl acetate (7:3, v/v) and hexane-ethyl acetate (1:1, v/v) fractions and α-boswellic acid, β-boswellic acid and acetyl-11-keto-boswellic *acid* reduce the *S. typhi, E. cloacae, S. pneumoniae* ATCC491619*, E. coli* ATCC25322*, P. aeruginosa* HM801.

The present study showed that, fractions and pure isolated compounds from the dicloromethane–methanol (1:1) extract of the stem barks of *Boswellia dalzielii* possess interesting antibacterial properties against *S. typhi, S. aureus, E. cloacae, S. pneumoniae* ATCC491619 *and P. aeruginosa HM801*. The bio guided studies on the actives fractions have led to the identification of some bioactive molecules in the stem barks of *B. dalzielii* with good activities; the most active compounds against the bacteria strains tested were α-boswellic acid, β-boswellic acid and acetyl-11-keto-boswellic. From these results, it can be concluding that fractionation has led to an increase of the activity.

These preliminary results obtained from the in vitro assays are consistent with the uses of the plant to treat microbial diseases in the northern part of Cameroun and are also in agreement with previously reported antibacterial activity of the tested compounds. (Abdallah *et al*., 2009 ; Camarda *et al*., 2007 ; Kasali *et al*., 2002 ; Weckessera *et al*., 2007)

Results on acute oral toxicity of aqueous extract of BDF did not show intoxication syndrome in rats at doses of 2000 and 5000 mg / kg. In rats given the extract, no deaths were observed for 14 days after administration of the extract suggesting that the LD 50 is greater than 5000 mg / kg (OECD, 2001). In addition, no clinical signs of toxicity were observed either on the behavior, or on the body weight of the animals, or on the weight of the organs after administration of the test substance and during the 14 days of experimentation.
Thus, according to the globally harmonized classification system (SCGH), the aqueous extract of BDF can be classified in category 5 of non-toxic substances because of its harmlessness.

GENERAL CONCLUSION AND PERSPECTIVES

The aim of this work was to evaluate the antibacterial activities of extracts, fractions and isolated compounds of stem barks and branches of *Boswellia dalzielii* (Burseraceae).

The crude extract of the stem barks of *Boswellia dalzielii* exhibited moderate antibacterial activity against *S. aureus, E. cloacae and S. pneumoniae* ATCC491619 with MIC of 250 *µg/ml*. Hexane/ethyl acetate (7:3) fraction and hexane/ethyl acetate (1:1) fraction showed significant activities with MICs ranging from 7.8 to 125 *µg/ml* against these strains, while *α*-boswellic acid (**59**), *β*-boswellic acid (**17**) and acetyl-11-keto-boswellic (**20**) acid from these fractions exhibited strong activities with MIC value of 3.125 *µg/mL* against *S. aureus* ATCC43300, *S. typhi*, *E. coli* (ATCC25322 *E. cloacae* NR4674, *S. pneumoniae* ATCC491619 and *P. aeruginosa* HM801. These preliminary results obtained from the in vitro assays are consistent with the uses of this plant to treat microbial diseases in the northern part of Cameroon and are also in agreement with previously reported antibacterial activity of the tested compounds.

The bio guided study of the stem barks and branches of *Boswellia dalzielii* afforded twenty-eight compounds with one new derivative dalzienoside (**82**) and twenty-seven known compounds. The structures of these compounds were established by comprehensive 1D and 2D NMR spectroscopy and Mass spectra.

Amongst the twenty-eight compounds, fourteen are pentacyclic triterpenes, two are steroids, and one is tirucalane once again confirming the fact that triterpenes are the chemotaxonomic markers of the *Boswellia* genus.

Four flavonoids: 4',5-dihydroxy-7-methoxyflavanone (**75**), 5,4´-dihydroxy-7-(γ,γ dimethylallyloxy)dihydroflavonol (**77**) , 3-Acetoxy-4',5-dihydroxy-7-methoxyflavanone(**78**), Soforaflavanone B (**76**) and four other phenolic compounds: 7-(3,4-Dihydroxyphenyl)-1-(4-hydroxyphenyl)-3-heptanol (**81**) , Angolensin (**79**), Aurantiamide acetate (**80**), 4-methoxy-2-*O-α-D* glucopyranosylphenyl methanol (**83**) are reported here for the first time from the genus *Boswellia* and contribute to the chemotaxonomy significance of this genus.

The acute toxicity was also done on the extract; this study was performed according to the protocol of the OECD (2001) to the guideline 423.

The results on acute oral toxicity of aqueous extract of stem bark did not show intoxication syndrome in rats at doses of 2000 and 5000 mg / kg. In rats given the extract, no deaths were observed for 14 days after administration of the extract suggesting that the LD 50 is greater than 5000 mg / kg (OECD, 2001). In addition, no clinical signs of toxicity were

observed either on the behavior, or on the body weight of the animals, or on the weight of the organs after administration of the test substance and during the 14 days of experimentation. Thus, according to the globally harmonized classification system (SCGH), the aqueous extract of BDF can be classified in category 5 of non-toxic substances because of its harmlessness.

In the future, we are going to perform others biological tests

CHAPTER 3 : MATERIALS AND METHODS

3.1. Instruments and general methods

The different masses of extracts, fractions and pure compounds were been measured using the electronic scales the type Cobos model D-6000-SX with precision at 10^{-1} and Ohaus pioneer with precision at 10^{-4} available in our laboratory**.** High resolution mass spectra were obtained with a QTOF Compact Spectrometer (Bruker, Germany) equipped with a HRESI and a HRAPCI sources. The spectrometer was operated in positive and negative modes (mass range: 50-1500, with a scan rate of 1.00 Hz) with automatic gain control to provide high-accuracy mass measurements within 1 *ppm* deviation using Na Formate as calibrant. The following parameters were used for experiments: spray voltage of 4.5 kV, capillary temperature of 200 °C. Nitrogen was used as sheath gas (4 l/min). 1D NMR spectra (^{1}H NMR, 500 MHz; ^{13}C NMR and DEPT 135; 125 MHz) and 2D NMR spectra (HMQC, HSQC, HMBC, COSY and NOESY) were measured on a Bruker TopSpin 3.0 spectrometer equipped with cryoprobe, with TMS as an internal reference. Methyl, methylene and methane carbons were distinguished by DEPT experiments. Homonuclear 1H connectivities were determined by using the COSY experiment. ^{1}H-^{13}C one bond connectivities were determined with HSQC gradient pulse factor selection. Two- and three-bond connectivities were determined by HMBC experiments. Chemical shifts are reported in δ (ppm) using TMS as internal standard, and coupling constants (J) were measured in Hz. Column chromatography was carried out on silica gel (230-400 mesh ASTM, Merck). Thin layer chromatography (TLC) was performed on Merck precoated silica gel 60 F254 aluminium foil, and spots were detected using UV light (254 nm) and (365 nm), and spraying with 10% H_2SO_4 in EtOH followed by heating at about 110^0C.

3.2. Plant material

The stem bark and branches of *Boswellia dalzielii* (Burceraceae) were collected in December, 2018 at Moutourwa in far North Region of Cameroon. The plant was identified by Doctor Souaré Konssala, a Botanist at the University of Maroua and then confirmed at the Cameroon National Herbarium in Yaoundé where a voucher specimen N°64939/HNC is kept.

3.3. Extraction and isolation
3.3.1. Extraction

Stems barks powder (5 Kg) and branches (3.4 Kg) were macerated into 20 L and 15 L of MeOH-CH_2Cl_2 (1/1, v/v) respectively, at room temperature for 72 h, then filtered through Whatman filter paper. Extracts were concentrated to dryness under vacuum at low temperature

to give 417.0 g (a brown extract) and 124.8 g (a green extract) of stem bark and branches, respectively.

3.3.2 Isolation

3.3.2.1. Column chromatography of the stem bark MeOH extract of *Boswellia dalzielii*

The crude extract of the stems bark 250.0 g was dissolved in methanol and adsorbed on 400.0 g of coarse silica gel (70-230 mesh) and subjected to to flash chromatography and eluted with solvents and mixture of solvents, starting with n-hexane and gradually increasing the polarity with ethyl-acetate and finally methanol to give seven fractions: Hexane-EtOAc 8/2 (14.6 g), Hexane-EtOAc 7/3 (11.5 g), Hexane-EtOAc 1/1 (3g) and EtOAc (43,7g), EtOAc- MeOH 8/2 (72g) and MeOH (127,6g) fractions.

3.3.2.1.1. Separation of Hexane-EtOAc 8/2 (F1) (14.6 g)

Fraction F1(14.6 g) was adsorbed on 20.0 g of coarse silica gel (70-230 mesh) and subjected to column chromatography over 150.0 g of coarse silica gel (70-230 mesh), using column chromatography of 3 cm of diameter and 1 m of length and eluted with *n*-hexane/EtOAc mixture starting from 100% *n*-hexane to 50% of the mixture of hexane/EtOAc. A total of 100 fractions of 125 ml each were collected, evaporated and regrouped based on their TLC profiles. This resulted in the isolation of fridelin (**56**) (33 mg), lupeol (**25**) (24 mg), *β*-sitosterol (**66**) and stigmasterol (**65**) (52.1 mg).

Table 39: Chromatogram of fraction F1 from the CH_2Cl_2/MeOH extract of the stem bark of *Boswellia dalzielii*

Eluent	Fraction N°	Observations	Compounds
100% Hexane	1-20	Oily fraction and mixture of about 6 compounds	BDF2A (**56**)
Hex-EtOAc (95 :05)	21-40	Mixture of about 4 compounds	BDF2B (**25**)
Hex-EtOAc (90 :10)	41-55	Mixture of about 3 compounds	BDF2C (**65** and **66**)
Hex-EtOAc (85 :15)	56-70	Mixture of about 6 compounds	_
Hex-EtOAc (80 :20)	71-80	Mixture of about 5 compounds	_
Hex-EtOAc (70 :30)	81-90	Mixture of about 5 compounds	_
Hex-EtOAc (60 :40)	91-100	Mixture of about 5 compounds	_

After evaporation of solvent, fractions 11-14 precipitated to give compound BDF2A (**56**) (33mg) soluble in DCM.

Fractions 21-40 were left at room temperature for one day and then fractions 24-27 precipitated like white powder to give BDF2B (**25**) (24mg) soluble in DCM.

Fractions 41-70 have been grouped on the basis of the CCM under two major fractions A and B and then evaporated. Fraction A left at room temperature precipitated to give BDF2C (**65**) and (**66**) (52.1mg)

3.3.2.1.2. Separation of Hexane-EtOAc 7/3 (F2) (11.5 g)

This fraction (11.5 g) was adsorbed on 15.0 g of coarse silica gel (70-230 mesh) and subjected to column chromatography of 3 cm of diameter and 1m of length, and eluted with *n*-hexane/EtOAc mixture starting from hexane/EtOAc 15% to ethyl acetate 100%. The column was packed with 100.0 g of silica gel (70-230 mesh). At the end of chromatography we obtained 5 pure compounds. These compounds are: 3α-acetyl-β-boswelic acid (**19**) (14.0 mg), betulinic acid (**62**) (18.6 mg), α-boswelic acid (**59**) (28.4 mg), β-boswelic acid (**17**) (13 mg), Acetyl-11-keto-boswellic (**20**) (7.8 mg)

Table 40: Chromatogram of fraction F2 from the MeOH extract of the stem bark of *Boswellia dalzielii*

Eluent	Fraction N°	Observations	Compounds
Hex-EtOAc (85 :15)	1-10	Mixture of about 6 compounds	_
Hex-EtOAc (80 :20)	11-20	Mixture of about 3 compounds	_
Hex-EtOAc (77.5:22.5)	21-35	Mixture of about 4 compounds	BDF3A (**19**)
Hex-EtOAc (75 :25)	36-50	Mixture of about 3 compounds	BDF3 (**62**)
Hex-EtOAc (72.5 :27.5)	51-65	Mixture of about 5 compounds	BDF3B (**59**) BDF3C (**17**)
Hex-EtOAc (70 :30)	66-80	Mixture of about 3 compounds	BDF3d (**20**)
Hex-EtOAc (60 :40)	81-95	Mixture of several compounds	_
EtOAc 100 %	96-115	Mixture of several compounds	_

Fractions 23-26 were precipitated to give BDF3A (**19**) (14.0 mg) as white powder soluble in DCM.

On the basis of the CCM, fraction 39-45 were grouped and left at room temperature. After one day they precipitated to give BDF3 (**62**) (18.6 mg) white powder soluble in DCM

Fractions 51-65 have been grouped on the basis of the CCM and purified using silica gel with mixture of Hex-DCM (2/8, v/v) to give BDF3B (**59**) (28.4 mg) and BDF3C (**17**) (13 mg) as white powder each other soluble in DCM.

Fraction 66-80 was subjected to column chromatography on Sephadex LH-20 using MeOH/DCM (4-6 v/v) as eluent to yield compound BDF3d (**20**) (8.4 mg) like white powder soluble in DCM.

3.3.2.1.3. Separation of Hexane-EtOAc 1/1 fraction (F3) (3g)

Hexane-EtOAc 1/1 fraction (3.0 g) was adsorbed on 5.0 g of coarse silica gel (70-230 mesh) and subjected to column chromatography over 50.0 g of coarse silica gel (70-230 mesh), using column chromatography of 2 cm of diameter and 1 m of length and eluted with hexane/EtOAc mixture starting from 30% of the mixture of hexane/EtOAc to 100% EtOAc. A total of 80 fractions of 125 ml each were collected, evaporated and regrouped based on their TLC profiles to yield 3-*O*-acetyl-28-hydroxylupeolic acid (**63**) (23 mg) and angolensin (**72**) (91 mg).

Table 41: Chromatogram of fraction F3 from the MeOH extract of the stem bark of *Boswellia dalzielii*

Eluent	Fraction N°	Observations	Compounds
Hex-EtOAc (70 :30)	1-10	Mixture of about 4 compounds	_
Hex-EtOAc (65 :35)	11-20	Mixture of about 3 compounds	_
Hex-EtOAc (60 :40)	21-30	Mixture of about 3 compounds	BDF4A (**63**)
Hex-EtOAc (55 :45)	31-40	Mixture of about 5 compounds	_
Hex-EtOAc (50 :50)	41-50	Mixture of about 5 compounds	BDRA (**72**)
Hex-EtOAc (40:60)	51-60	Mixture of about 6 compounds	_
Hex-EtOAc (30 :70)	61-70	Mixture of several compounds	_
EtOAc 100 %	71-80	Mixture of several compounds	_

Fractions 21-30 were left at room temperature for one night and then tomorrow morning we have observed the white powder into fractions 23, 24, 25 namely BDF4A (**63**) (23 mg) soluble in DCM.

Fractions 41-50 were subjected to column chromatography on Sephadex LH-20 using MeOH as eluent to yield compound BDRA (**72**) (91 mg) like brown paste soluble in DCM and MeOH.

3.3.2.1.4. Separation of EtOAc fraction (F4) (13 g)

This fraction (13 g) was adsorbed on 20.0 g of coarse silica gel (70-230 mesh) and subjected to column chromatography over 160.0 g of coarse silica gel (70-230 mesh), then eluted with *n*-hexane/EtOAc/MeOH mixture starting from hexane/EtOAc 40% to EtOAc-MeOH 10%. A total of 110 fractions of 125 ml each were collected, evaporated and regrouped based on their TLC profiles. The column has 3 cm of diameter and 1 m of length. Through this process, 2 compounds were obtained: *β*-Sitosterol-*3-O-β-D*-glucopyranoside (**67**) (73mg) and BDF4B (21mg). The structure of BDF4B was very complex we could not determine the structure.

Table 42: Chromatogram of fraction F4 from the MeOH extract of the stem bark of *Boswellia dalzielii*

Eluent	Fraction N°	Observations	Compounds
Hex-EtOAc (40 :60)	1-10	Mixture of about 4 compounds	_
Hex-EtOAc (35 :65)	11-20	Mixture of about 5 compounds	_
Hex-EtOAc (30 :70)	21-35	Mixture of about 5 compounds	BDF5A (**67**)
Hex-EtOAc (25 :75)	36-50	Complex mixture	_
Hex-EtOAc (20 :80)	51-60	Complex mixture	
Hex-EtOAc (10:90)	61-70	Complex mixture	_
EtOAc 100%	71-85	Complex mixture with one major compound	BDF4B
EtOAc/MeOH (95/5)	86-95	Complex mixture	_
EtOAc/MeOH (95/5)	95-110	Complex mixture	_

Fraction 27-32 precipitated as a white powder in the elution solvent. This powder was filtered and washed with methanol to give BDF5A **(67)** soluble in pyridine.

After evaporation of solvent into fraction 71-85, we added methanol and then a white powder precipitated in the flacons 72, 73, 74 namely BDF4B (21 mg) soluble in pyridine.

3.3.2.1.5. Separation of EtOAc/MeOH (8/2) fraction. (F5) (72 g)

Fraction **F5** (72 g) was adsorbed on 80.0 g of coarse silica gel (70-230 mesh) and eluted with EtOAc/MeOH mixture starting from 100% EtOAc to 20% EtOAc/MeOH. A total of 75 fractions of 250 ml each were collected, evaporated and regrouped based on their TLC profiles. The column (4 cm and 1 m) was packed with 400.0 g of silica gel. Through this process, 3

mixture of compounds were obtained. This mixture was purified to column chromatography over 100 g of silica gel and Sephadex LH-20 using DCM/MeOH as solvent to yield 3 compounds: 4-methoxy-1-(methoxymethyl)-2-*O-α-D*-Glucopyranosylbenzene (dalzienoside) (**74**) (30 mg), 4-methoxy-2-*O-α-D*-glucopyranosylphenylmethanol (**75**) (27 mg), desoxyrhapontigenin-3-O-rutinoside (**76**) (204 mg).

Table 43: Chromatogram of fraction F5 from the MeOH extract of the stem bark of *Boswellia dalzielii*

Eluent	Fraction N°	Observations	Compounds
EtOAc 100%	1-10	Complex mixture	_
EtOAc/MeOH (97.5/2.5)	11-20	Mixture of about 3 compounds	_
EtOAc/MeOH (95/5)	21-30	Mixture of about 3 compounds	BDCA10 (**74**)
EtOAc/MeOH (92.5/7.5)	31-40	Mixture of about 5 compounds	BDCA8 (**75**)
EtOAc/MeOH (90/10)	41-50	Mixture of about 5 compounds	BDF5B (76)
EtOAc/MeOH (85/15)	51-60	Mixture of about 6 compounds	_
EtOAc/MeOH (80/20)	61-70	Complex mixture	_
MeOH 100%	71-75	Complex mixture	_

Fraction 21-30 were subjected to column chromatography on Sephadex LH-20 using MeOH/DCM (7-3 v/v) as eluent to yield compound BDCA10 **(74)** (30 mg) as brown paste soluble in MeOH and acetone.

In the same way fraction 31-40 have been grouped on the basis of the CCM and also subjected to column chromatography on Sephadex LH-20 using MeOH as eluent to yield compound BDCA8 **(75)** (27 mg) as brown paste soluble in MeOH and acetone.

Fractions 41-50 were purified using silica gel with mixture of DCM/MeOH (1/1, v/v) to led BDF5B **(76)** (204 mg) as amorphous paste.

3.3.2.2. Column chromatography of the branches MeOH extract of *Boswellia dalzielii*

The crude extract of branches (90.0 g) was dissolved in methanol and adsorbed on 100.0 g of coarse silica gel (70-230 mesh). Then subjected to flash chromatography using 250.0 g of coarse silica gel (70-230 mesh) and eluted with solvents and mixture of solvents, starting with n-hexane and gradually increasing the polarity with ethyl-acetate and finally methanol to give

six fractions such as: hexane (3.1g), Hexane-EtOAc 7/3 (31.4g), Hexane-EtOAc 1/1 (16.0 g), EtOAc (6.4g), EtOAc- MeOH 8/2 (11.0 g) and MeOH (7.6 g) fractions.

3.3.2.2.1. Separation of Hexane-EtOAc 7/3 fraction. (F2) (31.4g)

Fraction **F2** (31.4g) was adsorbed on 35.0 g of coarse silica gel (70-230 mesh) and separated using column chromatography of 3cm of diameter and 1 m of length, through 150.0 g silica gel using solvent and mixture of solvent such as hexane, hexane/EtOAc with increasing polarity to give five compounds These compounds are: β-amyrin acetate (**60**) (20.0mg) , lup-20(29)-en-3-one (**22**) (8.4mg), mixture of α-amyrin and β-amyrin (**26**) and (**58**) (31.7 mg), mixture of 3α-acetyl-α-boswelic acid (**61**) and 3α-acetyl-β-boswelic acid (**19**) (28.0 mg), 4',5 dihydroxy-7-methoxyflavanone (**68**) (13.6mg), Urs-12-ene-3α,24β-diol (**57**) (11.3), Aurantiamide acetate (**77**) (22.4 mg)

Table 44: Chromatogram of fraction F2 from the MeOH extract of branches of *Boswellia dalzielii*

Eluent	Fraction N°	Observations	Compounds
Hexane	1-10	Mixture of about 5 compounds	BDb1 (**60**)
Hex-EtOAc (95 :5)	11-20	Mixture of about 3 compounds	BDb2 (**22**)
Hex-EtOAc (90:10)	21-35	Mixture of several compounds	BDR1 (**26** and **58**) BDb16 (**61** and **19**)
Hex-EtOAc (85 :15)	36-50	Mixture of several compounds	_
Hex-EtOAc (80 :20)	51-65	Mixture of about 5 compounds	BDb3 (**68**) BDC1 (**57**)
Hex-EtOAc (70 :30)	66-80	Mixture of about 3 compounds	BDb5 (**77**)
Hex-EtOAc (60 :40)	81-95	Mixture of several compounds	_
EtOAc 100 %	96-115	Mixture of several compounds	_

Fractions 3-6 precipitated as a white powder in the elution solvent. This powder was filtered and washed with methanol to give BDb1 (**60**) (20.0 mg) soluble in DCM.

Fractions 11-20 have been grouped on the basis of the CCM and then fractions 14-16 precipitated as a white powder to give BDb2 (**22**) (8.4 mg) soluble in DCM

Fractions 21-35 have been grouped on the basis of the CCM and purified using silica gel over column chromatography to give BDb16 (**61** and **19**) (28.0 mg) and BDR1 (31.7 mg) (**26** and **58**) soluble in DCM

Fractions 51-65 were purified using silica gel with mixture of Hex-EtOAc (75/15; 80/20, v/v) to led BDb3 (**68**) (13.6mg) as white powder soluble in DCM and BDC1 (**57**) (11.3 mg) as white powder (11.3mg) soluble in DCM

Fractions 66-80 were purified using silica gel with mixture of Hex-EtOAc (7/3, v/v) to give BDb5 (**77**) (22.4 mg) as white powder soluble in DCM.

3.3.2.2.2. Separation of Hexane-EtOAc 1/1 fraction. (F3) (16.0g)

Fraction F3 (16.0 g) was adsorbed on 20.0 g of coarse silica gel (70-230 mesh) and subjected to column chromatography over 120.0 g of coarse silica gel (70-230 mesh), using column chromatography of 3 cm of diameter and 1 m of length and eluted with *n*-hexane/EtOAc mixture starting from 20% of the mixture of hexane/EtOAc to 100% EtOAc. A total of 100 fractions of 125 ml each were collected, evaporated and regrouped based on their TLC profiles. This resulted in the isolation of four compound: lanos-7,24-dien-3-one (**64**) (22.6 mg), 7-(3,4-Dihydroxyphenyl)-1-(4-hydroxyphenyl)-3-heptanol (**73**) (12.4 mg), Soforaflavanone B (**69**) (16.4 mg) and one insoluble compound.

Table 45: Chromatogram of fraction F3 from the MeOH extract of branches of *Boswellia dalzielii*

Eluent	Fraction N°	Observations	Compounds
Hex-EtOAc (80 :20)	1-20	Mixture of about 5 compounds	BDR3 (**64**)
Hex-EtOAc (70 :30)	21-35	Mixture of about 3 compounds	BDb8 (**73**)
Hex-EtOAc (60 :40)	36-45	Mixture of several compounds	_
Hex-EtOAc (1 :1)	46-55	Mixture of about 5 compounds	
			BDb11 (**69**)
Hex-EtOAc (40 :60)	56-75	Mixture of several compounds	
Hex-EtOAc (30 :70)	76-90	Mixture of several compounds	_
EtOAc 100 %	91-100	Mixture of several compounds	_

Fraction 1-20 have been grouped on the basis of the CCM and also subjected to column chromatography on silica gel using DCM as eluent to yield compound BDR3 (**64**) (22.6 mg) as white powder soluble in DCM.

Fractions 21-35 have been grouped on the basis of the CCM and then fractions precipitated as a white powder to give BDb8 (**73**) (38.0 mg) soluble in DCM

Fractions 46-55 were purified using silica gel with mixture of DCM/MeOH (95/5, v/v) to led mixture of BDb10 and BDb11 (204mg) as amorphous paste. This mixture was purified on Sephadex LH-20 using DCM/MeOH (2/8, v/v) as eluent to yield compound BDb10 and BDb11 (**69**) (16.4 mg)

3.3.2.2.3. Separation of EtOAc fraction. (F4) (6.4g)

EtOAc fraction (6.4 g) was adsorbed on 10.0 g of coarse silica gel (70-230 mesh) and subjected to column chromatography over 80.0 g of coarse silica gel (70-230 mesh), using column chromatography of 2 cm of diameter and 1 m of length and eluted with hexane/EtOAc mixture starting from 40% of the mixture of hexane/EtOAc to EtOAc/MeOH. A total of 110 fractions of 125 ml each were collected, evaporated and regrouped based on their TLC profiles to yield 4 compounds: 5,4´-dihydroxy-7-(γ,γ dimethylallyloxy)dihydroflavonol) (**70**) (12.3 mg), 3-Acetoxy-4',5-dihydroxy-7-methoxyflavanone (**71**) (13.5 mg) and two others not elucidated

Table 46: Chromatogram of fraction F4 from the MeOH extract of branches of *Boswellia dalzielii*

Eluent	Fraction N°	Observations	Compounds
Hex-EtOAc (40 :60)	1-10	Complex mixture with one major compound	BDb14
Hex-EtOAc (35 :65)	11-20	Mixture of about 3 compounds	BDb15
Hex-EtOAc (30 :70)	21-35	Mixture of about 5 compounds	BDb17 (**71**) ;BDb18 (**70**)
Hex-EtOAc (25 :75)	36-50	Complex mixture	_
Hex-EtOAc (20 :80)	51-60	Complex mixture	_
Hex-EtOAc (10:90)	61-70	Complex mixture	_
EtOAc 100%	71-85	Complex mixture	_
EtOAc/MeOH (95/5)	86-95	Complex mixture	_
EtOAc/MeOH (95/5)	95-110	Complex mixture	_

Fractions 1-10 have been grouped on the basis of the CCM and then purified with silica gel using HEX/EA (1/1, v/v) to give BDb14 (14.0 mg) as a white powder insoluble

Fraction 11-20 was subjected to column chromatography on Sephadex LH-20 using MeOH/DCM (7-3, v/v) as eluent to yield compound BDb15 (17.6 mg) as white powder insoluble.

Fraction 21-35 were subjected to column chromatography on Sephadex LH-20 using MeOH/DCM (7-3 v/v) as eluent following to purification using silica gel with mixture of Hex-EtOAc (45/55, v/v) to led BDb17 (**71**) (13.5 mg) as white powder soluble in DCM and BDb18 (**70**) (12.3 mg) as white powder soluble in DCM.

3.4. Physicochemical characteristics of isolated compounds from *Boswellia dalzielii*
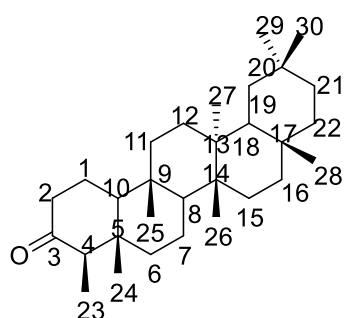
BDF2A: Fridelin **(56)**

Physical state: White powder

Molecular formular: $C_{30}H_{50}O$

^{1}H NMR (500 MHz, CDCl$_3$) and **^{13}C NMR** (125 MHz, CDCl$_3$) data see (Table XI).
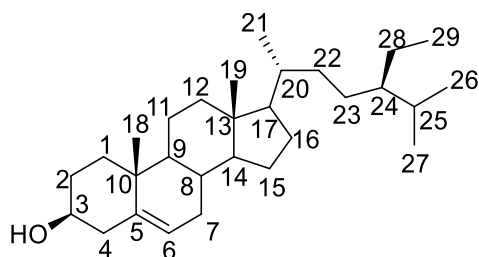
BDF2C: *β*-sitosterol **(66)**

Physical state: White powder

Molecular formular: $C_{29}H_{50}O$
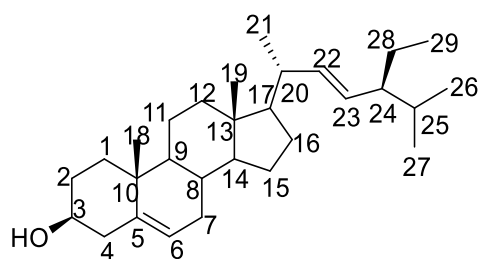
BDF2C: stigmasterol **(65)**

Physical state: White powder

Molecular formular: $C_{29}H_{48}O$
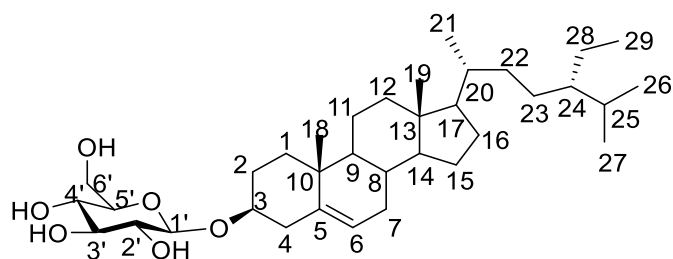
BDF5A: β-Sitosterol-3-O- β- D-glucopyranoside **(67)**

Physical state: White powder;

Molecular formular: $C_{35}H_{60}O_6$
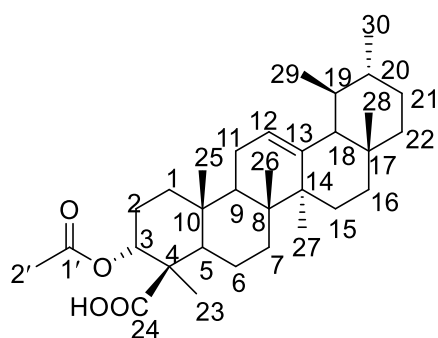
BDF3A: 3α-acetyl-β-boswellic acid **(19)**

Physical state: White powder

Molecular formular: $C_{32}H_{50}O_4$

¹H NMR (500 MHz, CDCl₃) and **¹³C NMR** (125 MHz, CDCl₃) data see (Table XII).
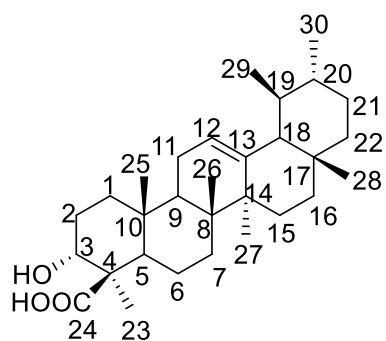
BDF3C: 3*β*-boswelic acid (**17**)

Physical state: White powder

Molecular formular: $C_{30}H_{48}O_3$

¹H NMR (500 MHz, CDCl₃) and **¹³C NMR** (125 MHz, CDCl₃) data see (Table XIII).
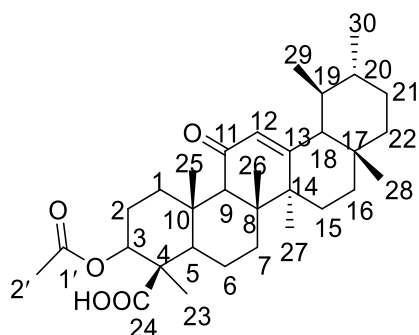
BDF3d: Acetyl-11-keto-boswellic (**20**)

Physical state: White powder

Molecular formular: $C_{32}H_{48}O_5$

¹H NMR (500 MHz, CDCl₃) and **¹³C NMR** (125 MHz, CDCl₃) data see (Table XIV).
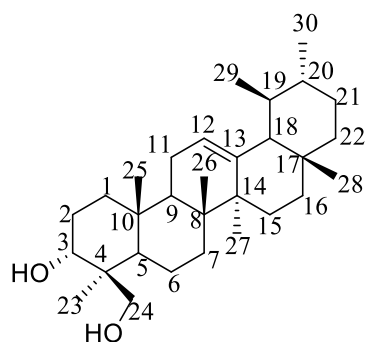
BDC1: Urs-12-ene-*3α*,24*β*-diol (**57**)

Physical state: White powder

Molecular formular: $C_{30}H_{50}O_2$

¹H NMR (500 MHz, CD₃OD) and **¹³C NMR** (125 MHz, CD₃OD) data see (Table XV).
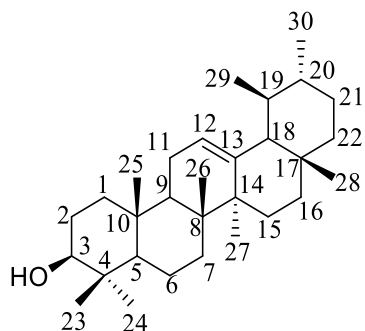
BDR1: *α*-amyrin **(26)**

Physical state: White powder

Molecular formular: $C_{30}H_{50}O$

¹H NMR (500 MHz, CD₃OD) and **¹³C NMR** (125 MHz, CD₃OD) data see (Table XVI).
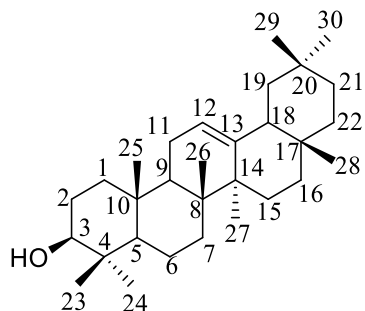
BDR1: *β*-amyrin **(58)**

Physical state: White powder

Molecular formular: $C_{30}H_{50}O$

¹H NMR (500 MHz, CD₃OD) and **¹³C NMR** (125 MHz, CD₃OD) data see (Table XVI).
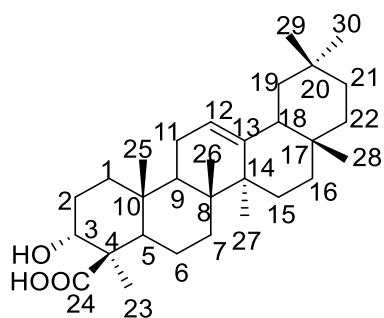
BDF3B: *α*-boswelic acid **(59)**

Physical state: White powder

Molecular formular: $C_{30}H_{48}O_3$

^{1}H NMR (500 MHz, CDCl$_3$) and **^{13}C NMR** (125 MHz, CDCl$_3$) data see (Table XVII).
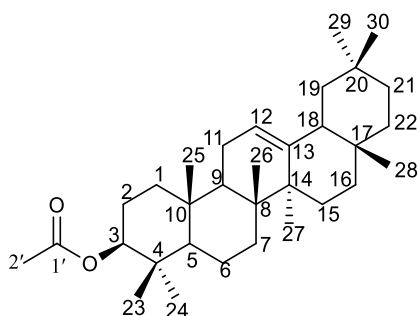
BDb1: *β*-amyrin acetate **(60)**

Physical state: White powder

Molecular formular: $C_{32}H_{52}O_2$

^{1}H NMR (500 MHz, CDCl$_3$) and **^{13}C NMR** (125 MHz, CDCl$_3$) data see (Table XVIII).
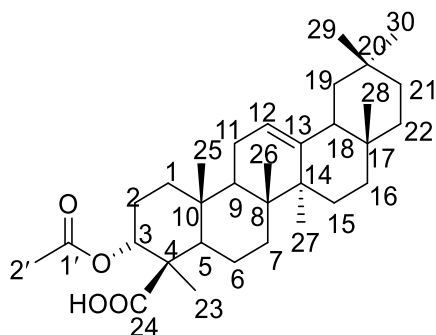
BDb16: 3*α*-acetyl-*α*-boswellic acid **(61)**

Physical state: White powder

Molecular formular: $C_{32}H_{50}O_4$

^{1}H NMR (500 MHz, CDCl$_3$) and **^{13}C NMR** (125 MHz, CDCl$_3$) data see (Table XIX).
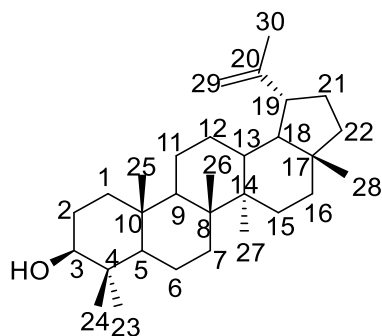
BDF2B: Lupeol **(25)**

Physical state: White powder

Molecular formular: $C_{30}H_{50}O$

White powder; ^{1}H NMR (500 MHz, CDCl$_3$) and ^{13}C NMR (125 MHz, CDCl$_3$) data see (Table XX).
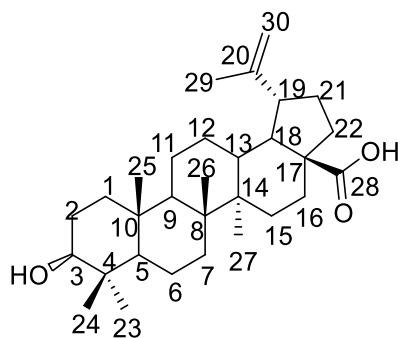
BDF3: betulinic acid **(62)**

Physical state: White powder

Molecular formular: $C_{30}H_{48}O_3$

White powder; ^{1}H NMR (500 MHz, CDCl$_3$) and ^{13}C NMR (125 MHz, CDCl$_3$) data see (Table XXI).
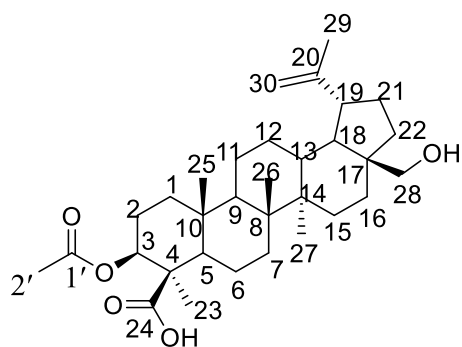
BDF4A: 3-*O*-acetyl-28-hydroxylupeolic **(63)**

Physical state: White powder

Molecular formular: $C_{32}H_{50}O_5$

White powder; ^{1}H NMR (500 MHz, $CDCl_3$) and ^{13}C NMR (125 MHz, $CDCl_3$) data see (Table XXII).
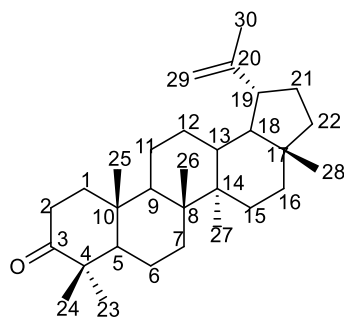
BDb2: lupenone **(22)**

Physical state: White powder

Molecular formular: $C_{30}H_{48}O$

^{1}H NMR (500 MHz, $CDCl_3$) and ^{13}C NMR (125 MHz, $CDCl_3$) data see (Table XXIII).
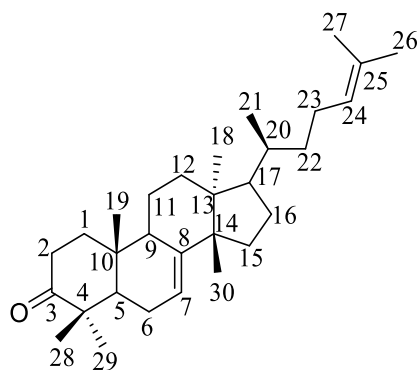
BDR3: lanosta-7,24-dien-3-one **(64)**

Physical state: White powder

Molecular formular: $C_{30}H_{48}O$

^{1}H NMR (500 MHz, CDCl$_3$) and ^{13}C NMR (125 MHz, CDCl$_3$) data see (Table XXIV).
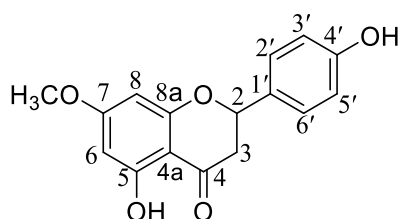
BDb3: 4', 5-dihydroxy-7-methoxyflavanone **(68)**

Physical state: White powder

Molecular formular: $C_{16}H_{14}O_5$

^{1}H NMR (500 MHz, CDCl$_3$) and **^{13}C NMR** (125 MHz, CDCl$_3$) data see (Table XXV).
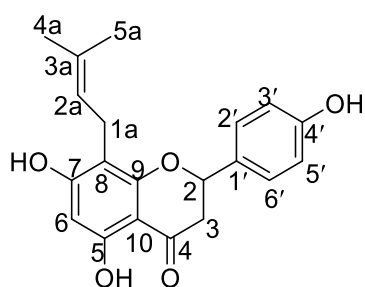
BDb11: Soforaflavanone B **(69)**

Physical state: White powder

Molecular formular: $C_{20}H_{20}O_5$

^{1}H NMR (500 MHz, CDCl$_3$) and **^{13}C NMR** (125 MHz, CDCl$_3$) data see (Table XXVI).
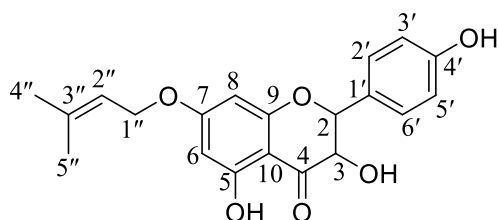
BDb18 : 5,4′-Dihydroxy-7-(γ,γ-dimethylallyloxy)dihydroflavonol **(70)**

Physical state: White powder

Molecular formular: $C_{20}H_{20}O_6$

^{1}H NMR (500 MHz, CDCl$_3$) and **^{13}C NMR** (125 MHz, CDCl$_3$) data see (Table XXVII).
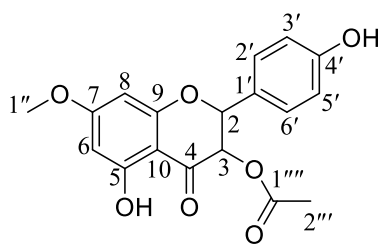
BDb17: 3-Acetoxy-4',5-dihydroxy-7-methoxyflavanone **(71)**

Physical state: White powder

Molecular formular: C$_{18}$H$_{16}$O$_7$

^{1}H NMR (500 MHz, CDCl$_3$) and **^{13}C NMR** (125 MHz, CDCl$_3$) data see (Table XXVIII).
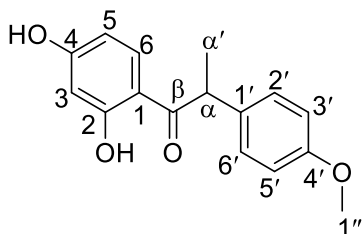
BDRA: angolensin (72)

Physical state: Brown paste

Molecular formular: C$_{16}$H$_{16}$O$_4$

^{1}H NMR (500 MHz, CDCl$_3$) and **^{13}C NMR** (125 MHz, CDCl$_3$) data see (Table XXIX).
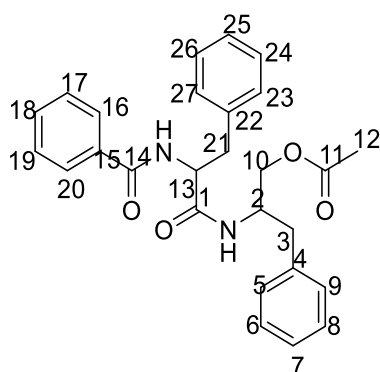
BDb5: Aurantiamide acetate (77)

Physical state: White powder

Molecular formular: $C_{27}H_{28}N_2O_4$

^{1}H NMR (500 MHz, CDCl$_3$) and **^{13}C NMR** (125 MHz, CDCl$_3$) data see (Table XXXIV).
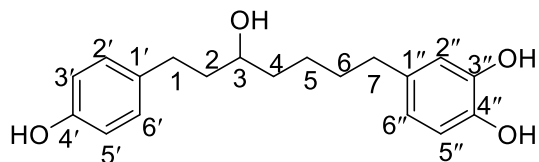
BDb8: 7-(3, 4-Dihydroxyphenyl)-1-(4-hydroxyphenyl)-3-heptanol **(73)**

Physical state: White powder

Molecular formular: $C_{19}H_{24}O_4$

^{1}H NMR (500 MHz, CDCl$_3$) and **^{13}C NMR** (125 MHz, CDCl$_3$) data see (Table XXX).
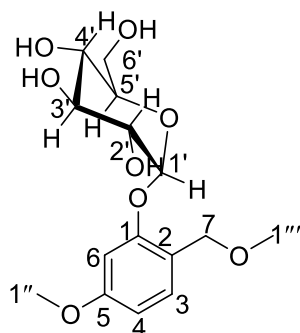
BDCA10: (dalzienoside) **(74)**

Physical state: Brown paste

Molecular formular: $C_{15}H_{22}O_8$

^{1}H NMR (500 MHz, acetone) and **^{13}C NMR** (125 MHz, acetone) data see (Table XXXI).
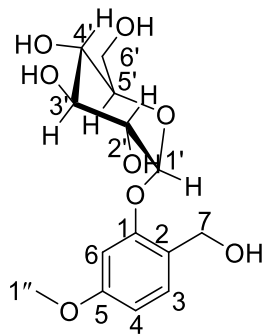
BDCA8: 4-methoxy-*2-O-α-D*-glucopyranosylphenylmethanol **(75)**

Physical state: Brown paste

Molecular formular: $C_{14}H_{20}O_8$

¹H NMR (500 MHz, acetone) and **¹³C NMR** (125 MHz, acetone) data see (Table XXXII).
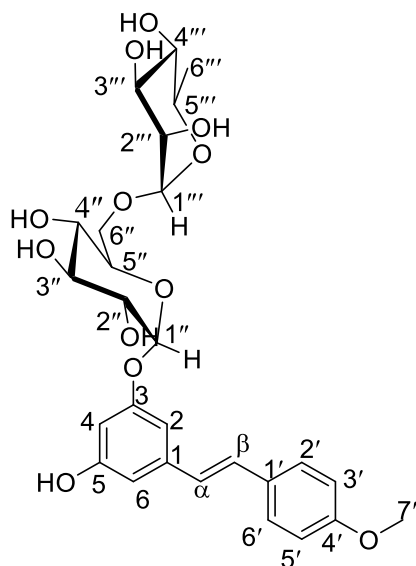
BDF5B: desoxyrhapontigenin-3-O-rutinoside **(76)**

Physical state: Yellowish amorphous powder

Molecular formular: $C_{27}H_{34}O_{12}$

¹H NMR (500 MHz, MeOD) and **¹³C NMR** (125 MHz, MeOD) data see (Table XXXIII).

3.5. Characteristic Analytical Tests

3.5.1. Liebermann-Burchard test: identification of terpenes and sterols

Objective: Identification of triterpenes and sterols.

Reagents: $CHCl_3$, AC_2O, concentrated H_2SO_4 (50 mL / 20 mL / 1 mL). To a $CHCl_3$ solution of the sample to be analysed, add a few drops of acetic anhydride, followed by concentrated H_2SO_4. The presence of triterpenes and their saponins is indicated by a change of colour from brick red, through purple, then blue and finally to green. Sterols give a blue colour that rapidly changes to green.

3.5.2. Molish's Test

Objective: Identification of sugars

Reagents: EtOH, α-naphtol, concentrated H_2SO_4. The sample to be analysed is introduced into a test tube and dissolved in a solution of 1 % ethanol in α-naphtol. A few drops of concentrated

H_2SO_4 are added, letting it flow down the side of the tube. The appearance of a purple–red ring at the interface, between the liquids indicates the presence of a sugar.

3.5.3. Ferric Chloride Test

Objective: Identification of phenols.

Reagents: $FeCl_3$, an alcoholic solution of the sample, add a few drops of $FeCl_3$. A colour change from yellow to purple indicates the presence of phenols.

3.5.4. Flavonoids test

Objective : Identification of flavonoids.

Reagents: MeOH, H_2SO_4, Magnesium ribbon. 2 mg of the pure compound were dissolved in 2 ml of methanol, then 3 drops of concentrated sulphuric acid and 0.5g of Magnesium ribbon were added. A pink or red colouration that disappears after three minutes indicates the presence of flavonoids

3.6. Protocol of biological activities

Antibacterial activities assay was conducted on a total of six bacterial strains, two from American Type Culture Collection, *E coli* ATCC 25322 and *Streptococcus Pneumoniae* ATCC 491619, one from BEI Resources namely *Pseudomonia aeruginosa* HM 801 and finally three clinical isolate strains from Laboratory collection namely *Salmonela typhi* (CPC and CHU), *Enterobacter cloacae* (CPC) and *Escherichia coli* CPC

The bacterial strains were maintained on agar slant at 4 °C and subcultured on a fresh appropriate agar plates 24 h prior to any antibacterial test. The minimal inhibitory concentration of extracts, fractions and compounds were assessed using the broth microdilution method as described by Eloff, (1998) with slight modifications. The tests were performed in duplicates. Each test sample was dissolved in dimethylsulfoxide (DMSO) to give a stock solution. In each well of the microtiter plate was introduced, 100 μL of Mueller Hilton broth (MHB). Then, 100 μL of each sample stock solution (2000 μg/mL) was added to the first wells, and then distributed to all other wells according to a geometric progression of reason 2, with final concentrations varying from 3.8 to 500 μg/mL and from < 0.15 to 500 μg/mL for ciprofloxacin. Then, 100 μL of the liquid culture medium (MHB) inoculated with the test germ ($2x10^6$ CFU/mL) were introduced into the wells to obtain a final concentration of 10^6 CFU/mL. The reference antibiotic (ciprofloxacin) serves as a positive control. The negative controls consist of wells containing only the culture medium on the one hand, and wells containing a mixture of culture broth and germ on the other hand. The micro culture plates were covered and incubated at 37

°C for 18 hours. 20 Microliters (20 μL) of Resazurin were then introduced into all wells and the micro-plates are incubated again at 37 °C for 30 minutes (Mativandlela *et al*. 2006). The colour shift from blue to pink was observed. The MIC was the lowest concentration of the extract that did not permit any visible growth compared to the control well. The minimum inhibitory concentration (MIC) was defined as the lowest concentration of the sample that prevented bacterial growth. The antibacterial activity of a sample of plant-isolated compounds was strong, moderate or weak if the MIC of the plants was $\leq$ 10 μg/mL, 10<MIC$\leq$100 μg/mL or >100 μg/mL, respectively. However, the activity of plant extracts will be classified as significant (MIC < 100 μg/mL), moderate (100 < MIC $\leq$ 625 μg/mL) or weak (MIC > 625 μg/mL) (Kuete, 2010).

3.6.1. Acute oral toxicity study on aqueous extract

The study was performed according to the protocol of the OECD (2001) according to the guideline 423. For this toxicity study, 9 adult female rats and not pregnant were used. These animals were randomly divided into 3 groups of 3 animals each, of which group 1, taken as a test control, was treated with distilled water at the single dose of 10ml / kg; the other two groups (test batches) received extract in single doses of 2000 and 5000 mg / kg, respectively. The animals were fasted without water 12 hours before the start of the experiment and 4 hours after. Oral administration of the extract and distilled water was done through a gastric tube. After administration, animals were observed individually for the first 4 hours and daily for 14 days after treatment. Special care should be taken during the first 30 minutes after administration of the substance. Any signs of immediate toxicity such as aggressiveness, mobility, possible tremors, and changes in coat, convulsions and other apparent signs of toxicity were recorded during the experiment as well as changes in body weight. At the end of the experiment, the animals were sacrificed, their organs (liver, kidneys, spleen, lungs and heart) were removed and weighed in order to perform an autopsy on a macroscopic scale

REFERENCES

Abdallah E. M., Khalid A. S., Ibrahim N. **2009**. Antibacterial activity of oleo-gum resins of Commiphora molmol and *Boswellia papyrifera* against methicillin resistant Staphylococcus aureus (MRSA). *Scientific Research and Essa*y, 4: 351-356.

Ageta H. and Arai Y. **1983**. Fern constituents: pentacyclic triterpenoids isolated from *Polypodium niponicum and P. formosanum. Phytochemistry*, 22(8): 1801-1808.

Agrawal P. K. **1989**. Carbons -13 NMR of flavonoids. *Central Institute of Medicinal and Aromatics Plants*. 106-107.

Ahmed A. A. A. **2013**. Valorisation pharmacologique de dracaena cinnabari balf, boswellia elongata balf et rumex nervosus vahl : plantes du yemen: toxicite, potentiel analgesique, anti inflammatoire, et anti spasmodique. Thèse de doctorat : Pharmacologie, Toxicologie et Pharmacognosie. Rabat : Faculté de Médecine et de Pharmacie de Rabat, 19-21.

Aksamija A. **2012**. Étude chimique des matériaux résineux : oliban, dammar et mastic. Application à des prélèvements artistiques et archéologiques. Thèse de doctorat, chimie, Avignon, Université d'Avignon et des Pays de Vaucluse, 39-40.

Alarcón R., Flores R. C., Ocampos S., Lucatti A., Galleguillo L. F., Tonn C., Sosa V. **2008**. Flavonoids from *Pterocaulon alopecuroides* with Antibacterial Activity. *Planta Medica*, 74: 1463-1467.

Alborn W., Allen N. & Preston D. **1991**. Deptomycin disrupts membrane potential in growing *Staphylococcus aureus*. *Antimicrobial Agents and Chemotherapy*, 31(7): 1093-1099.

Alemika T. E., Onawunmi G.O., Tiwalade A.O. **2004**. Isolation and characterization of incensole from *Boswellia dalzielii* stem bark. *Journal of Pharmacy and Bioresources*, 1(1): 7-11.

Al-Harrasi A., Hidayat H., Csuk R., Husain Y. K. **2019**. Biological Activities of *Boswellia* Extract. Chemistry and Bioactivity of Boswellic Acids and Other Terpenoids of the Genus *Boswellia*, 111-125.

Aliyu R., Gatsing D., Kiri H. J. **2007**. The effects of *Boswellia dalzielii* (Burseraceae) aqueous bark extract on rat liver function. *Asian journal of biochemistry*, 2(5): 359-363.

Allard S. and Ourisson G. **1957**. Remarques sur la nomenclature des triterpènes. *Tetrahedron,* 1(4): 277-283.

Amarinder S., Arvinda S., Surjeet S., Jyotsna S., Surinder K., Dilip M. M., Gurdarshan S., Ram V. **2017**. (Urs-12-ene-3α,24β-diol) a plant based derivative of boswellic acid protect Cisplatin induced urogenital toxicity. *Toxicology and Applied Pharmacology*, S0041-008X(17): 30031-30035.

Aminov R. I. **2010**. A brief history of the antibiotic era: Lessons learned and challenges for the future. Front Microbiol. 1(134): 1 -7.

Atta-ur-Rahman, Humera N., Fadimatou, Talat M., Amsha Y., Naheed F., Ngounou F. N, Kimbu S. F, Sondengam B. L, Choudhary M. I. **2005**. Bioactive Constituents from *Boswellia papyrifera*. *Natural Product*, 68:189-193.

Augustin J. M., Kuzina V., Andersen S. B., Bak S. **2011**. Molecular activities, biosynthesis and evolution of triterpenoid saponins. *Phytochemistry,* 72(6): 435-457.

Ayad R. **2008**. Recherche et Détermination structurale des métabolites secondaires de l'espèce, *Zygophyllum cornutum* (Zygophyllaceae). Mémoire de master, phytochimie. Algérie : Université Mentouri de Constantine, 41-44.

Ayafor F., Connolly J. D. **1981**. *2R,3R-(+)-3-Acetoxy-4',5-dihydroxy-7-methoxyflavanone and* 2R,3R- (+)-3-Acetoxy-4', 5, 7-trihydroxyflavanone: Two New 3-Acetylated dihydrofIavonols from *Aframomum pruinosum* Gagnepain (Zingiberaceae). *Journal Chemistry Society*, 2563-2565.

Baggnian I., Abdou L., Yameogo J. T., Moussa I., Toudou A. **2018**. Étude ethnobotanique des plantes médicinales vendues sur les marchés du centre ouest du Niger. *Journal of Applied Biosciences*, 132: 13392- 13403.

Belkacem, S. **2009**. Investigation phytochimique de la phase *n*-butanol de l'extrait hydroalcoolique des parties aériennes de *Centaurea parviflora* (Compositae). Thèse de Doctorat. Université Mentouri-Constantine ; Constantine, Algérie, Pp 20-32.

Belsner K., Buchele B., Werz U., Syrovets T., Simmet T. **2003**. Structural analysis of pentacyclic triterpenes from the gum resin of *Boswellia serrata* by NMR spectroscopy. *Magnetic resonance in chemistry*, 41: 115-122.

Benguerba A. **2008.** Etude phytochimique et de la phase butanolique de l'espece *inula crithmoides l.* Mémoire de magister, phytochimie, Algérie, Universite Mentouri Constantine, 26-27.

Bohlmann F., Abraham W. R, king R. M., Robinson H. **1981**. Thiophene acetylenes and flavanols from *Pterocaulon virgatum. Phytochemistry*, 20 (4): 825-827.

Brooks G. F., Butel J. S. & Morse S. A. **2004**. Jawetz, Melnick and Adelberg''s Medical Microbiology, 23rd Edition. McGraw Hill Companies, Singapore.

Bruneton J. **1993.** Pharmacognosie, phytochimie et plantes médicinales. 2e Edition, technique documentation Lavoisier, Ed Paris. 625-642, 816-822.

Bruneton J. **1999**. Phytochimie et plantes médicinales. Pharmacognosie, tome III, 3e édition Technique et Documentation. Paris, 266-293.

Bugg T. D. H. & Walsh C. T. (1992). Intracellular steps of bacterial cell wall peptidoglycan biosynthesis: Enzymology, antibiotics, and antibiotic resistance. *Natural Product Reports*, 9: 199-215.

Burkill, H. M. **1985.** *Boswellia dalzielii hutch* (family Burseraceae). The useful plants of west tropical Africa vol1

Camarda L., Dayton T., Di Stefano V., Pitonzo R., Schillaci D. **2007**. Chemical composition and antimicrobial activity of some oleo gum resin essential oils from Boswellia spp. (Burseraceae). *Annali Di Chimica*, 97(9): 837-844.

Carla C. M., Luciana Q. S., Frederico G. C., Nidia F. R. **2009**. New (9*βH*)-Lanostanes and Lanostanes from *Mikania* aff. *jeffreyi* (Asteraceae). *Chemistry and biodiversity*, 6: 1463-1470

Caron L. **2013**. Etude de l'influence de la tordeuse des bourgeons de l'épinette (*Choristoneura fumiferana Clem.*) sur la composition chimique du Sapin Baumier (*Abies Balsamea* (L.) Mill) en forêt Boréale, Mémoire de Magister, Ressources Renouvelables, Québec, Université du Québec à Chicoutimi, 28-31.

Chen C. R., Malik M., Snyder M. & Drlica K. **1996**. DNA gyrase and topoisomerase IV on the bacterial chromosome: quinolone – induced DNA cleavage. *Journal of molecular Biology*, 258: 627-637.

Chopra I., Roberts M. **2001**. Tetracycline antibiotics: Mode of action, applications, molecular biology, and epidemiology of bacterial resistance. Microbiol. *Molecular Biology Review*, 65(2): 232-260.

Chopra R., Alderborn G., Podczeck F. **2002**. The influence of pellet shape and surface properties on the drug release from uncoated and coated pellets. *International Journal of Pharmacology* 239: 171-178.

Clark A. M. **1996**. Natural products as sources for new drugs. *Pharmacology Research* 16: p1996.

Coder K. D. **2011**. *Frankincense & myrrh: A gift of tree history*. University of Georgia, Georgia, USA.

Connolly J., Hill A. **1991**. Methods in plant biochemistry. *7 academy press limited*, 331-359.

Cox P. A. **1994**. The *ethnobotanical approach to drug discovery: strengths and limitations*. In Prance GT (Ed) Ethnobotany and the search for new drugs. Wiley Chichester: 25-41.

Culioli G., Mathe C., Archier P., Vieillescazes C. **2003**. A lupane triterpene from frankincence Boswellia sp. (Burseraceae). *Phytochemistry*, 62(4): 537-541.

Daly D., Harley M., Martínez-Habibe M., Weeks A. **2010**. Burseraceae Flowering Plants. *Eudicots. Springer*, 76–104.

DeCarlo A., Johnsona S., Okeke-Agulub K. I., Dosokya N. S., Wax S. J., Owolabi M. S., Setzer W. N. **2019**. Compositional analysis of the essential oil of Boswellia dalzielii frankincense from West Africa reveals two major chemotypes. *Phytochemistry*, 164: 24-32.

Delfaut B. **2018**. *Boswellia serrata Roxb. ex Colebr.* : Une plante ancienne aux propriétés nouvelles. Thèse de doctorat, sciences pharmaceutiques, Bordeaux, U.F.R. des sciences pharmaceutiques, 23-24.

Demizu S. K., Kajiyama K., Takahashi Y., Hiraga S., Yamamoto Y., Tamura K., Okada T., Kinoshita T. **1998**. Antioxidant and antimicrobial constituent of licorice: isolation and structure elucidation of a new benzofurane derivative. *Chemical Pharmacology Bulletin* 36: 3474-3479.

De-Nova J. A., Medina R., Montero J. C., Weeks A., Rosell J. A., Olson M. E., Eguiarte L. E., Magallón S. **2012**. Insights into the historical construction of species-rich Mesoamerican seasonally dry tropical forests: the diversification of Bursera (Burseraceae, Sapindales). *New Phytologist,* 193(1): 276-287.

Denyer S. P., Hodges N. A., German S. P. **2004**. Introduction to pharmaceutical microbiology. In: Denyer SP, Hodges NA & German SP (eds.) Hugo and Russell‟s Pharmaceutical Microbiology. 7th Ed. Blackwell Science, UK. Pp. 3-8.

Dethlefsen, L., McFall-Ngai, M., Relman, D.A. **2007**. An ecological and evolutionary perspective on human microbe mutualism and disease. *Nature,* 449 (7164): 811-818. Available from: https://doi.org/10.1038/nature06245.

Douanla P. D., Tchuendem M. H. K., Tchinda A. T., Tabopda T. K., Zofou D., Cieckiewicz E., Frederich M., & Nkengfack A. E. **2018.** Chemical constituents of the leaves of *Caloncoba welwitschii* Gilg. *Phytochemistry Letters*, 23: 5-8.

Douthwaite S. **1992**. Interaction of the antibiotics clindamycin and lincomycin with *Escherichia coli* 23S ribosomal RNA. *Nucleic Acids Res*earch, 20: 4717-4720.

Doyle J. A. and Hotton C. L. **1991**. Diversifiation of early angiosperm pollen in a cladistic context. *Pollen and spores: patterns of diversification*, 44: 169-195.

Ebimieowei E. and Ibemologi A. **2016**. Antibiotics: Classification and mechanisms of action with emphasis on molecular perspectives. *International Journal of Appllied Microbiology and Biotechnololy Research*, 4: 90-101.

Eisenberg D. M., Kessler R. C., Foster C., Norlock F. E., Calkins D. R., Delbanco T. L. **1993**. Unconventional medicine in the United States: Prevalence, cost and pattern of use. *National England Journal of Medicine,* 328: 246-252

Emmanuel A. O., Adediji J. A., Ehimigbai A. R. O. **2015**. Histological effects of aqueous extract of *Boswellia dalzielii* stem bark on the testes of adult wistar rats. *Journal of pharmaceutical and scientific innovation*, 3(5): 280-283.

Epe B., Woolley P. **1984**. The binding of 6-demethylchlortetracycline to 70S, 50S and 30S ribosomal particles: A quantitative study by fluorescence anisotropy. *EMBO Journal*, 3: 121 - 126.

Eslamieh J. **2010**. Creating "Perfect" Boswellia. *Cactus and Succulent Journal*, 82(3): 126-131.

Etebu E. **2013**. Potential panacea to the complexities of polymerase chain reaction (PCR). *Advances in Life Science and Technoloy*, 13:1-8.

Falagas M. E., Rafailidis P. I., Matthaiou D. K. **2010**. Resistance to polymyxins: Mechanisms, frequency and treatment options. *Drug Resistance Update*, 13: 132-138.

Fukui H., Goto K., Tabata M. **1988**. Two antimicrobial flavonoids from the leaves of *Glyzyrrhiza glabra. Chemical Pharmacology Bulletin,* 36: 4174-4176.

Furuya T., **1987**. Saponins (ginseng saponins). In Vasil, I.K. (Ed.), "Cell Cultures and Somatic Cell Genetics of Plants". 5, Academic Press, San Diego, CA: 213-234.

Gadek P. A., Fernando E. S., Quinn C. J., Hoot S. B., Terrazas T., Sheahan M. C., Chase, M. W. **1996**. Sapindales: molecular delimitation and infraordinal groups. *American Journal of Botany,* 83(6): 802-811.

Gale E., Cundliffe E., Reynolds P. E., Richmond M. H., Waring M. J. **1981**. The molecular basis of antibiotic action. 2nd Ed. John Wiley & Sons, New York. 670p.

Gera Y., Ume U., Tor-Anyiin T. A., Iheukwumere C. C. **2015**. Ethnobotanical survey of anti-diarrheal medicinal plants among Tiv people of Nigeria. *Archives of Applied Science Research*, 7(6): 16-21.

Gonzalez-Cortazar M., Lopez-Gayou V., Tortoriello J., Dominguez-Mendoza B. E., Rıos-Cortes A. M., Delgado-Macuil R., Hernandez-Beteta E. E., Ble-Gonzalez E. A., Zamilpa A. **2019**. Antimicrobial gastrodin derivatives isolated from Bacopa procumbens. *Phytochemical Letter*, 31: 33-38

Gormo J., Nizesete B. D. **2013**. Des végétaux et leurs usages chez les peuples du Nord Cameroun: sélection et mode d'emploi du XIXe au XXe siècle. História, Ciências, Saúde – Manguinhos, Rio de Janeiro, 20(2): 587-607.

Group A. P. **2009**. An update of the Angiosperm Phylogeny Group classification for the orders and families of flowering plants: APG III. *Botanical Journal of the Linnean Society,* 161(2):105-121.

Gualerzi C. O., Brandi L. B., Caserta E., La Teana A., Spurio R., Tomsic J., Pon C. L. **2000**. Translation initiation in bacteria. In: Garrett R. A., Douthwaite S. R., Liljas A., Matheson A. T., Moore P. B. & Noller H. F. (eds.). The ribosome: Structure, function, antibiotics, and cellular interactions. ASM Press, Washington, DC. Pp. 477-494.

Guardabassi L., Courvalin P. **2006**. Modes of antimicrobial action and mechanisms of bacterial resistance. *In Aarestrup F.M. (Ed.), Antimicrobial resistance in bacteria of animal origin. ASM Press: Washington*, 1-18.

Habib M. R., Nikkon F., Rahman M., Haque M. E., Karim M. R. **2007**. Isolation of Stigmasterol and β-Sitosterol from Methanolic Extract of Root Bark of *Calotropis gigantea* (Linn). *Pakistan Journal of Biological Sciences,* 10: 4174-4176.

Hanaa H. A., Ahmed A. A., Amal Z. H., Soheir E. K. **2015**. Phytochemical Analysis and Anti-cancer Investigation of *Boswellia Serrata* Bioactive Constituents in Vitro. *Asian Pacific Journal of Cancer Prevention*, 16(16): 7179-7188.

Haralampidis K., Trojanowska M., Osbourn A. E. **2002**. Biosynthesis of Triterpenoid Saponins in Plants. *Advances in Biochemical Engineering/ Biotechnology*, 75: 31-49.

Harbone J.B. **1988**. The flavonoids: advance in research since 1980. Vol.2, Springer US. p. 621.

Harley M. M. and Daly D. C. **1995**. Burseraceae Kunth.: Protieae March. em. Engl. *World pollen and spore flora,* 20.

Hay R., Higuero I., Camarena I., De Meulenaer T., Gaynor K., Caromel A., Gray J. **2019**. Convention sur le commerce international des espèces de faune et de flore sauvages menacées d'extinction, Conférence des Parties Colombo 2019, Sri Lanka, 1-4.

Hepper F. N. **1969**. Arabian and African frankincense trees. *The Journal of Egyptian Archaeology,* 55(1): 66-72.

Herbert R. B. **1981**. The biosynthesis of secondary metabolites. (Ed). Chapman and Hall: London, Pp 89-90.

Holtje J. V. **1998**. Growth of the stress bearing and shape maintaining murein sacculus of *Escherichia coli*. *Microbioly and Molecular Biology Reviews*, 62: 181-189.

Hong W., Zeng J. & Xie J. **2014**. Antibiotic drugs targeting bacterial RNAs. *Acta Pharmaceutica Sinica B*. 4(4): 258-265.

Ii A. **2003**. An update of the Angiosperm Phylogeny Group classification for the orders and families of flowering plants: APG II. *Botanical Journal of the Linnean Society,* 141(4): 399-436.

Imane B. **2017**. Cours de chimie des produits naturels 2, Chimie organique appliquée, Algérie, Universite Ziane Achour – Djelfa : 19.

James J.T. & Dubery I.A. **2009**. Pentacyclic Triterpenoids from the Medicinal Herb, *Centella asiatica* (L.) Urban. *Molecules* 14: 3922 – 3941

Jiang-Bo H., Yong-Ming Y., Xiu-Jing M., Qing L., Xue-Song L., Jia S., Yan L., Guang-Ming L., Yong-Xian C. **2011**. Sesquiterpenoids and Diarylheptanoids from Nidus Vespae and Their Inhibitory Effects on Nitric Oxide Production. *Chemistry and biodiversity*, 8: 2270-2276.

Jinqian Y., Hongwei Z., Daijie W., Xiangyun S., Lei Z., Xiao W. **2017**. Extraction and purification of five terpenoids from Olibanum by ultrahigh pressure technique and high-speed countercurrent chromatography. *Journal of Separation Science*, 40(13): 2732-2740.

Jinqian Y., Yanling G., Hongwei Z., Xiao W. **2018**. Diterpenoids from the gum resin of *Boswellia carterii* and their biological activities. *Tetrahedron*, 74: 5858-5866

Josephine H. R., Kumar I. & Pratt R. F. **2004**. The Perfect Pencillin? Inhibition of a bacterial DD-peptidase by peptidoglycan-mimetic betalactams. *Journal of the American Chemical Society*, 126: 81222-81223.

Kapche F. **2000**. Contribution à l'étude phytochimique de deux plantes médicinales du Cameroun: *Dorsténia poinsettiifolia* et *Dorsténia psilurus* (Moraceae) et Hémisynthèse de quelques Flavanones. Thèse de doctorat de 3e cycle en chimie organique, Université de Yaoundé I, faculté des sciences, Cameroun: 30

Kasali A. A., Adio A. M., Kundaya O. E., Oyedeji A. O., Eshilokun A. O., Adefenwa M. **2002**. Antimicrobial activity of the essential oil of Boswellia serrata Roxb. *Journal Essent Oil Bearing Plants*, 5(3): 173-175.

Katz L. & Ashley G. W. **2005**. Translation and protein synthesis: macrolides. *Chemical Reviews*, 105: 499-528.

Kémeuzé V. A., Mapongmetsem P. M., Tientcheu M. A., Nkongmeneck B. A., Jiofack R. B. **2012**. *Boswellia dalzielii* Hutch : état du peuplement et utilisation traditionnelle dans la région de Mbé (Adamaoua-Cameroun). *Sécheresse*, 23: 278-283.

Koné D. **2009**. Enquête ethnobotanique de six plantes médicinales maliennes : extraction, identification d'alcaloïdes - caractérisation, quantification de polyphénols : étude de leur activité antioxydante. Thèse de doctorat, chimie organique, Bamako, Faculté des Sciences et Techniques de Bamako: 22.

Kuete V., Alibert-Franco S., Eyong K., Ngameni B., Folefoc G., Nguemeving J., Tangmouo J., Fotso G., Komguem J., Ouahouo B. **2011**. Antibacterial activity of some natural products against bacteria expressing a multidrug-resistant phenotype. *Internatinal Journal of Antimicrobial Agents*. 37(2):156–161.

Kyeong W., Ji Y., Sang U., Ki H., Kang R. **2014**. Triterpenes from Perilla frutescens var. acuta and their cytotoxic activity. *Natural Product Sciences*, 20: 71-75.

Lawrence G. H. M. **1951**. Taxonomy of Vascular Plants. New York: The Macmillan Company. *Science Education,* 36(5): 311-311.

Levy S. B and Engl N. **1993**. The antimicrobial paradox. How miracle drugs are destroying the miracle. *Journal of Medicine*, 328:1792

Levy S. B., Chadwick D. J., Goode J., Chichester U. K. **2007**. Antibiotic Resistance: Antibiotic Resistance: An Ecological Imbalance, in Ciba Foundation Symposium 207- antibiotic Resistance: Origins, Evolution, Selection and Spread. *Clinical Microbiology Review* 13: 602-614.

Lim Y. H., Kim I. H. and Seo J. J. **2007**. In vitro Activity of Kaempferol Isolated from the Impatiens balsamina alone and in Combination with Erythromycin or Clindamycin against Propionibacterium acnes. *The Journal of Microbiology* 45 : 473−477.

Lipp E. K, Huq A., Colwell R. R. (**2002**). Effects of global climate on infectious disease: the cholera model. *Clinical Microbiologie Review*. 15(4): 757-770.

Madigan M. T. and Martinko J. M. **2006**. Brock biology of microorganisms. 11th edition. Pearson Prentice Hall Inc.

Mahato B. S., Nandy K. A., Roy G. **1992**. Triterpenoids. *Phytochemistry* 31(1): 2199-2249.

Mahato S. and Kundu A. **1994**. 13C NMR spectra of pentacyclic triterpenoids –A compilation and some salient features. *Phytochemistry*, 37: 1517-1575.

Mahato S. B. and Sen S. **1997**. Advances in triterpenoid research, 1990–1994. *Phytochemistry,* 44(7): 1185-1236.

Manase M. J. **2013**. Étude chimique et biologique de saponines isolées de trois espèces Malgaches appartenant aux familles des Caryophyllaceae, Pittosporaceae et Solanaceae. Thèse de doctorat, pharmacognosie, Bourgogne, Universite de Bourgogne, 34-35.

Manguro L. O. A. and Wagai S. O. **2016**. Ursane and tirucallane-type triterpenes of *Boswellia rivae* oleo-gum resin. *Journal of Asian Natural Products Research*, 18(9): 854-864.

Mbiantcha M., Ngouonpe A., Dawe A., Yousseu W., Ateufack G. **2017**. Antinociceptive Activities of the Methanolic Extract of the Stem Bark of *Boswellia dalzielii* Hutch. (Burseraceae) in Rats Are NO/cGMP/ATP-Sensitive-K$^+$ Channel Activation Dependent. *Evidence-Based Complementary and Alternative Medicine*, 12.

Menninger J. R. and Otto D. P. **1982**. Erythromycin, carbomycin, and spiramycin inhibit protein synthesis by stimulating the dissociation of peptidyl-tRNA from ribosomes. *Antimicrobial Agents and Chemotherary,* 21: 811-818.

Motahareh N., Tanja G., Stephen J. T., Helen M. W., Mohammad K., Ronald J. Q., Peter R. B. **2014**. Chemical Constituents of Kino Extract from *Corymbia torelliana*. *Molecules*, 19: 17862-1787.

Nacoulma P.A. **2012**. Reprogrammation métabolique induite dans les tissus hyperplasiques formés chez le tabac infecté par Rhodococcus fascians: aspects fondamentaux et applications potentielles. Thèse de doctorat, Sciences Biomédicales et Pharmaceutiques, Bruxelles, Ecole Doctorale en Sciences Pharmaceutiques, 17.

Nacoulma-Ouédraogo G. **1996**. Plantes médicinales et pratiques médicinales traditionnelles au Burkina Faso. Cas du plateau central. Université de Ouagadougou.

Nazifi A. B., Danjuma N. M., Olurishe T.O., Ya'u J. **2017**. Behavioural Effects of Methanol Stem Bark Extract of *Boswellia dalzielii* Hutch (Burseraceae) in Mice. *African Journal of Biomedical Research*, 20: 103-108.

Nissen P., Hansen J., Ban N., Moore P. B., Steitz T. A. **2000**. The structural basis of ribosome activity in peptide bond synthesis. *Sciences*, 289: 920-930.

Nitu T. **2018**. Antibiotic resistance: causes, consequences, prevention and control. *Agriways*, 6 (2): 47-49.

Noushahi H. A., Khan H. A., Noushahi F. U., Hussain M., Javed T., Zafar M., Batool M., Ahmed U., Liu K., Harrison T. M., Saud S., Fahad S., Shu S. **2022**. Biosynthetic pathways of triterpenoids and strategies to improve their biosynthetic efficiency. *Plants Growth regulation* 97 : 439─454.

Nwude N., Ibrahim M. A. **1980**. Plants used in traditional veterinary medical practice in Nigeria. *Journal of veterinary pharmacology and therapeutics*, 3: 261-273.

OECD. **2001**. Acute oral toxicity - method by acute toxicity class. OECD Guideline for the Testing of Chemicals, Guideline 423, 14p.

Ogunkoya L. **1981**. Application of mass spectrometry in structural problems in triterpenes. *Phvtochemistry,* 20: 121-126.

Onana J. **2018**. Flore du Cameroun 43 Burseraceae. London, Raynes Park.

Onobrudu D. A. **2017**. Saponins and Polyphenolics of Methanol Leaf Extract of *Boswellia dalzielii Hutch*. *Archives of Current Research International,* 8(3): 1-6.

Ouedraogo A., Thiombiano A., Hahn-Hadjali K., Guinko S. **2006**. Régénération sexuée de *Boswellia dalzielii* Hutch., un arbre médicinal de grande valeur au Burkina Faso. Bois et Forêts des Tropiques, 289(3): 41-48.

Park J. T. and Uehara T. **2008**. How bacteria consume their own exoskeleton (turnover and recycling of cell wall-peptidoglycan). *Microbiology and Molecular Biology*, 72: 211-227.

Patel U., Yan Y. P., Hobbs F. W. Jr., Kaczmarczyk J., Slee A. M., Pompliano D. L., Kurilla M. G., Bobkova E. V. **2001**. Oxazolidinones mechanism of action: Inhibition of the first peptide bond formation. *Journal of Biological Chemistry*, 276(40): 37199-37205.

Perotto C. **2013**. L'utilisation des plantes et de leurs principes actifs dans le traitement de la douleur à travers le monde. Thèse de doctorat, pharmacie, Limoges, Faculté de Pharmacie, 79-80.

Philippe B. **2000.** Etude bibliographique des flavonoïdes sulfatés : répartition, structure et propriétés biologiques. Thèse de doctorat, pharmacie, Grenoble, Faculté de Pharmacie de Grenoble, 22.

Prasain J. K., Wang C.-C. and Barnes S. **2004**. Mass spectrometric methods for the determination of flavonoids in biological samples. Free Radical Biology and Medicine 37: 1324─1350.

Pu L., Pan H., Rui-Xue D., Ru L., Li Y., Wei-Ping Y. **2011**. Triterpenoids from the Flowers of Salvia miltiorrhiza. *Helvetica Chimicaa Acta*, 94: 136-141.

Qu W., Wu F. H., Li J., Liang J. Y. **2011**. Alkaloids from *Houttuynia cordata* and Their Antiplatelet Aggregation Activities. *Chinese Journal of Natural Medicines*, 9(6): 0425-0428

Qurishi Y., Abid H., Zargar M. A., Shashank K. S., Ajit K. S. **2010**. Potential role of natural molecules in health and disease: Importance of boswellic acid. *Journal of Medicinal Plants Research,* 4: 2778-2785.

Russell A. D. **2004**. Types of antibiotics and synthetic antimicrobial agents. In: Denyer S. P., Hodges N. A. & German S. P. (eds.) Hugo and Russell‟s pharmaceutical microbiology. 7th Ed. Blackwell Science, UK. Pp. 152-186.

Sandjo L. P. **2009**. Sphingolipides, Triterppènoides et autres métabolites secondaires des variétés sauvage et cultivée de l'espèce *Triumfetta cordifolia* A. Rich. (Tiliaceae) : Transformations chimiques et évaluation des propriétés biologiques de quelques composés isolés. Thèse de Doctorat/Ph.D en Chimie Organique. Universite paul-verlaine de metz, Université de Yaoundé I, faculté des sciences, Cameroun, 22-23.

Sandjo L. P. and Kuete V. **2013**. Triterpenes and Steroids from the Medicinal Plants of Africa. *Medicinal Plant Research in Africa*, 135-202.

Sarada N. C. and Geetha V. **2016**. A review on ethnobotany, Phytochemistry and Pharmacology of *Boswellia ovalifoliolata*. *International Journal of Chemistry Technology Research*, 9(1): 95-104.

Sarnim G., Sanjay S. T., Roshan A., Vedamurthy A. B., Hoshker J. H. **2013**. Artemisia indica extracts as Anthalminthic agent against Pheretima Posthuma. *International Journal of Pharmacy and Pharmaceutical Sciences*, 5: 259-262.

Satyal P., Paudel P., Kafle A., Pokhare S. K., Lamichhane B., Dosoky N. S., Moriarity D. M., Setzer W. N. **2012**. Bioactivities of volatile components from Nepalese Artemisia species. *Natural Product Communications*, 12: 1651-8122.

Schlegel H. G. **2003**. General microbiology. 7th Ed. Cambridge University Press, Cambridge.

Shenvi S., Rijesh K., Diwakar L., Chandrasekara G. R. **2014**. Beckmann rearrangement products of methyl 3-oxo-tirucall-8, 24-dien-21-oate from *Boswellia serrata* gum and their anti-tumor activity. *Phytochemistry Letters*, 7: 114-119.

Shi Y. R., Hyun S. L., Young K. K., Sung H. K. **1997**. Determination of Isoprenyl and Lavandulyl Positions of Flavonoids from *Sophoraflavescens* by NMR Experiment. *Archives of Pharmacal Research,* 20(5): 491-495.

Songue J. L., Kouam , Dongo E., Mpondo T. N., Robert L. W. **2012.** Chemical Constituents from Stem Bark and Roots of *Clausena anisate. Molecules*, 17: 13673-13686.

Subhashini P. D., Satyanarayana B., Tarakeswara M. N. **2014**. Phytochemical Screening for Secondary Metabolites in *Boswellia serrata* Roxb. and *Wrightia tinctoria* Roxb. R.Br. *Notulae Scientia Biologicae*, 6(4): 474-477.

Szakiel A., Pączkowski C., Pensec F., Bertsch C. **2012**. Fruit cuticular waxes as a source of biologically active triterpenoids. *Phytochemistry Reviews,* 11(2-3): 263-284.

Talaro K. P. and Chess B. **2008**. Foundations in microbiology. 8th Ed. McGraw Hill, New York.

Talom T. B., Tagne S. R., Talla E., Fodouop C. S. P., Njateng G. S. S., Nyemb J. N., Almas J., Huma A. B., Rukesh M., Tatsadjieu N. L., Kuiate J. R. **2019.** Antimicrobial and Immunomodulatory Properties of Crude Extract and Compounds from *Boswellia dalzielii* Hutch. *International Journal of Biosciences*, 14(2): 161-171.

Tarek B. **2012.** Biodiversité, Bioactivité des Composés Terpéniques Volatils des Lavandes Ailées, *Lavandula stoechas Sensu Lato*, un Complexe d'Espècs Méditérrnéennes d'Intérêt Pharmacologique, Thèse de doctorat, Biologie et Ecophysiologie Végétale, ENS de Kouba Algérie, Université Jean Monnet-Saint Etienne, 7-10.

Thimmappa R., Geisler K., Louveau T., O'Maille P., Osbourn A. **2014**. Triterpene biosynthesis in plants. *Annual Review of Plant Biology*, 65: 225-257.

Thulin M. and Warfa A. M. **1987**. The frankincense trees (Boswellia spp., Burseraceae) of northern Somalia and southern Arabia. *Kew Bulletin*, 42(3): 487-500.

Timo D. S., Mtui D. J., Balemba O.B. **2013**. Ethnopharmacological survey of plants used in the traditional treatment of gastrointestinal pain, inflammation and diarrhea in Africa: future perspectives for integration into modern medicine. *Animals*. 3(1): 158-227.

Tommy Ö., May-Britt T., Tone F B., Helena B., Anders A., Mattias H., Trygve A. **2014**. Identification of metabolites from 2D ^{1}H-^{13}C HSQC NMR using peak correlation plots. *Biomedical central Bioinformatics*, 15: 413

Toshihiro A., Yumiko K., Wilhelmus C. M. C., Kokke, Sei-ichi T., Ken Y., Toshitake T. **2016**. Tirucalla-5,24-dien-3β-ol[(13α,14β,17α,20S)-lanosta-5,24-dien-3β-ol] And three other unsaturated tirucallanes from the roots of *Bryonia dioica* Jacq.: the first naturally occurring C-10 methylated tetracyclic triterpene alcohols with a monounsaturated skeleton. *Journal Chemistry Society*, 1: 2379-2384

Uzama D., Gbubele J. D., Bwai M. D., Galadanchi K. M. **2015**. Phytochemical, Nutritional and Antimicrobial Screening of Hexane, Ethyl Acetate and Ethanolic Extracts of *Boswellia Dalzielii* Leaves and Bark. *American Journal of Bioscience and Bioengineering*, 3(5): 76-79.

Vaishnav V. and Janghel U. **2018**. A note on the clonal propagation of depleted threatened species Boswellia serrata Roxb. Through branch cuttings. *Tropical Plant Research*, 5(1): 27-28

Vannuffel P. and Cocito C. 1996. Mechanism of action of streptogramins and macrolides. Drugs. 51(1): 20-30.

Verhoff M., Seitz S., Michael P., Stefan M. N., Jauch J., Schuster D., Werz O. 2014. Tetra- and Pentacyclic Triterpene Acids from the Ancient Antiinflammatory Remedy Frankincense as Inhibitors of Microsomal Prostaglandin E2 Synthase-1. *Journal of Natural Products*, 77(6): 1445-1451.

Verhoff M, Seitz S, Northoff H, Jauch J, Schaible AM, Werz O. 2012. A novel C(28)-hydroxylated lupeolic acid suppresses the biosynthesis of eicosanoids through inhibition of cytosolic phospholipase A2. *Biochemecal Pharmacology*, 84: 681-691.

Wafo P., Ramsay S. T., Kamdem, Zulfiqar A., Shazia A., Shamsun N. K., Afshan B., Karsten K., Berhanu M. A., Bonaventure T. N., Muhammad I. C. 2010. Duboscic Acid: A Potent r-Glucosidase Inhibitor with an Unprecedented Triterpenoidal Carbon Skeleton from *Duboscia macrocarpa*. *Organic Letters*, 12(24): 5760-5763.

Walsh C. 2003. Antibiotics: actions, origins, resistance. 1 st Ed. ASM Press, Washington, DC. 345p.

Wang Y.G., Ma Q.G., Tian J., Ren J., Wang A.G., Ji T.F., Yang J.B., Su Y.L. 2016. Hepatoprotective triterpenes from the gum resin of *Boswellia carterii. Fitoterapia*, 109: 266-273.

Wansi J. D. 2000. Contribution à l'étude phytochimique de deux plantes médicinales du Cameroun : *Gambeya africana* (Sapotacée) et *Drypetes molunduana* (Euphorbiacée), Thèse de Doctorat 3e cycle en chimie organique, Université de Yaoundé I - Cameroun, 22-23.

Weckessera S., Engela K., Simon-Haarhausa B., Wittmerb A., Pelzb K., Schemppa C. M. 2007. Screening of plant extracts for antimicrobial activity against bacteria and yeasts with dermatological relevance. *Phytomedicine*, 14: 508-516.

Weeks A., Daly D. C., Simpson B. B. 2005. The phylogenetic history and biogeography of the frankincense and myrrh family (Burseraceae) based on nuclear and chloroplast sequence data. *Molecular Phylogenetics and Evolution,* 35(1): 85-101.

WHO. 2000. General Methodical Principles for Traditional Medicine Research and Evaluation 2015: Summary. WHO / EDT / TRMP. World Health Organization, Geneva, Switzerland, 87p.

Wright G. D. 2010. Q & A: Antibiotic resistance: Where does it come from and what can we do about it? *Biomedical central Biology*, 8:123. http://doi.org/10.1186/1741 -7007-8-123.

Yan-Gai W., Qin-Ge M., Jin T., Jin R., Ai-Guo W., Teng-Fei J., Jian-Bo Y., Ya-Lun S. 2016. Hepatoprotective Triterpenes from the Gum Resin of *Boswellia carterii. Fitoterapia*, 109: 266-273.

Yi-Chun L., Chien-Kuang C., Wan-Wan L., Shoei-Sheng L. 2012. A comprehensive investigation of anti-inflammatory diarylheptanoids from the leaves of Alnus formosana. *Phytochemistry*, 73:84-94.

Yili A., Mutalipu A. H. A., Isaev M. I. 2009. Betulinic acid and sterols from *Astragalus altaicus. Chemistry of Natural Compounds*, 45: 592-594.

Younoussa L., Nchiwan N. E., Danga Y.S.P., Okechukwu E. C. **2014**. Larvicidal activity of *Annonasenegalensis* and *Boswellia dalzielii* leaf extract against Aedesaegypti (Diptera: colicidac). *International Journal of Mosquito Research*, 1(4): 25-29

Younoussa L., Nchiwan N. E., Okechukwu E. C. **2016.** Toxicity of *Boswellia dalzielii* (Burseraceae) Leaf fractions Against Immature Stages of Anopheles gambiae (Giles) and Culex quinquefasciatus (Say) (Diptera: Culicidae). *International Journal of Insect Science*, 8: 23-31.